PB82-258609

# Green River Air Quality Model Development: Meteorological Data August 1980 Field Study in the Piceance Creek Basin Oil Shale Resources Area

Battelle Pacific Northwest Labs.
Richland, WA

Prepared for

Environmental Sciences Research Lab.
Research Triangle Park, NC

Jun 82

U.S. Department of Commerce
National Technical Information Service
NTIS

EPA-600/7-82-047
June 1982

PB82-258609

# GREEN RIVER AIR QUALITY MODEL DEVELOPMENT
## Meteorological Data - August 1980 Field Study in the Piceance Creek Basin Oil Shale Resources Area

by

C. D. Whiteman, N. S. Laulainen
G. A. Sehmel, J. M. Thorp

Battelle, Pacific Northwest Laboratory
Richland, Washington 99532

Interagency Agreement AD-89-F-0-097-0

Project Officer

Alan H. Huber
Meteorology and Assessment Division
Environmental Sciences Research Laboratory
Research Triangle Park, North Carolina 27711

This study was jointly funded by the United States Environmental Protection Agency and the United States Department of Energy

REPRODUCED BY
NATIONAL TECHNICAL
INFORMATION SERVICE
U.S. DEPARTMENT OF COMMERCE
SPRINGFIELD, VA. 22161

ENVIRONMENTAL SCIENCES RESEARCH LABORATORY
OFFICE OF RESEARCH AND DEVELOPMENT
U.S. ENVIRONMENTAL PROTECTION AGENCY
RESEARCH TRIANGLE PARK, NORTH CAROLINA 27711

BEGIN FIRST LINE OF TEXT HERE
CENTER OF PAGE
TOP OF IMAGE AREA
DROPPED HEAD: BEGIN SECTIONS HERE
6-1/2"
9-1/8"
BEGIN LAST LINE OF TEXT
3/8"
PAGE NUMBER
BOTTOM OF IMAGE AREA; OUTSIDE DIMENSION FOR TABLES AND ILLUSTRATIONS
EPA Form 2350-4 (4-80)
[PREVIOUSLY CIN. EPA FORM 287]
☆ U.S. GOVERNMENT PRINTING OFFICE 1980-660-639
TYPING GUIDE SHEET

## TECHNICAL REPORT DATA

*(Please read Instructions on the reverse before completing)*

| | | |
|---|---|---|
| 1. REPORT NO.<br>EPA-600/7-82-047 | 2.<br>ORD Report | 3. RECIPIENT'S ACCESSION NO.<br>PB82 258609 |
| 4. TITLE AND SUBTITLE<br>GREEN RIVER AIR QUALITY MODEL DEVELOPMENT<br>Meteorological Data - August 1980 Field Study in the Piceance Creek Basin Oil Shale Resources Area | | 5. REPORT DATE<br>June 1982<br>6. PERFORMING ORGANIZATION CODE |
| 7. AUTHOR(S)<br>C. D. Whiteman, N. S. Laulainen, G. A. Sehmel, and J. M. Thorp | | 8. PERFORMING ORGANIZATION REPORT NO. |
| 9. PERFORMING ORGANIZATION NAME AND ADDRESS<br>Pacific Northwest Laboratory<br>Richland, Washington 99532 | | 10. PROGRAM ELEMENT NO.<br>CDAN1A/03-0726 (FY-82)<br>11. CONTRACT/GRANT NO.<br>AD-89-F-0-097-0 |
| 12. SPONSORING AGENCY NAME AND ADDRESS<br>Environmental Sciences Research Laboratory - RTP, NC<br>Office of Research and Development<br>U.S. Environmental Protection Agency<br>Research Triangle Park, North Carolina 27711 | | 13. TYPE OF REPORT AND PERIOD COVERED<br>Final<br>14. SPONSORING AGENCY CODE<br>EPA/600/09 |

15. SUPPLEMENTARY NOTES

This study was jointly funded with the U.S. Department of Energy, Washington, DC 20545

16. ABSTRACT

Special meteorological and air quality studies were conducted during August 1980 in the Piceance Creek Basin oil shale resource area of Northwestern Colorado as part of the EPA-sponsored Green River Ambient Model Assessment program. The objective of the limited field program was to collect initial data to aid in the development, calibration, and validation of a mesoscale air quality model. The specific goals of the program were to investigate the growth and characteristics of convective boundary layers that form over the area during the daytime, to characterize background pollutant levels, visibility, and atmospheric structure over the area, and to investigate, by means of tracer experiments, the dispersion and dry deposition of pollutants released in nocturnal valley drainage flows.

An instrumented DC-3 aircraft was the primary means of collecting background air quality and visibility data. A balloon-borne upper air sounding system was used to monitor temporal changes in convective boundary layer structure. Dual tracer experiments were conducted on four occasions in the shallow Corral Gulch near tract C-a using non-depositing $SF_6$ gas and depositing lithium-traced particles collected on two to five sampling arcs during well-defined drainage flow events.

17. KEY WORDS AND DOCUMENT ANALYSIS

| a. DESCRIPTORS | b. IDENTIFIERS/OPEN ENDED TERMS | c. COSATI Field/Group |
|---|---|---|
| | | |

| | | |
|---|---|---|
| 18. DISTRIBUTION STATEMENT<br>RELEASE TO PUBLIC | 19. SECURITY CLASS *(This Report)*<br>UNCLASSIFIED | 21. NO. OF PAGES<br>172 |
| | 20. SECURITY CLASS *(This page)*<br>UNCLASSIFIED | 22. PRICE |

EPA Form 2220-1 (9-73)

## NOTICE

Mention of trade names or commercial products does not consititute endorsement or recommendation for use.

BEGIN FIRST LINE OF TEXT HERE
CENTER OF PAGE
TOP OF IMAGE AREA
DROPPED HEAD: BEGIN SECTIONS HERE

# ABSTRACT

Special meteorological and air quality studies were conducted during August 1980 in the Piceance Creek Basin oil shale resource area of Northwestern Colorado by the Pacific Northwest Laboratory, operated for the U.S. Department of Energy by Battelle Memorial Institute. The objective of the limited field program was to collect initial data to aid in the development, calibration, and validation of a mesoscale air quality model. The specific goals of the program were to investigate the growth and characteristics of convective boundary layers that form over the area during the daytime, to characterize background pollutant levels, visibility, and atmospheric structure over the area, and to investigate, by means of tracer experiments, the dispersion and dry deposition of pollutants released in nocturnal valley drainage flows.

An instrumented DC-3 aircraft was the primary means of collecting background air quality and visibility data. It also was used to determine spatial variations in atmospheric structure over the Piceance Basin. A balloon-borne upper air sounding system was used to monitor temporal changes in convective boundary layer structure. The sondes, measuring atmospheric temperature, humidity, and winds, were released from a point near federal oil shale tract C-a, from which supporting solar and terrestrial radiation and soil temperature data were collected. Dual tracer experiments were conducted on four occasions in the shallow Corral Gulch near tract C-a using non-depositing $SF_6$ gas and depositing lithium-traced particles collected on two to five sampling arcs during well-defined drainage flow events.

This report, which presents the data from these initial field experiments, is being submitted in partial fulfillment of the U.S. Environmental Protection Agency Interagency Agreement AD-89-F-097-0 with the U.S. Department of Energy. Interpretation and analysis of these data are separate tasks that will be presented in future reports under the Green River Ambient Model Assessment program. The objective of this program is to produce improved, site-specific air quality models for analyzing the environmental impacts from the anticipated development of the Green River Oil Shale Formation.

BEGIN LAST LINE OF TEXT
BOTTOM OF IMAGE AREA; OUTSIDE DIMENSION FOR TABLES AND ILLUSTRATIONS

PAGE NUMBER
EPA Form 2350-4 (4-80)
(PREVIOUSLY CIN. EPA FORM 287)
☆ U.S. GOVERNMENT PRINTING OFFICE 1980-660-639
TYPING GUIDE SHEET

## CONTENTS

ABSTRACT . . . iii

FIGURES . . . vii

TABLES . . . xiv

ACKNOWLEDGEMENTS . . . xvi

1.0 INTRODUCTION . . . 1

2.0 EXPERIMENTAL DESIGN . . . 3

    2.1 Location . . . 4

    2.2 Synoptic Situation . . . 7

    2.3 Instrumentation . . . 13

        2.3.1 Mobile Van Instrumentation . . . 13

        2.3.2 Aircraft Instrumentation . . . 15

        2.3.3 Tracer Instrumentation . . . 18

3.0 DATA SUMMARY . . . 26

    3.1 Surface and Background Meteorological Measurements . . . 26

        3.1.1 Grand Junction, Colorado Upper Air Data . . . 26

        3.1.2 Balloon-Borne Sonde Data . . . 27

        3.1.3 Solar and Terrestrial Radiation Data . . . 34

        3.1.4 Soil Temperature Data . . . 37

    3.2 Aircraft Measurements . . . 37

        3.2.1 Temperature and Wind Profiles . . . 39

        3.2.2 Ozone Profiles and $SO_2$ Concentrations . . . 39

        3.2.3 Aerosol Light Scattering and Aitken Nuclei Profiles . . . 47

        3.2.4 Aerosol Physical and Chemical Properties . . . 47

        3.2.5 Solar and Ultraviolet Radiation . . . 55

3.3 Tracer Experiment Measurements . . . . . . . . . . . . . . . . . . 55

  3.3.1 Run 1, August 5 to 6 . . . . . . . . . . . . . . . . . 59

  3.3.2 Run 2, August 7 to 8 . . . . . . . . . . . . . . . . . 63

  3.3.3 Run 3, August 9 to 10 . . . . . . . . . . . . . . . . 71

  3.3.4 Run 4, August 11 to 12 . . . . . . . . . . . . . . . . 71

4.0 RECOMMENDATIONS . . . . . . . . . . . . . . . . . . . . . . . . 79

REFERENCES . . . . . . . . . . . . . . . . . . . . . . . . . . . . 80

APPENDIX A - INDIVIDUAL AIRSONDE PLOTS . . . . . . . . . . . . . . . . 81

APPENDIX B - COMPOSITE AIRSONDE SOUNDINGS . . . . . . . . . . . . . . . 115

APPENDIX C - AIRSONDE SUBPOINT TRAJECTORIES . . . . . . . . . . . . . . 125

APPENDIX D - SOLAR AND TERRESTRIAL RADIATION AND SOIL TEMPERATURE DATA . . . . . . . . . . . . . . . . . . . 139

APPENDIX E - AIRCRAFT-MEASURED PROFILES OF AIR QUALITY . . . . . . . . . 147

# FIGURES

Number | Page

1. Map of the Green River Oil Shale Formation Showing the Major Rivers and Towns of the Area . . . . . . . . . . . . . . . . 5

2. Map of the Piceance Basin of Colorado Showing the Primary Physical Features of the Region. The Dot Near Oil Shale Tract C-a is the Location of the Experimental Site. Circles Marked A and B Show the Locations From Which the Photographs in Figures 3 and 4 Were Taken . . . . . . . . . . . . 6

3. Aerial Photograph of the Cathedral Bluffs Southwest of the Experimental Area as Taken From Location A in Figure 2. . . . 8

4. Aerial Photograph of the Topography Within the Piceance Basin as Taken From Location B in Figure 2 . . . . . . . . . . . 9

5. Photograph of the Piceance Creek Valley, Looking Down-Valley From the Road Leading to Tract C-a . . . . . . . . . . . . 10

6. Topographic Map of the Experimental Area Near Tract C-a, Showing the Locations of Tracer Release and Sampling Sites. Tract C-a's Visitor's Center and Meteorological Site 3 (MET-3) are Indicated. The Contour Interval is 20 feet . . . . . . . . 11

7. Photograph Looking Down Corral Gulch From the Valley Sidewall North of Tract C-a's Visitor's Center. Meteorological Site 3 and the Battelle Mobile Van are on the Valley Floor in the Center of the Picture . . . . . . . . . . . . . . . . . . . 12

8. Lithium-Traced Particle Generation Equipment . . . . . . . . . . 21

9. Real-Time Sampling Station at Meteorological Site 3 . . . . . . . 22

10. Radio-Controlled $SF_6$ Bag Sampling Station. Air Samples at This Sequential Sampling Station are Drawn Through Tubes Located at the 1.7-m Level . . . . . . . . . . . . . . . . . . . 25

11. Example of Airsonde Data Plot, Corral Creek, Colorado, August 5, 1980 . . . . . . . . . . . . . . . . . . . . . . . . 32

12. Example of Potential Temperature Composite Profiles, Corral Creek, Colorado, August 11, 1980 . . . . . . . . . . . . 35

13. Atmospheric Radiation Measurements Taken at Corral Creek, Colorado, August 11, 1980. $K_{ext}$ is Extraterrestrial Solar Radiation, $K\downarrow$ is Incoming Solar Radiation, $K\uparrow$ is Outgoing Solar Radiation, $Q^*$ is Net Radiation, and D is Diffuse Solar Radiation . . . . . . . . . . . . . . . . . . . . . . . . 36

14. Soil Temperature Measurements Taken at Corral Creek, Colorado, August 11, 1980 . . . . . . . . . . . . . . . . . . . . . . . . . . 38

15. Aircraft-Measured Temperature Profiles, August 5, 1980, 1228 to 1346 MDT. The Dry Adiabatic Lapse Rate ($\Gamma_d$) is Given For Reference . . . . . . . . . . . . . . . . . . . . . . . 40

16. Aircraft-Measured Temperature Profiles, August 8, 1980, 2102 to 2357 MDT . . . . . . . . . . . . . . . . . . . . . . . 41

17. Aircraft-Measured Temperature Profiles, August 9, 1980, 0832 to 1040 MDT . . . . . . . . . . . . . . . . . . . . . . . 42

18. Aircraft-Measured Temperature Profiles, August 9, 1980, 1040 to 1759 MDT . . . . . . . . . . . . . . . . . . . . . . . 43

19. Aircraft-Measured Temperature Profiles, August 14, 1980, 0528 to 0655 MDT . . . . . . . . . . . . . . . . . . . . . . . 44

20. Aircraft-Measured Temperature Profiles, August 14, 1980, 0713 to 0828 MDT . . . . . . . . . . . . . . . . . . . . . . . 45

21. Envelopes of Vertical Profiles of Ozone Concentrations, Light Scattering Coefficients ($b_{scat}$), and Condensation Nuclei Concentrations (CNC) for Aircraft Flights of August 5 and August 8, 1980. Rayleigh Scattering Coefficients for Clean Air are Plotted for Reference . . . . . . 48

22. Envelopes of Vertical Profiles of Ozone Concentrations, Light Scattering Coefficients ($b_{scat}$), and Condensation Nuclei Concentrations (CNC) for Aircraft Flights of August 9 and August 14, 1980 . . . . . . . . . . . . . . . . . 49

23. Average Particle Size Distributions Obtained From Four Aircraft Flights in August, 1980 . . . . . . . . . . . . . . . . . . . 50

24. Particle Size Distributions Obtained From Aircraft on August 8, 1980, 2135 to 2357 MDT . . . . . . . . . . . . . . . . 51

25. Particle Size Distributions Obtained From Aircraft on August 9, 1980, 0842 to 1114 MDT . . . . . . . . . . . . . . . . 52

26. Particle Size Distributions Obtained From Aircraft on August 9, 1980, 1114 to 1759 MDT . . . . . . . . . . . . . . . . 53

27. Particle Size Distributions Obtained From Aircraft on August 14, 1980, 0545 to 0831 MDT . . . . . . . . . . . . . . . 54

28. Airborne Tracer Particle and $SF_6$ Concentrations as a Function of Time, Night of August 5 to 6, 1980 . . . . . . . . . 62

29. $SF_6$ Concentrations at 1.7-m as a Function of Cross Valley Position on Sampling Line 1 for Three Sampling Time Intervals, Night of August 5 to 6, 1980 . . . . . . . . . 64

30. $SF_6$ Concentrations at Three Heights as a Function of Cross Valley Position on Sampling Line 2, Night of August 5 to 6, 1980 . . . . . . . . . . . . . . . . . . . . . . 65

31. $SF_6$ Concentrations at Three Heights as a Function of Cross Valley Position on Sampling Line 4, Night of August 5 to 6, 1980 . . . . . . . . . . . . . . . . . . . . . . 66

32. $SF_6$ Concentrations as a Function of Time, Night of August 7 to 8, 1980 . . . . . . . . . . . . . . . . . . . . . . 67

33. $SF_6$ Concentrations at 1.7-m as a Function of Cross Valley Position on Sampling Line 1 for Three Sampling Time Intervals, Night of August 7 to 8, 1980 . . . . . . . . . . 68

34. $SF_6$ Concentrations at Three Heights as a Function of Cross Valley Position on Sampling Line 2, Night of August 7 to 8, 1980 . . . . . . . . . . . . . . . . . . . . . . 69

35. $SF_6$ Concentrations as a Function of Cross Valley Position as Determined From Four Mobile Traverses With Syringe Samplers, Night of August 7 to 8, 1980 . . . . . . 70

36. Airborne Tracer Particle and $SF_6$ Concentrations as a Function of Time, Night of August 9 to 10, 1980 . . . . . . . . . 72

37. $SF_6$ Concentrations at Three Heights as a Function of Cross Valley Position on Sampling Line 2, Night of August 9 to 10, 1980 . . . . . . . . . . . . . . . . . . . . . . 73

38. $SF_6$ Concentrations at 1.7-m as a Function of Cross Valley Position on Sampling Line 3, Night of August 9 to 10, 1980 . . . . . . . . . . . . . . . . . . . . . . 74

39. $SF_6$ Concentrations at Three Heights as a Function of Cross Valley Position on Sampling Line 4, Night of August 9 to 10, 1980 . . . . . . . . . . . . . . . . . . . . . . 75

40. $SF_6$ Concentrations as a Function of Cross Valley Position as Determined From Four Mobile Traverses With Syringe Samplers, Night of August 9 to 10, 1980 . . . . . . . . . 76

41. Airborne Tracer Particle and $SF_6$ Concentrations as a Function of Time, Night of August 11 to 12, 1980 . . . . . . . . 77

42. SF Concentrations as a Function of Cross Valley Position as Determined From Three Mobile Traverses With Syringe Samplers, Night of August 11 to 12, 1980 . . . . . . 78

43. Airsonde Sounding #1, 1158 MDT, August 5, 1980 . . . . . . . . . . 82

44. Airsonde Sounding #2, 1503 MDT, August 5, 1980 . . . . . . . . . . 83

45. Airsonde Sounding #3, 1542 MDT, August 5, 1980 . . . . . . . . . . 84

46. Airsonde Sounding #4, 1855 MDT, August 5, 1980 . . . . . . . . . . 85

47. Airsonde Sounding #5, 1231 MDT, August 7, 1980 . . . . . . . . . . 86

48. Airsonde Sounding #6, 1510 MDT, August 7, 1980 . . . . . . . . . . 87

49. Airsonde Sounding #7, 0912 MDT, August 8, 1980 . . . . . . . . . . 88

50. Airsonde Sounding #8, 1201 MDT, August 8, 1980 . . . . . . . . . . 89

51. Airsonde Sounding #9, 1455 MDT, August 8, 1980 . . . . . . . . . . 90

52. Airsonde Sounding #10, 0837 MDT, August 9, 1980 . . . . . . . . . 91

53. Airsonde Sounding #11, 1152 MDT, August 9, 1980 . . . . . . . . . 92

54. Airsonde Sounding #12, 1720 MDT, August 9, 1980 . . . . . . . . . 93

55. Airsonde Sounding #13, 1943 MDT, August 9, 1980 . . . . . . . . . 94

56. Airsonde Sounding #14, 2200 MDT, August 9, 1980 . . . . . . . . . 95

57. Airsonde Sounding #15, 0618 MDT, August 10, 1980 . . . . . . . . . 96

58. Airsonde Sounding #16, 0734 MDT, August 10, 1980 . . . . . . . . . 97

59. Airsonde Sounding #17, 0859 MDT, August 10, 1980 . . . . . . . . . 98

60. Airsonde Sounding #18, 1125 MDT, August 10, 1980 . . . . . . . . . 99

61. Airsonde Sounding #19, 1411 MDT, August 10, 1980 . . . . . . . . . 100

62. Airsonde Sounding #20, 0823 MDT, August 11, 1980 . . . . . . . . . 101

63. Airsonde Sounding #21, 1150 MDT, August 11, 1980 . . . . . . . . . 102

64. Airsonde Sounding #22, 1453 MDT, August 11, 1980 . . . . . . . . . 103
65. Airsonde Sounding #23, 1744 MDT, August 11, 1980 . . . . . . . . . 104
66. Airsonde Sounding #24, 0911 MDT, August 12, 1980 . . . . . . . . . 105
67. Airsonde Sounding #25, 1207 MDT, August 12, 1980 . . . . . . . . . 106
68. Airsonde Sounding #26, 1515 MDT, August 12, 1980 . . . . . . . . . 107
69. Airsonde Sounding #27, 0850 MDT, August 13, 1980 . . . . . . . . . 108
70. Airsonde Sounding #28, 1146 MDT, August 13, 1980 . . . . . . . . . 109
71. Airsonde Sounding #29, 1430 MDT, August 13, 1980 . . . . . . . . . 110
72. Airsonde Sounding #30, 1450 MDT, August 13, 1980 . . . . . . . . . 111
73. Airsonde Sounding #31, 0835 MDT, August 14, 1980 . . . . . . . . . 112
74. Airsonde Sounding #32, 1140 MDT, August 14, 1980 . . . . . . . . . 113
75. Airsonde Sounding #33, 1349 MDT, August 14, 1980 . . . . . . . . . 114
76. Composite Airsonde Profiles, August 5, 1980 . . . . . . . . . . . 116
77. Composite Airsonde Profiles, August 7, 1980 . . . . . . . . . . . 117
78. Composite Airsonde Profiles, August 8, 1980 . . . . . . . . . . . 118
79. Composite Airsonde Profiles, August 9, 1980 . . . . . . . . . . . 119
80. Composite Airsonde Profiles, August 10, 1980 . . . . . . . . . . . 120
81. Composite Airsonde Profiles, August 11, 1980 . . . . . . . . . . . 121
82. Composite Airsonde Profiles, August 12, 1980 . . . . . . . . . . . 122
83. Composite Airsonde Profiles, August 13, 1980 . . . . . . . . . . . 123
84. Composite Airsonde Profiles, August 14, 1980 . . . . . . . . . . . 124
85. Airsonde #1 Subpoint Trajectory, 1158 MDT, August 5, 1980 . . . . . . . . . . . . . . . . . . . . . . . . 126
86. Airsonde #2 Subpoint Trajectory, 1503 MDT, August 5, 1980 . . . . . . . . . . . . . . . . . . . . . . . . 126
87. Airsonde #3 Subpoint Trajectory, 1542 MDT, August 5, 1980 . . . . . . . . . . . . . . . . . . . . . . . . 127

88. Airsonde #5 Subpoint Trajectory, 1231 MDT, August 7, 1980 . . . . . . . . . . . . . . . . . . . . . . . . 128

89. Airsonde #6 Subpoint Trajectory, 1510 MDT, August 7, 1980 . . . . . . . . . . . . . . . . . . . . . . . . 128

90. Airsonde #7 Subpoint Trajectory, 0912 MDT, August 8, 1980 . . . . . . . . . . . . . . . . . . . . . . . . 129

91. Airsonde #8 Subpoint Trajectory, 1201 MDT, August 8, 1980 . . . . . . . . . . . . . . . . . . . . . . . . 129

92. Airsonde #9 Subpoint Trajectory, 1455 MDT, August 8, 1980 . . . . . . . . . . . . . . . . . . . . . . . . 130

93. Airsonde #10 Subpoint Trajectory, 0837 MDT, August 9, 1980 . . . . . . . . . . . . . . . . . . . . . . . . 130

94. Airsonde #11 Subpoint Trajectory, 1152 MDT, August 9, 1980 . . . . . . . . . . . . . . . . . . . . . . . . 131

95. Airsonde #20 Subpoint Trajectory, 0823 MDT, August 11, 1980 . . . . . . . . . . . . . . . . . . . . . . . . 132

96. Airsonde #21 Subpoint Trajectory, 1150 MDT, August 11, 1980 . . . . . . . . . . . . . . . . . . . . . . . . 132

97. Airsonde #22 Subpoint Trajectory, 1453 MDT, August 11, 1980 . . . . . . . . . . . . . . . . . . . . . . . . 133

98. Airsonde #23 Subpoint Trajectory, 1744 MDT, August 11, 1980 . . . . . . . . . . . . . . . . . . . . . . . . 133

99. Airsonde #24 Subpoint Trajectory, 0911 MDT, August 12, 1980 . . . . . . . . . . . . . . . . . . . . . . . . 134

100. Airsonde #25 Subpoint Trajectory, 1207 MDT, August 12, 1980 . . . . . . . . . . . . . . . . . . . . . . . . 134

101. Airsonde #26 Subpoint Trajectory, 1515 MDT, August 12, 1980 . . . . . . . . . . . . . . . . . . . . . . . . 135

102. Airsonde #27 Subpoint Trajectory, 0850 MDT, August 13, 1980 . . . . . . . . . . . . . . . . . . . . . . . . 135

103. Airsonde #28 Subpoint Trajectory, 1146 MDT, August 13, 1980 . . . . . . . . . . . . . . . . . . . . . . . . 136

104. Airsonde #29 Subpoint Trajectory, 1430 MDT, August 13, 1980 . . . . . . . . . . . . . . . . . . . . . . . . 136

105. Airsonde #30 Subpoint Trajectory, 1450 MDT, August 13, 1980 . . . . . . . . . . . . . . . . . . . . . . 137

106. Airsonde #31 Subpoint Trajectory, 0835 MDT, August 14, 1980 . . . . . . . . . . . . . . . . . . . . . . 137

107. Airsonde #32 Subpoint Trajectory, 1140 MDT, August 14, 1980 . . . . . . . . . . . . . . . . . . . . . . 138

108. Airsonde #33 Subpoint Trajectory, 1349 MDT, August 14, 1980 . . . . . . . . . . . . . . . . . . . . . . 138

109. Vertical Profiles of Ozone Concentration, Light Scattering Coefficient, and Condensation Nuclei Concentration for Aircraft Flights of August 5, 1980. Rayleigh Scattering Coefficients for Clean Air are Plotted for Reference . . . . . . . . . . 148

110. Vertical Profiles of Ozone Concentration, Light Scattering Coefficient, and Condensation Nuclei Concentration for Aircraft Flights of August 8, 1980 . . . . 149

111. Vertical Profiles of Ozone Concentration, Light Scattering Coefficient, and Condensation Nuclei Concentration for Aircraft Flights of August 9, 1980 . . . . 150

112. Vertical Profiles of Ozone Concentration, Light Scattering Coefficient, and Condensation Nuclei Concentration for Aircraft Flights of August 9, 1980 . . . . 151

113. Vertical Profiles of Ozone Concentration, Light Scattering Coefficient, and Condensation Nuclei Concentration for Aircraft Flights of August 14, 1980, 0528 - 0655 MDT . . . . . . . . . . . . . . . . . . . . . . 152

114. Vertical Profiles of Ozone Concentration, Light Scattering Coefficient, and Condensation Nuclei Concentration for Aircraft Flights of August 14, 1980, 0713 - 0837 MDT . . . . . . . . . . . . . . . . . . . . . . 153

## TABLES

Number Page

1. Specifications of Airsonde Data Collection System . . . . . . . . . 15
2. Radiation and Soil Temperature Sensors . . . . . . . . . . . . . . 15
3. Summary of Aircraft Flight Patterns and Locations . . . . . . . . . 17
4. Aircraft Instrumentation . . . . . . . . . . . . . . . . . . . . . 19
5. Grand Junction, Colorado Winds (deg, m $\sec^{-1}$) . . . . . . . . . . . . 28
6. Grand Junction, Colorado Temperatures (°C) and Potential Temperatures (°K) . . . . . . . . . . . . . . . . . . . . 29
7. Summary of Corral Creek Upper Air Soundings . . . . . . . . . . . . . 30
8. Aircraft-Measured Winds From Selected Constant-Altitude, Straight-Line Flight Legs . . . . . . . . . . . . . . . . . . 46
9. Particulate Elemental Composition as Determined by X-Ray Fluorescence Analysis of Filter Samples . . . . . . . . . . 56
10. Ionic Composition of Atmospheric Particulates Derived From Aircraft Filter Samples by Ion Chromatography . . . . . . . . . . . . . . . . . . . . . . . . 57
11. Ratio of Elemental Composition Results From X-Ray Fluorescence Analysis and Neutron Activation For Four Filter Samples . . . . . . . . . . . . . . . . . . . . . . . 57
12. Solar and Ultraviolet Radiation Over the Oil Shale Area During August 1980 . . . . . . . . . . . . . . . . . . 58
13. Summary of Tracer Releases . . . . . . . . . . . . . . . . . . . . 60
14. Figure Listing for Tracer Data . . . . . . . . . . . . . . . . . . 61
15. Radiation and Soil Temperature Data, Corral Creek, Colorado, August 8, 1980 . . . . . . . . . . . . . . . . . . . . . 140
16. Radiation and Soil Temperature Data, Corral Creek, Colorado, August 9, 1980 . . . . . . . . . . . . . . . . . . . . . 141
17. Radiation and Soil Temperature Data, Corral Creek, Colorado, August 10, 1980 . . . . . . . . . . . . . . . . . . . . 142
18. Radiation and Soil Temperature Data, Corral Creek, Colorado, August 11, 1980 . . . . . . . . . . . . . . . . . . . . 143

19. Radiation and Soil Temperature Data, Corral Creek, Colorado, August 12, 1980 . . . . . . . . . . . . . . . . . . . . . 144

20. Radiation and Soil Temperature Data, Corral Creek, Colorado, August 13, 1980 . . . . . . . . . . . . . . . . . . . . . 145

21. Radiation and Soil Temperature Data, Corral Creek, Colorado, August 14, 1980 . . . . . . . . . . . . . . . . . . . . . 146

# ACKNOWLEDGEMENTS

The work presented in this report includes contributions from many individuals. Battelle contributors include:

O.B. Abbey
E.G. Chapman
W.E. Davis
R.L. Drake
R.C. Easter
R.V. Hannigan
T.R. Heimbigner
W.H. Hodgson
F.D. Lloyd
M.M. Orgill

Dr. Jack Clark and Dr. Gary Bertolin of the Rio Blanco Oil Shale Company, a partnership of the Gulf Oil Corporation and Standard Oil of Indiana, arranged for important field support at the measurement sites near federal oil shale lease tract C-a.

Dr. Dan Golomb of the Office of Research and Development, Mr. Frank Schiermeier of the Terrain Effects Branch of the Environmental Sciences Research Laboratory and Mr. Terry Thoem and Mr. Richard Fisher of Region VIII, U.S. Environmental Protection Agency; and Dr. David Ballantine of the U.S. Department of Energy provided essential aid in obtaining funds for the field experiments.

Dr. Sumner Barr and Dr. Bill Clements of Los Alamos National Laboratory, among others at that laboratory, made initial field arrangements and provided an important cooperative spirit that resulted in a successful joint field effort for participants of all the field programs.

Computer programs used to process atmospheric sounding data were developed under National Science Foundation support while one of the authors (C.D. Whiteman) was at Colorado State University.

The work reported here, except for the tracer experiment, was supported by the U.S. Environmental Protection Agency Interagency Agreement

TYPING GUIDE SHEET
BEGIN FIRST LINE OF TEXT HERE
CENTER OF PAGE
TOP OF IMAGE AREA
DROPPED HEAD; BEGIN SECTIONS HERE
6-1/2"
9-1/8"
BEGIN LAST LINE OF TEXT
BOTTOM OF IMAGE AREA; OUTSIDE DIMENSION FOR TABLES AND ILLUSTRATIONS
3/8"
PAGE NUMBER

AD-89-F-0-097-0 with the U.S. Department of Energy. The tracer experiment was supported entirely by the U.S. Department of Energy under contract DE-AC06-76RLO-1830. Dr. George A. Sehmel was the Principal Investigator for the tracer experiment.

EPA-287 (Cin.)
(4-76)

# 1.0 INTRODUCTION

A special meteorological measurement program was conducted in the complex terrain of the Piceance Basin of Northwestern Colorado during August, 1980. The program was performed by the Pacific Northwest Laboratory (PNL), operated for the Department of Energy by Battelle Memorial Institute. The objective of the program was the collection of data to aid in the design, calibration, and validation of a mesoscale air quality model that is being developed at PNL. The specific goals of the 2-week field program were:

- to investigate the growth and characteristics of convective boundary layers (CBLs) or mixing layers that form over the oil shale region during the daytime,
- to characterize background pollutant levels, atmospheric visibility, and atmospheric structure over the region, and
- to investigate, by means of a dual tracer experiment using a particulate and a gaseous tracer, the dispersion and deposition of pollutants released into well-developed, nocturnal, valley drainage flows.

In the early planning stages of the experimental program it was clearly recognized that a single 2-week program would be insufficient to fully characterize the meteorological phenomena investigated. It was expected, however, that the initial experimental design and results of the experiments would lead to improved experimental designs and refined physical hypotheses that could be tested further in future experiments.

The purpose of this report is to present the processed data obtained in the initial field program in a basic form that will allow its use by other investigators and will facilitate a scientific interchange of ideas that may lead to progress in understanding the meteorology and air quality of this complicated terrain region. Data analysis will be reported in separate documents.

While this report concerns meteorological observations collected in support of a model development program called, "The Green River Ambient Model Assessment Program," it is important to point out that the field experiments were conducted jointly with other investigators who performed related work in the oil shale region during the same experimental period. By combining forces with other investigators, it was possible to effect cost savings and, at the same time, obtain a larger data set for use by all investigators. The field program described in this report was conducted cooperatively with investigators from the University of California's Los Alamos National Laboratory, who, under U.S. Department of Energy and Environmental Protection Agency sponsorship, investigated the transport and diffusion of $SF_6$ tracer material in the nocturnal drainage flows of Corral Gulch near the federal oil shale lease tract C-a. Their work included upper air and tethered balloon profiles taken to characterize atmospheric conditions during the tracer experiments, and the operation of an acoustic sounder and surface meteorological stations. The meteorological and tracer data collected in their investigations has been published in a separate report (Clements et al. 1981). Additionally, meteorological and air quality data were being collected routinely on oil shale tract C-a by the Rio Blanco Oil Shale Company (RBOSC). These data, collected by RBOSC as one of the conditions of its lease of the federal tract, were processed and transmitted to the U.S. Geological Service's Conservation Division, Oil Shale Office in Grand Junction, Colorado and are available from the Oil Shale Office in a processed form, or are available in a summarized form in RBOSC's annual report (RBOSC 1981).

## 2.0 EXPERIMENTAL DESIGN

### CONVECTIVE BOUNDARY LAYER EXPERIMENT

The convective boundary layer (CBL) experiments were designed to allow frequent soundings through the entire depth of the CBL, or mixed layer, so that its height, temperature structure, and wind structure could be determined as a function of time during the day. This was accomplished primarily by balloon-borne sondes released from a point on the ground within the Piceance Basin. Soundings were released at approximately 3-hour intervals from sunrise until late afternoon. Release times were coordinated, as much as possible, to allow comparison of Piceance Basin profiles with rawinsonde profiles over Grand Junction and with aircraft profiles over other parts of the Piceance Basin. Further characteristics of the convective boundary layer were determined from aircraft soundings made within the CBL, including observations of temperature, wind, and pollutant profiles with height, atmospheric aerosol characteristics within the layer, and visibility measurements.

### BACKGROUND AND AIR QUALITY EXPERIMENT

In addition to the supporting role that the aircraft was to play in the design of the convective boundary layer experiments, separate experiments were designed to make use of the aircraft as a platform from which to measure background pollutant concentrations in the oil shale region and to better define horizontal variations in atmospheric structure over the region during both daytime and nighttime flights. The special equipment aboard the aircraft and the flight plans and procedures used to obtain these data are discussed further in later sections of this report.

### TRACER EXPERIMENT

The tracer experiments were designed to answer basic scientific questions about the transport, diffusion, and deposition of pollutants introduced into a valley drainage flow. In these experiments two types of tracer materials were utilized. The first type was a gaseous $SF_6$ tracer released by the Los Alamos National Laboratory. The second type, a lithium-traced aerosol, was released by PNL so that comparisons could be made between gas and aerosol tracer concentrations to determine how diffusion and deposition will affect pollutant concentrations downwind of the pollutant sources. These experiments were designed to be conducted during the nighttime when the valley drainage flow had become well established and had attained a near-steady state. Tracers were released for an hour so that the transport velocities within the drainage flow would allow tracer to be carried through the length of the sampling station grid. Sampling stations were located along multiple lines perpendicular to the valley axis at various downwind distances from the source. The lines extended across the valley floor and up the valley sidewalls. Using this grid and the two tracer materials, the experiments allowed a determination of transport, diffusion, and aerosol deposition as a function of downwind distance from the tracer source.

The next sections describe the topographic location of the experiments, the synoptic weather patterns observed during the experimental period, and the instrumentation used in the field data collection programs.

## 2.1 Location

Experiments were conducted in the Piceance Creek Basin of Northwestern Colorado (Figure 1), one of several basins in Colorado, Utah, and Wyoming which are part of the Green River Oil Shale Formation. The Piceance Basin is a shallow basin which is inclined toward the north-northeast. The two major drainages in the basin, Piceance Creek and Yellow Creek, drain northward into the westward-flowing White River, a major tributary to the Green River and ultimately, to the Colorado River. The major topographical features of the region (Figure 2) include the Cathedral Bluffs--the steep cliffs forming the western rim of the basin, the Roan Plateau--the name given to the flat topped highlands on the south edge of the basin, and the Grand Hogback, a sharp ridge of resistant rock running from north to south making up the eastern boundary of the basin. The Rocky Mountains rise toward their crest east of the basin, but the terrain is quite complicated, consisting of various mountain subranges containing valleys of different size and orientation. Seventy kilometers east of the basin is the rugged

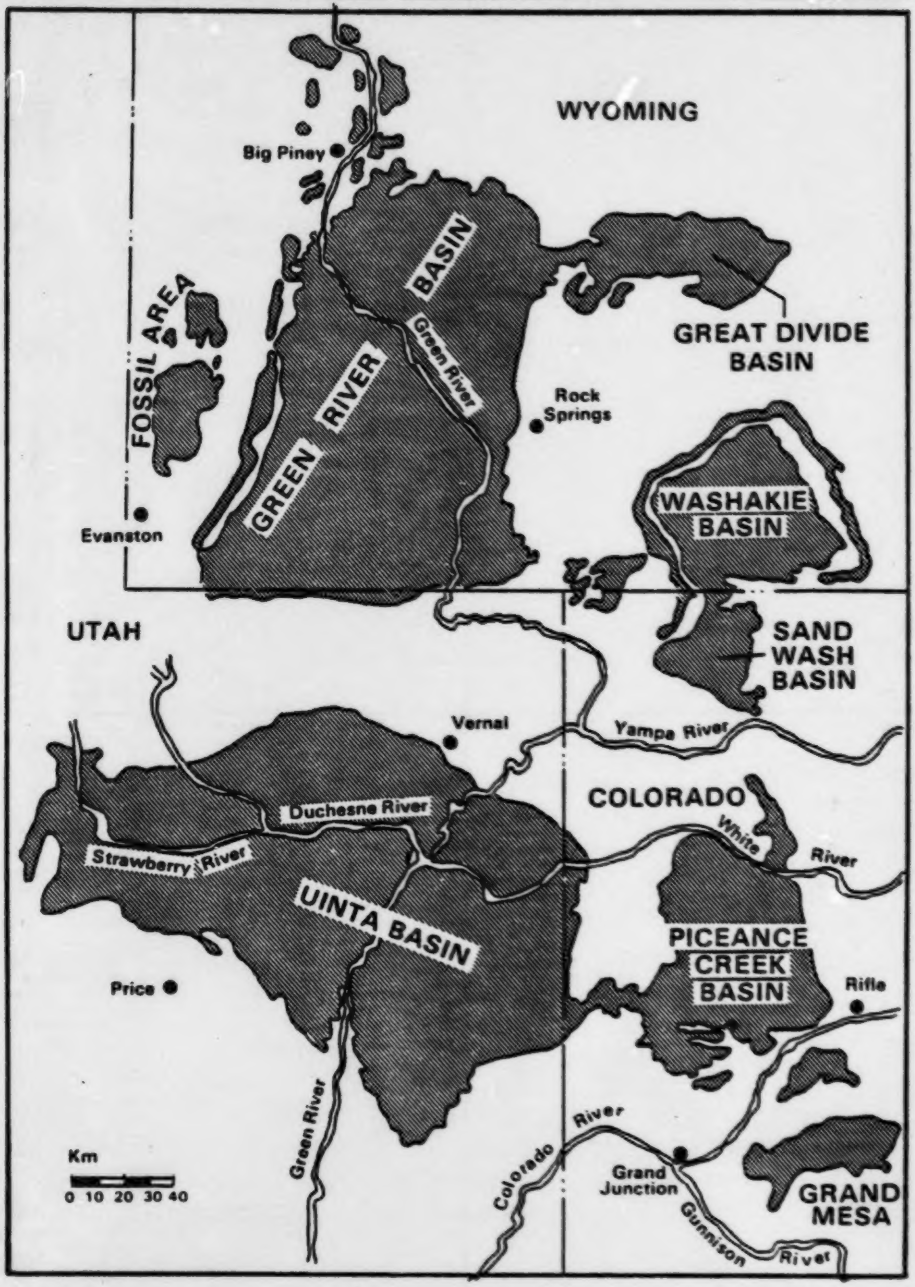

FIGURE 1. Map of the Green River Oil Shale Formation Showing the Major Rivers and Towns of the Area.

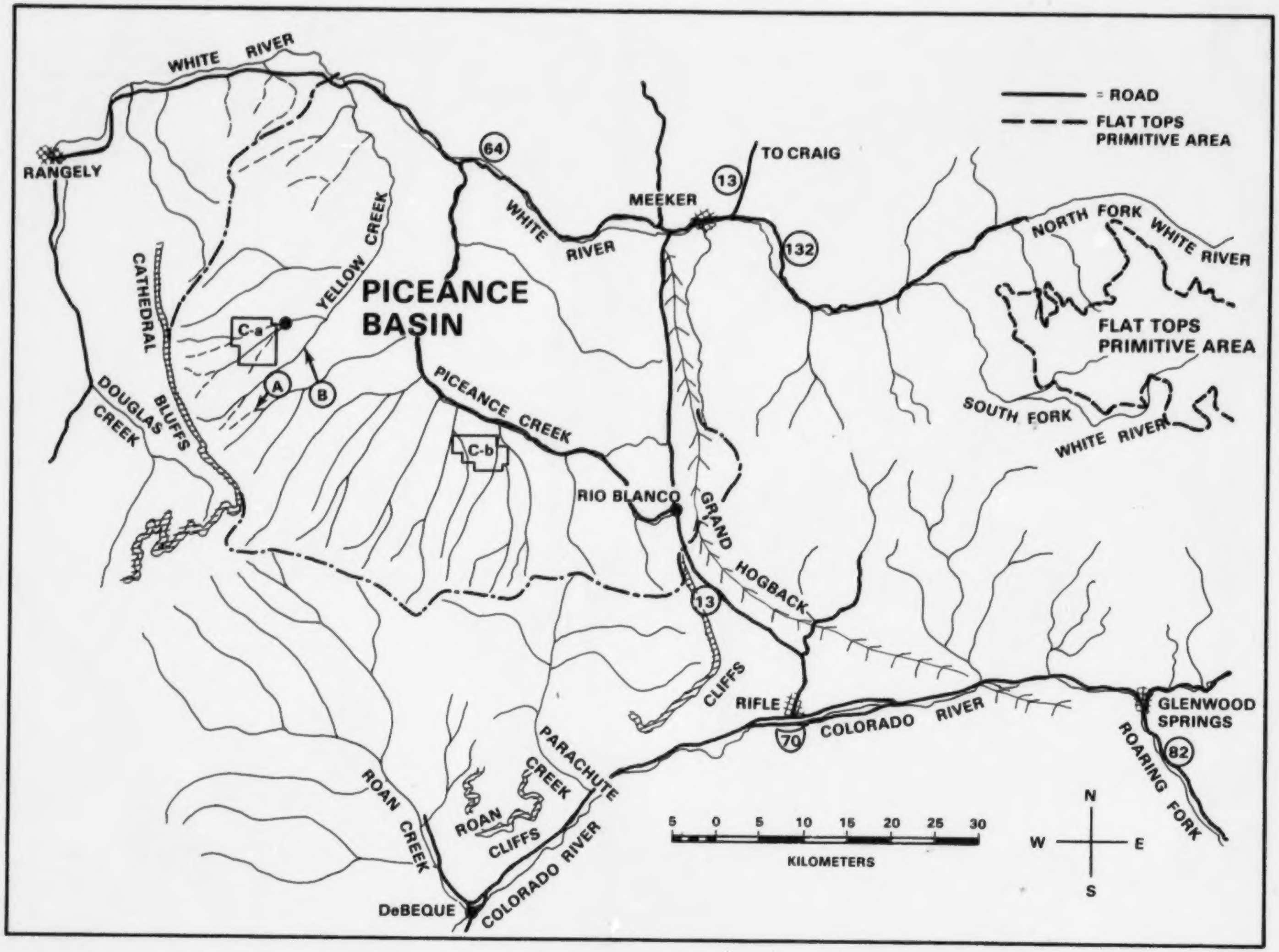

FIGURE 2. Map of the Piceance Basin of Colorado Showing the Primary Physical Features of the Region. The Dot Near Oil Shale Tract C-a is the Location of the Experimental Site. Circles Marked A and B Show the Locations From Which the Photographs in Figures 3 and 4 Were Taken.

Flat Tops Primitive Area, a Class I PSD air quality area that is situated predominantly on the relatively flat tops of an elevated plateau region.

Aerial photographs are presented as Figures 3 and 4 to give the reader a better feeling for the topography of the Piceance Basin. The points from which the photographs were taken are indicated on Figure 2. The parallel nature of the shallow linear valleys is clear in both photographs. The major valleys in the basin, Piceance Creek and Yellow Creek, are narrow, (0.3- to 0.6-km wide), flat-bottomed, valleys having steep sidewalls (Figure 5) and local relief of 50- to 150-m. The smaller tributaries, such as those shown in the foreground of Figure 3, are nearly v-shaped, but have about the same local relief as the major valleys.

Surface observations during the experiments were conducted from a mobile van located on Corral Gulch, a tributary to the Yellow Creek drainage, at Meteorological Site No. 3 (lat. 39° 55' 13" N, long. 108° 28' 14" W, elevation 2003-m) of the federal oil shale lease tract C-a (Figure 6). A photograph of Corral Gulch, taken from the south-facing sidewall WNW of the field site, is presented as Figure 7.

## 2.2 Experimental Weather Conditions

Warm, dry weather prevailed over northwest Colorado and the Corral Creek area during August 5 to 12, 1980. A weak cold front across Wyoming on August 5 and 6 edged into northern Colorado the afternoon of August 7. No significant weather was observed with this front in northwestern Colorado, but an increase in instability cloudiness was observed during the afternoons of August 8 and 9. Greatest convective activity occurred on August 9 with a light thundershower occurring at Corral Creek.

The afternoon convective activity decreased on August 10 and 11 as a surface high pressure cell moved eastward across and beyond Colorado. Several large thunderheads (cumulo-nimbus) were observed distant in the east, late on the 11th.

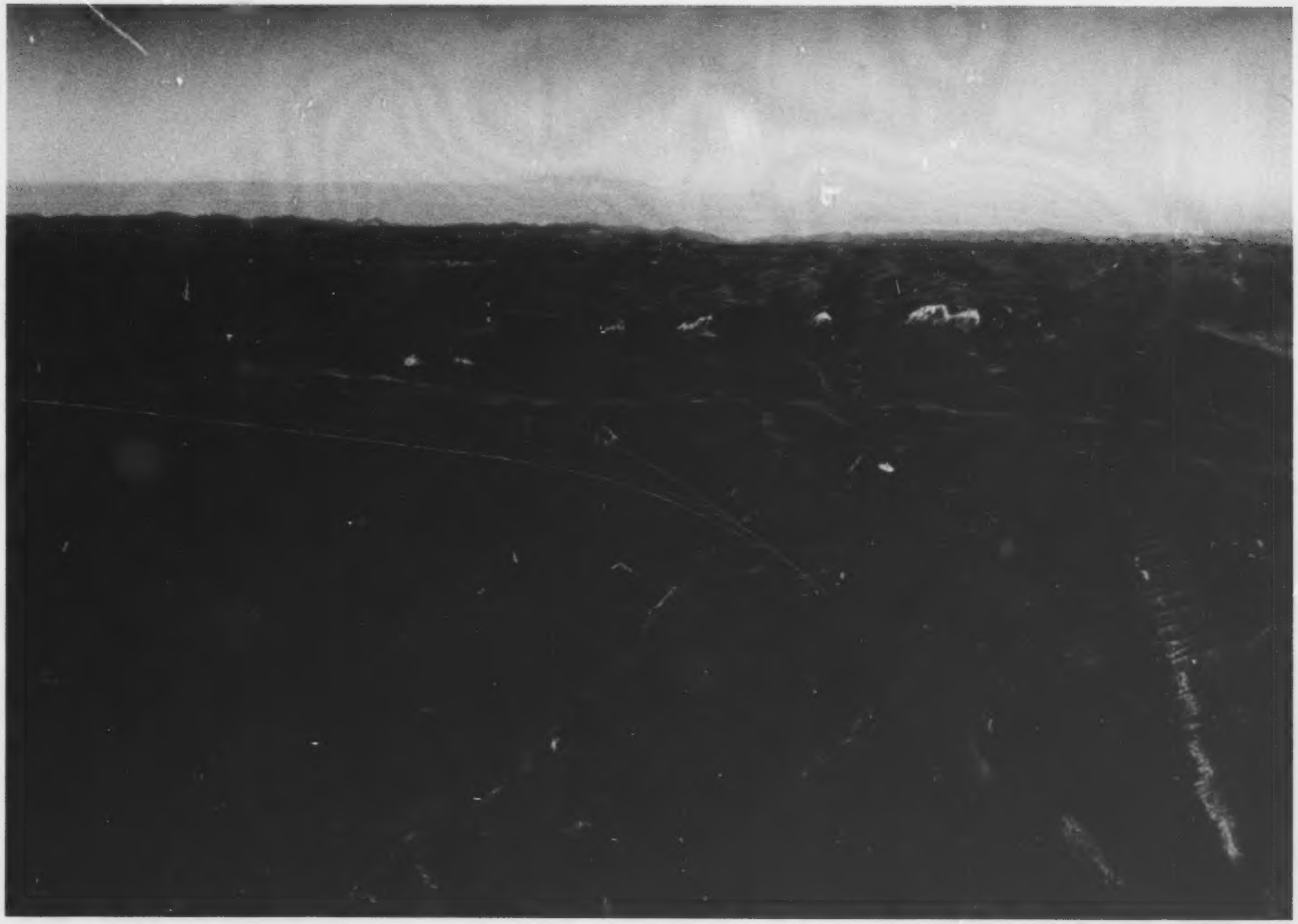

FIGURE 3. Aerial Photograph of the Cathedral Bluffs Southwest of the Experimental Area as Taken From Location A in Figure 2.

**FIGURE 4.** Aerial Photograph of the Topography Within the Piceance Basin as Taken From Location B in Figure 2.

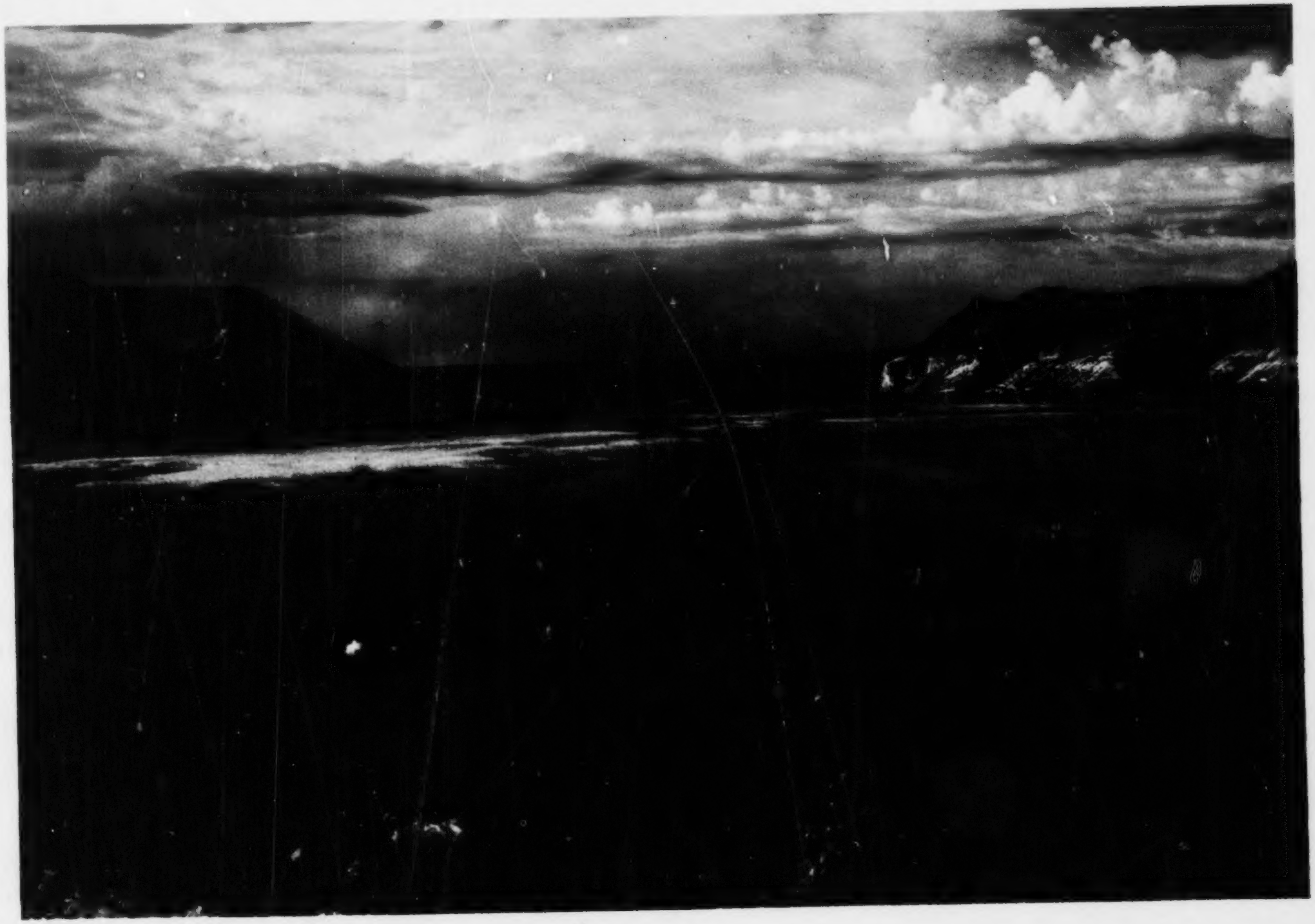

FIGURE 5. Photograph of the Piceance Creek Valley, Looking Down-Valley From the Road Leading to Tract C-a.

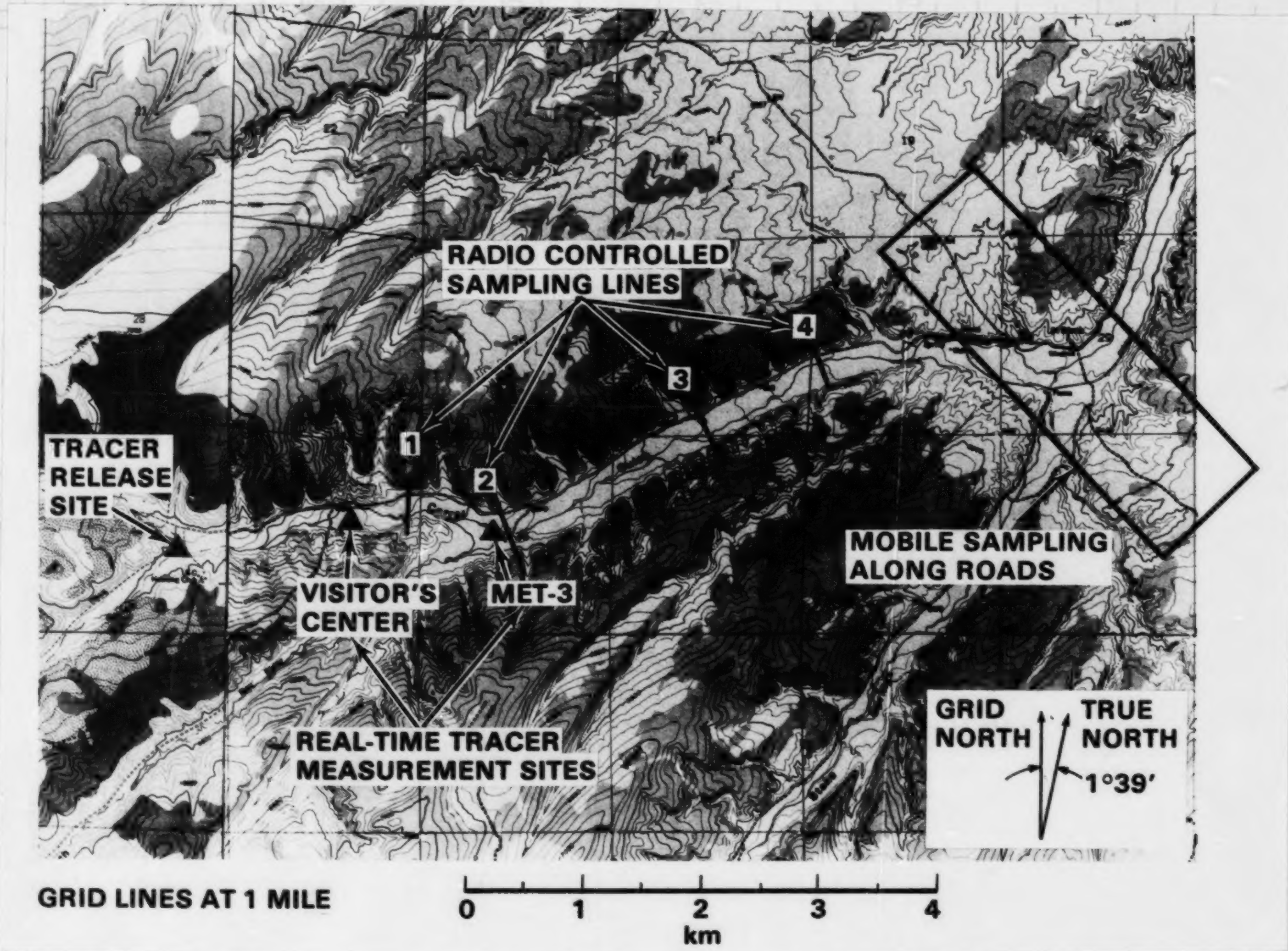

FIGURE 6. Topographic Map of the Experimental Area Near Tract C-a, Showing the Locations of Tracer Release and Sampling Sites. Tract C-a's Visitor's Center and Meteorological Site 3 (MET-3) are Indicated. The Contour Interval is 20 feet.

Neg. 80J402-16

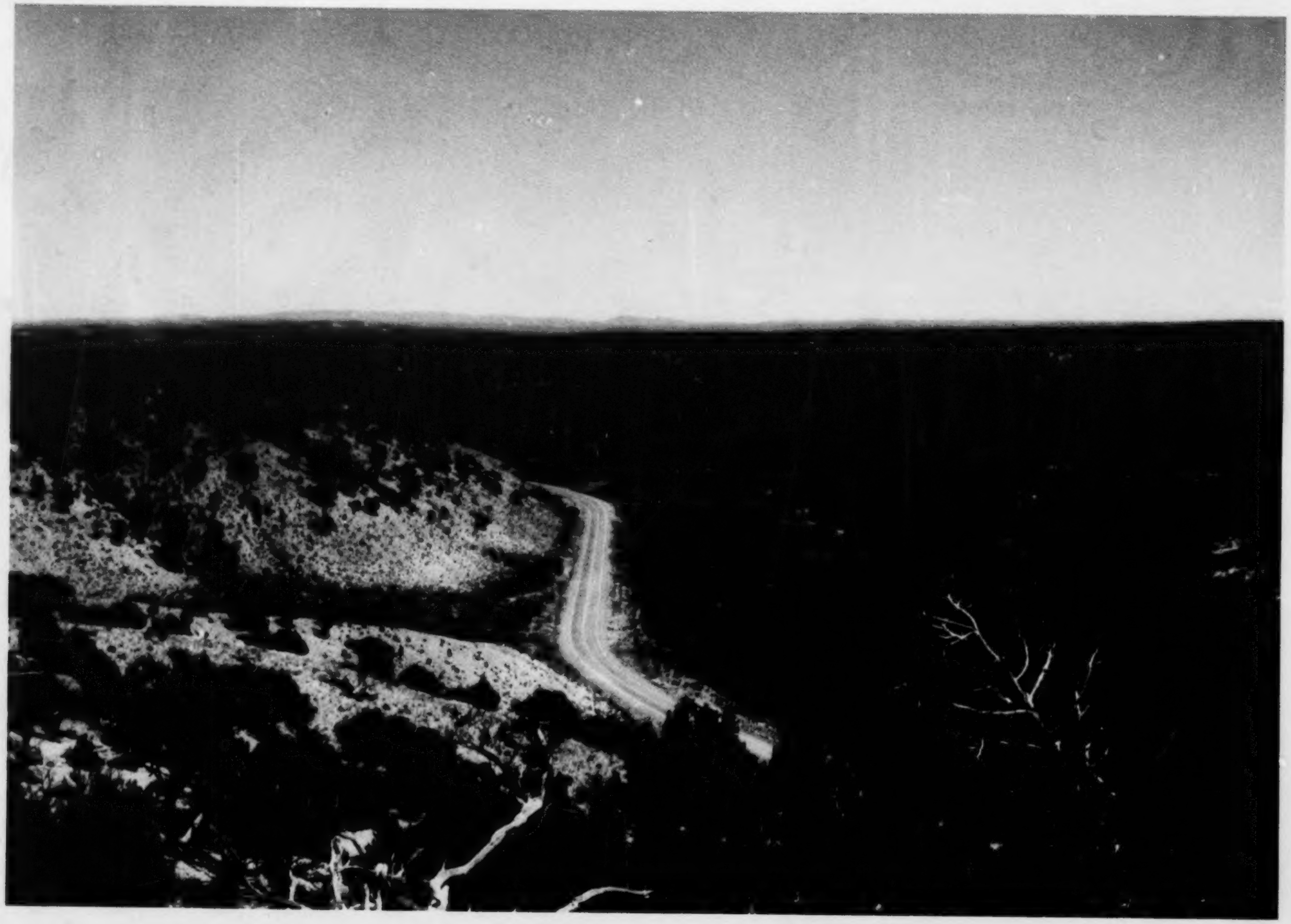

FIGURE 7. Photograph Looking Down Corral Gulch From the Valley Sidewall North of Tract C-a's Visitor's Center. Meteorological Site 3 and the Battelle Mobile Van are on the Valley Floor in the Center of the Picture.

Increasing cloudiness occurred on August 12 with light afternoon showers and thunder showers at the Corral Gulch site. An intensifying cold front across southern Wyoming the afternoon of the 12th became stalled over northwest Colorado on August 13 and 14. Considerable cloudiness and cooler weather with afternoon showers and thunder showers occurred both days with this frontal system.

## 2.3 Instrumentation

### 2.3.1 Mobile Van Instrumentation

The surface-based field experiments were conducted from a mobile van parked near tract C-a's Meteorological Station 3 in Corral Gulch. The site was chosen for its location relative to the tracer experiments, its accessibility, and its 110 VAC power supply. The two basic types of data collected from the mobile van site included upper air data and surface energy budget data.

The upper air data were obtained using a commercial balloon-borne sounding system.* The system uses expendable sondes that are towed aloft by a 50-gm helium-filled balloon. The time-multiplexed radio frequency data transmitted at 403.5 Mhz from the rising sonde is received by a ground receiving station and decoded into time, pressure, temperature, and wet bulb temperature information. The decoding is accomplished by a microprocessor in the ground station using sonde calibration information keyed into the ground station before the sonde is released. The processed data are printed out on a Hewlett Packard HP-97 printer/calculator as the sonde ascends, and is also recorded in a digital form on an audio cassette recorder. The microprocessor in the ground station has been programmed so that this digital data can be played back into the ground station at a later time and transferred directly into a computer data file.

The multiplexing rate of the sonde (approximately one full scan of data in six seconds) and the nominal ascent rates utilized (200-m $\text{min}^{-1}$)

---

* Airsonde® Data Collection System, Model TS-2A, Atmospheric Instrumentation Research Co., Boulder, CO 80301.

allowed vertical data resolution of about 20 meters. The sondes could generally be tracked to about the 430 millibar pressure level or the 6500-m MSL (21,000 ft MSL) level before signals became weak and data quality became a problem. Since data quality was consistently good up to 6000-m MSL, the sonde data are plotted only to this height. Airsonde system specifications are summarized in Table 1. For further information on system characteristics and performance, the reader is referred to an article by the manufacturer of the Airsonde system, (Call and Morris 1979), and to independent tests of the Airsonde system conducted by Whiteman (1980). Actual data collected with the system are presented in later sections.

Upper air winds were obtained for the Airsonde ascents by merging the Airsonde-derived height data with data obtained with an optical theodolite. The procedure for theodolite tracking was to record the position (azmiuth and elevation) of the sonde at 30-second intervals from the release time. Upper air winds and the trajectory of the sonde's subpoint were then calculated using the well-known single theodolite wind reduction equations. It is important to note that the equations used do not rely on the sonde ascending through the atmosphere at a fixed, estimated rate of rise, but depends, instead, on derived heights as calculated hydrostatically from sonde-measured pressure and temperature data. The vertical resolution of wind data, determined by balloon ascent rates and the 30-second theodolite observation interval, is approximately 100-m.

Energy budget data constitute the second type of data obtained at the mobile van. These data were collected at a site just north of the mobile van in a small area where the natural surface of the valley floor was undisturbed. The surface characteristics of this site were representative of the valley floor in general, having a sparse cover of sagebrush, bare soil, and natural grasses. At this site solar and net radiation instruments were mounted at the one-meter level on booms that extended out one meter from a guyed mast. Nearby was a small plot of ground in which soil temperature sensors were inserted into undisturbed soil from the walls of a 20-cm deep excavated pit at depths of 2-, 5-, and 20-cm. All sensors were connected through signal conditioning electronics to a multichannel recording system.

TABLE 1. Specifications of Airsonde Data Collection System

| Parameter | Sensor | Range | Precision | Resolution | Time Constant |
|---|---|---|---|---|---|
| Dry and wet bulb temperature | aspirated bead thermistor | -70°C to +50°C | ± 0.5°C | 0.1°C | 3 sec dry bulb<br>12 sec wet bulb |
| Barometric pressure | temperature compensated aneroid capacitance | 1050 to 300 mb | ± 3.0 mb | 0.1 mb | |

Radiation instruments were calibrated before and after the field experiment, and field data were corrected using this calibration information. The types of sensors and their characteristics are listed below in Table 2.

TABLE 2. Radiation and Soil Temperature Sensors

| Sensor | Description | Manufacturer |
|---|---|---|
| net radiometer | temperature compensated miniature net radiometer (Fritschen), Model No. MNR | Micromet Instruments, Bothell, Washington |
| downward- and upward-looking pyranometers | LiCor cosine corrected silicon cell pyranometer, Model LI-200S with rotating shadow band | Lambda Instruments Corp. Lincoln, Nebraska |
| soil thermometers | YSI 10K thermistors with linearizing bridge | Yellow Springs Instrument Co., Inc., Yellow Springs, Ohio |

### 2.3.2 Aircraft Instrumentation

The primary objective of the aircraft sampling program was to provide a means of intercomparing air temperature profile data from the geographical region of the Green River Oil Shale Formation with those obtained on a regular basis at Grand Junction (rawinsonde soundings) and those obtained during the intensive experimental period at the tract C-a site (Airsonde

8

soundings). In addition, the DC-3 aircraft provided a platform for measuring various air quality parameters, including ozone and sulfur dioxide concentrations, aerosol concentrations, and light scattering coefficients, as well as aerosol size distributions and elemental compositions. Vertical profiles were made over the oil shale region at altitudes generally between 2300- and 4300-m MSL.

Several aircraft flight patterns were adopted in order to meet the objectives of the experimental program. These patterns include a descending spiral, a modified ascending spiral, and a fixed heading flight. Descent profiles of 2000-m in height were in the form of a spiral and were made in about 20 minutes. These profiles were coordinated, where possible, with rawinsonde and Airsonde releases. Ascent profiles required about 40 minutes to complete because of the relatively high altitudes and slow climb rate of the DC-3. The flight pattern in this case was modified to include a straight and level flight leg at discrete altitudes in order to obtain wind speed and direction data from the aircraft navigation system. Finally, fixed heading flights were sometimes utilized to obtain vertical profile data on ascent or descent or to obtain data at discrete flight levels.

A typical flight began with departure from the airport at Grand Junction, Colorado, and a modified spiral ascent profile over the Grand Junction area or a direct ascending flight profile to tract C-a. A descending spiral pattern was then flown over tract C-a. The aircraft then moved to a location upwind of the site (in this case to the west of the Cathedral Bluffs) where a modified spiral ascent was made. After the upwind profile was completed, a second descent over tract C-a was carried out. The aircraft then ascended along a line due east toward the Flat Tops Primitive Area. Once past the Flat Tops, a descending spiral was made over the Yampa Valley (to the north of Flat Tops) or over the Glenwood Springs area (to the south of Flat Tops). Upon completion of this spiral the DC-3 ascended to a convenient VFR flight altitude for return to base. On one occasion a descending spiral from 4200- to 2300-m MSL was made prior to landing at Grand Junction (August 8, 1980). A summary of flight information is given in Table 3. T3

## TABLE 3. Summary of Aircraft Flight Patterns and Locations

| | Flight Locations or Legs* | | | | | | | | |
|---|---|---|---|---|---|---|---|---|---|
| Date+ | GJT | Tract C-a | Upwind | Yampa | Glenwood Springs | GJT to Tract. C-a | Tract C-a to Flat Tops | Yampa to GJT | Glenwood Springs to GJT |
| August $5_a$ | MAS | DS | | | DS | | FHA | | FHL |
| August $8_n$ | MAS, DS | DS | MAS | | | FHL | FHA | FHL | |
| August $9_a$ | | DS (2) | MAS | DS | | FHA | FHA | FHL | |
| August $9_p$ | MAS | | | | | FHL | | | |
| August $14_a$ | | DS (2) | MAS | DS | | FHA | FHA | | |

+ a = morning flight
p = afternoon flight
n = night flight

* MAS = modified ascending spiral
DS = descending spiral
FHA = fixed heading ascent
FHL = fixed heading, level
FHD = fixed heading descent

Instrumentation on board the DC-3 aircraft during the August 1980 field experiment is listed in Table 4. Atmospheric state parameters which were measured included air temperature, relative humidity, pressure altitude and, when possible, wind speed and direction from the aircraft navigation system. The latter system also provided geographic coordinates (latitude, longitude). Real-time air quality parameters were limited to total aerosol concentrations (Aitken nuclei or condensation nuclei concentrations), aerosol light scattering coefficients and ozone concentrations. The remaining air quality measurements required integrated samples; these included $SO_2$ concentration (by means of bubbler samples using a tetrachloro mercurate solution) and aerosol chemical composition (by means of various high volume filter samples). The integrated samples were analyzed later in the laboratory. Aerosol size distributions in the diameter range 0.01- to 5-μm were determined by combining data collected with an electrical aerosol analyzer (EAA) and an optical particle counter (OPC). Finally, measurements of incident short wave and ultraviolet radiation were made. Data from all instruments, including the high volume filter flowrate, were recorded on magnetic tape with selected outputs displayed on multichannel strip chart recorders.

Several laboratory procedures were followed in the analysis of the integrated samples. Bubbler samples were analyzed by a modified West-Gaeke method to determine $SO_2$ concentration. The high volume filter samples (mostly IPC but also a few Teflon® * coated glass fiber filters) were split in half with one half used for x-ray fluorescence (XRF) and neutron activation analysis (NAA) and the other half rinsed and analyzed by the ion chromatographic (IC) techniques. The XRF and NAA analyses provided data on elemental abundances while the IC analysis provided data on soluble ionic species such as sulfates, nitrates, etc.

### 2.3.3 Tracer Instrumentation

Atmospheric transport and plume depletion investigations were conducted with dual tracers released from federal oil shale lease trace C-a. The tracers, simultaneously released from adjacent release points (Figure 6)

---

* Trademark of E. I. duPont de Nemours, Wilmington, DE 19898.

## TABLE 4. Aircraft Instrumentation

| Parameter | Instrument | Comment |
|---|---|---|
| **Atmospheric State** | | |
| Temperature | Rosemont | |
| Relative Humidity | ERC, Model BR Lyman-Alpha Humidiometer | Calibration approximately set with sling psychrometer |
| Pressure Altitude | Metrodata MB | Manual aircraft altimeter used as a backup |
| Wind Speed, Direction | Omega Global Navigation System | Winds valid only when aircraft moving with a fixed heading |
| **Air Quality** | | |
| Aitken Nuclei Concentration | General Electric CNC-II Condensation Nuclei Counter | Total aerosol concentration |
| Aerosol Light Scattering Coefficient | MRI Integrating Nephelometer Model 1560 | Total integrated aerosol light scattering; periodic clean air checks |
| Particle Size Distribution | Thermo Systems Electrical Aerosol Analyzer, Model 3030 | Size distributions in the diameter range 0.01 to 0.5 μm by electrical mobility method |
| | Royco Optical Particle Counter, Model 220 | Pulse height analysis of light scattering from individual particles interfaced with a 15-channel data system: range 0.5 to 5 μm. |
| Particle Composition | High volume filter samples | IPC, Teflon® coated glass fiber filters. Analyses by XRF, NAA, and IC. Elemental and ionic anlayses. |
| Ozone Concentration | Bendix Ozone Analyzer, Model 8002 | |
| $SO_2$ Concentration | Spectrex Bubbler Sampler, Model PAS-3000 | Integrated sample. TCM solution used to fix $SO_2$ |
| **Other** | | |
| Aircraft Location | Omega Global Navigation System | Geographic coordinates (latitude, longitude) |
| UV Radiation | Eppley UV Radiometer, Model TUVR | Incident UV radiation |
| Solar Radiation | Lambda Silicon Cell Pyranometer, Model LI-200S | Incident solar (short-wave) radiation |
| High Volume Flow | Cox Turbine Flowmeters | |
| Selected Output Display | Brush Chart Recorder, Model 260,<br>Houston Omni-Scribe Recorder | 6-channel<br>2-channel |

12

were non-depositing $SF_6$ gas and depositing lithium-traced particles. The $SF_6$ tracer was released from tanks in which the $SF_6$ was in the gas phase. The lithium-traced particles were generated from a 10 g/ℓ lithium carbonate water solution sprayed from four sonic nozzles* mounted on the back of a pick-up truck. The truck, water solution tank, spray nozzles, and air compressor are shown in the foreground of Figure 8.

F8

Airborne tracer concentrations downwind of the release point were measured using one of three methods:

- Samples of $SF_6$ and lithium-traced particles were collected and detected in real time at the tract C-a Visitor's Center and at Meteorological Site 3 using commercial instrumentation.
- Samples of $SF_6$ were collected using bag samplers that were distributed along four radio-controlled sampling lines oriented perpendicular to the valley axis at distances of 1.6-, 2.5-, 4.6-, and 5.6-km downvalley from the release point. $SF_6$ concentrations were determined from these samples after collection.
- Samples of $SF_6$ were collected in syringes at various points along a road which runs perpendicular to the valley axis approximately 6.8-km below the release point. Concentrations were determined from these samples after collection.

F9

The real-time measurements of $SF_6$ and lithium particle concentrations were made using the instrumentation shown in Figure 9. Shown in the figure are two laboratory carts holding identical detection equipment. Actually, three such laboratory carts were located at each of the two real-time measurement sites. When operated in the real-time mode, the three sets of instruments at each site were operated in sequence, with the sequencing speed dependent on the rapidity with which the detectors returned to baseline. Each of the carts holds both lithium particle detectors and $SF_6$ detectors. The gas cylinders necessary to operate the equipment are located nearby.

---

* Spray Nozzle Model 900-3, Heat Systems-Ultrasonics, Inc., Plainview, NY 11803.

13

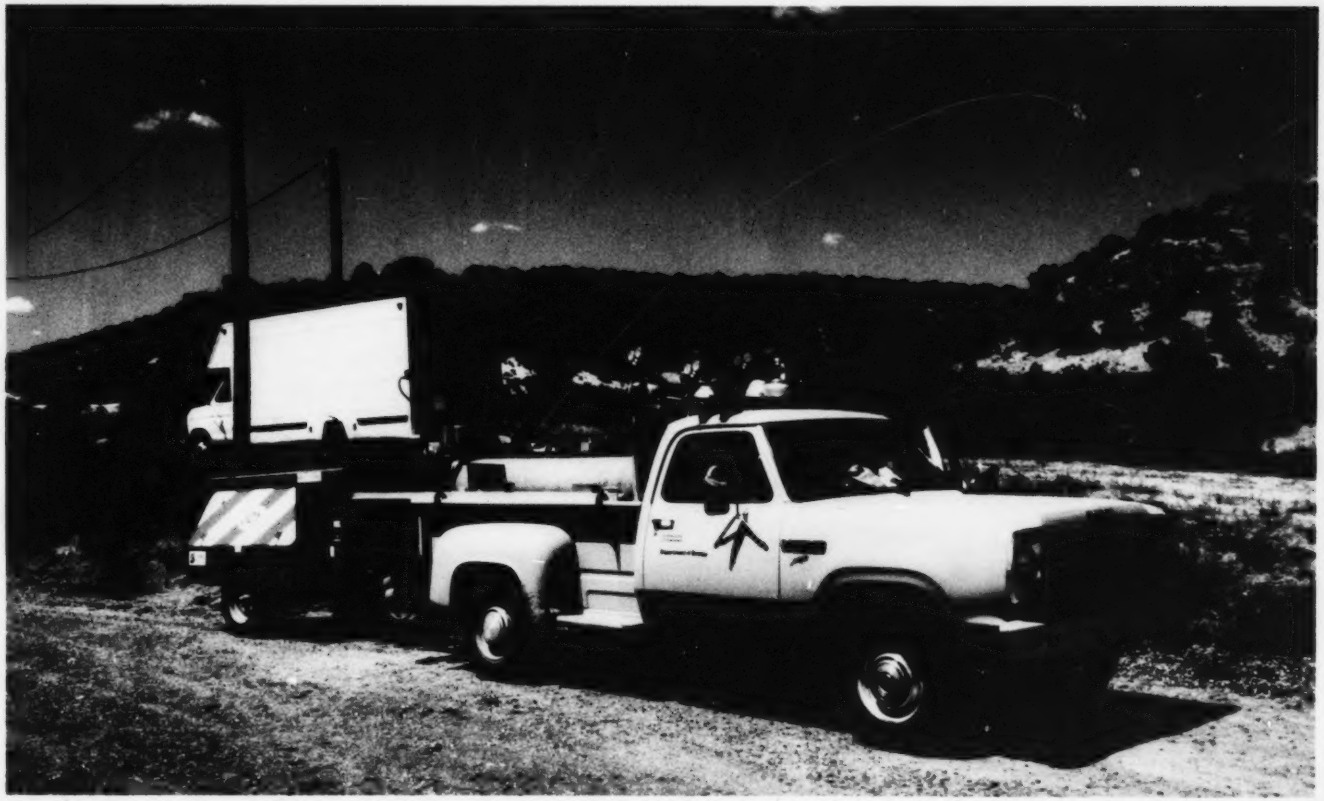

FIGURE 8. Lithium-Traced Particle Generation Equipment.

Neg. 81B936-3

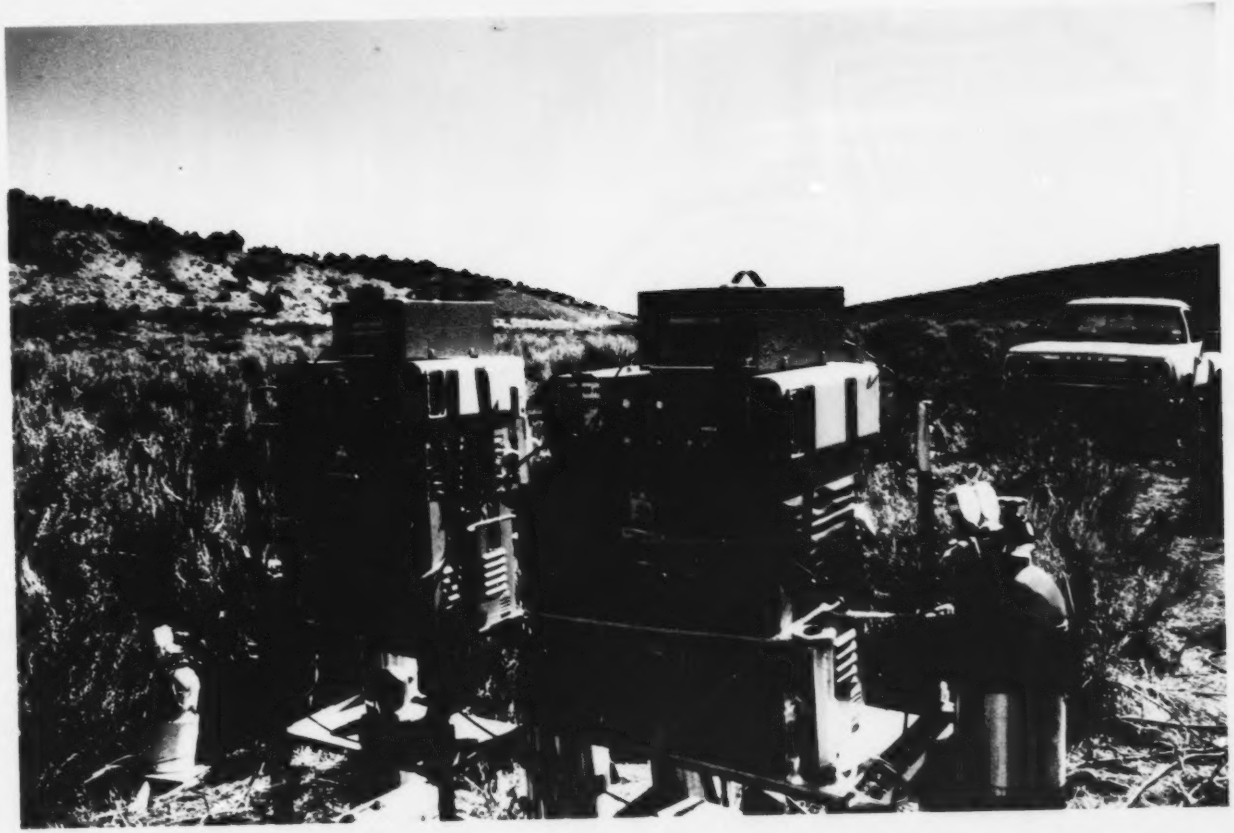

FIGURE 9. Real-Time Tracer Sampling Station at Meteorological Site 3.

Neg. 81B936-1

Gases include 99.95% purity hydrogen for burning in the lithium detector, oxygen-free nitrogen for the carrier gas in the gas chromatograph $SF_6$ detector, and $SF_6$ gas in ultra-pure air for calibration of the $SF_6$ detector.

The instrument placed directly on the laboratory cart in Figure 9 is a real-time lithium-traced particle monitor* which uses a flame ionization detector. The particle detector response is particle size dependent and counts are accumulated for each particle sensed. Lithium-traced particles generated from lithium carbonate solution are detected in the narrow size range from about 0.5- to 1.5-μm diameter. Particles below 0.5-μm contain insufficient lithium for detection, while particles larger than 1.5-μm are not detected due either to sampling line losses or burning characteristics. For detection, ambient air is sampled at an air flow rate of 50 cc/min and subsequently burned in a hydrogen flame. Light from the flame is focused by a lens onto the face of a red-sensitive photomultiplier tube. An optical interference filter passes only the lithium spectrum (6708 Å strong emission). Sensed light pulses are automatically recorded. Airborne lithium-traced particle concentrations were measured for air sampling intervals of one minute or longer. The gas chromatograph** used to detect $SF_6$ tracer gas is located on top of the particle detector in Figure 9. Detection is by electron capture. The upper-most instrument is a strip chart recorder for the $SF_6$ detector.

Bag samples were collected at sampling stations along the four radio-controlled sampling lines previously mentioned. Each of the lines consisted of 7 or 8 sampling stations, three or four on the valley floor and two on each sidewall. Each station had three sampling bags***, each attached to its own separate air pump. On sampling lines 1 and 3, tubing inlets for the air pumps were secured at the 1.7-m level. On these sampling lines the pumps could be activated sequentially to collect three consecutive air samples from the same height level. Thus, airborne $SF_6$ concentrations could be investigated as a function of time at a given point. On sampling lines 2 and 4, on the other hand, the tubing inlets for the air pumps were secured at the 0.3-, 1.3-, and 5-m levels. These sampling lines were activated by radio control so that all pumps were turned on simultaneously, allowing the determination of $SF_6$ concentration profiles as a function of height for a single time interval.

---

* Lithium Particle Monitor, Environment One, Schenectady, NY 12309

** Field-Portable Tracer Gas Monitor, Model 215AUP, Systems, Science and Software, LaJolla, CA 92038

*** Industry Bag, 10 by 15 inches, 2.5 mil, flow meter fully inserted, no tubes. B Bar B, Suite 34, 121 West Whittier Blvd., LaHabra, CA 90631.

A photograph of a sequential sampling station is presented as Figure 10. At this sampling site an antenna is attached to a bamboo pole, 5.2-m in height, taped to a steel fence post. The antenna is attached to a battery-powered radio signal decoder, seen in the foreground on the cement block. Electrical wires run upward from the decoder to the three pumps taped to the bamboo pole above an open cardboard box. Inlet tubing is connected to sampling bags housed in the cardboard box, which can be closed to hinder bag exposure to sunlight and the elements. Experimental procedure called for the tubing to be flushed with ambient air before each experiment to remove residual $SF_6$ from the prior experiment. Samples were collected after each experiment and, within the constraints of time and personnel, selected samples were analyzed in the field for $SF_6$ concentration using the real-time gas chromatographic equipment previously described.

After tracer generation had ended, syringe* samples of ambient air were collected from a vehicle driven along roads which crossed the valley approximately 6.8-km below the $SF_6$ release point. These samples were analyzed using the real-time gas chromatographic equipment previously described. The lower detection limits of the tracer analysis equipment were $10^{-12}$ parts by volume for $SF_6$ and $2x10^{-2}$ particles/$cm^3$ for lithium particulates.

---

* Plastipak Single-Use Syringe, BD-5663, Becton-Dickinson, Rutherford, NJ 07070.

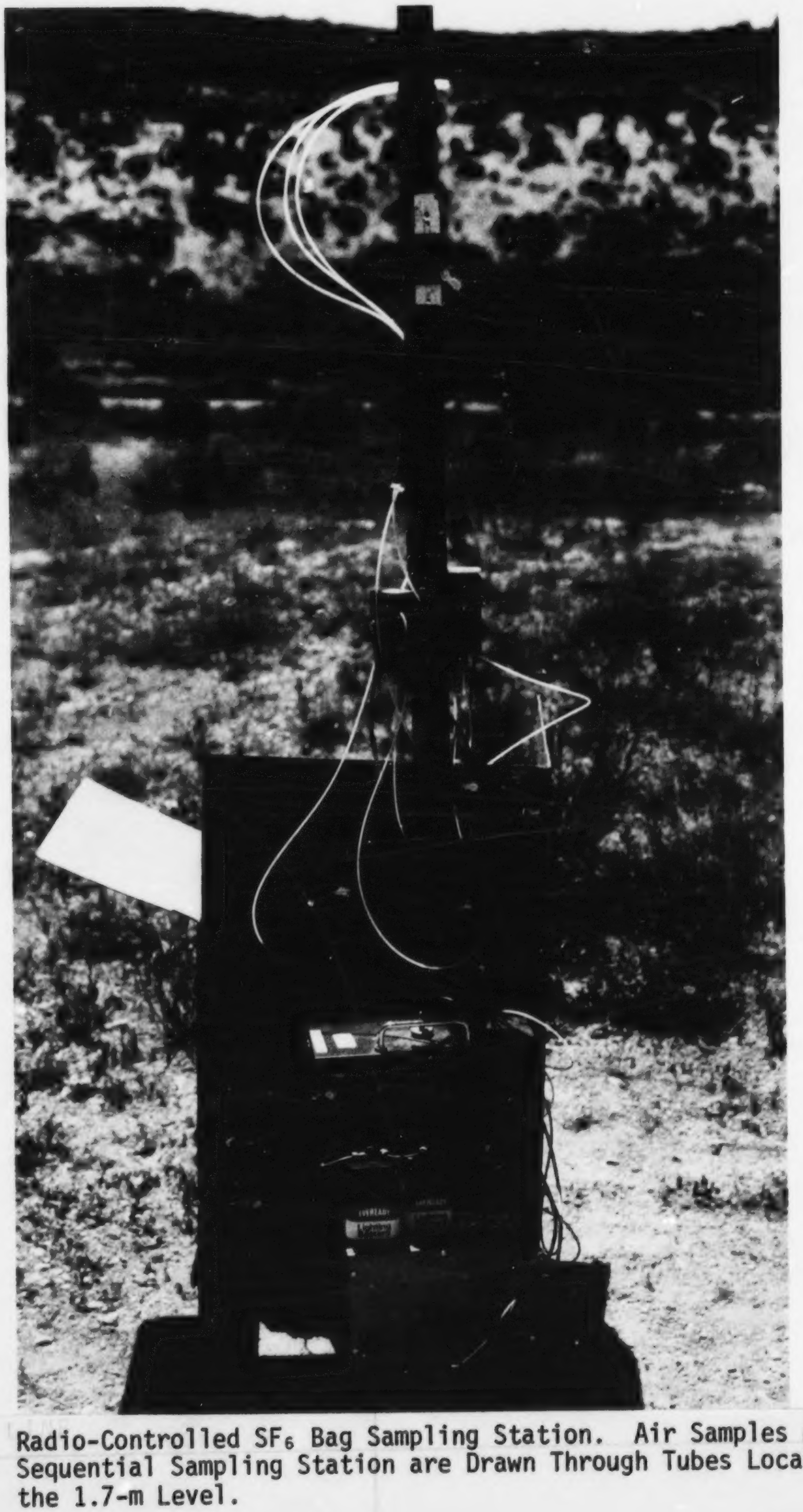

**FIGURE 10.** Radio-Controlled $SF_6$ Bag Sampling Station. Air Samples at This Sequential Sampling Station are Drawn Through Tubes Located at the 1.7-m Level.

Neg. 80G653-3CN

## 3.0 DATA SUMMARY

In this section, data collected in the field experiments will be summarized by means of tables, composite figures, or data samples. Detailed individual soundings or data sets will be found in Appendices at the end of the data report. For ease in presentation, the data summaries are broken into three sections. The first deals with surface and background meteorological observations, while the second deals with data collected in the aircraft flight program, and the third deals with data taken in the tracer experiments.

## 3.1 Surface and Background Meteorological Measurements

### 3.1.1 Grand Junction, Colorado Upper Air Data

A general description of the weather conditions encountered during the field program has been provided in an earlier section. For completeness Tables 5 and 6 are given, listing the surface, 700-mb and 500-mb Grand Junction, Colorado wind and temperature observations obtained from rawinsondes launched twice per day by the National Weather Service (NWS). The Grand Junction rawinsonde site, located at an elevation of 1474-m MSL, 120-km (75 miles) south-southwest of the field measurement site, is the closest rawinsonde site to the experimental area. The site is located in the broad SE-NW oriented Grand Valley of the Colorado River. The nominal release time for rawinsondes at NWS sites is 0000 and 1200 Greenwich Mean Time (GMT). In the United States, however, the general practice of the National Weather Service is to begin rawinsonde ascents at 1115 and 2315 GMT, respectively. Times in this report are given in Mountain Daylight Time (MDT) in hours and minutes using a 24-hr clock. The time relationship with Greenwich (England) Mean Time was MDT=GMT-6 hrs. Thus, a nominal rawinsonde release time of 0000 GMT on August 8, 1980 actually indicates a release at 2315 GMT on August 7 or 1715 MDT on August 7. A nominal release time of 1200 GMT on August 8, 1980 indicates an actual release time of 0515 MDT.

A summary of rawinsonde data follows. Table 5 lists the winds at the surface, 700-mb and 500-mb levels at the rawinsonde release times. The morning surface winds are drainage winds, flowing parallel to the valley axis. The winds are generally from 110° to 130° at 2- to 6-m sec$^{-1}$. The afternoon surface winds are stronger and, while generally flowing up the valley, are more variable in direction. Upper level (700 and 500-mb) winds during the experimental period were generally blowing from the western quadrants. 500-mb wind speeds averaged about 8-m sec$^{-1}$.

Due to the fine weather during the experimental periods and the lack of traveling weather disturbances, ambient air temperatures at the surface and other levels remained remarkably constant over Grand Junction from day to day (Table 6). Diurnal temperature oscillations (between 0000 GMT and 1200 GMT soundings) were readily apparent at the surface and at 700-mb with amplitudes of 13.3°C and 2.2°C, respectively.

### 3.1.2 Balloon-Borne Sonde Data

Table 7 provides a summary of the 33 upper air soundings taken from the Corral Creek field site over a period of 9 days. Included in this table are the sounding number, release time, number of theodolite observations, pressure level attained, cloud conditions at Airsonde release time, and special comments on the data. A special intensive 30-hr observational period was begun with the 0837 MDT sounding of August 9. Observations to complete the 30-hr series during the evening of August 9 and early morning of August 10 were collected by the Los Alamos personnel and are presented in their data report, previously referenced.

Upper air soundings from the balloon-borne sondes were processed, and plotted by computer in two forms. The first form (Figure 11) includes plots of dry bulb temperature (°C), wet bulb temperature (°C), mixing ratio (gm kg$^{-1}$), relative humidity (percent), wind speed and wind direction, as functions of height. Special symbols, indicated for every 10th frame of data, identify the wet bulb temperature and relative humidity profiles.

## TABLE 5. Grand Junction, Colorado Winds (deg, m sec$^{-1}$)

| Date | | Surface | | 700 mb | | 500 mb | |
|---|---|---|---|---|---|---|---|
| | | 0000 GMT | 1200 GMT | 0000 GMT | 1200 GMT | 0000 GMT | 1200 GMT |
| August | 5 | — | 130/6 | — | 250/7 | — | 260/14 |
| | 6 | 300/4 | — | 265/5 | — | 240/10 | — |
| | 7 | 310/5 | 120/5 | 255/7 | 255/11 | 220/14 | 250/9 |
| | 8 | 340/5 | 130/3 | 280/3 | 230/9 | 215/7 | 225/10 |
| | 9 | 320/4 | 130/3 | 295/4 | 250/9 | 230/13 | 230/10 |
| | 10 | 320/6 | 130/4 | 270/8 | 250/8 | 280/6 | 260/8 |
| | 11 | 270/7 | 110/2 | 315/5 | 360/2 | 300/11 | 300/7 |
| | 12 | 320/7 | 120/3 | 265/7 | 225/6 | 255/9 | 275/8 |
| | 13 | 160/4 | 110/2 | 160/6 | 250/6 | 285/8 | 305/2 |
| | 14 | 160/5 | 160/3 | 240/3 | 240/8 | 290/5 | 250/5 |
| | 15 | 290/3 | — | 245/4 | — | 215/4 | — |
| Average Speed | | 5 | 3 | 5 | 7 | 9 | 8 |

18

## TABLE 7. Summary of Corral Creek Upper Air Soundings

| Date | No. | Release[1] Time | Theodolite[2] Readings | Pressure[3] Attained | Cloud Conditions and Comments |
|---|---|---|---|---|---|
| August 5 | 1 | 1157 | 38 | 494 | 3/10 Cu. Line overhead E-W. Bad signal mid-flight. |
| | 2 | 1503 | 36 | 705 | 3/10 Cu + 1/10 Ci. Slow rising balloon. |
| | 3 | 1541 | 9 | 689 | 3/10 Cu + 1/10 Ci W. Interference with No. 2. |
| | 4 | 1854 | -- | 757 | Equipment failure. |
| August 7 | 5 | 1231 | 41 | <440 | Clear, few Cu. Two balloons. Early burst. |
| | 6 | 1511 | 48 | 430 | Clear, few Cu mostly E. |
| August 8 | 7 | 0912 | 53 | 480 | Clear, few Sc distant E. |
| | 8 | 1201 | 69 | 300 | Clear, few Cu and Fcu → 0.1 to 0.2 Cu. 30 sec → 1 min. |
| | 9 | 1455 | 58 | 500 | 65 sctd Cu. Slow rise. 30 sec →1 min. |
| August 9 | 10 | 0837 | 39 | 479 | 65 sctd Sc. |
| | 11 | 1152 | 69 | 351 | 65 sctd Cu and swelling Cu. Cu increasing. |
| | 12 | 1721 | -- | 350 | 0.5 to 0.6 Cu with virga → 0.4 Cu. |
| | 13 | 1943 | -- | 318 | 0.2 Cu, virga SE. Sunset 1953. |
| | 14 | 2200 | -- | 505 | 0.2 Cu mostly SW-SE. |
| August 10 | 15 | 0618 | -- | 335 | 0.1 Ac, mostly NE-SE. |
| | 16 | 0735 | -- | 429 | Clear, few Ac E. |
| | 17 | 0859 | -- | 444 | Clear. |
| | 18 | 1125 | -- | 469 | Clear. |
| | 19 | 1411 | -- | 369 | Clear, few Cu distant E. Strong surface winds. Winds picked up suddenly at 1310. |

## TABLE 7. (continued)

| Date | No. | Release[1] Time | Theodolite[2] Readings | Pressure[3] Attained | Cloud Conditions and Comments |
|---|---|---|---|---|---|
| August 11 | 20 | 0823 | 56 | 396 | Clear. |
| | 21 | 1150 | 58 | 366 | Clear. |
| | 22 | 1453 | 46 | 422 | Clear. |
| | 23 | 1744 | 56 | 386 | Clear, 3 Cb distant E. |
| August 12 | 24 | 0911 | 44 | 384 | Clear, few Ac and Acc, virga. |
| | 25 | 1207 | 52 | 351 | 0.1 Ac, few swelling Cu E, few heavy Cu distant E. |
| | 26 | 1516 | 23 | 480 | 65 sctd 80 ovcst RW--, virga and RWU SW-W-N. BINOVC S, mammatus W and overhead. Conditions changing rapidly. |
| August 13 | 27 | 0850 | 39 | 511 | E 90 sctd Ac, few Ci. |
| | 28 | 1146 | 66 | 410 | Clear, few Cu and TCU E and SE. Few Ac. |
| | 29 | 1430 | 8 | 681 | E 65 brkn. Cs horizon NW, TCU, Cb. RWU E and W. |
| | 30 | 1450 | 25 | 400 | E 70 brkn T. Cs horizon NW, TCU and Cb all quadrants, RWU E and W. |
| August 14 | 31 | 0835 | 39 | 494 | 100 sctd 250 sctd, few Sc. |
| | 32 | 1140 | 23 | 583 | E 90 ovcst, BINOVC ENE-N-WSW near horizon. Few Cu and TCU distant ENE. |
| | 33 | 1349 | 60 | 348 | 70 sctd 120 sctd 220 sctd. RWU ENE. TCU and Cb in vicinity. |

---

1. Mountain Daylight Time
2. Number of theodolite observations at 30 sec intervals (unless noted).
3. Millibars

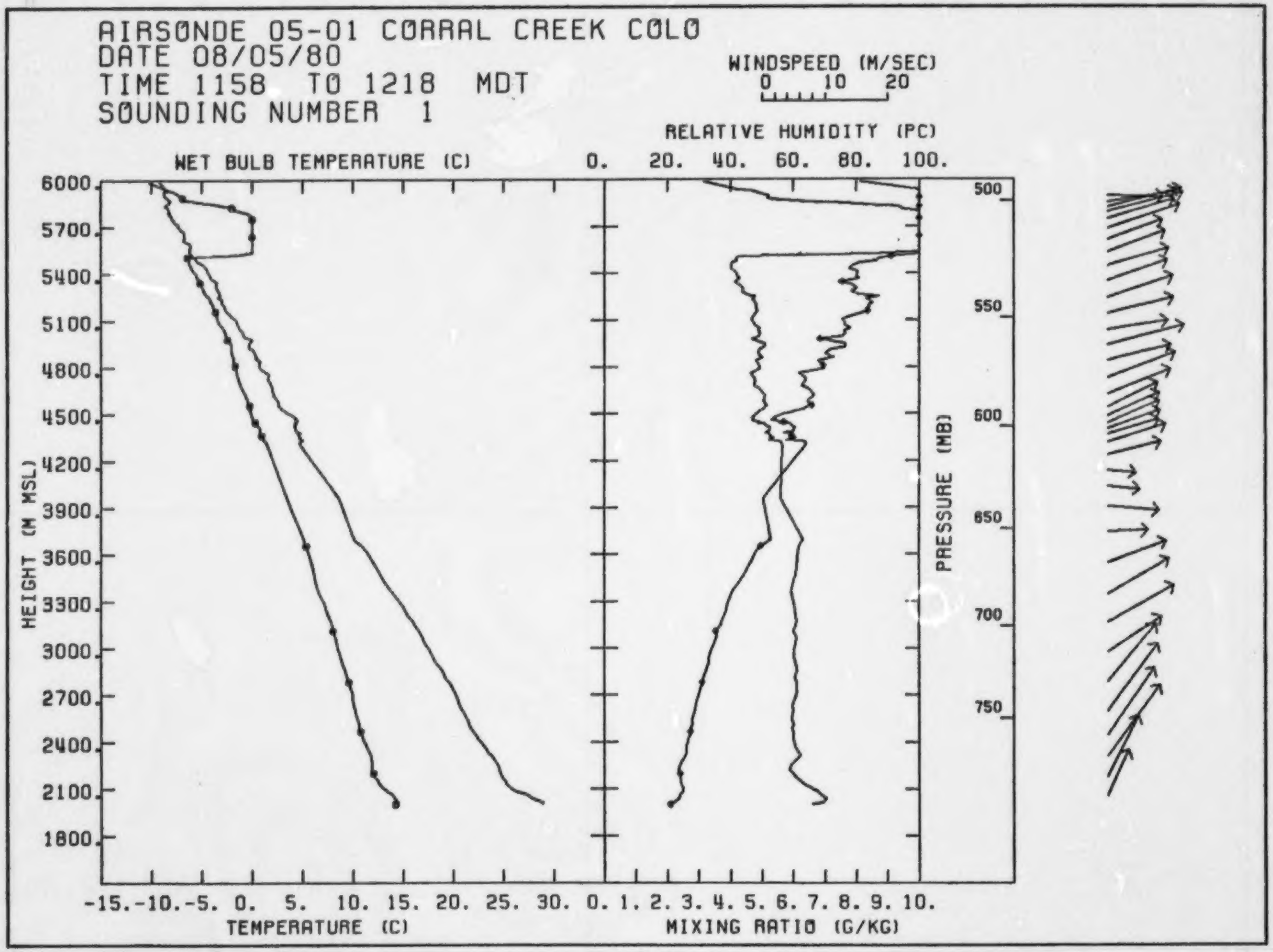

FIGURE 11. Example of Airsonde Data Plot, Corral Creek, Colorado, August 5, 1980.

Since some frames of data were discarded in the editing process before plotting due to reception problems, one should not attempt to determine sonde ascent rates from symbols on the figures. Humidity data (wet bulb temperature, relative humidity and mixing ratios) above a certain height are affected by the freezing of the water covered wick on the wet bulb thermistor. The height at which freezing occurs varies from sounding to sounding depending on the height of the atmospheric freezing level and the degree of supercooling attained by the wick before nucleation of ice occurs. The freezing of the wick occurs at a temperature of 0°C. After the wick has frozen, the existence of solid ice on the wet bulb increases the time constant of the wet bulb sensor. Thus, it takes a period of time after freezing before the wet bulb temperature approaches an equilibrium with the ambient temperature. As a result, the humidity data are erroneously high during, and for a time after, the freezing of the water on the wet bulb thermistor.

The fact that the water on the wet bulb freezes at 0°C allows an independent check of the Airsonde manufacturer's temperature calibration of the sonde. If freezing occurred at an indicated temperature other than 0°C, the temperature data could be assumed in error by the temperature differential, and the data could be corrected by this differential. This procedure has been applied to all Airsonde temperature data (wet bulb and dry bulb) collected in the field experiments. The procedure was applied to the dry bulb temperatures, as well as to the wet bulb temperatures, since temperature sensors were identical, carefully-matched, thermistors that underwent identical pre-launch calibrations (in which the wet bulb was left dry) by the Airsonde manufacturer.

Temperature differential checks at the freezing point for 28 sondes indicated that the average sonde indicated freezing at -0.05°C. The standard deviation of the temperature discrepancies was 0.09°C. The largest error was 0.38°C. We conclude from these tests that the sondes seem to be giving quite accurate indications of temperature, although as previously mentioned, wet bulb temperatures are seriously in error for a period of time after the wet bulb freezes.

On the right margin of Figure 11 are theodolite-derived wind vector profiles. A vector pointing straight up toward the top of the figure would be a wind blowing toward the north (in meteorological parlance, a south wind), while a vector oriented toward the right of the figure would be a west wind. Wind speeds in meters per second can be determined by referring to the wind speed scale. For ease in conversion, 1 m $\text{sec}^{-1}$ = 2.24 miles $\text{hr}^{-1}$ = 1.94 kts equals 3.6 km $\text{hr}^{-1}$. The winds, derived from single theodolite angular measurements, and heights as calculated hydrostatically from Airsonde temperature and pressure measurements, are averages over 30 second intervals. Figure 11 is merely an example of one Airsonde profile. The remaining profiles are presented in Appendix A. Airsonde subpoint trajectories for the profiles are presented in Appendix B. These trajectory plots on a 1 km x 1 km grid provide information on the plan position of the Airsonde during its profile. Most sondes drifted east of the site toward the center of the basin during their ascents. No major topographic features that could be expected to affect Airsonde-measured parameters are present in that direction within 30 to 45 minutes of Airsonde travel time.

The second form of Airsonde data presentation (see, e.g., Figure 12) is a daily composite plot of potential temperature ($\theta$) soundings, where $\theta \equiv T \left(\frac{1000}{P}\right)^{0.286}$ and P is the atmospheric pressure in millibars. This form of plot is very useful for analysis of layer stability and boundary layer dynamics. In particular, layers having constant potential temperature as a function of height can be identified as mixed layers in which the dry adiabatic temperature lapse rate is achieved. Airsonde release times (LT) are plotted on the figure. On the right margin of the figure the rawinsonde-derived upper air winds at Grand Junction are given for reference as vectors at the approximate height of the 700- and 500-mb surfaces. A complete set of plots for the individual days of the experiments is given in Appendix C.

F 12

### 3.1.3 Solar and Terrestrial Radiation Data

Solar and terrestrial radiation data were obtained using the instruments listed in Table 2. An example of the results is given in Figure 13 where the radiation measurements are plotted against time for the clear

F 13

24

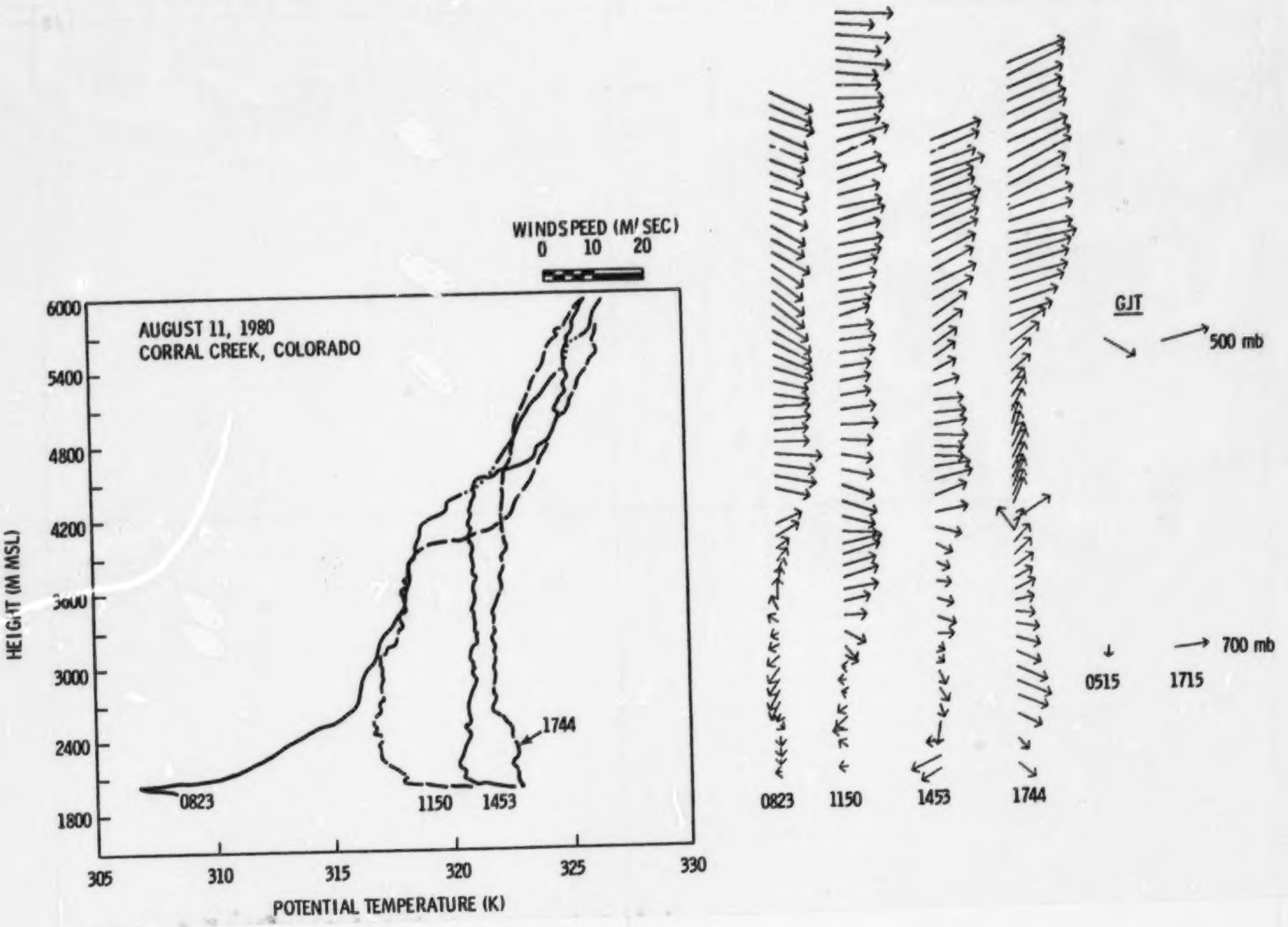

FIGURE 12. Example of Potential Temperature Composite Profiles, Corral Creek, Colorado, August 11, 1980.

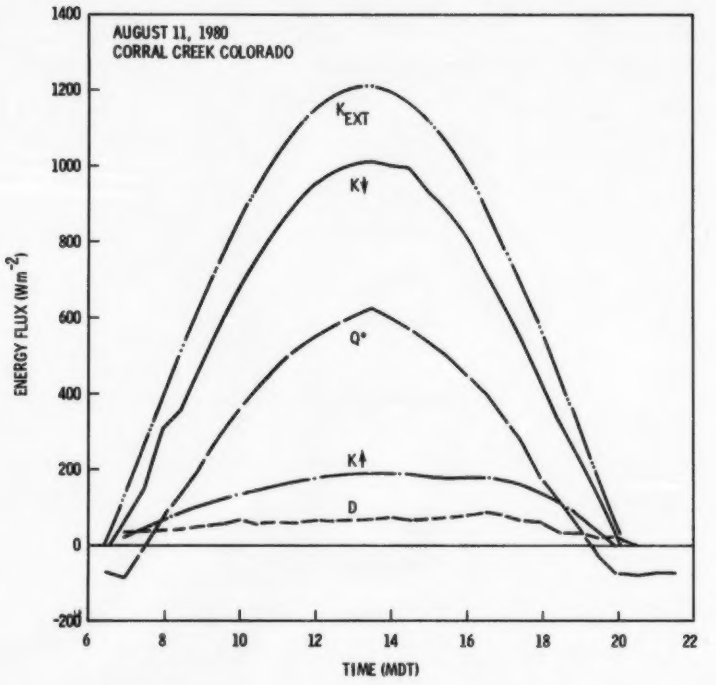

**FIGURE 13.** Atmospheric Radiation Measurements Taken at Corral Creek, Colorado, August 11, 1980. $K_{ext}$ is Extraterrestrial Solar Radiation, $K\downarrow$ is Incoming Solar Radiation, $K\uparrow$ is Outgoing Solar Radiation, $Q^*$ is Net Radiation, and D is Diffuse Solar Radiation.

day of August 11, 1980. Also plotted on the figure is the solar radiation that would be received at the location of the field site if the site's horizon were unobstructed by mountains and the earth had no atmosphere. This theoretical solar radiation, calculated by a computer model, is termed the extraterrestrial radiation and is given the symbol $K_{ext}$. Listings of the solar and extraterrestrial data collected in the field experiment are provided in Appendix D.

### 3.1.4 Soil Temperature Data

Using equipment as described in Table 2, soil temperatures were measured at depths of 2-, 5-, and 20-cm. An example of the results for a clear day are shown in Figure 14. Data for the entire period of the field experiment are presented in data tables in Appendix D.

## 3.2 Aircraft Measurements

A summary of aircraft atmospheric state and air quality measurements is given in the following sections. Detailed summaries are given in Appendix E. Several general observations about the results are appropriate, however, before addressing the various measurements. First, the atmosphere above the oil shale region during the August 1980 period was well mixed up to some level above the highest altitude attained by the aircraft. This conclusion is based on observations of the measured temperature profiles (both Airsonde and aircraft soundings), which essentially followed a dry-adiabatic lapse rate for all flight days except August 14, and the measured aerosol and ozone profiles, which showed either uniform concentrations with altitude or concentrations decreasing in proportion with air density. Second, the air was relatively clean and was near continental background levels. This result is primarily based on the very low aerosol mass and $SO_2$ concentrations which were observed. Apparently, the vigorous vertical mixing of materials released near the surface to heights in excess of 2-km diluted these emissions to near background conditions. Finally, inspection of the elemental composition of the aerosol and the measured size distributions suggests that crustal components are probably responsible

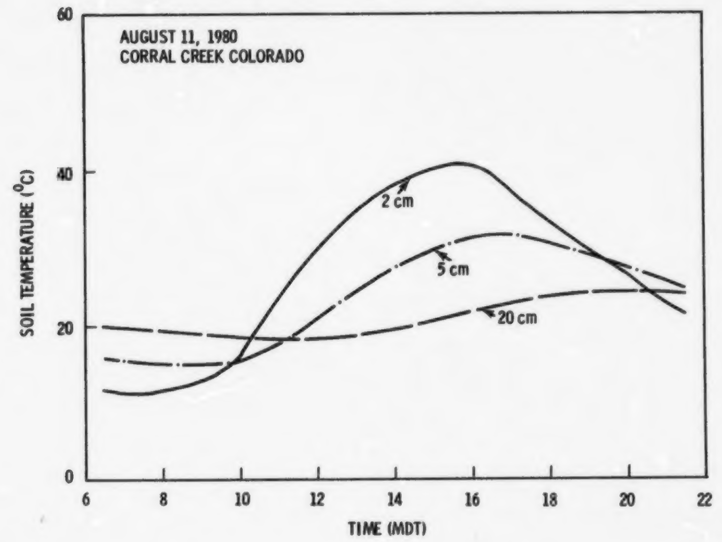

FIGURE 14. Soil Temperature Measurements Taken at Corral Creek, Colorado, August 11, 1980.

for more than half of the aerosol mass, with emissions from local vehicular traffic accounting for the remainder.

### 3.2.1 Temperature and Wind Profiles

F 15 – 20

Temperature profiles for the flights listed in Table 3 are shown in Figures 15 through 20. The temperature data are plotted as 30-second averages. Except for some structural detail near 3000-m MSL during the morning profiles between 0830 and 1000 MDT, the soundings obtained on August 5, August 8, and August 9 are very similar in lapse rate and approximate that of a dry adiabat. The August 14 flight day followed several days of vigorous thunderstorm activity; on this day the profiles showed lapse rates which were less than the dry adiabat.

The mid-day flight of August 5 (Figure 15) showed a significant warming of the air in the CBL during a one-hour interval. A similar observation is apparent in the profile data for August 9 (Figure 17 and 18) especially in the near surface layers. By late afternoon (1700 MDT) the air temperature had increased by 1 to 2°C with hardly any of the structure observed in the morning hours. Smaller changes in the atmospheric heating rate are observed in the early morning flight of August 14 (Figures 19 and 20). The night flight of August 8 (2100 to 2400) (Figure 16) shows little change in the temperature profile above 2800-m MSL, but a noticeable cooling in the near surface layer over Grand Junction. Generally, the profiles shown in Figures 15 to 20 tend to promote good vertical mixing.

Wind profile measurements were more difficult to obtain with the aircraft because of the requirement of straight-line flight for valid wind computations by the aircraft navigation system. A summary of wind data for constant altitude straight-line legs is given in Table 8. Some caution should be exercised in using the results of this table since the accuracy of the navigation system for wind determination has not been established.

T 8

### 3.2.2 Ozone Profiles and $SO_2$ Concentrations

Ambient $SO_2$ levels were below the minimum detection level of 0.3 μmol/ℓ by the West-Gaeke method for the range of sampling times used during the study (between 70 and 200 minutes). This detection limit implies that the average $SO_2$ concentration over the oil shale area was <1.0 ppbv during August 1980 sampling flights.

59

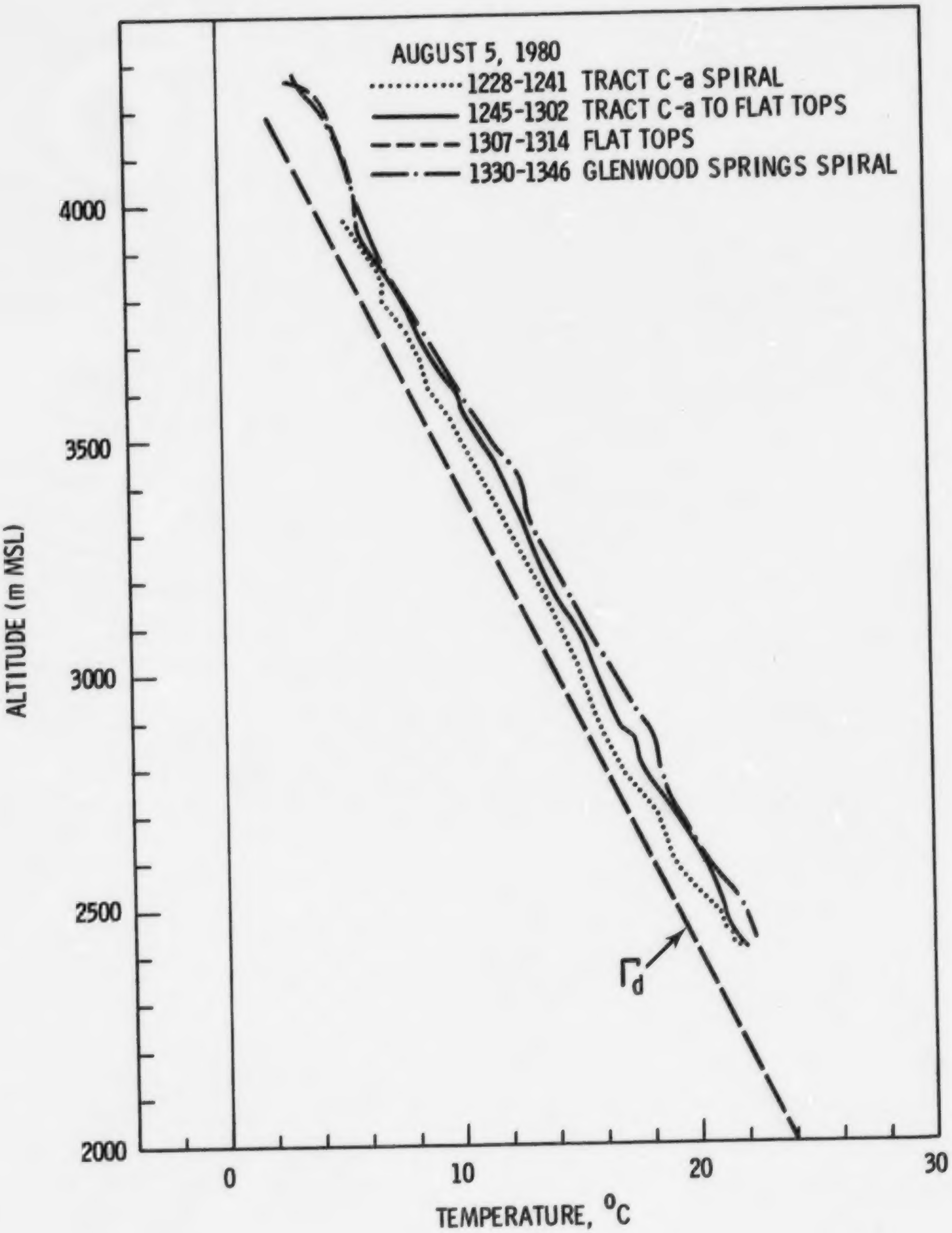

FIGURE 15. Aircraft-Measured Temperature Profiles, August 5, 1980, 1228 to 1346 MDT. The Dry Adiabatic Lapse Rate ($\Gamma_d$) is Given For Reference.

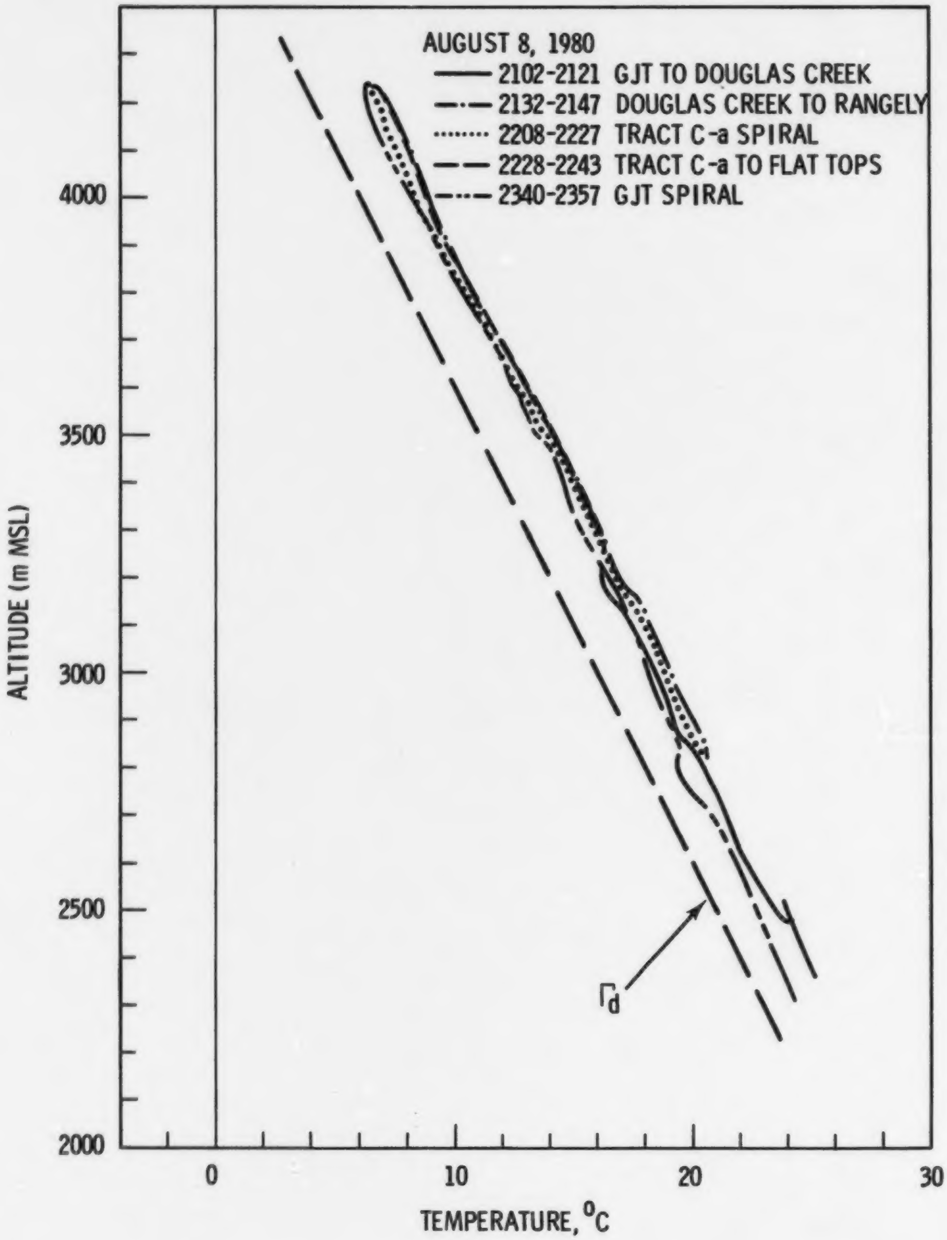

FIGURE 16. Aircraft-Measured Temperature Profiles, August 8, 1980, 2102 to 2357 MDT.

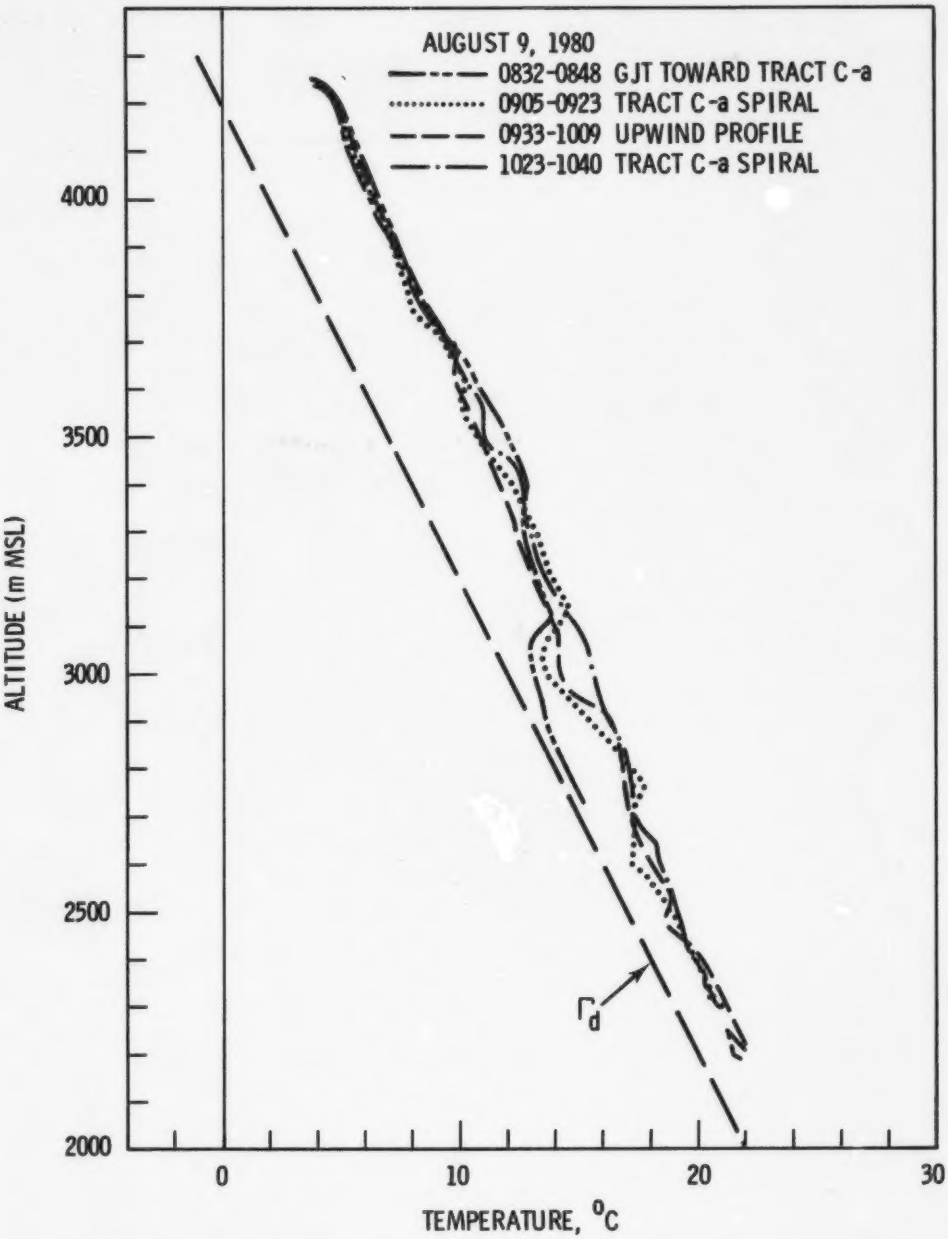

FIGURE 17. Aircraft-Measured Temperature Profiles, August 9, 1980, 0832 to 1040 MDT.

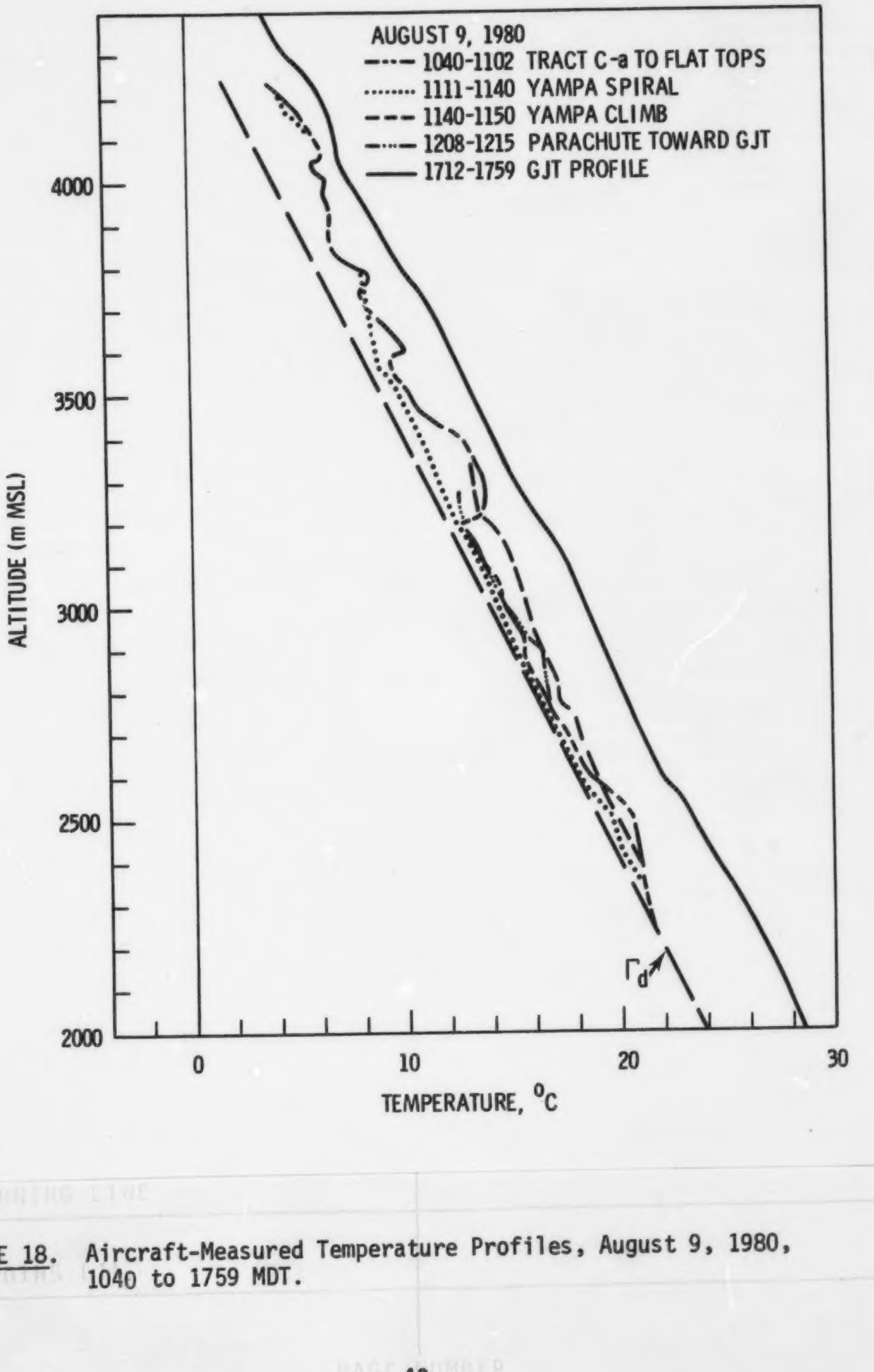

FIGURE 18. Aircraft-Measured Temperature Profiles, August 9, 1980, 1040 to 1759 MDT.

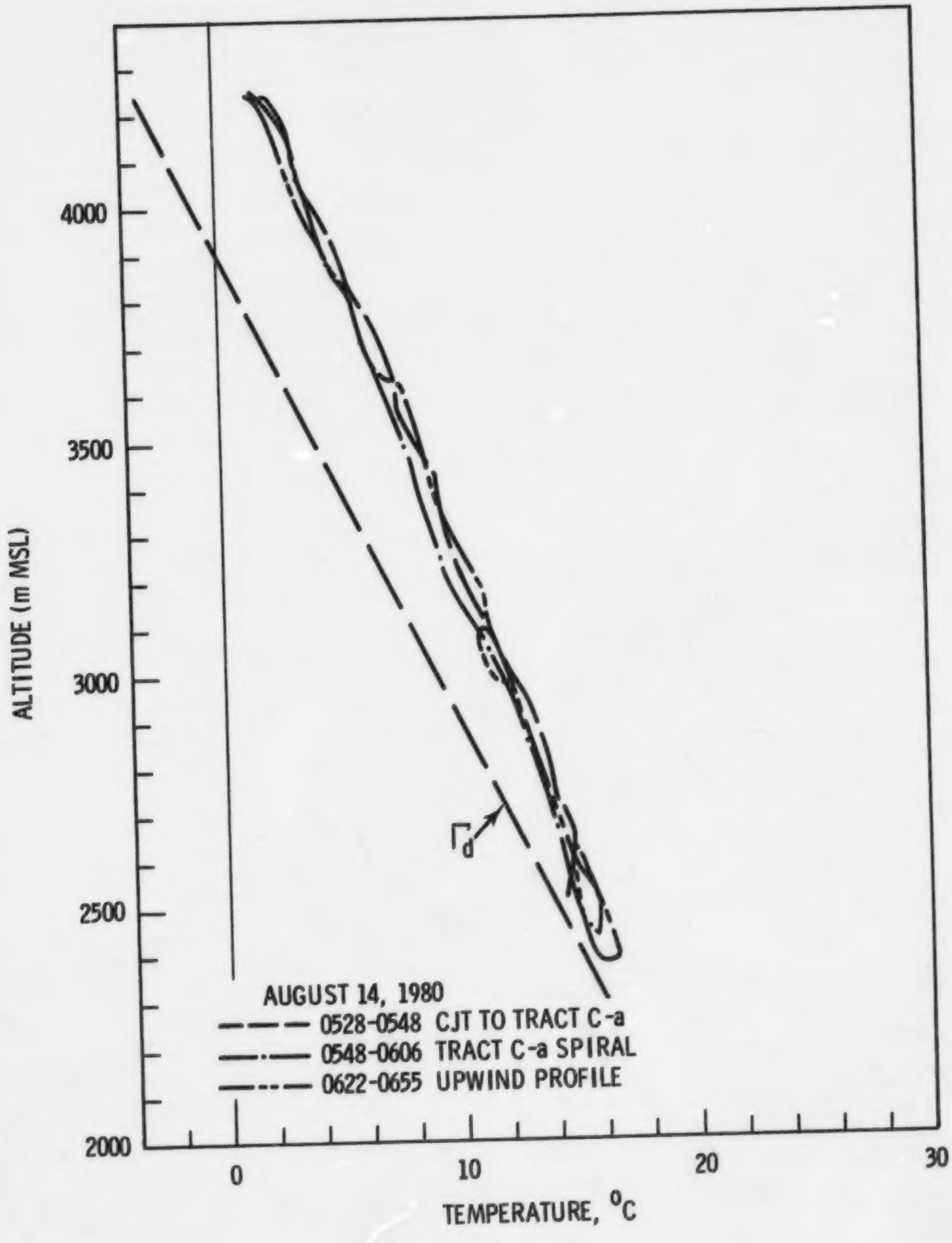

FIGURE 19. Aircraft-Measured Temperature Profiles, August 14, 1980, 0528 to 0655 MDT.

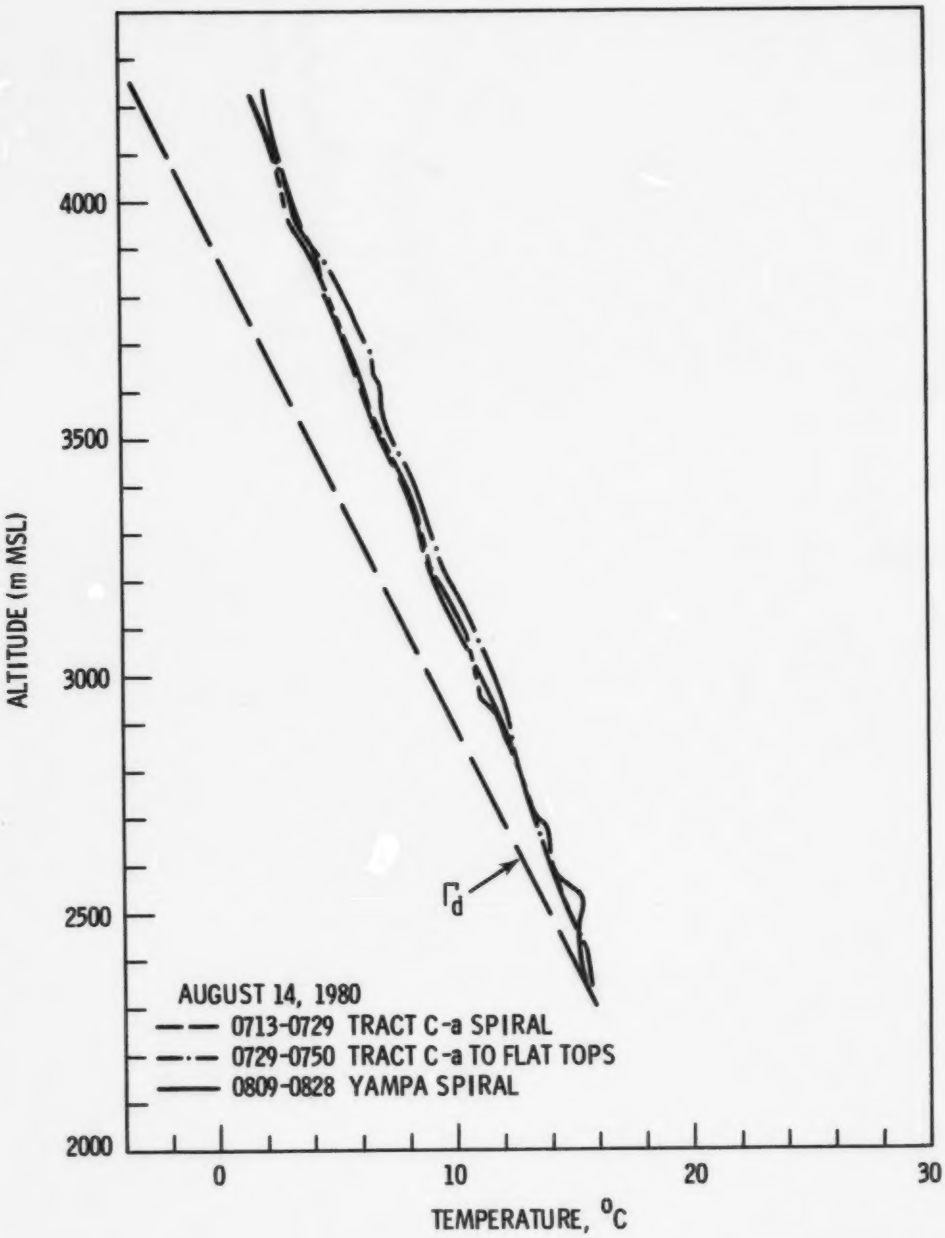

FIGURE 20. Aircraft-Measured Temperature Profiles, August 14, 1980, 0713 to 0828 MDT.

## TABLE 8. Aircraft-Measured Winds From Selected Constant-Altitude, Straight-Line Flight Legs

| Date | Time | Altitude (m-MSL) | Average Temperature (°C) | Wind Speed (m/s) | Wind Direction (°) | Flight Direction |
|---|---|---|---|---|---|---|
| August 5 | 1112-1122 | 1810 | -- | 7.3 | 171 | WNW |
| | 1127-1133 | 2431 | -- | 2.0 | 79 | ESE |
| | 1140-1151 | 3211 | 12.8 | 8.0 | 201 | WNW |
| | 1156-1204 | 3972 | 5.3 | 3.7 | 250 | ESE |
| | 1204-1226 | 3970 | 5.4 | 8.7 | 239 | N |
| | 1302-1308 | 3969 | 6.0 | 10.7 | 296 | E |
| | 1312-1330 | 4255 | 3.3 | 7.6 | 257 | WNW to S |
| | 1312-1317 | 4244 | 3.6 | 11.3 | 257 | WNW |
| | 1318-1330 | 4259 | 3.15 | 5.9 | 259 | S |
| | 1344-1410 | 2435 | 22.0 | 4.6 | 225 | W |
| August 8 | 2147-2209 | 4241 | 6.1 | 8.1 | 249 | ESE |
| | 2242-2326 | 4236 | 6.1 | 9.9 | 282 | E, WSW |
| | 2326-2338 | 4236 | 6.1 | 5.9 | 279 | WSW |
| August 9 | 0833-0906 | 4224 | 4.4 | 6.6 | 267 | N |
| | 0822-0934 | 2374 | 19.9 | 6.2 | 266 | WNW |
| | 0934-0939 | 2233 | 21.6 | 4.7 | 242 | S |
| | 0944-0950 | 2968 | 14.4 | 4.7 | 244 | N |
| | 0955-1003 | 3607 | 9.6 | 8.2 | 257 ± 15 | S |
| | 1008-1015 | 4237 | 4.2 | 8.6 | 263 ± 10 | N |
| | 1017-1026 | 4183 | 4.8 | 11.2 | 254 | ESE |
| | 1152-1208 | 3301 | 12.7 | 12.1 | 290 | WSW |
| | 1701-1712 | 1841 | 30.3 | 5.5 | 279 | WNW |
| | 1717-1726 | 2594 | 22.0 | 6.1 | 250 | ESE |
| | 1728-1737 | 3370 | 14.5 | 7.3 | 292 | WNW |
| | 1748-1757 | 4310 | 4.5 | 7.6 | 275 | ESE |
| August 14 | 0627-0637 | 2998 | 11.7 | 4.3 | 258 | N |
| | 0655-0705 | 4235 | 1.9 | 4.5 | 246 | S |
| | 0706-0713 | 4237 | 1.95 | 3.7 | 269 | ESE |
| | 0749-0758 | 4231 | 1.4 | 13.2 | 218 | E |
| | 0759-0810 | 4233 | 1.3 | 8.1 ± 3.8 | 116 ± 40 | NNW |

F 21 22

Ozone profiles are shown in Figures 21 and 22. Except for the single ascent in the late afternoon of August 9 (shown in Figure 22), the profiles are shown as the range of ozone concentrations encountered during each flight. Individual profiles are shown in Appendix E. Horizontal bars in the figures indicate the range of data values encountered in horizontal flights at selected altitudes. Ozone concentration generally decreases with altitude with values ranging between 62 and 78 ppbv at 2500-m MSL and between 54 and 71 ppbv at 4000-m MSL. The surface values are somewhat higher than average values reported at tract C-a during August 1975 (Singh et al. 1978). Day to day variations are noticeable in present data.

### 3.2.3 Aerosol Light Scattering and Aitken Nuclei Profiles

Light scattering coefficients and Aitken or condensation nuclei concentrations are also shown in Figures 21 and 22 as a function of elevation. Aerosol light scattering varied from about 0.5 to 1.5 times Rayleigh or clean air scattering. Visual ranges based on these light scattering values lie between about 250- and 150-km, respectively. The vertical dependence of total light scattering closely follows that for clean air, indicating that aerosol light scattering is roughly constant with altitude, i.e., the aerosol is well mixed vertically.

Aitken nulcei concentration, on the other hand, appeared to increase slightly with altitude. If, in fact, this observed increase with altitude is real, then very fine particles were being produced in elevated layers. This effect needs to be examined in more detail in future field work.

### 3.2.4 Aerosol Physical and Chemical Properties

F 23 to 27

Average aerosol volume size distributions determined from each flight are shown in Figures 23 to 27. The fine particle mode between 0.1 and 1.0 μm was quite similar from flight to flight while the coarse particle mode varied by more than a factor of 2. With an assumed particle density of 1.5 $g/cm^3$, the fine particle mode contributed about 1.7 $\mu g/m^3$ to the total aerosol mass, while the coarse mode contributed about 2 to 4 $\mu g/m^3$. The fine particle mode provided the greater contribution to aerosol light scattering.

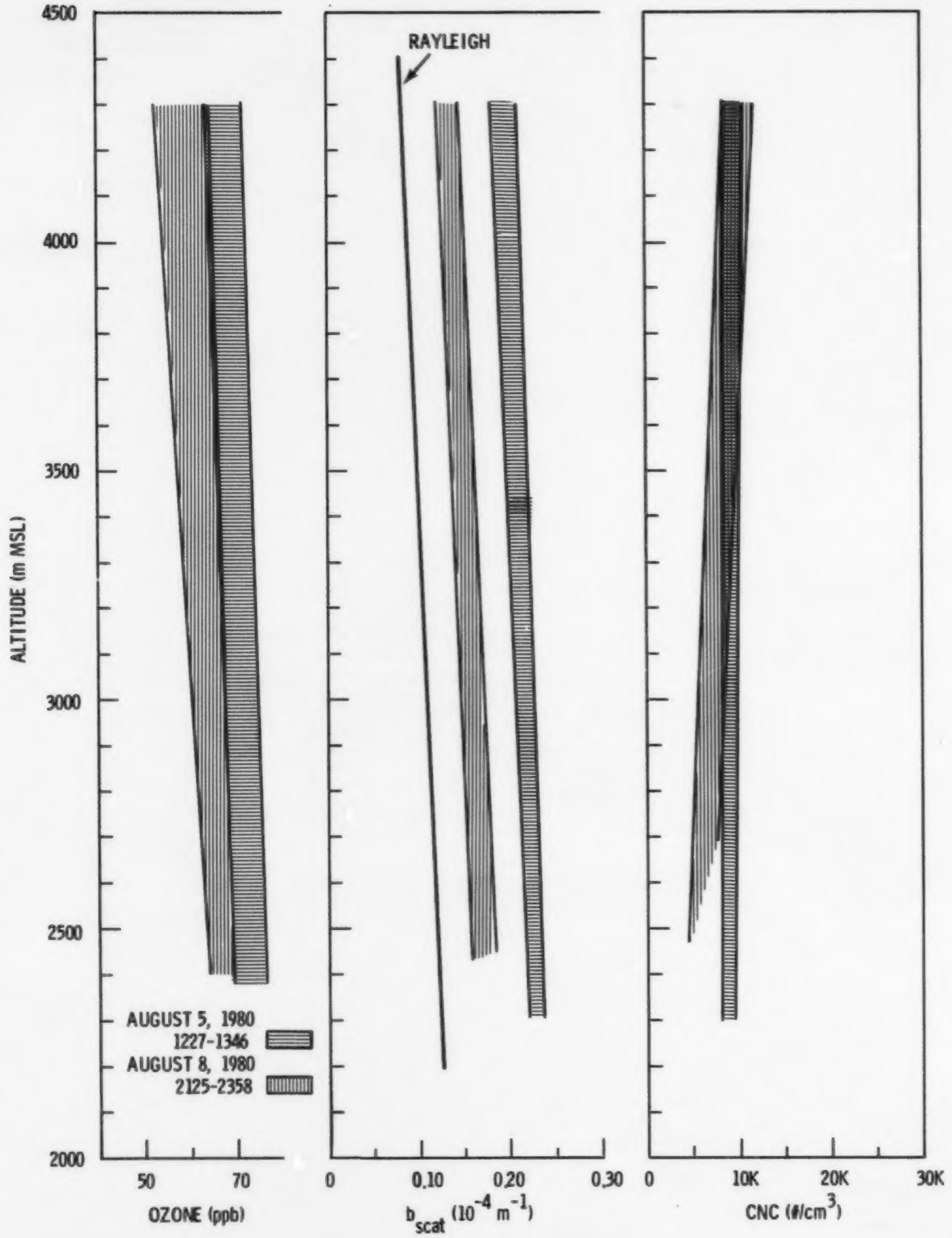

FIGURE 21. Envelopes of Vertical Profiles of Ozone Concentrations, Light Scattering Coefficients ($b_{scat}$), and Condensation Nuclei Concentrations (CNC) for Aircraft Flights of August 5 and August 8, 1980. Rayleigh Scattering Coefficients for Clean Air are Plotted for Reference.

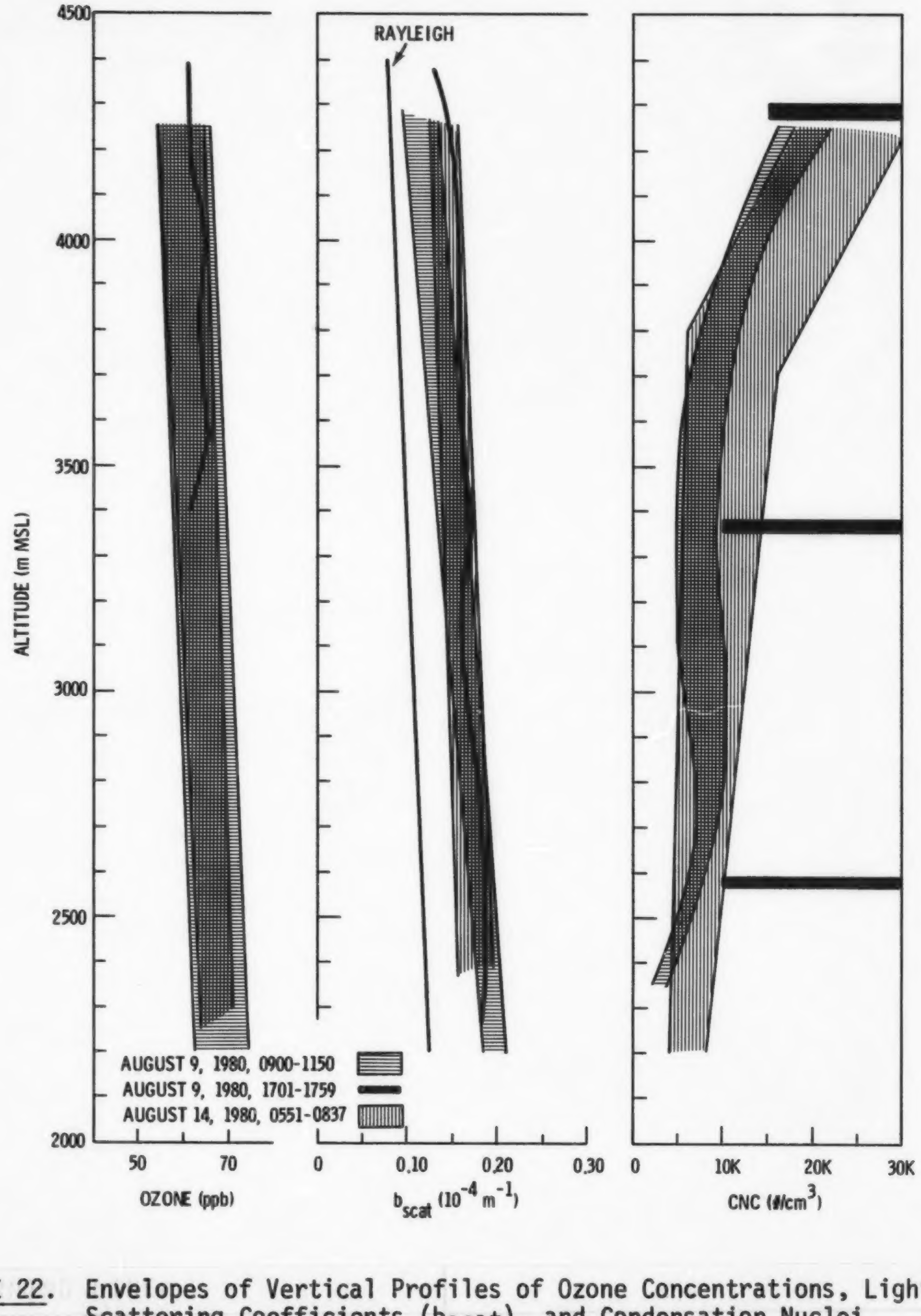

FIGURE 22. Envelopes of Vertical Profiles of Ozone Concentrations, Light Scattering Coefficients ($b_{scat}$), and Condensation Nuclei Concentrations (CNC) for Aircraft Flights of August 9 and August 14, 1980.

START LINE

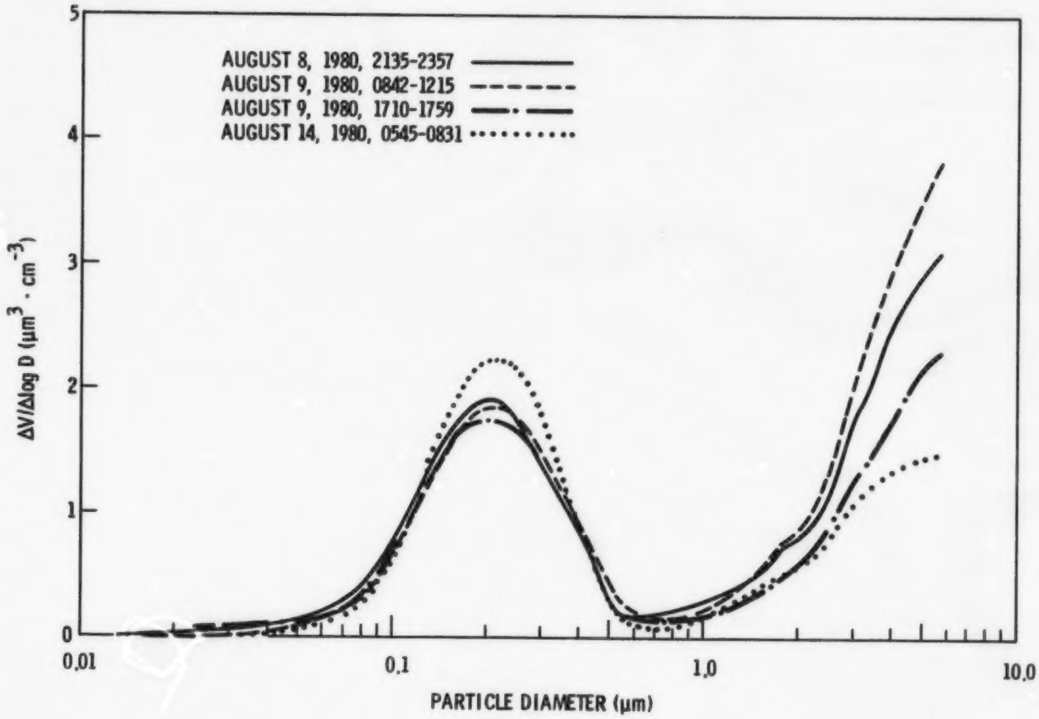

FIGURE 23. Average Particle Size Distributions Obtained From Four Aircraft Flights in August, 1980.

WARNING LINE

ENDING LINE

TYPIST PROOFER CORRECTED BY

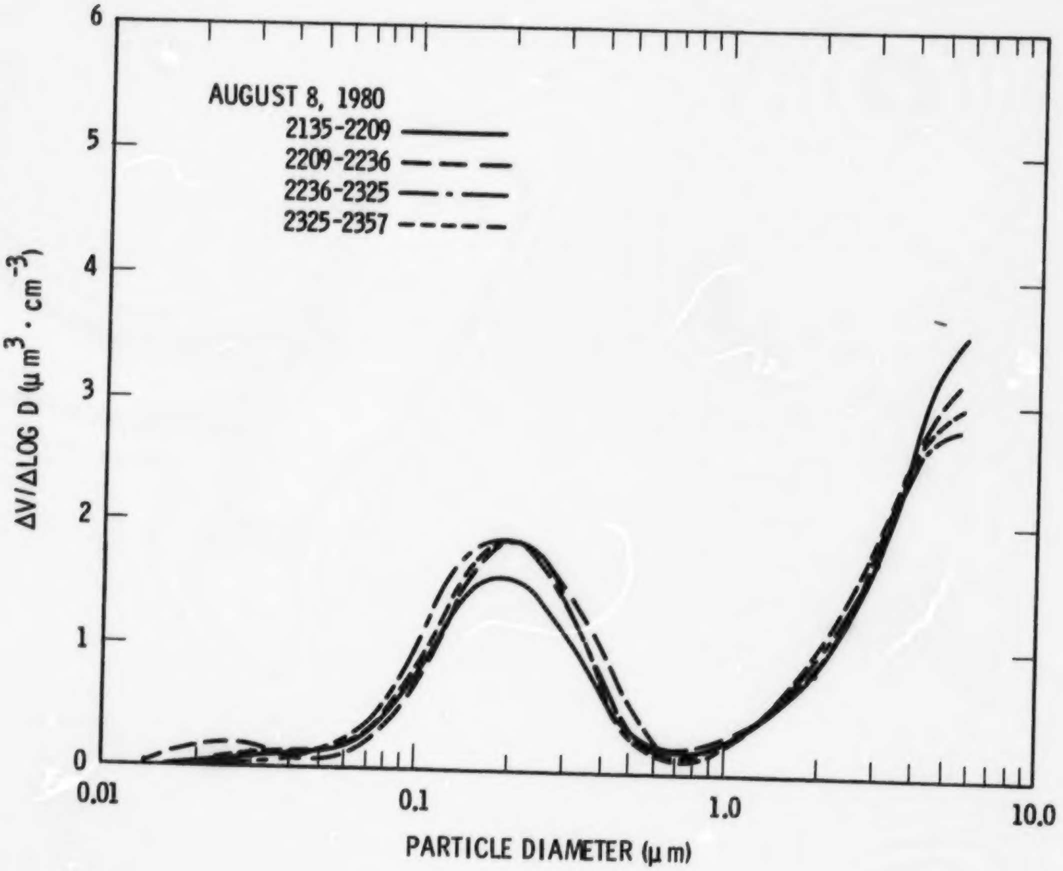

FIGURE 24. Particle Size Distributions Obtained From Aircraft on August 8, 1980, 2135 to 2357 MDT.

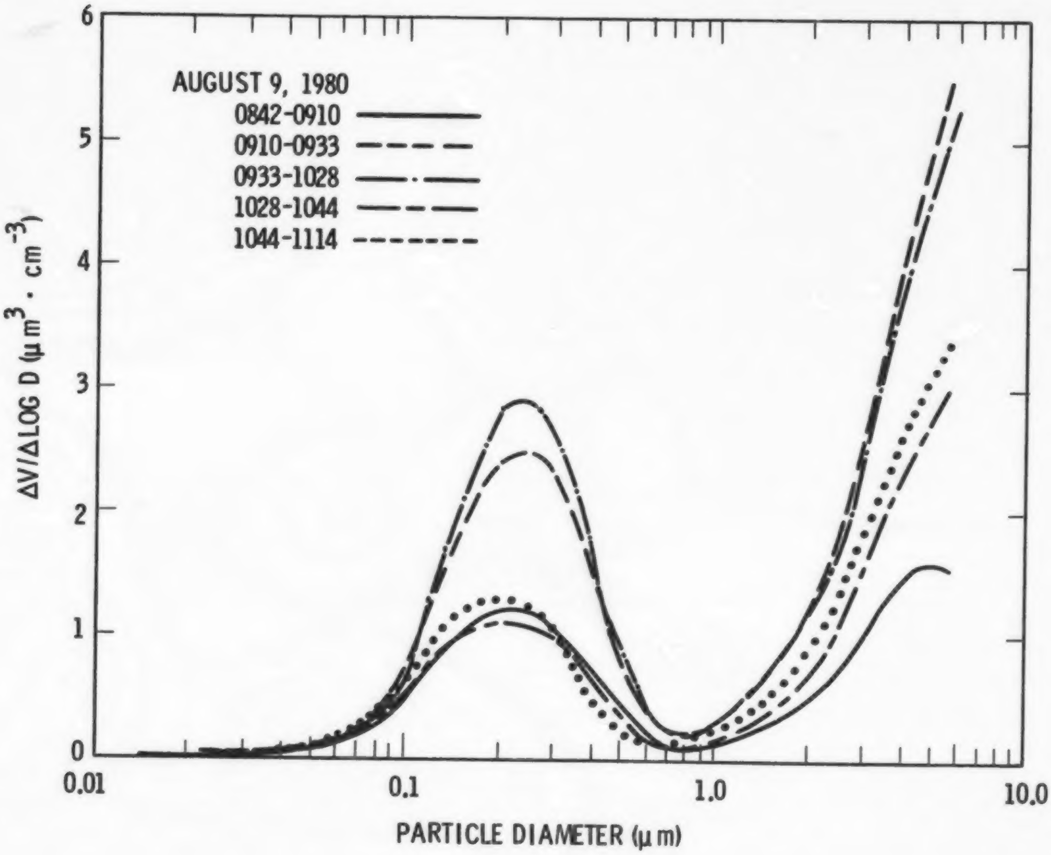

FIGURE 25. Particle Size Distributions Obtained From Aircraft on August 9, 1980, 0842 to 1114 MDT.

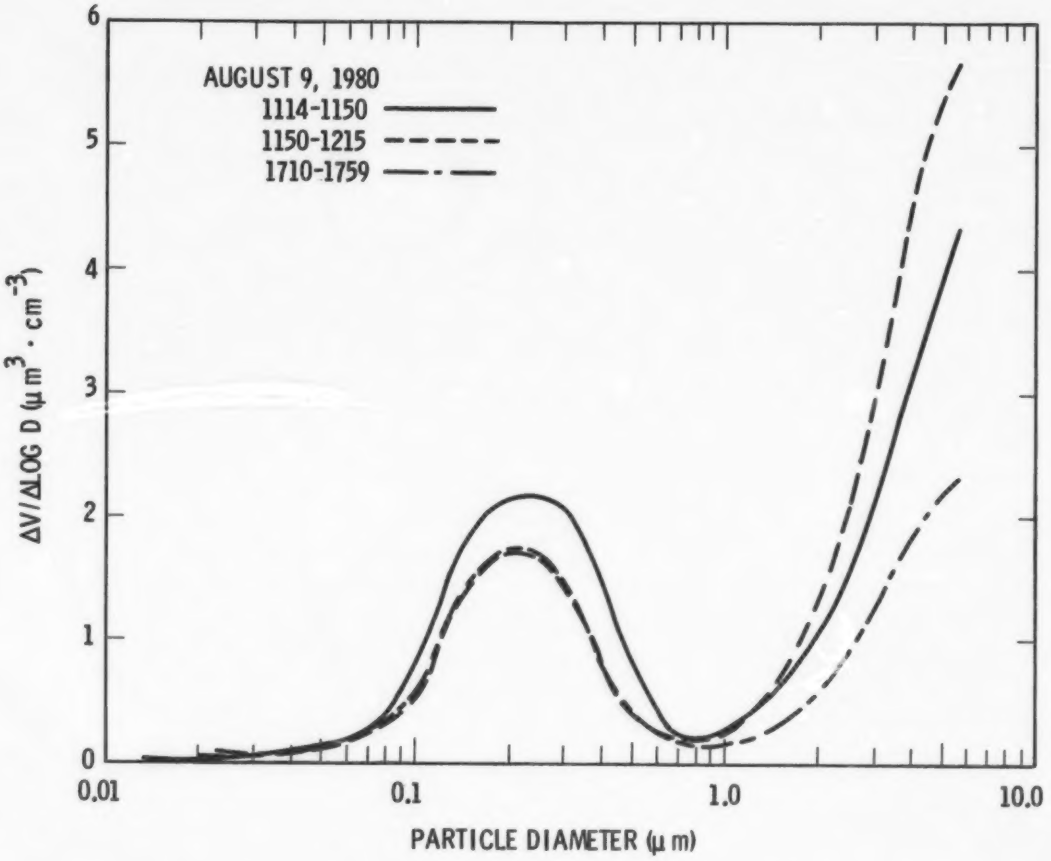

FIGURE 26. Particle Size Distributions Obtained From Aircraft on August 9, 1980, 1114 to 1759 MDT.

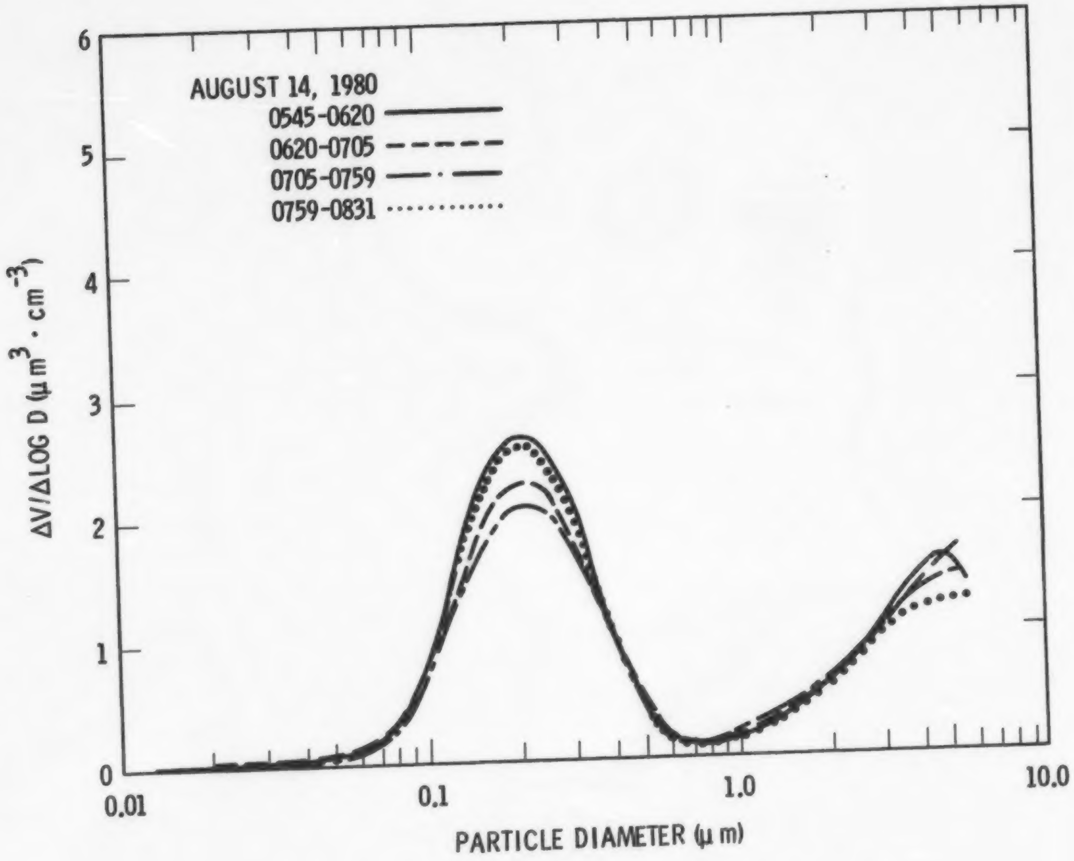

FIGURE 27. Particle Size Distributions Obtained From Aircraft on August 14, 1980, 0545 to 0831 MDT.

WARNING LINE

ENDING LINE

PAGE REF

TYPIST PROOFER CORRECTED BY

Elemental and ionic composition of aerosol collected on filters and analyzed by xray fluorescence (XRF), neutron activation (NAA), and ion chromatography (IC) are summarized in Tables 9 and 11. Standard deviations are given for reference, when available. Table 9 lists the element, the average crustal concentration (Bowen, 1966), minimum/maximum and average air concentration and the enrichment factor referenced to aluminum (Al) determined by XRF. Except for S, Br, and Pb (As, Se, Cd were very near the detection limit of XRF and are probably quite uncertain), all elements have no enrichment with respect to crustal materials. Enhanced concentrations of S, Br, and Pb indicate that automotive exhaust, presumably of local origin, contributed to the observed aerosol loadings. Table 10 lists the average ionic composition of the ambient aerosol as determined by IC. Only sulfate and perhaps nitrate were present in significant amounts. A comparison between XRF and IC methods is possible for sulfur. The average air concentration of $SO_4^{--}$ by IC was 0.71 ± 0.09 $\mu g/m^3$ while the value obtained from XRF (assuming that all sulfur is present as $SO_4^{--}$) was 1.10 ± 0.48 $\mu g/m^3$. Elemental concentrations determined by XRF and NAA are compared in Table 11 for several elements. In general, the two methods agree within the variance of the measurements.

### 3.2.5 Solar and Ultraviolet Radiation

The average solar and ultraviolet radiation measured by aircraft on constant altitude, fixed heading flight legs is presented in Table 12. The time intervals over which the measurements were taken, the flight altitudes, and the standard deviations of the measurements are given in the table.

## 3.3 Tracer Experiment Measurements

Dual tracers were used to investigate air motion and plume depletion by dry deposition. Plume depletion could be determined from the decrease in the $SF_6$ concentration/particle concentration ratio between the two real-time tracer measurement sites, i.e., between the Visitor's Center and Meteorological Site 3. In this section tracer concentration data will be presented in graphical form. Subsequent reports will also consider calibration factors to adjust measured responses for each lithium detector and the estimated tracer particle release rate. At that time both the $SF_6$ gas and lithium-traced

BEGIN FIRST LINE OF TEXT HERE
CENTER OF PAGE
TOP OF IMAGE AREA
DROPPED HEAD: BEGIN SECTIONS HERE
6-1/2"
9-1/2"
BEGIN LAST LINE OF TEXT
BOTTOM OF IMAGE AREA; OUTSIDE DIMENSION FOR TABLES AND ILLUSTRATIONS
3/8"
PAGE NUMBER
EPA Form 2350-4 (4-80)
(PREVIOUSLY CIN. EPA FORM 287)
☆ U.S. GOVERNMENT PRINTING OFFICE 1980-660-639
TYPING GUIDE SHEET

## TABLE 9. Particulate Elemental Composition as Determined by X-Ray Fluorescence Analysis of Filter Samples

| Element | Crustal[1] Concentration (ppm) | Minimum-Maximum Air Concentration (ng/m³) | Average Air[2] Concentration (ng/m³) | Enrichment[3] Factor E |
|---|---|---|---|---|
| Al | 71,000 | 110 - 1910 | 550 ± 16 | 1 |
| Si | 330,000 | 830 - 6090 | 1665 ± 640 | 0.65 ± 0.25 |
| S | 700 | 90 - 540 | 383 ± 122 | 71 ± 23 |
| Cl | -- | 20 - 360 | 105 ± 52 | -- |
| K | 14,000 | 60 - 520 | 172 ± 73 | 1.6 ± 0.7 |
| Ca | 13,700 | 10 - 1430 | 430 ± 200 | 4 ± 2 |
| Ti | 5,000 | 10 - 120 | 37 ± 16 | 1.0 ± 0.4 |
| V | 100 | 7 - 80 | 2.5 ± 1.0 | 3.2 ± 1.3 |
| Cr | 100 | 1 - 8 | 2.5 ± 1.4 | 3.2 ± 1.8 |
| Mn | 850 | 3 - 20 | 6.8 ± 2.6 | 1.0 ± 0.4 |
| Fe | 38,000 | 130 - 1230 | 310 ± 144 | 1.1 ± 0.5 |
| Ni | 40 | 0.5 - 6 | 2.2 ± 1.5 | 7 ± 5 |
| Cu | 20 | 2 - 6 | 2.8 ± 1.2 | 18 ± 8 |
| Zn | 50 | 6 - 15 | 9 ± 3 | 23 ± 8 |
| As | 6 | <1 - 4 | <2 ± 1 | <43 ± 22 |
| Se | 0.2 | <0.5 - 2 | <1.0 ± 0.6 | <210 ± 130 |
| Br | 5 | 2 - 3 | 2.7 ± 0.4 | 70 ± 10 |
| Cd | 0.06 | 4 - 21 | <10 ± 4 | ? |
| Ba | 500 | <19 - 80 | 50 ± 17 | 13 ± 4 |
| Pb | 10 | 4 - 13 | 7 ± 3 | 90 ± 40 |

---

1. From Bowen (1966).
2. Minimum/maximum values not included in average.
3. $E = \left[X_{air} / X_{air\ ref}\right] / \left[X_{crust} / X_{crust\ ref}\right]$, $X_{ref}$ = Al.

TABLE 10. Ionic Composition of Atmospheric Particulates Derived From Aircraft Filter Samples by Ion Chromatography

| Ion | Minimum-Maximum Air Concentration ($\mu g/m^3$) | Average Air Concentration ($\mu g/m^3$) |
|---|---|---|
| $SO_4^{--}$ | 0.61 - 0.82 | 0.71 ± 0.09[1] |
| $NO_3^-$ | 0.01 - 0.42 | 0.26 ± 0.14 |
| $NH_4^+$ | 0.06 - 0.15 | 0.10 ± 0.03 |
| $Na^+$ | 0.05 - 0.30 | 0.13 ± 0.08 |
| $K^+$ | 0.03 - 0.16 | 0.06 ± 0.04 |

TABLE 11. Ratio of Elemental Composition Results From X-Ray Fluorescence Analysis and Neutron Activation For Four Filter Samples

| Element | Ratio[1] |
|---|---|
| Al | 0.83 ± 0.38 |
| Cl | 1.00 ± 0.20 |
| Mn | 0.91 ± 0.33 |
| Ti | 0.94 ± 0.29 |
| Br | 1.00 ± 0.34 |

---

[1] $(X^{XRF}/X^{NAA})$

## TABLE 12. Solar and Ultraviolet Radiation Over the Oil Shale Area During August 1980[1]

| Date | Time (MDT) | Altitude m-MSL | Solar[1] (W/m²) | UV[1] (W/m²) |
|---|---|---|---|---|
| August 5 | 1113 - 1122 | 1810 | 841 ± 7 | 11.1 ± 0.1 |
| | 1127 - 1133 | 2430 | 791 ± 9 | 11.5 ± 0.1 |
| | 1141 - 1150 | 3200 | 870 ± 10 | 12.8 ± 0.1 |
| | 1156 - 1204 | 3970 | 851 ± 12 | 13.1 ± 0.2 |
| | 1204 - 1226 | 3970 | 923 ± 12 | 13.9 ± 0.2 |
| | 1320 - 1326 | 4257 | 941 ± 10 | 13.9 ± 0.1 |
| | 1350 - 1407 | 2433 | 920 ± 9 | 13.0 ± 0.2 |
| August 9 | 0926 - 0930 | 2490 | 563 ± 12 | 6.9 ± 0.1 |
| | 0934 - 0940 | 2230 | 542 ± 9 | 7.0 ± 0.1 |
| | 0945 - 0950 | 2970 | 615 ± 10 | 7.8 ± 0.1 |
| | 0955 - 1003 | 3610 | 630 ± 23 | 8.6 ± 0.3 |
| | 1008 - 1015 | 4240 | 703 ± 16 | 9.5 ± 0.2 |
| | 1017 - 1023 | 4230 | 652 ± 11 | 9.3 ± 0.1 |
| | 1042 - 1050 | 2820 | 718 ± 12 | 9.7 ± 0.2 |
| | 1050 - 1057 | 3540 | 754 ± 9 | 10.3 ± 0.2 |
| | 1057 - 1105 | 4080 | 777 ± 13 | 10.9 ± 0.2 |
| | 1107 - 1113 | 4200 | 876 ± 15 | 12.2 ± 0.2 |
| | 1141 - 1148 | 3050 | 868 ± 19 | 12.0 ± 0.3 |
| | 1148 - 1204 | 3300 | 878 ± 11 | 12.3 ± 0.2 |
| | 1204 - 1214 | 3250 | 897 ± 12 | 12.6 ± 0.2 |
| August 9 | 1704 - 1711 | 1835 | 521 ± 12 | 6.8 ± 0.1 |
| | 1718 - 1725 | 2590 | 550 ± 15 | 6.7 ± 0.2 |
| | 1729 - 1736 | 3380 | 472 ± 14 | 6.4 ± 0.1 |
| | 1748 - 1755 | 4290 | 476 ± 23 | 6.2 ± 0.2 |
| August 14 | 0752 - 0756 | 4240 | 216 ± 3 | 2.9 ± 0.1 |
| | 0803 - 0808 | 4230 | 284 ± 13 | 3.5 ± 0.1 |

---

[1] Averaged over constant altitude fixed heading flight legs.

BEGIN FIRST LINE OF TEXT HERE
CENTER OF PAGE
TOP OF IMAGE AREA
DROPPED HEAD: BEGIN SECTIONS HERE

particle concentrations will be normalized to their respective release rates and related to meteorological measurements.

A summary of the five tracer experiments is presented in Table 13. The first four experiments were conducted in nocturnal drainage flows, while the fifth was a daytime release. Tracer results for the four nighttime releases are summarized in the following sections. Insufficient data were obtained for the daytime release since air bag samplers were not operated and airflow only occasionally delivered $SF_6$ tracer to the real-time sampling sites. Supporting meteorological data for the tracer experiments were collected by the Los Alamos National Laboratory and by the Rio Blanco Oil Shale Company. These data, collected from a minisonde sounding system, pilot balloons, a tethered balloon sounding system and a network of towers, have been previously published by Clements et al. (1981).

Before discussing the data, it will be useful to summarize the experimental design of the radio-controlled bag sampling lines to clarify the relationship between sampling intervals on the different lines. Two radio-controlled signal tones were used to activate air pumps for bag sampling. The first signal tone activated (or deactivated) all air pumps on sampling lines 1 and 2. The second signal tone controlled pumps on lines 3 and 4. Sampling lines 1 and 3 consisted of sequential sampler stations, while lines 2 and 4 consisted of profile sampling stations. Thus, profile samples on lines 2 and 4 were collected during the same time intervals as the first sample in the sequential series on lines 1 and 3, respectively.

Tracer concentration data were obtained at the sampling sites and times given in Table 14. The table shows the figures in which the data can be found. As shown in the table, some data are missing. This is because:

- all equipment was not operational for the first experiments,
- some bag samples were contaminated due to delays in analysis, and
- some equipment was not operated during certain experiments.

The four nighttime experiments are summarized in the following sections.

BEGIN LAST LINE OF TEXT
3/8"
BOTTOM OF IMAGE AREA; OUTSIDE DIMENSION FOR TABLES AND ILLUSTRATIONS

PAGE NUMBER
EPA Form 2350-4 (4-80)
(PREVIOUSLY CIN. EPA FORM 287)
TYPING GUIDE SHEET

TABLE 13. Summary of Tracer Releases

| Run No. | Dates, August 1980 | Tracer Release Time, MDT, hr:min |  |  | TRACERS RELEASED |  |
|---|---|---|---|---|---|---|
|  |  | Start |  | End | $SF_6$, lbs/hr | Particulates |
| 1 | 6 | 00:01 | to | 01:02 | 12 | Yes |
| 2 | 7 to 8 | 23:15 | to | 00:15 | 12 | No |
| 3 | 9 to 10 | 23:15 | to | 00:15 | 12.5 | Yes |
| 4 | 11 to 12 | 23:46 | to | 00:46 | 16.5 | Yes |
| 5 | 13 | 15:05 | to | 15:59 | variable | No |

## TABLE 14. Figure Listing for Tracer Data

|  |  | Real-Time Tracer Data |  | Radio-Controlled Bag Sampling Stations[1] |  |  |  | Syringe Sample |
|---|---|---|---|---|---|---|---|---|
| Run No. | Dates August 1980 | $SF_6$ | Particulate | Line 1, Sequential[2] Stations at 1.6 km | Line 2, Profile[3] Stations at 2.5 km | Line 3, Sequential[2] Stations at 4.6 km | Line 4, Profile[3] Stations at 5.6 km | Line 5, From Vehicle at $\sim$6.8 km |
| 1 | 5 to 6 | Fig. 28 | Fig. 28 | Fig. 29 | Fig. 30 | -- | Fig. 31 | -- |
| 2 | 7 to 8 | Fig. 32 | -- | Fig. 33 | Fig. 34 | -- | -- | Fig. 35 |
| 3 | 9 to 10 | Fig. 36 | Fig. 36 | -- | Fig. 37 | Fig. 38 | Fig. 39 | Fig. 40 |
| 4 | 11 to 12 | Fig. 41 | Fig. 41 | -- | -- | -- | -- | Fig. 42 |

---

1. The distances listed are measured from the tracer release site.
2. Sequential stations (sampling at three selected time periods at a sampling height of 1.7-m.)
3. Profile stations (simultaneous sampling at three heights of 0.3-, 1.3, and 5-m.)

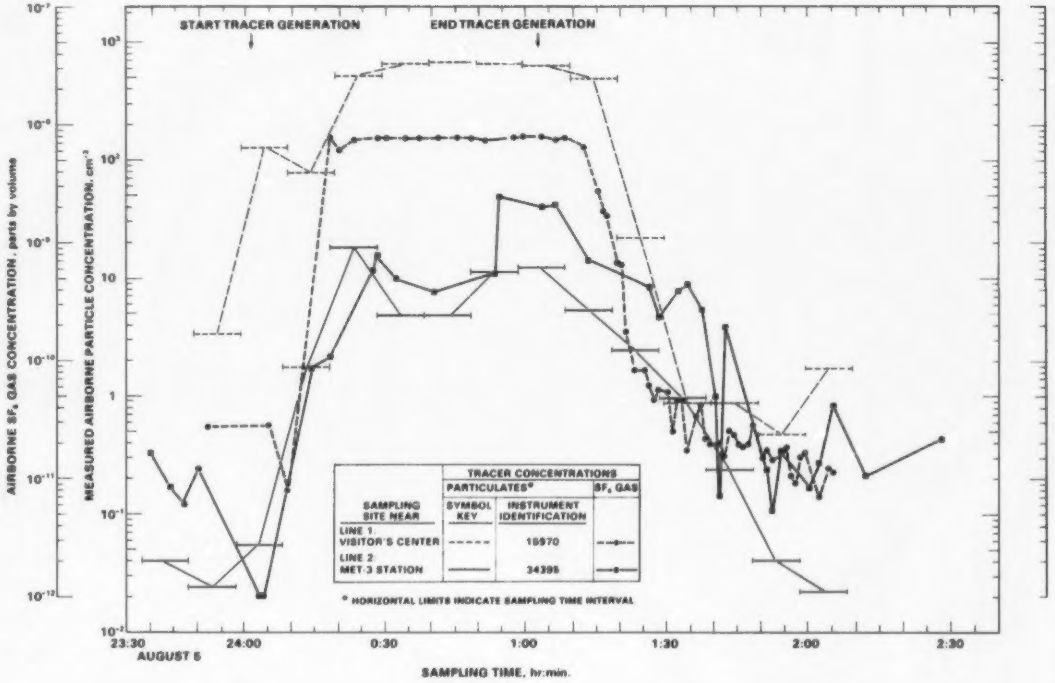

FIGURE 28. Airborne Tracer Particle and SF$_6$ Concentrations as a Function of Time, Night of August 5 to 6, 1980.

Neg. 80J402-15

BEGIN FIRST LINE OF TEXT HERE
CENTER OF PAGE
TOP OF IMAGE AREA
DROPPED HEAD; BEGIN SECTIONS HERE

### 3.3.1 Run 1, August 5 to 6

Real-time $SF_6$ gas and lithium-traced particulate concentrations are shown in Figure 28 for the Visitor's Center and Meteorological Site 3 sampling stations. Tracers were released from 0001 to 0102 MDT. For $SF_6$ tracer gas, measured concentrations are shown at each sampling time. Data points are connected by straight lines. For lithium-traced particulates, instrument counts were accumulated for 10-minute sampling intervals. Each time interval is indicated by a horizontal line with time limit bars. Straight lines are connected between mid-points of the time intervals.

Sequential sampling data for airborne $SF_6$ concentrations measured along sampling line 1 are shown in Figure 29. The data are shown in the upper sub-figure as a function of sampling time (0032 to 0042, 0050 to 0059, and 0017 to 0125 MDT) and distance from the Corral Gulch centerline. The ground contours and station locations are shown in the lower sub-figure. As indicated by the vertical lines on the valley cross section, three sampling stations were on the valley floor and two stations were located on each sidewall. Drainage flow is from the reader into the figure. North is to the left and south to the right.

Vertical profiles of $SF_6$ concentrations were taken on sampling lines 2 and 4. These data are presented in Figures 30 and 31, respectively. The Meteorological Site 3 sampling station is a real-time tracer measurement station and is directly upwind of sampling line 2. The location of this site's projection onto sampling line 2 is indicated in Figure 30 and in subsequent figures showing concentrations along line 2. Comparison of Figures 30 and 31 shows that the tracer plume initially traveled along the northern hillside of the valley, but diffused horizontally across the valley as it traveled between tracer lines 2 and 4.

### 3.3.2 Run 2, August 7 to 8

$SF_6$ concentrations for August 7 to 8 are shown in Figures 32 through 35. Due to a malfunction of the air compressor, lithium-traced particulates were not released in this experiment. Airborne $SF_6$ concentrations for the two real-time stations are shown in Figure 32. Concentrations measured as a

BEGIN LAST LINE OF TEXT
BOTTOM OF IMAGE AREA; OUTSIDE DIMENSION FOR TABLES AND ILLUSTRATIONS

PAGE NUMBER
EPA Form 2350-4 (4-80)
(PREVIOUSLY CIN. EPA FORM 287)
☆ U.S. GOVERNMENT PRINTING OFFICE: 1980-660-F39
TYPING GUIDE SHEET

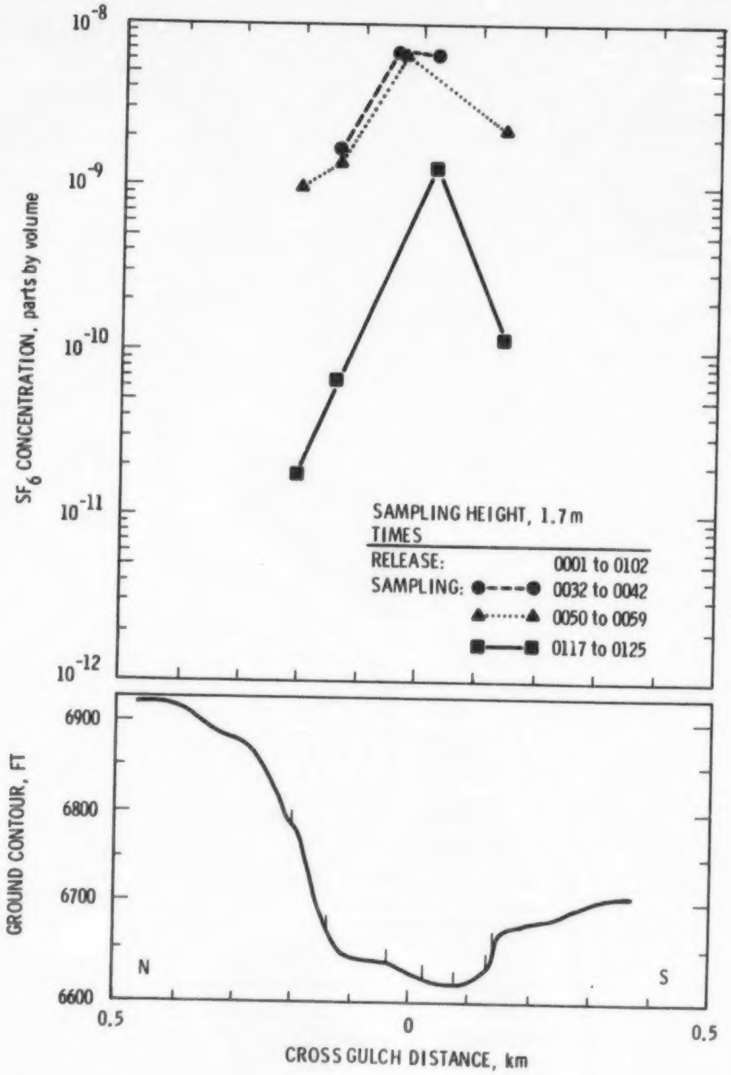

FIGURE 29. $SF_6$ Concentrations at 1.7-m as a Function of Cross-Valley Position on Sampling Line 1 for Three Sampling Time Intervals, Night of August 5 to 6, 1980.

Neg. 80J402-5

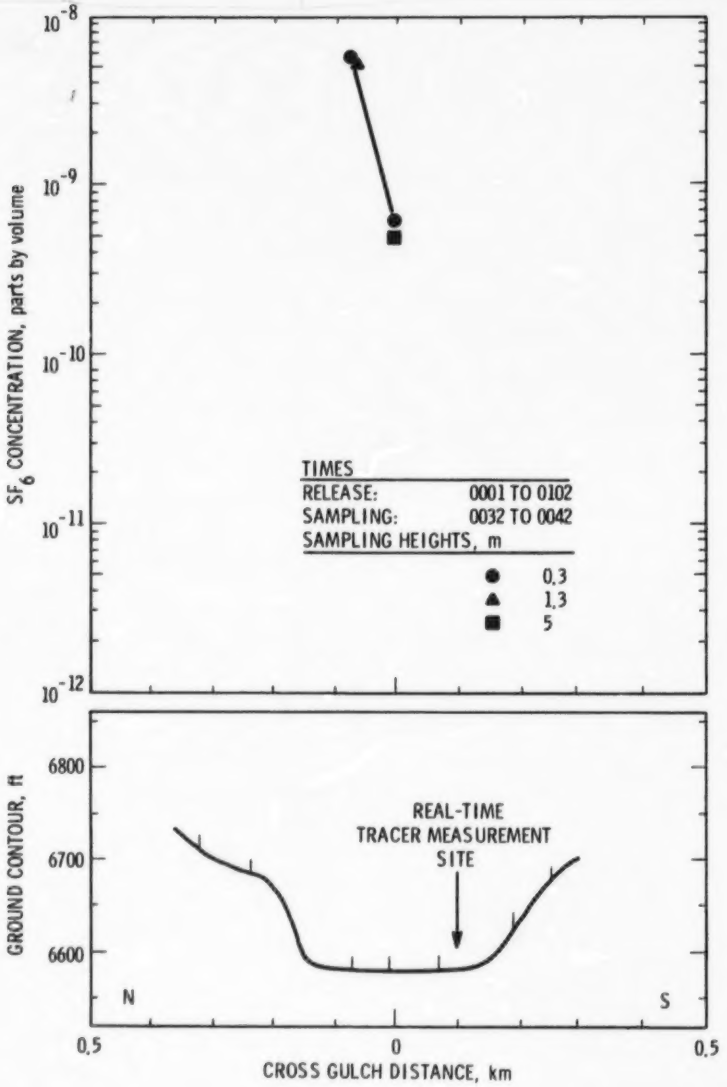

FIGURE 30. SF$_6$ Concentrations at Three Heights as a Function of Cross Valley Position on Sampling Line 2, Night of August 5 to 6, 1980.

Neg. 80J402-14

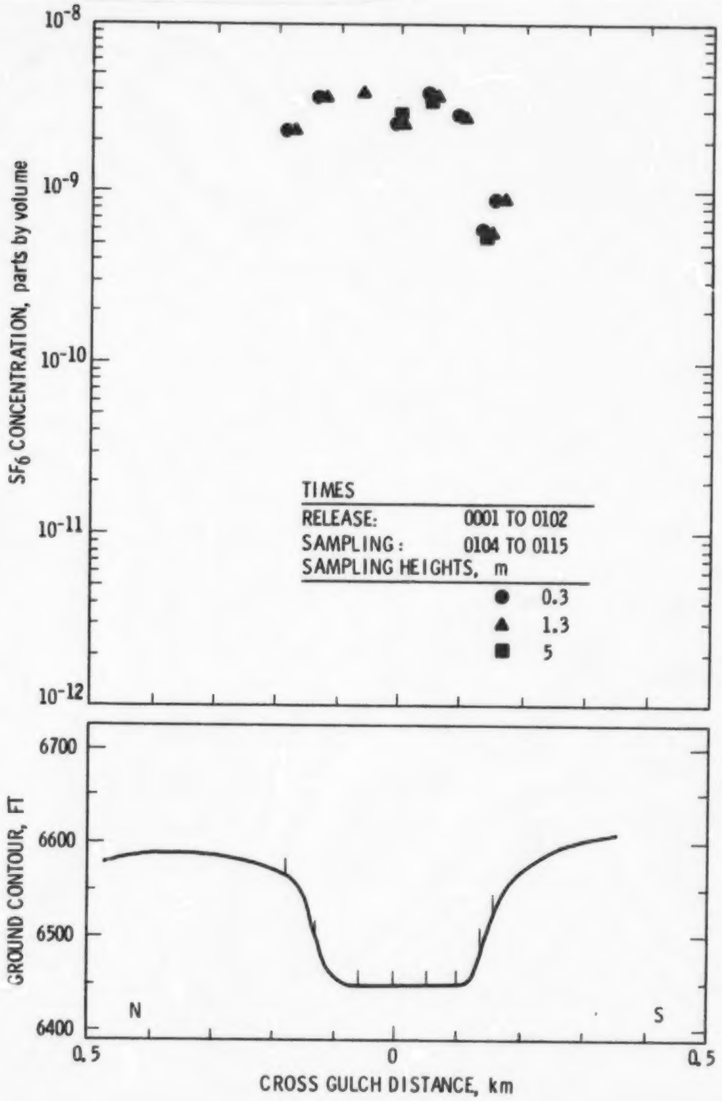

FIGURE 31. $SF_6$ Concentrations at Three Heights as a Function of Cross Valley Position on Sampling Line 4, Night of August 5 to 6, 1980. Neg. 80J402-3

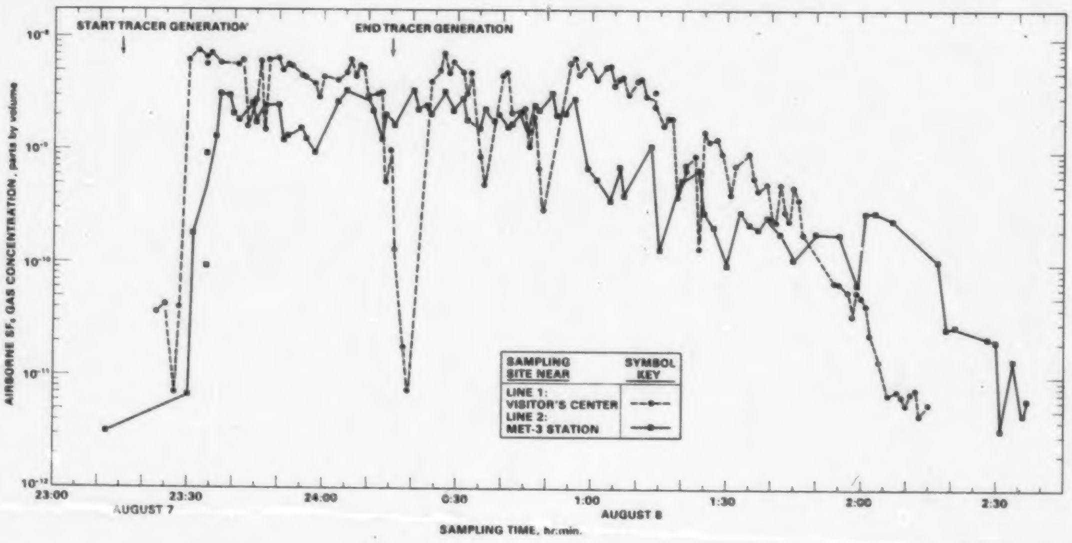

FIGURE 32. $SF_6$ Concentrations as a Function of Time, Night of August 7 to 8, 1980.

Neg. 80J402-11

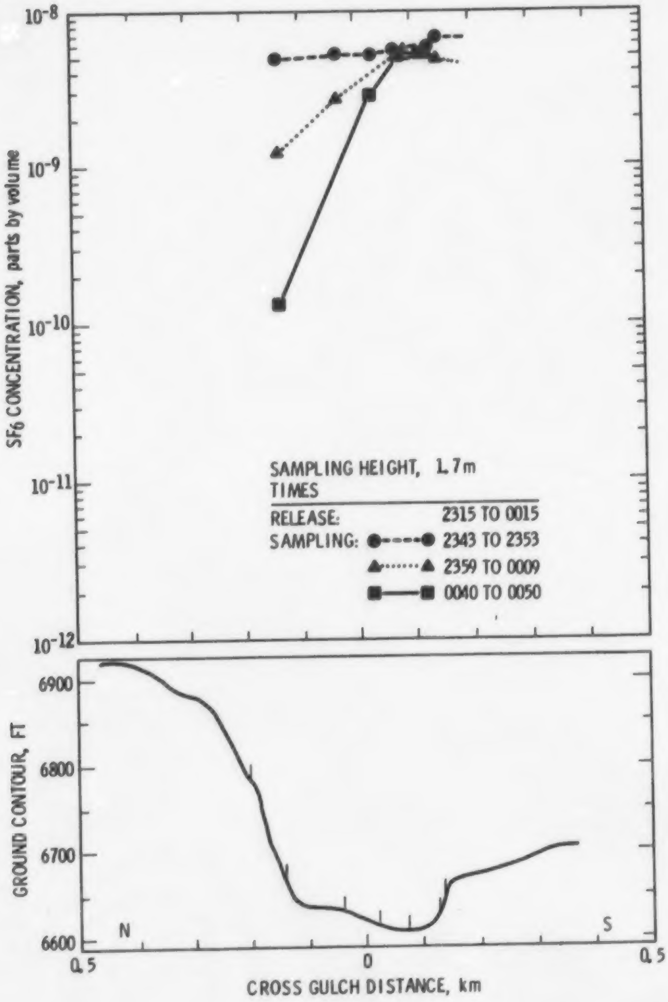

FIGURE 33. $SF_6$ Concentrations at 1.7-m as a Function of Cross Valley Position on Sampling Line 1 for Three Sampling Time Intervals, Night of August 7 to 8, 1980.

Neg. 80J402-13

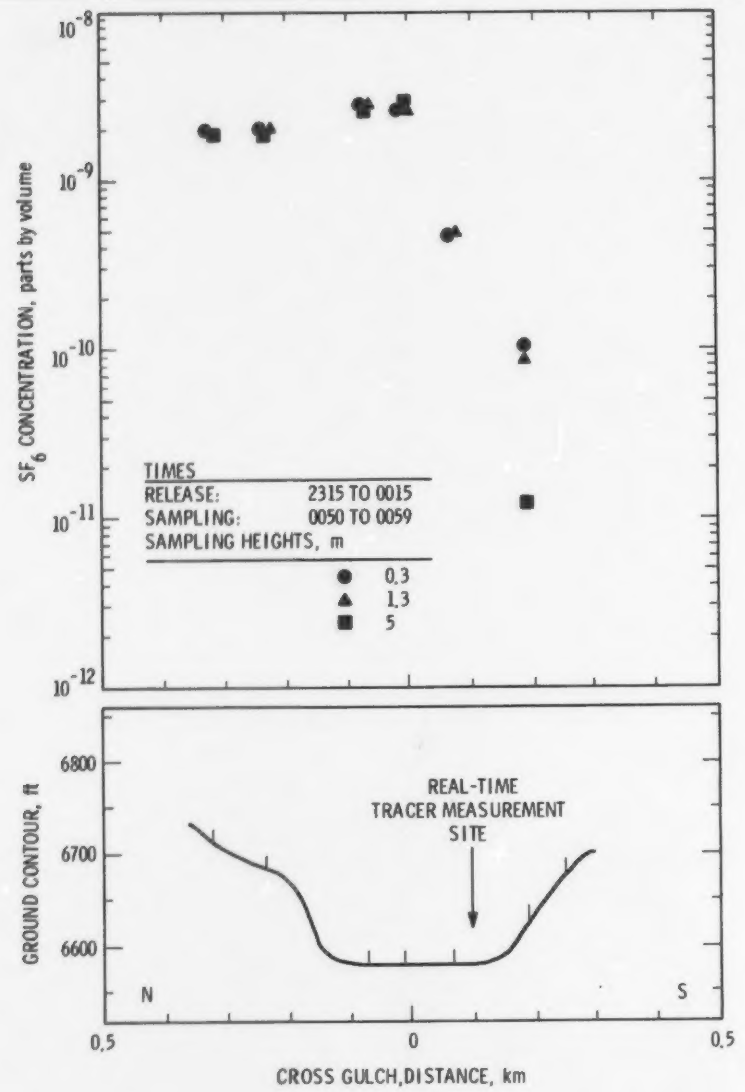

FIGURE 34. $SF_6$ Concentrations at Three Heights as a Function of Cross Valley Position on Sampling Line 2, Night of August 7 to 8, 1980. Neg. 80J402-10

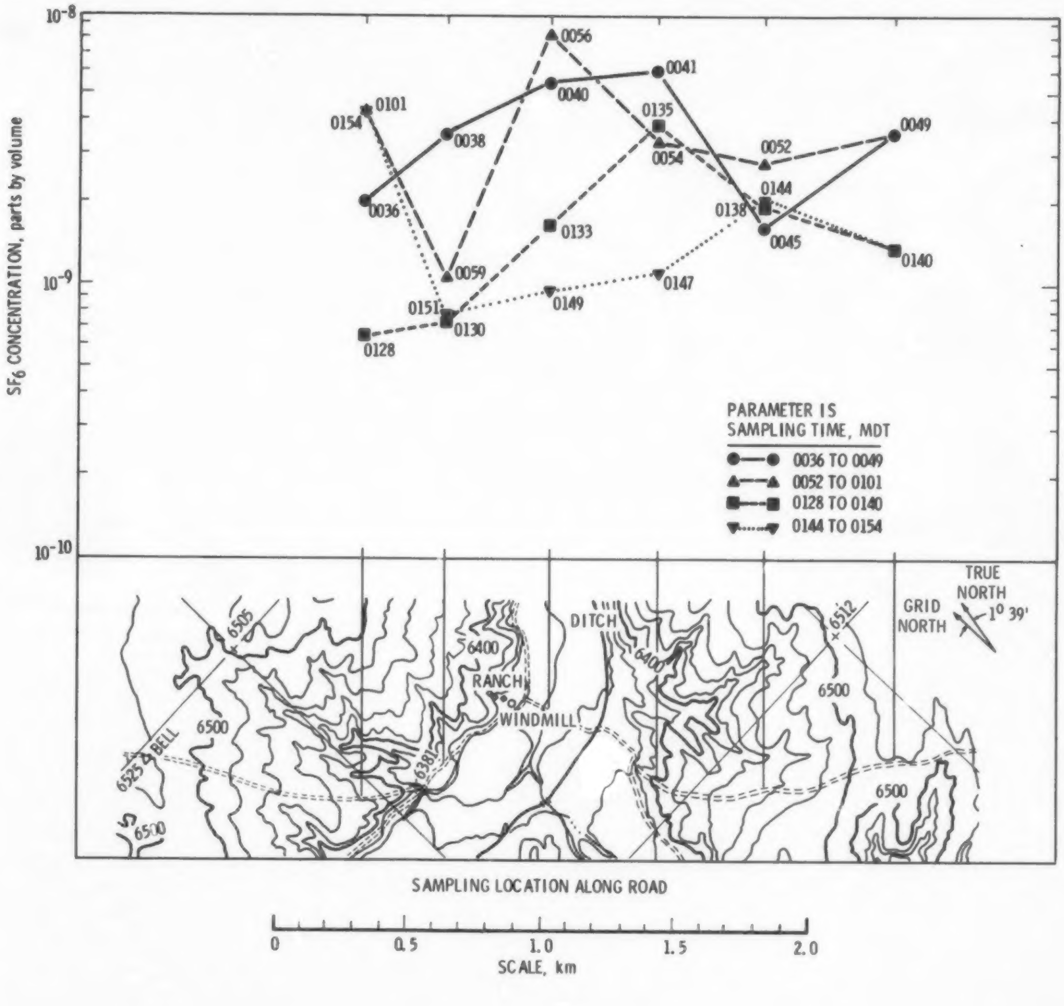

FIGURE 35. SF$_6$ Concentrations as a Function of Cross Valley Position as Determined From Four Mobile Traverses With Syringe Samplers, Night of August 7 to 8, 1980. Neg. 80J402-6

function of time along sampling line 1 are shown in Figure 33. Concentrations measured as a function of height along sampling line 2 are shown in Figure 34. A strong gradient in $SF_6$ concentrations across the valley is apparent in the figure.

$SF_6$ concentrations determined from syringe samples collected along roads approximately 6.8 km downwind of the release point are shown in Figure 35. Vertical lines extending from the topographic sub-figure of Figure 35 to the upper sub-figure identify the sampling locations. Samples were collected from a single vehicle in four sample collection traverses along the roads. The first traverse started at the left side of the figure at 0036 and ended at the right side of the figure at 0049 MDT. The sampling time is shown adjacent to each data symbol.

### 3.3.3 Run 4, August 9 to 10

Airborne tracer concentrations for August 9 to 10 are shown in Figures 36 to 40.

### 3.3.4 Run 4, August 11 to 12

Airborne tracer concentrations for August 11 to 12 are shown in Figures 41 and 42.

EPA Form 2350-4 (4-80)
(PREVIOUSLY CIN. EPA FORM 287)
TYPING GUIDE SHEET

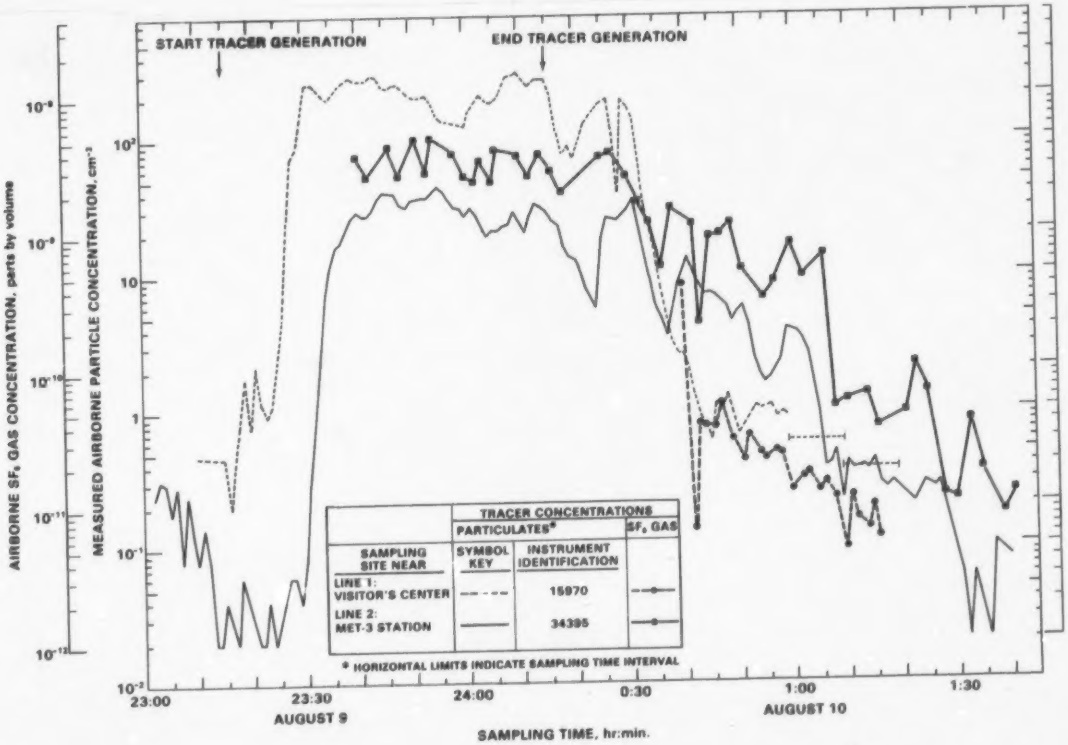

FIGURE 36. Airborne Tracer Particle and $SF_6$ Concentrations as a Function of Time, Night of August 9 to 10, 1980.

Neg. 80J402-9

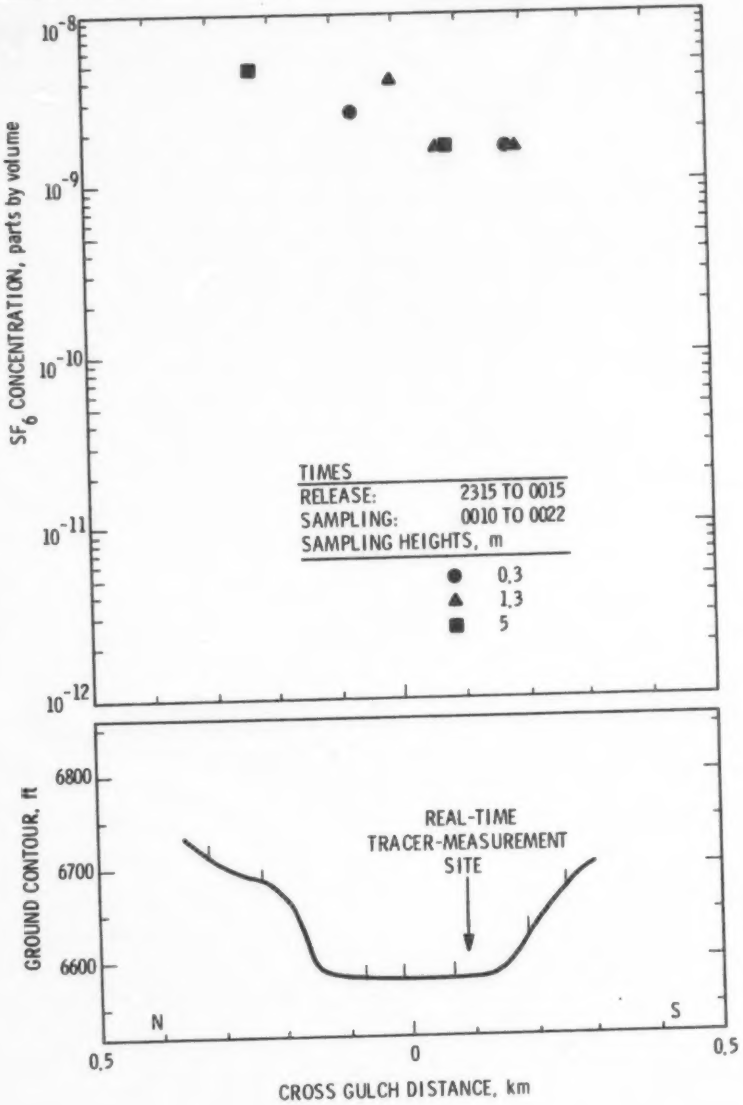

FIGURE 37. $SF_6$ Concentrations at Three Heights as a Function of Cross Valley Position on Sampling Line 2, Night of August 9 to 10, 1980. Neg. 80J402-1

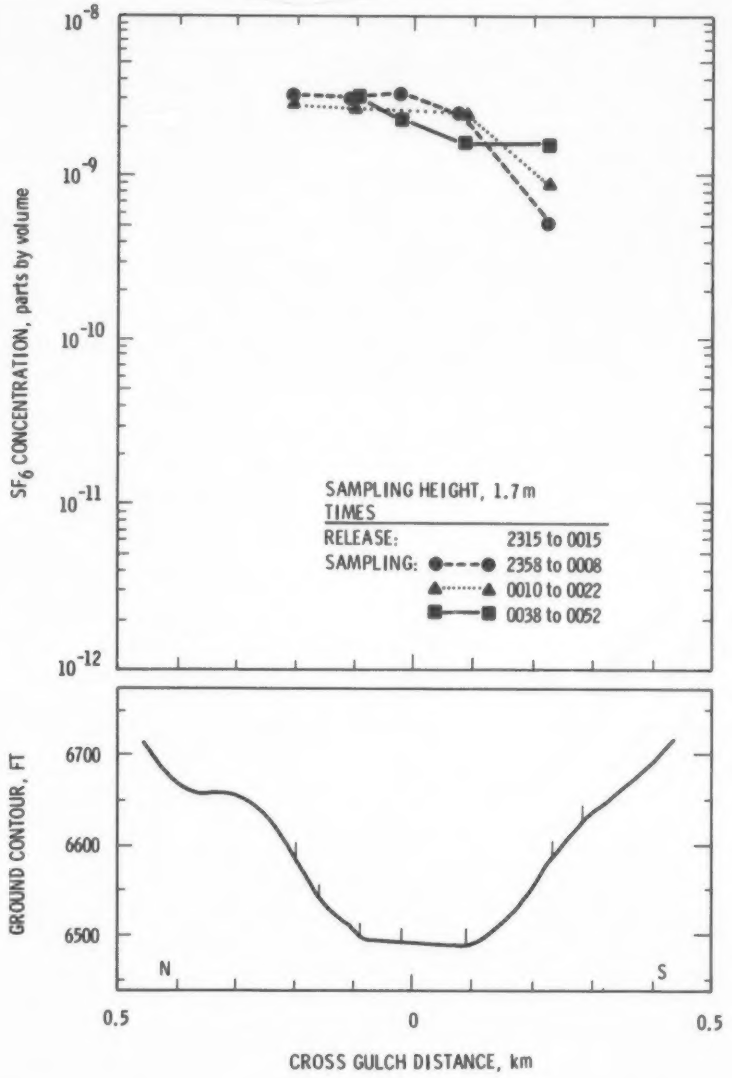

FIGURE 38. $SF_6$ Concentrations at 1.7-m as a Function of Cross Valley Position on Sampling Line 3, Night of August 9 to 10, 1980.

Neg. 80J402-2

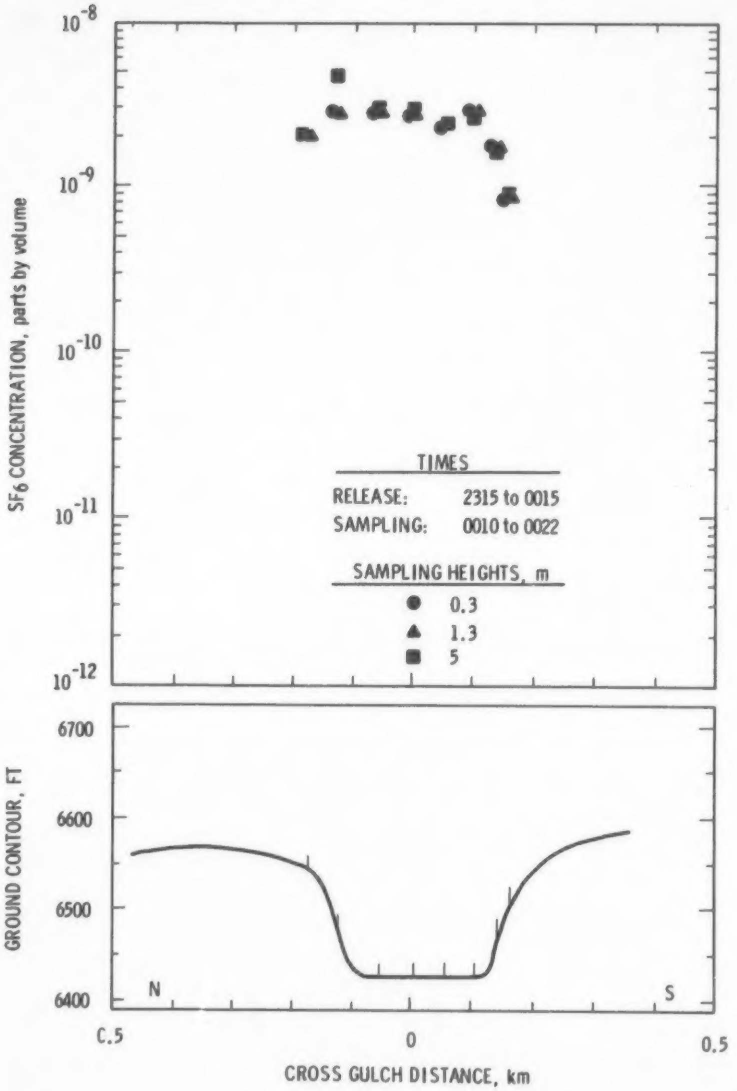

FIGURE 39. $SF_6$ Concentrations at Three Heights as a Function of Cross Valley Position on Sampling Line 4, Night of August 9 to 10, 1980. Neg. 80B935-3

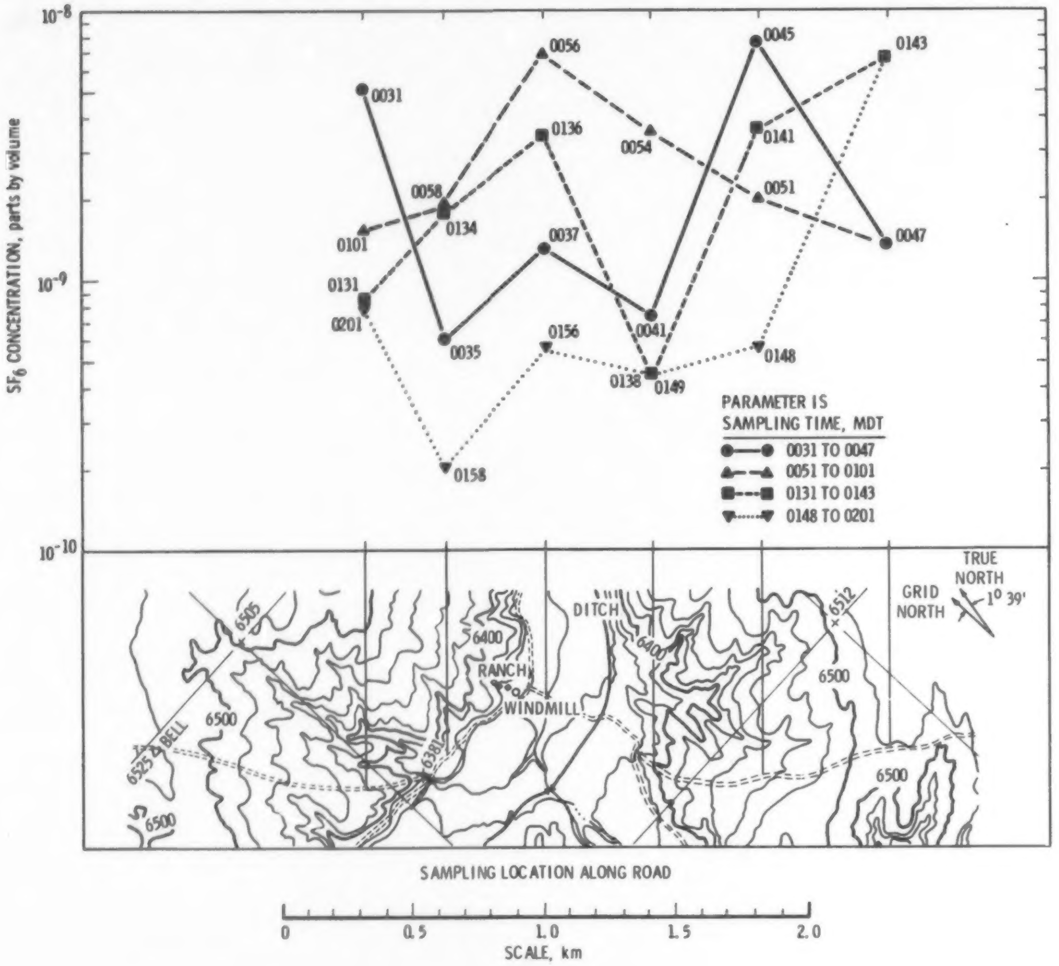

FIGURE 40. $SF_6$ Concentrations as a Function of Cross Valley Position as Determined From Four Mobile Traverses With Syringe Samplers, Night of August 9 to 10, 1980.

Neg. 80J402-8

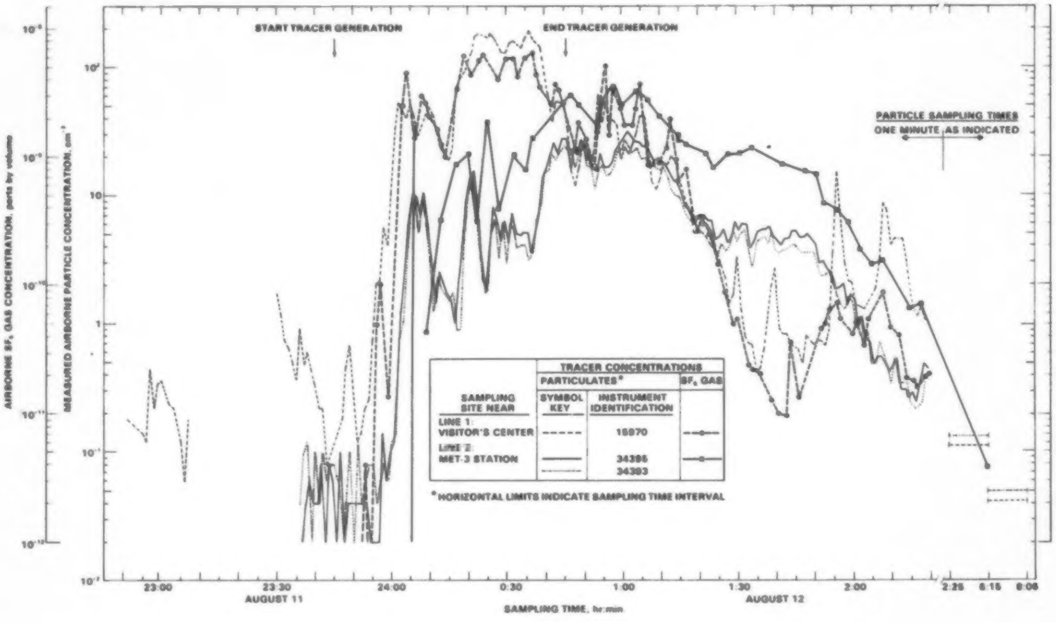

**FIGURE 41**. Airborne Tracer Particle and SF$_6$ Concentrations as a Function of Time, Night of August 11 to 12, 1980.

Neg. 80J402-7

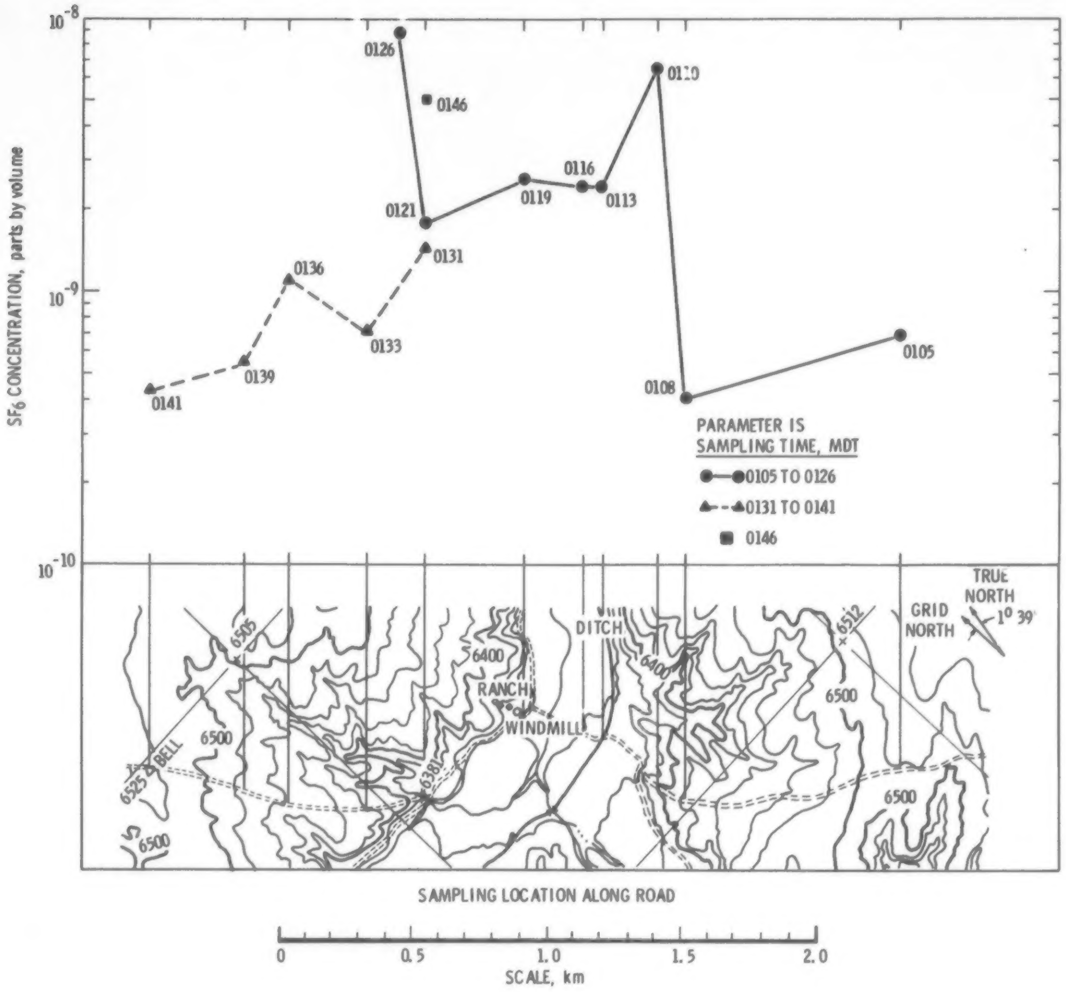

FIGURE 42. $SF_6$ Concentrations as a Function of Cross Valley Position as Determined From Three Mobile Traverses With Syringe Samplers, Night of August 11 to 12, 1980.
Neg. 80J402-12

## 4.0 RECOMMENDATIONS

This report has dealt with the design and execution of a set of field experiments conducted during a two-week period in August, 1980 in the Piceance Basin of Northwestern Colorado. The field experiments were described, the design and characteristics of the data collection systems were specified, and the data were summarized in the form of figures and tables. Experiments, rather than being focused on the collection of large quantities of general background meteorological and air quality data, were directed at investigating specific meteorological phenomena, including the evolution and characteristics of atmospheric mixing layers and the dispersion capabilities of nocturnal valley drainage flows. Separate work is proceeding on the further analysis of these data as this report is being written. The initial data reported here will constitute an important input to the development of a mathematical model of pollutant transport and diffusion in the oil shale region now being developed at PNL. It is important to point out, however, that further investigations of the meteorology and air quality of this data sparse and very complicated topographic region are essential. We recommend that a much more comprehensive set of experiments be initiated in the near future to obtain a better understanding of the regional environmental effects of the development of oil shale resources in the Piceance Basin. Modeling work will benefit from the phenomenological approach advocated here, but it will be necessary to observe other phenomena (e.g., the buildup and breakdown of temperature inversions, the evolution of local wind systems, the coupling and decoupling of synoptic and valley flows, etc.) and to expand the scope of the observational work in both time and space.

# REFERENCES

Bowen, H.J.M. 1966. Trace Elements in Biochemistry. Academic Press, 241 pp.

Call, D.B. and A.L. Morris. 1979. Airsonde® - Versatile New Sounding System. Atmospheric Instrumentation Research, Inc., Boulder, CO 21 pp.

Clements, W.E., S. Goff, J.A. Archuleta and S. Barr. 1981. Experimental Design and Data of the August 1980 Corral Gulch Nocturnal Wind Experiment, Piceance Basin, Northwestern Colorado. Los Alamos National Laboratory Report, LA-8895-MS, July 1981, 197 pp, University of California, Los Alamos, NM 87545.

Rio Blanco Oil Shale Company. 1981. Modular Development Phase Monitoring Report Seven, Vol. 1 of 3, Dec. 1979-Nov. 1980, Year End Report. Rio Blanco Oil Shale Co., 2851 So. Parker Road, Aurora, CO 80014. (Available from USGS Conservation Div., Oil Shale Office, 131 No. 6th St., Suite 300, Grand Junction, CO 81501.)

Singh, H.B., F.L. Ludwig and W.B. Johnson. 1978. "Tropospheric Ozone: Concentrations and Variabilities in Clean Remote Atmospheres." Atmospheric Environment, 12, p. 2185-2196.

Whiteman, C.D. 1980. Breakup of Temperature Inversions in Colorado Mountain Valleys. Atmospheric Science Paper No. 328, Colorado State University, Fort Collins, CO 80523, 250 pp.

# APPENDIX A

# INDIVIDUAL AIRSONDE PLOTS

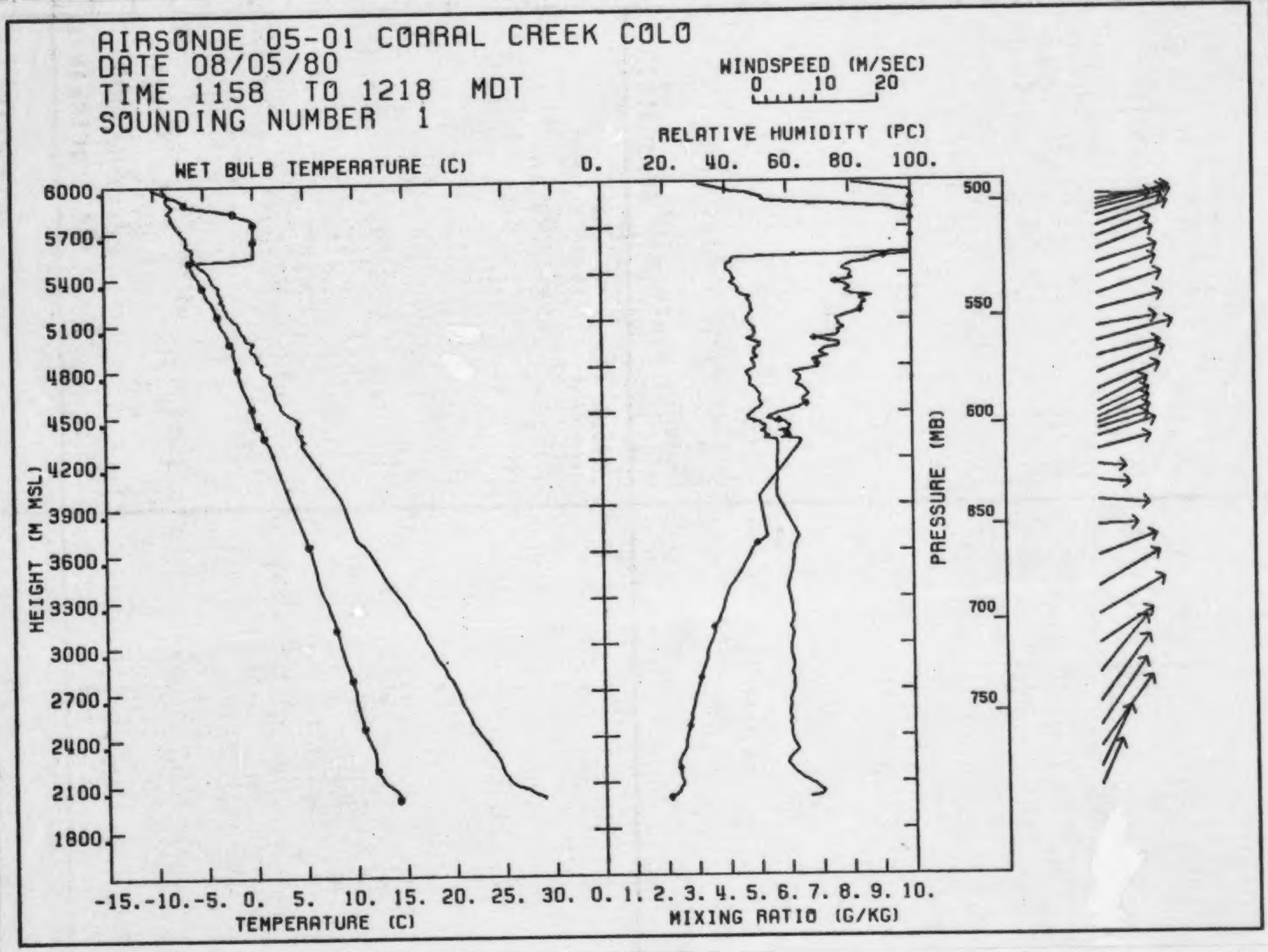

FIGURE 43. Airsonde Sounding #1, 1158 MDT, August 5, 1980.

START LINE

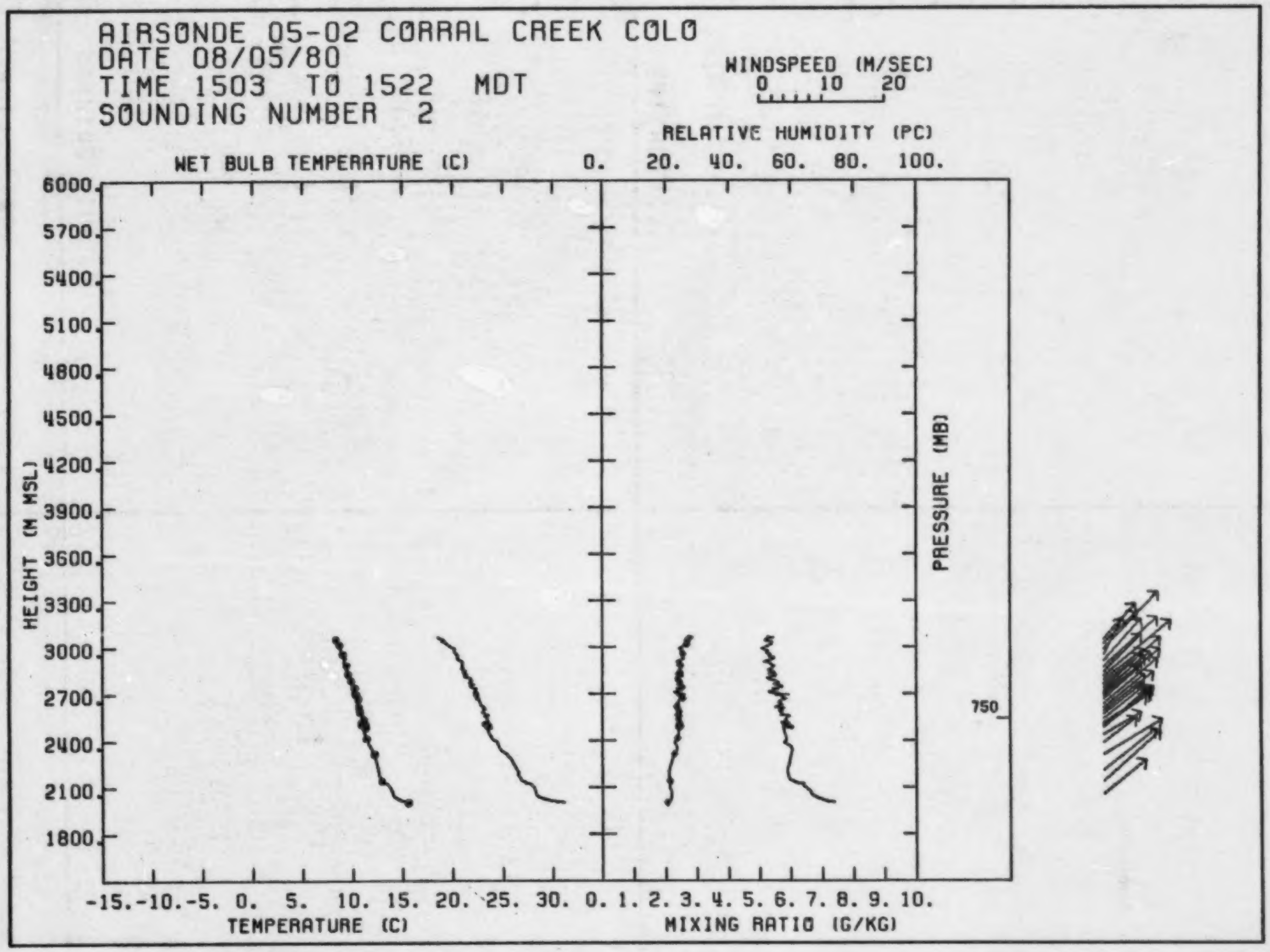

FIGURE 44. Airsonde Sounding #2, 1503 MDT, August 5, 1980.

TYPIST ____ PROOFER ____ CORRECTED BY ____

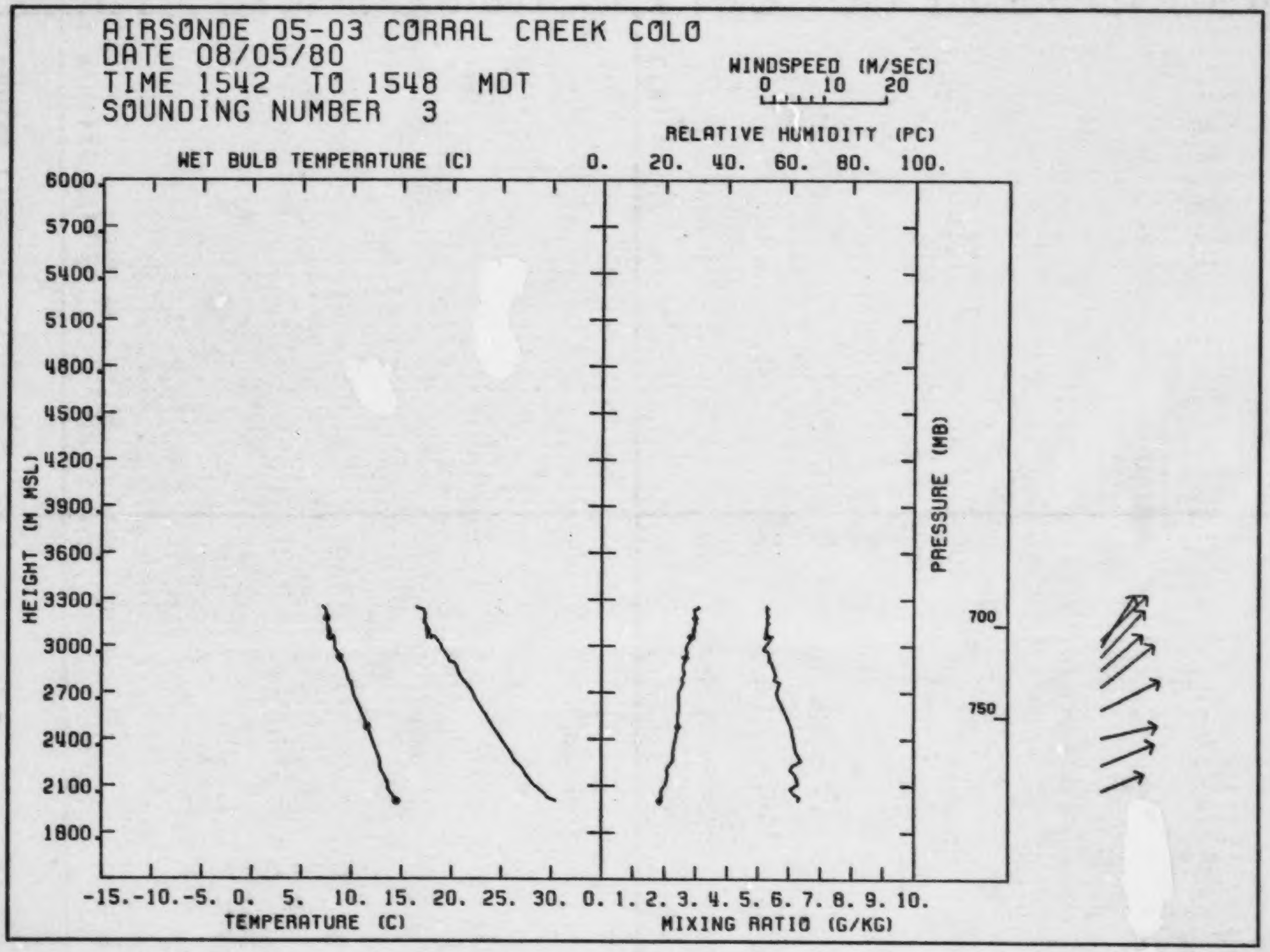

FIGURE 45. Airsonde Sounding #3, 1542 MDT, August 5, 1980.

START LINE

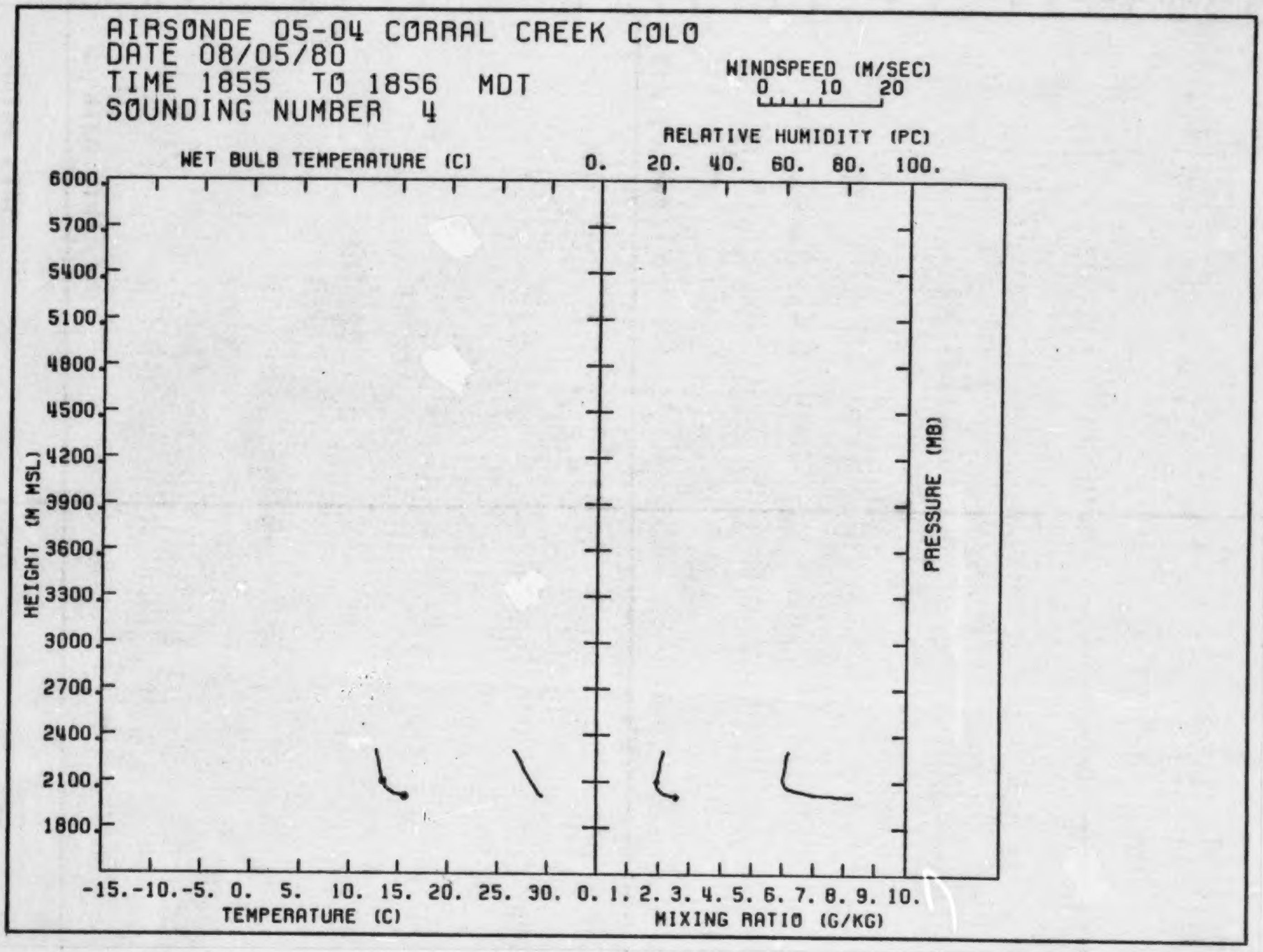

FIGURE 46. Airsonde Sounding #4, 1855 MDT, August 5, 1980.

TYPIST PROOFER CORRECTED BY

START LINE

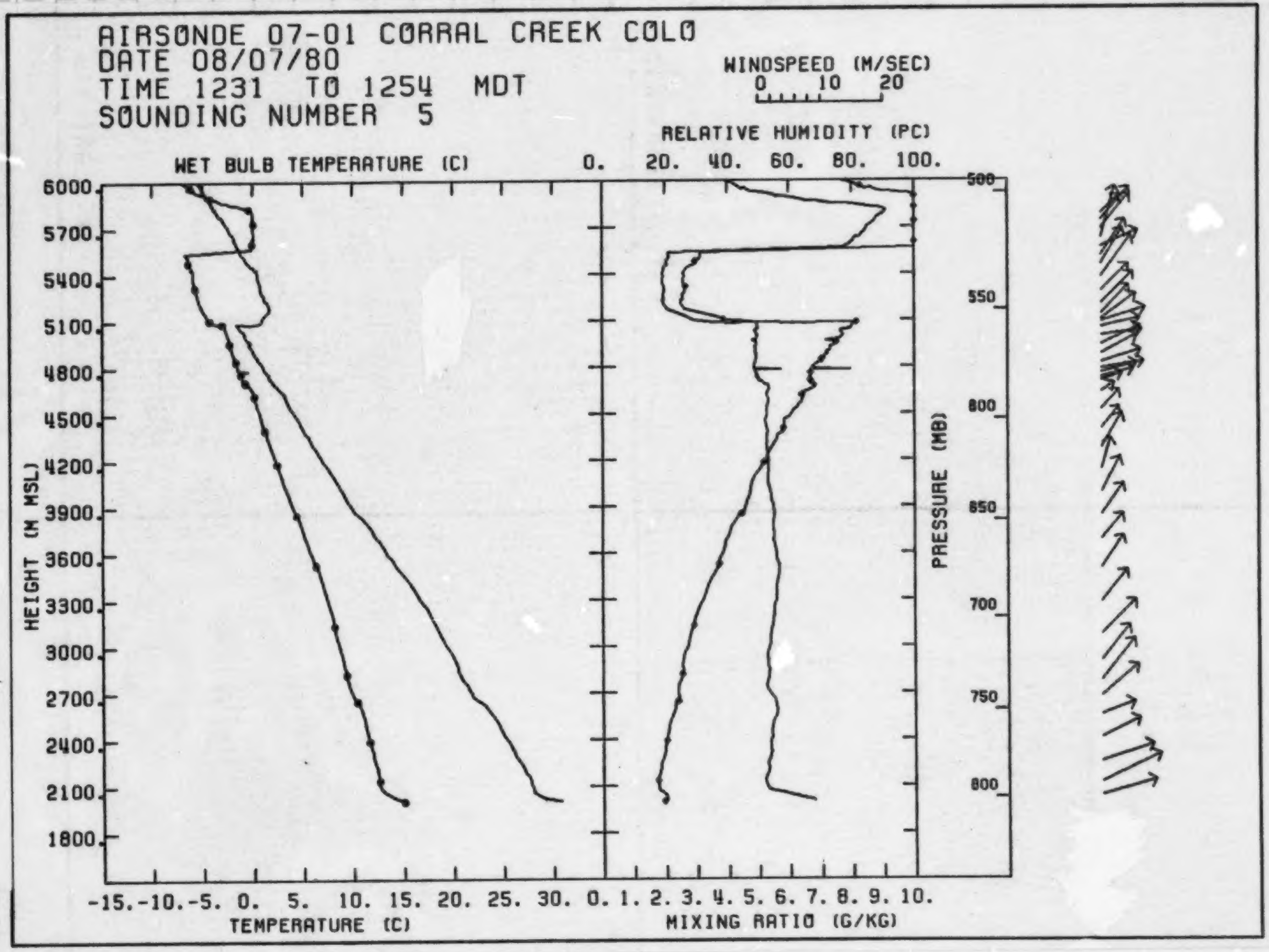

FIGURE 47. Airsonde Sounding #5, 1231 MDT, August 7, 1980.

TYPIST PROOFER CORRECTED BY

START LINE

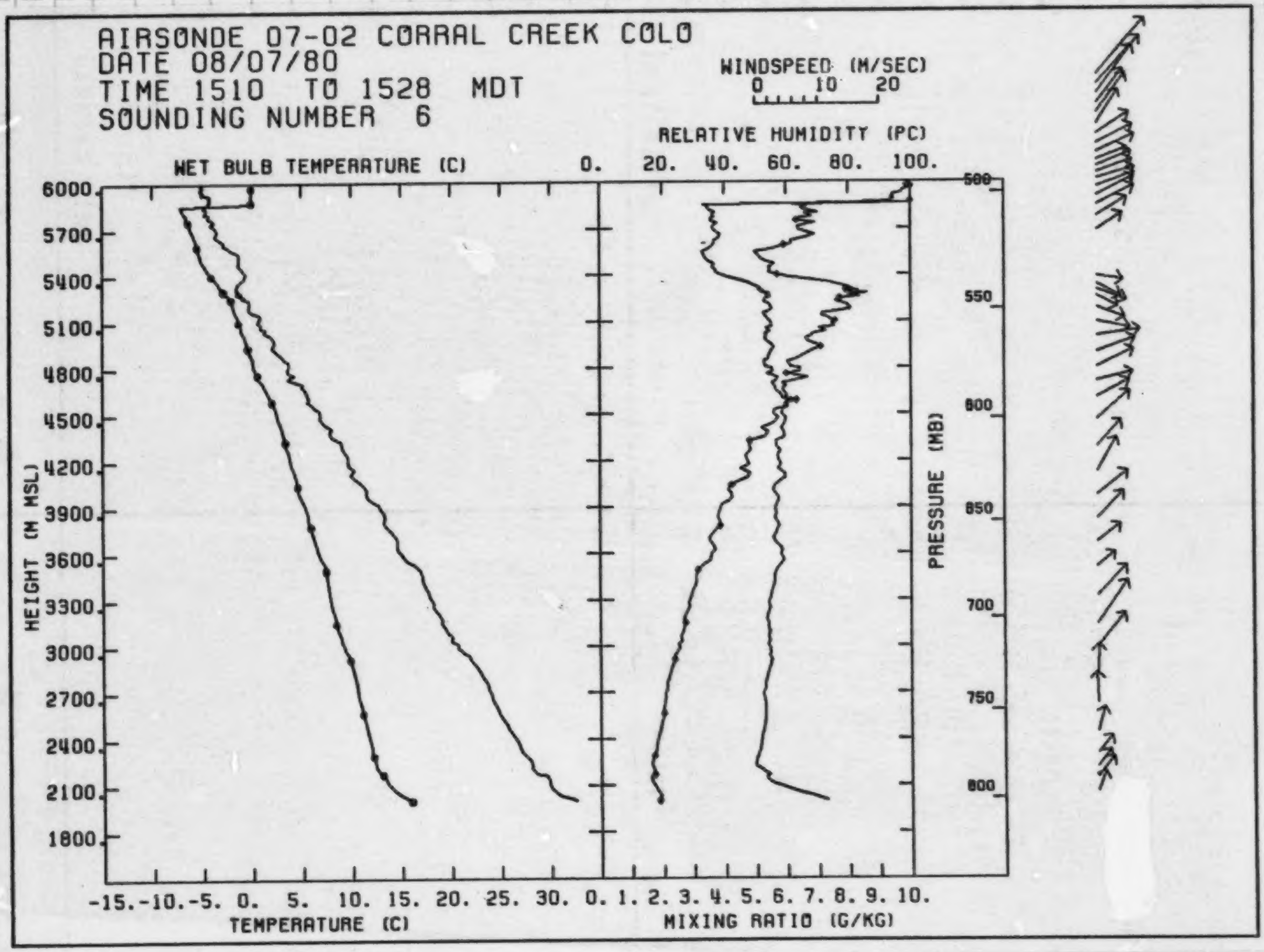

FIGURE 48. Airsonde Sounding #6, 1510 MDT, August 7, 1980.

TYPIST PROOFER CORRECTED BY

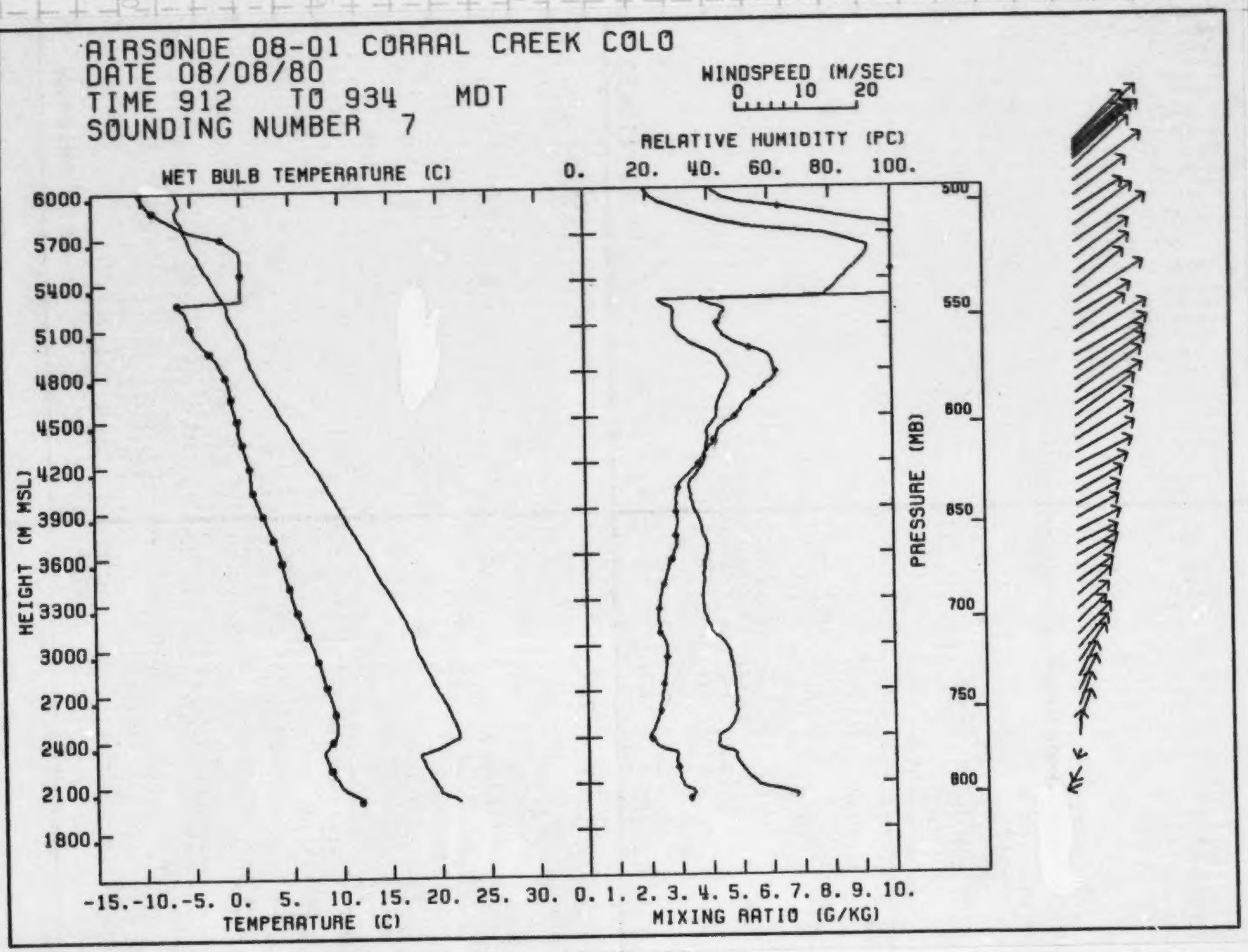

FIGURE 49. Airsonde Sounding #7, 0912 MDT, August 8, 1980.

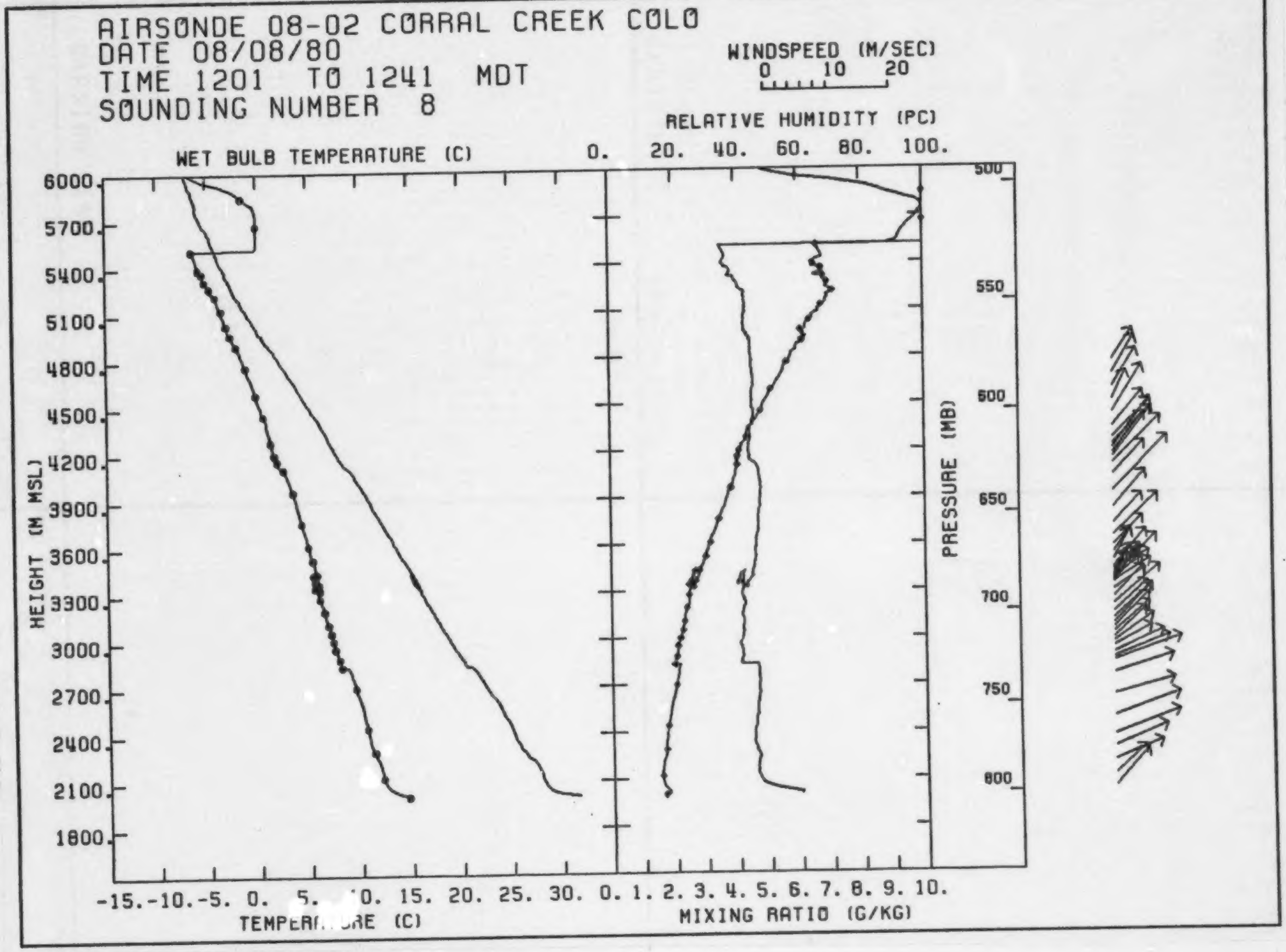

FIGURE 50. Airsonde Sounding #8, 1201 MDT, August 8, 1980.

START LINE

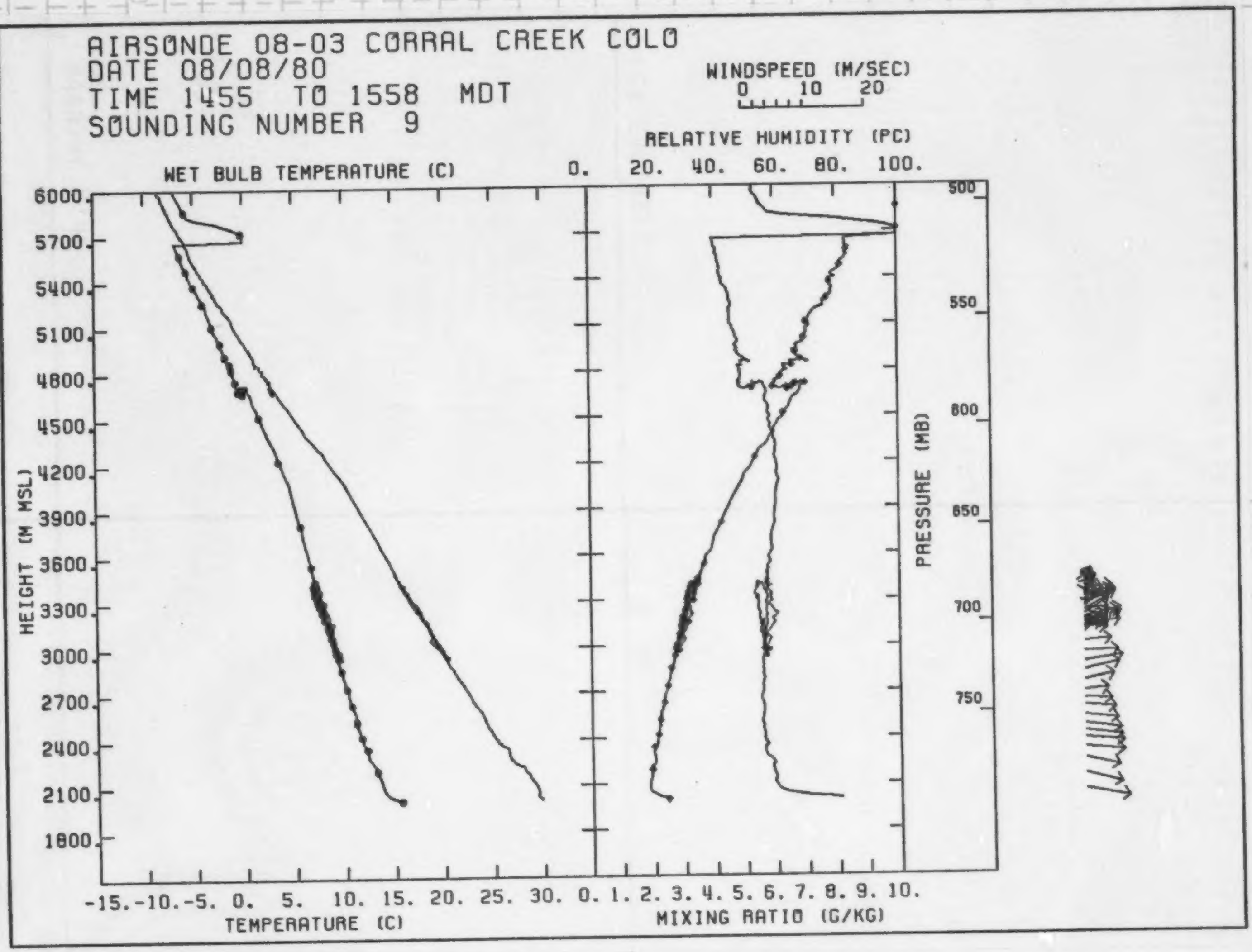

FIGURE 51. Airsonde Sounding #9, 1455 MDT, August 8, 1980.

PA ER
TYPIST PROOFER CORRECTED BY

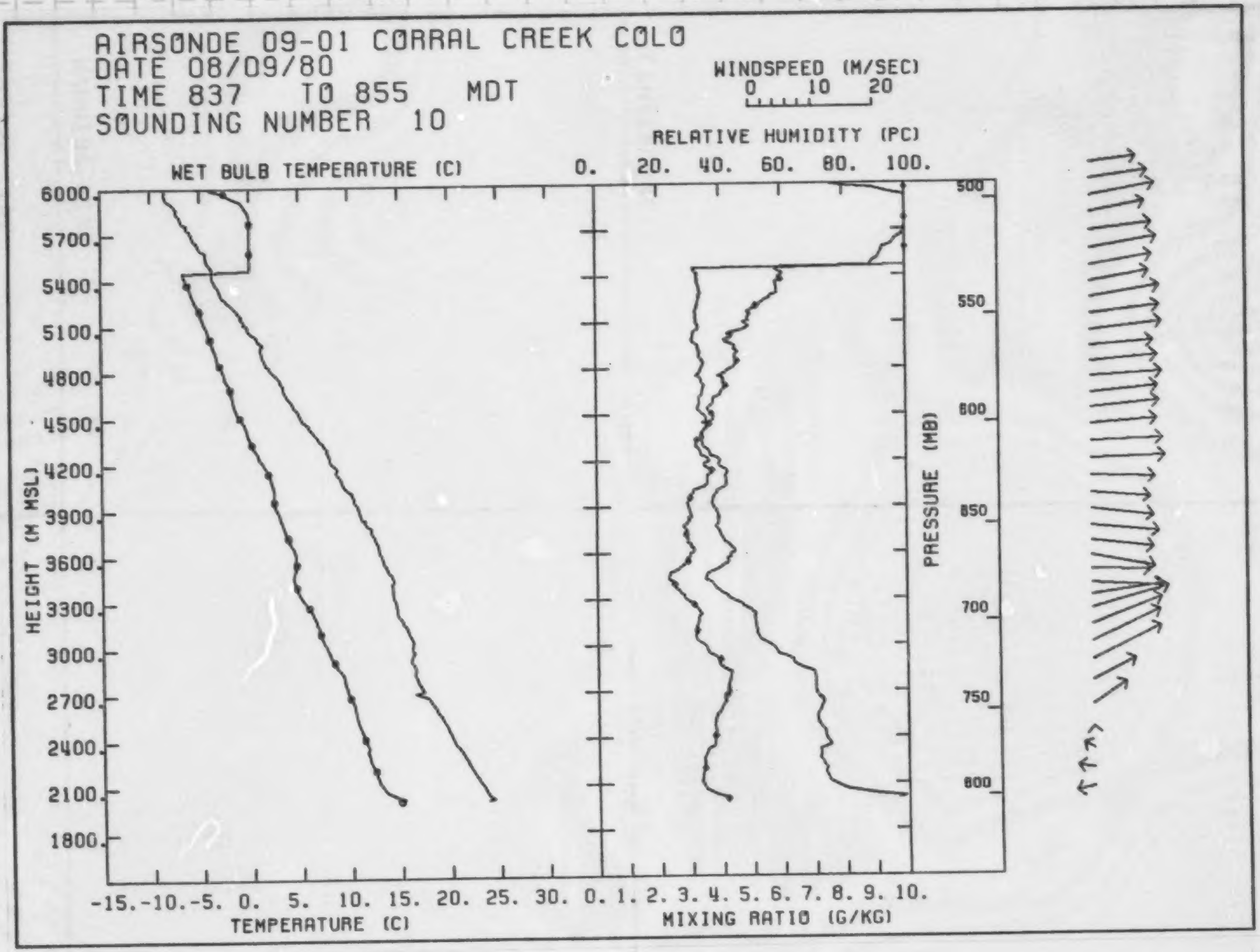

FIGURE 52. Airsonde Sounding #10, 0837 MDT, August 9, 1980.

START LINE

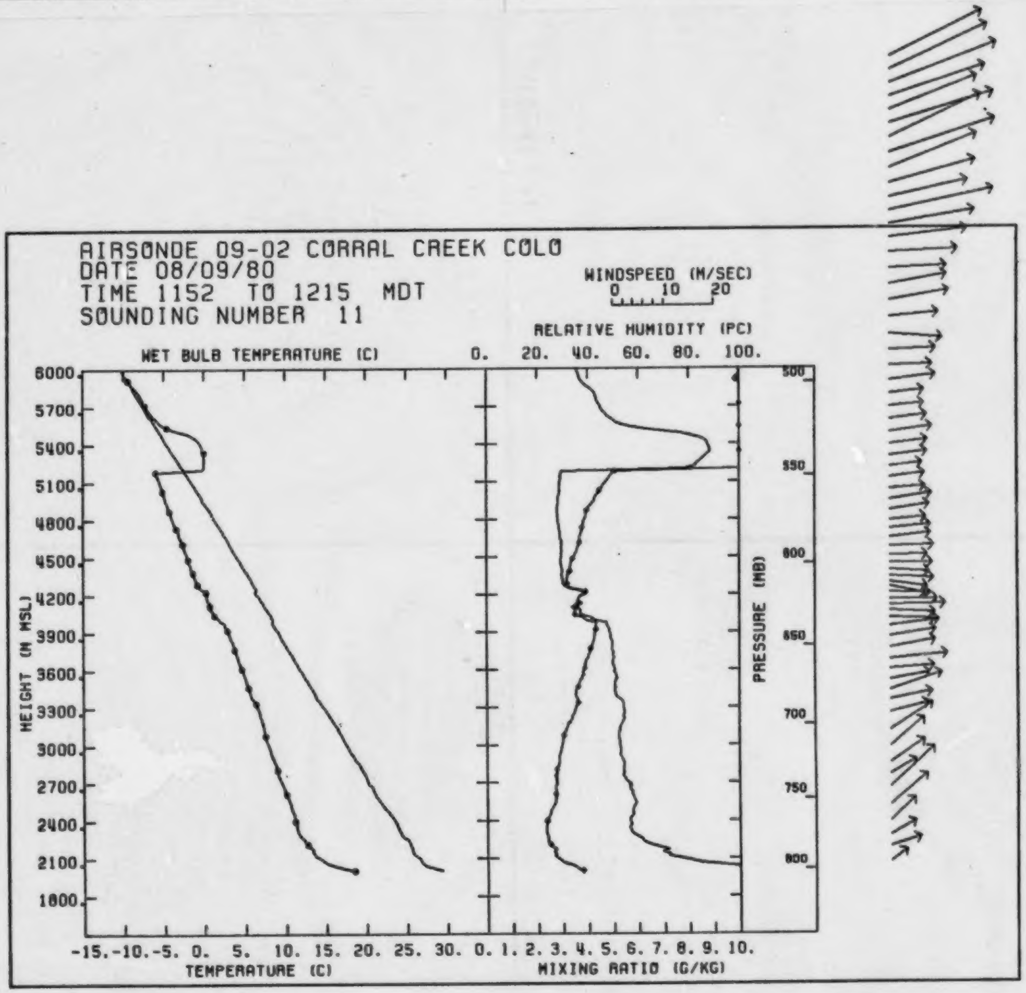

FIGURE 53. Airsonde Sounding #11, 1152 MDT, August 9, 1980.

ENDING LINE

TYPIST PROOFER CORRECTED BY

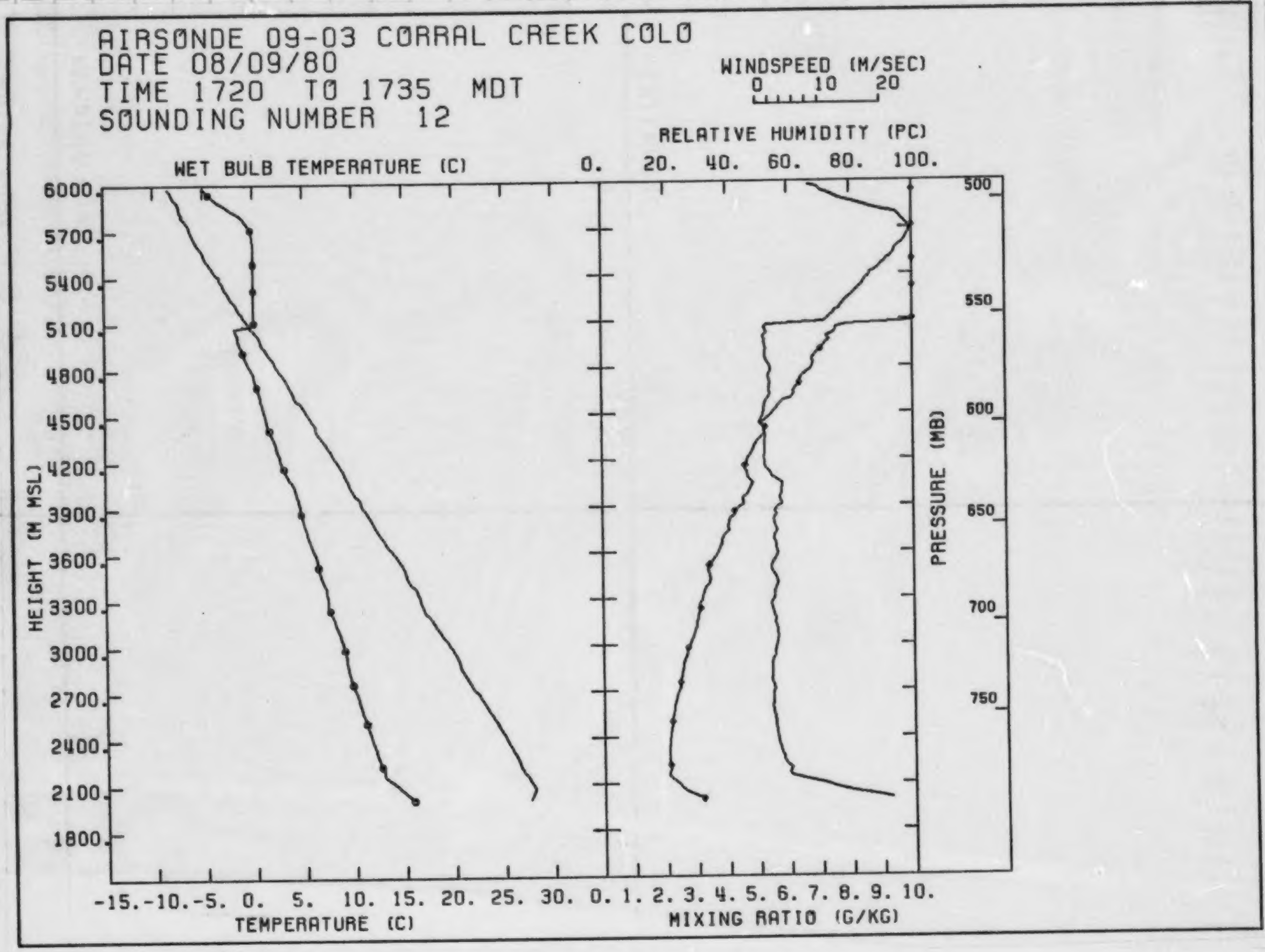

FIGURE 54. Airsonde Sounding #12, 1720 MDT, August 9, 1980.

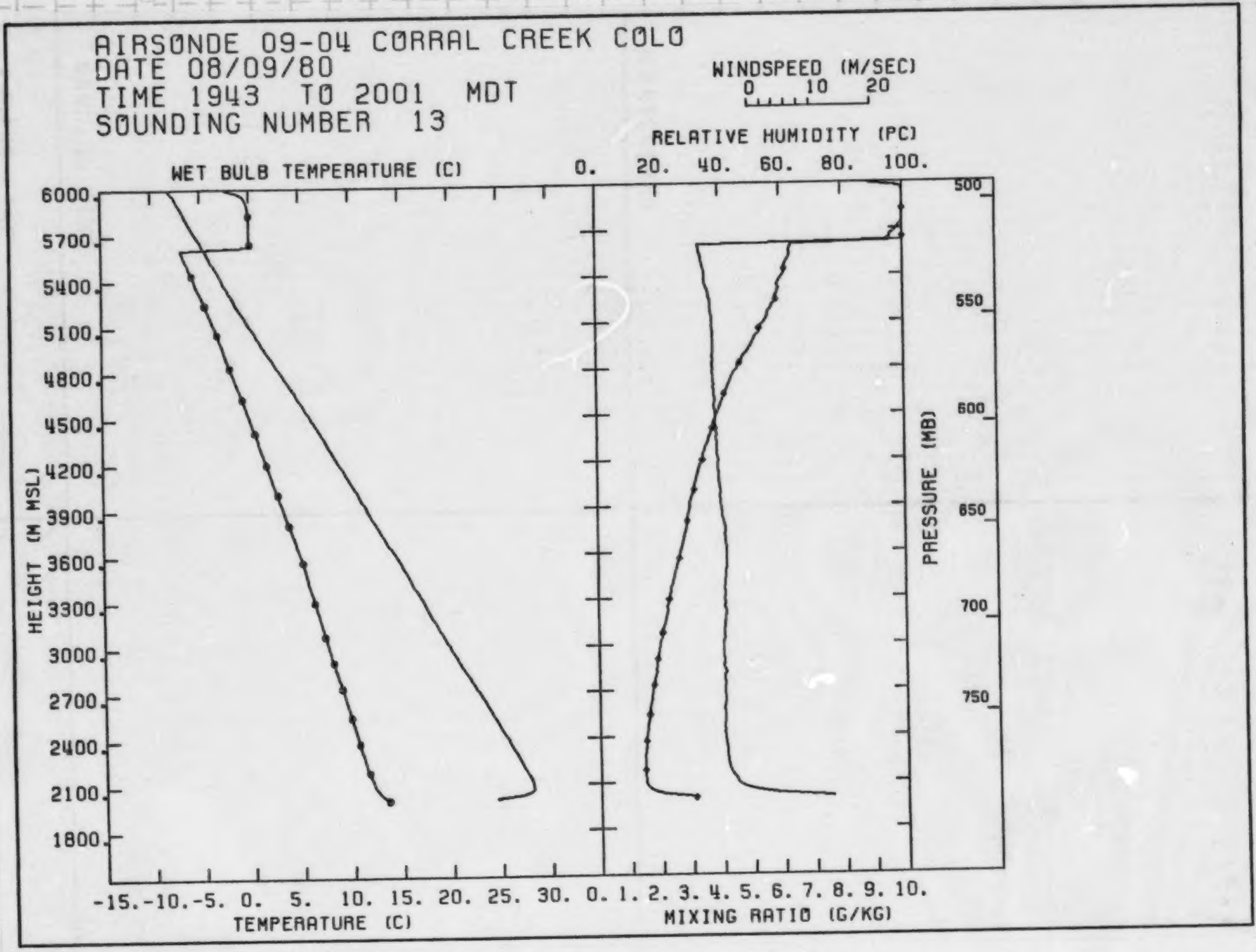

FIGURE 55. Airsonde Sounding #13, 1943 MDT, August 9, 1980.

START LINE

TYPIST PROOFER CORRECTED BY

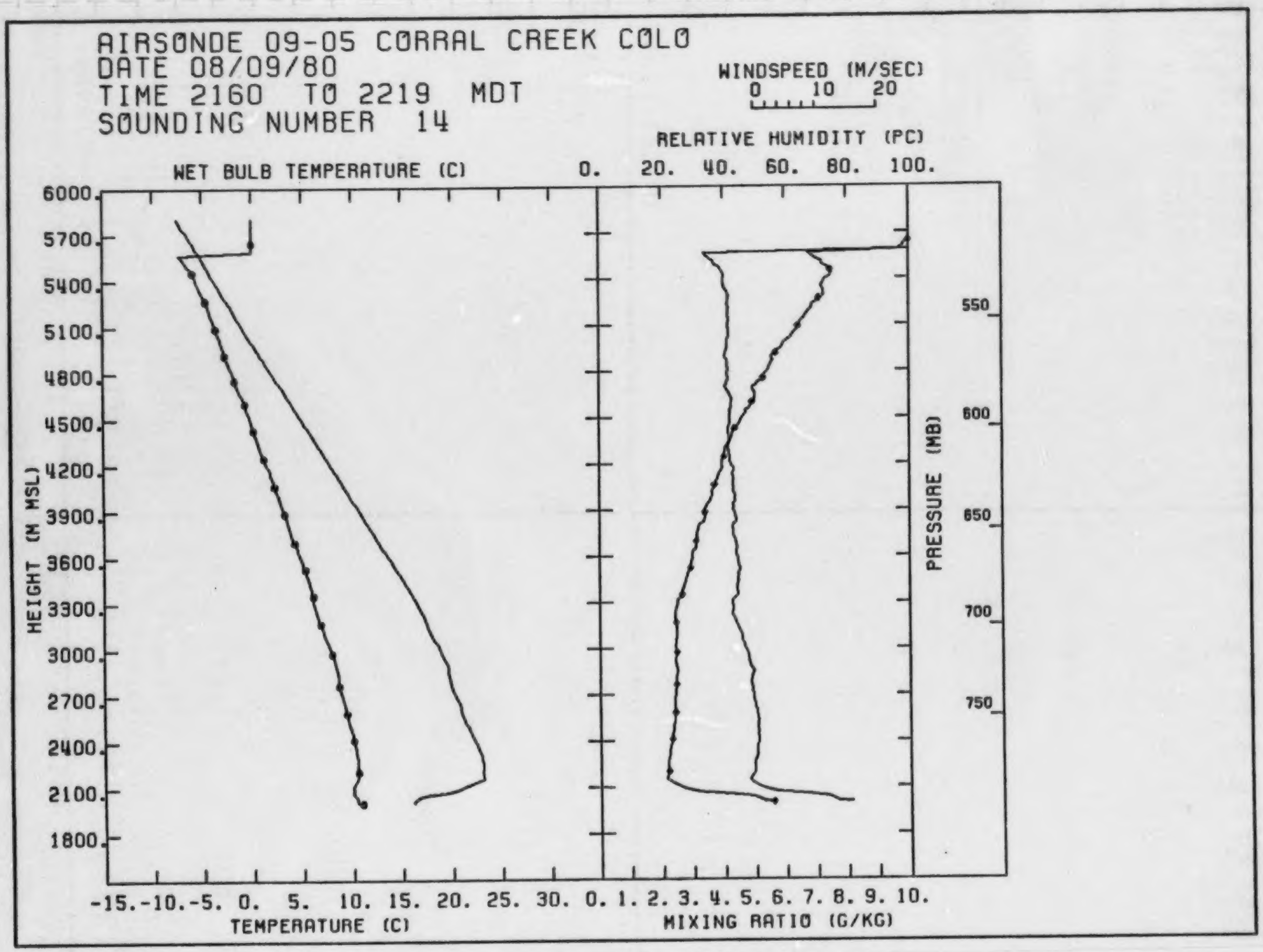

FIGURE 56. Airsonde Sounding #14, 2200 MDT, August 9, 1980

START LINE
TYPIST PROOFER CORRECTED BY

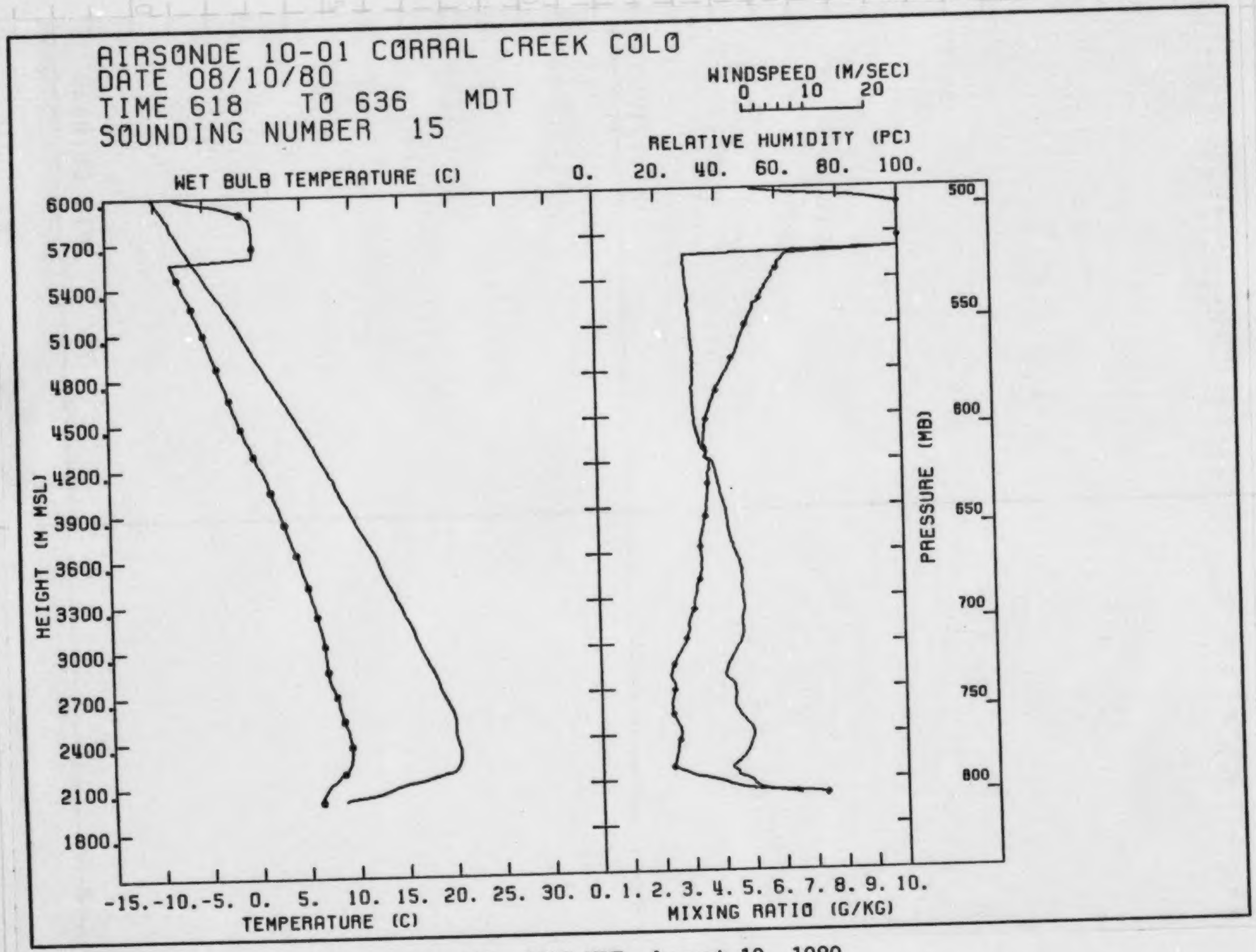

FIGURE 57. Airsonde Sounding #15, 0618 MDT, August 10, 1980.

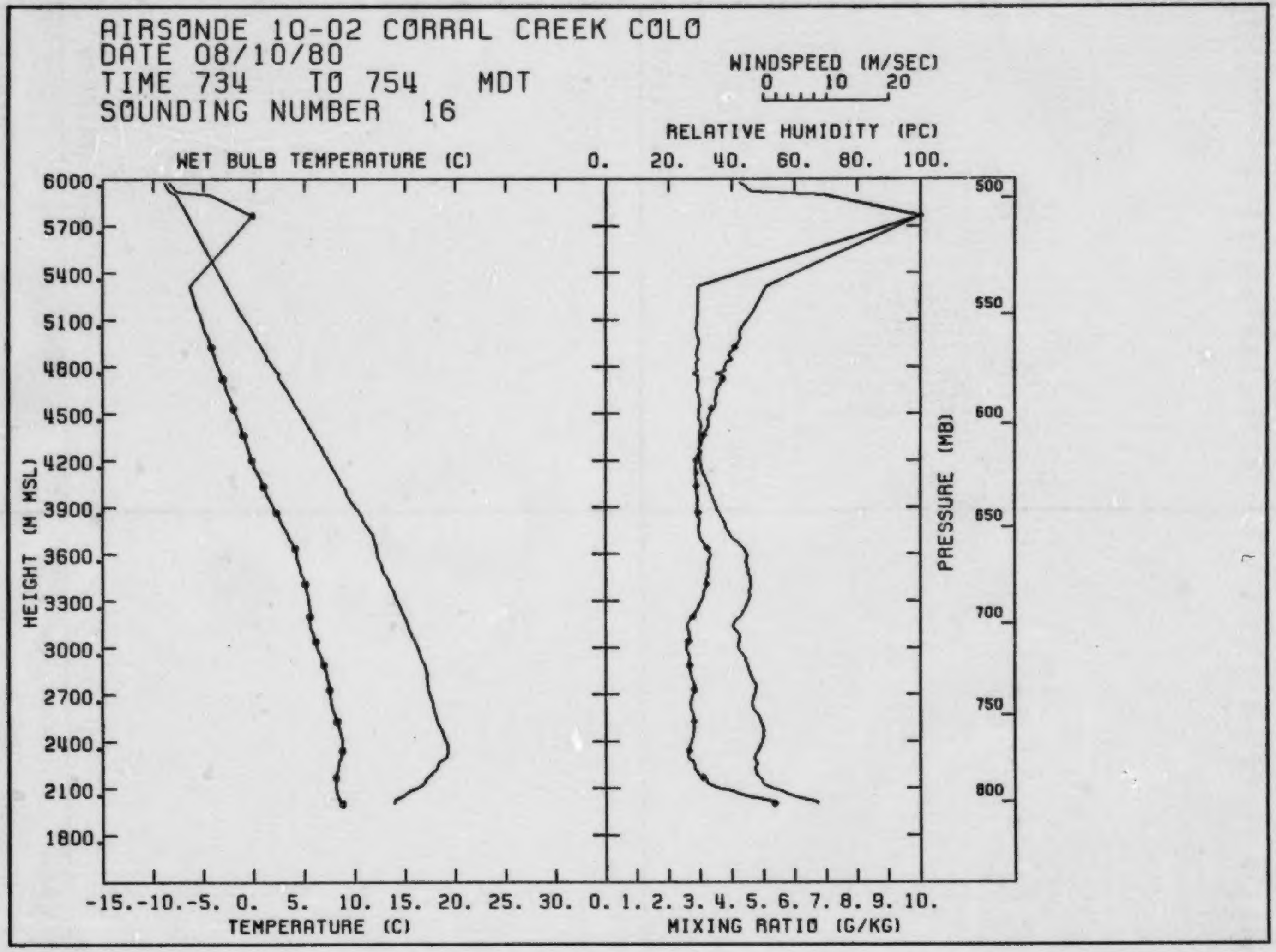

FIGURE 58. Airsonde Sounding #16, 0734 MDT, August 10, 1980.

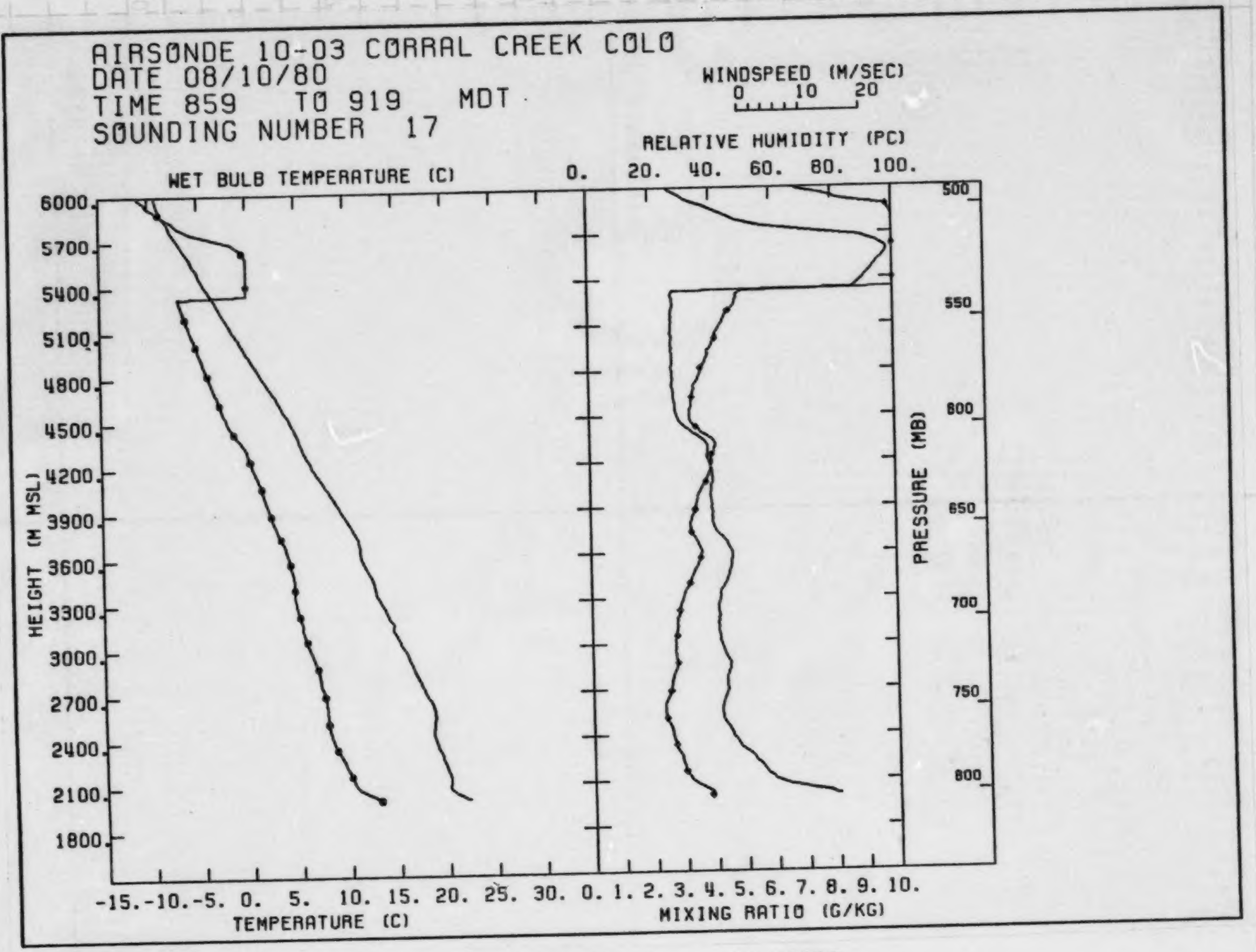

FIGURE 59. Airsonde Sounding #17, 0859 MDT, August 10, 1980.

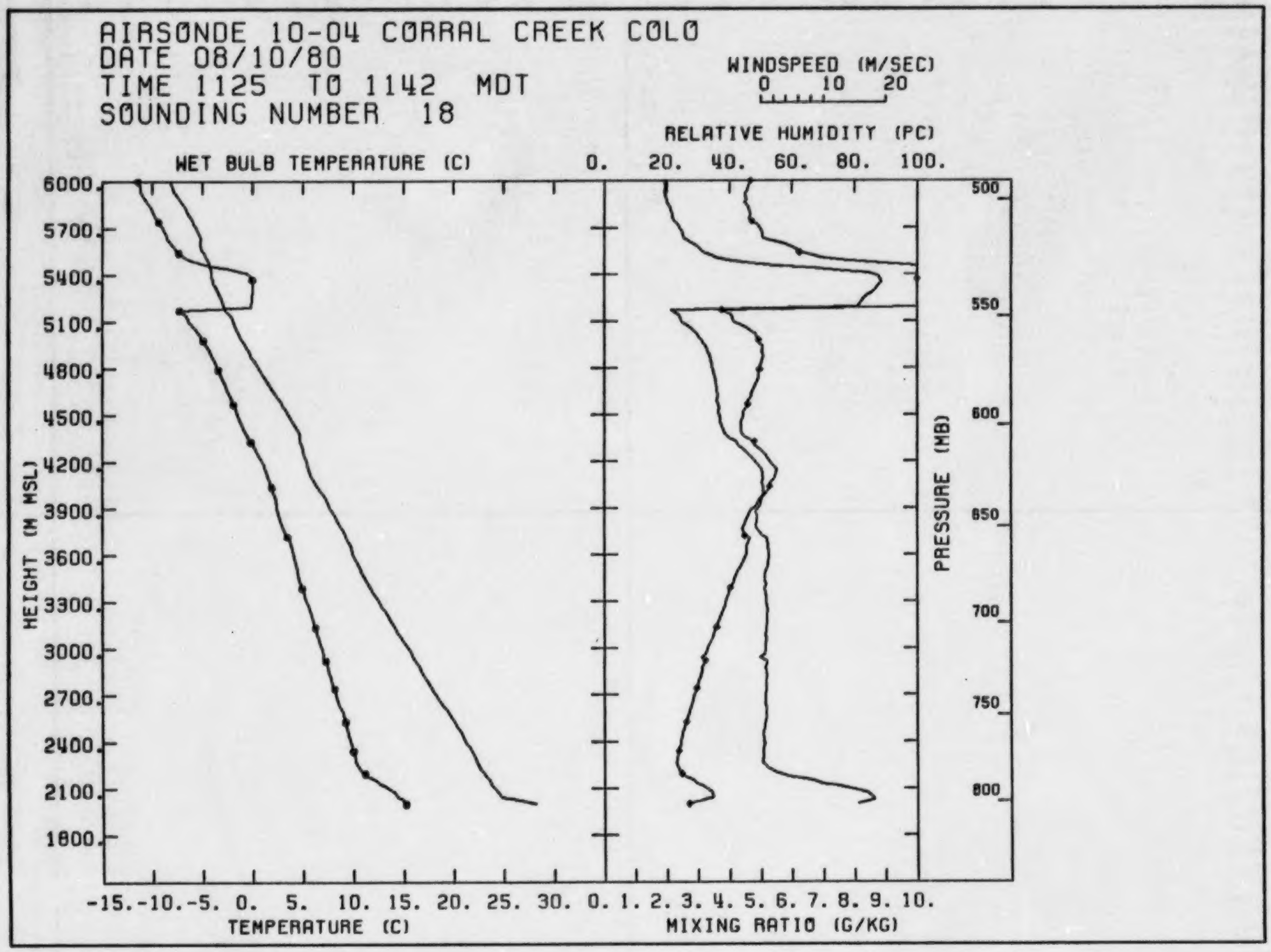

FIGURE 60. Airsonde Sounding #18, 1125 MDT, August 10, 1980.

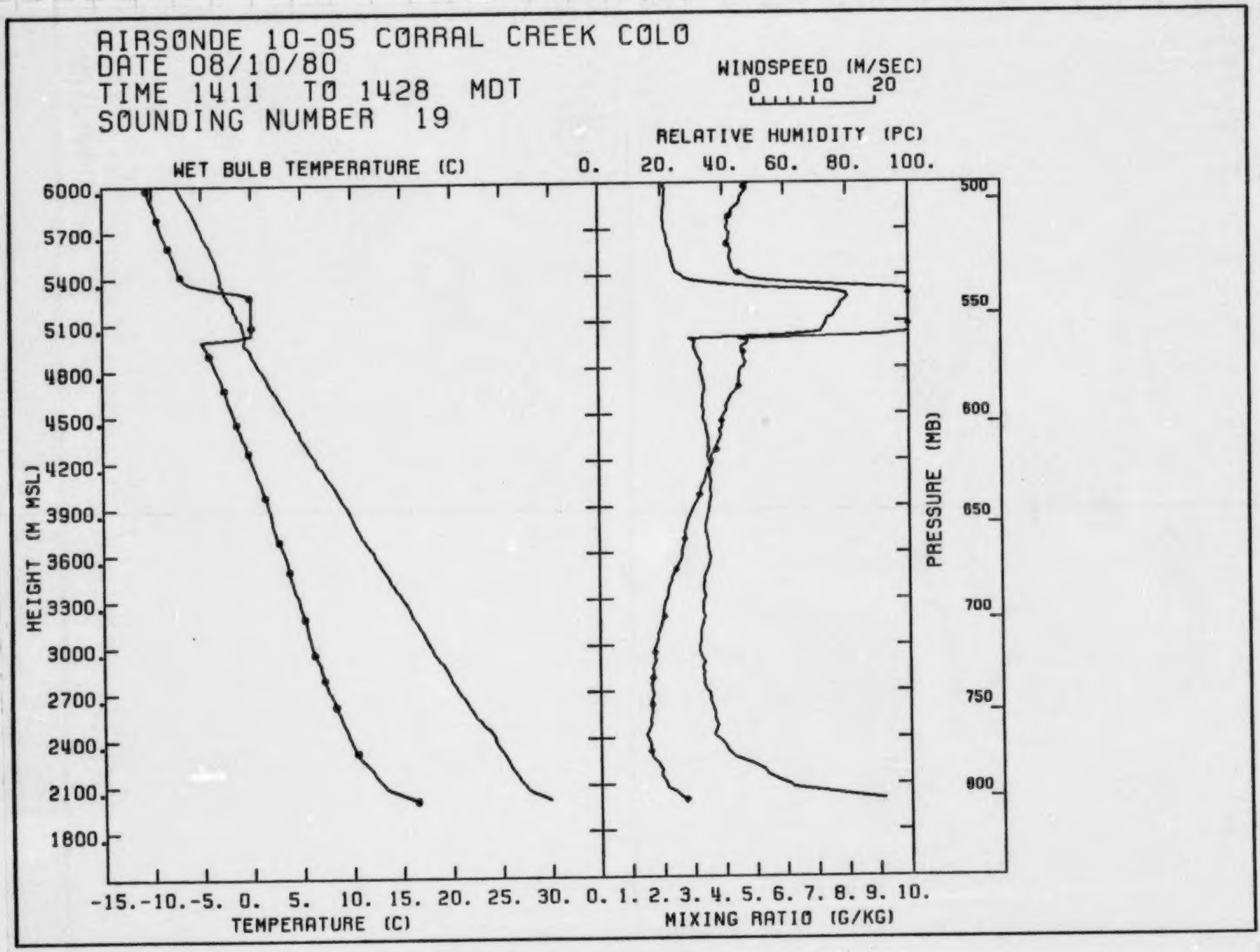

FIGURE 61. Airsonde Sounding #19, 1411 MDT, August 10, 1980.

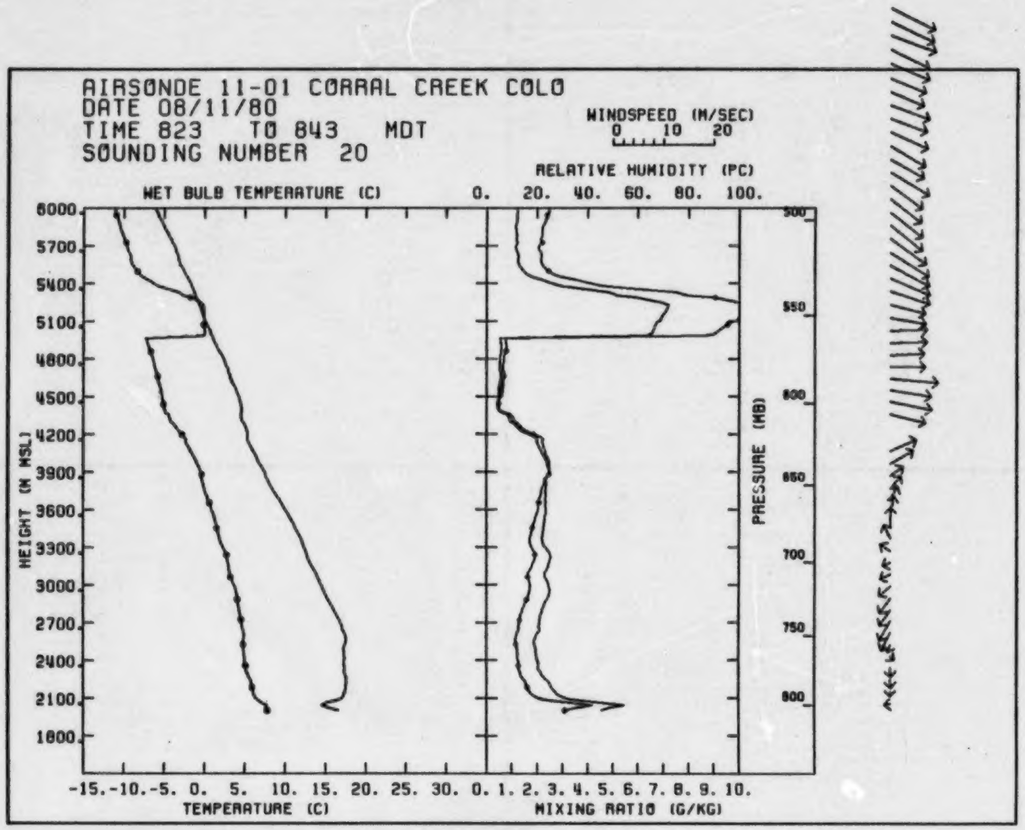

FIGURE 62. Airsonde Sounding #20, 0823 MDT, August 11, 1980.

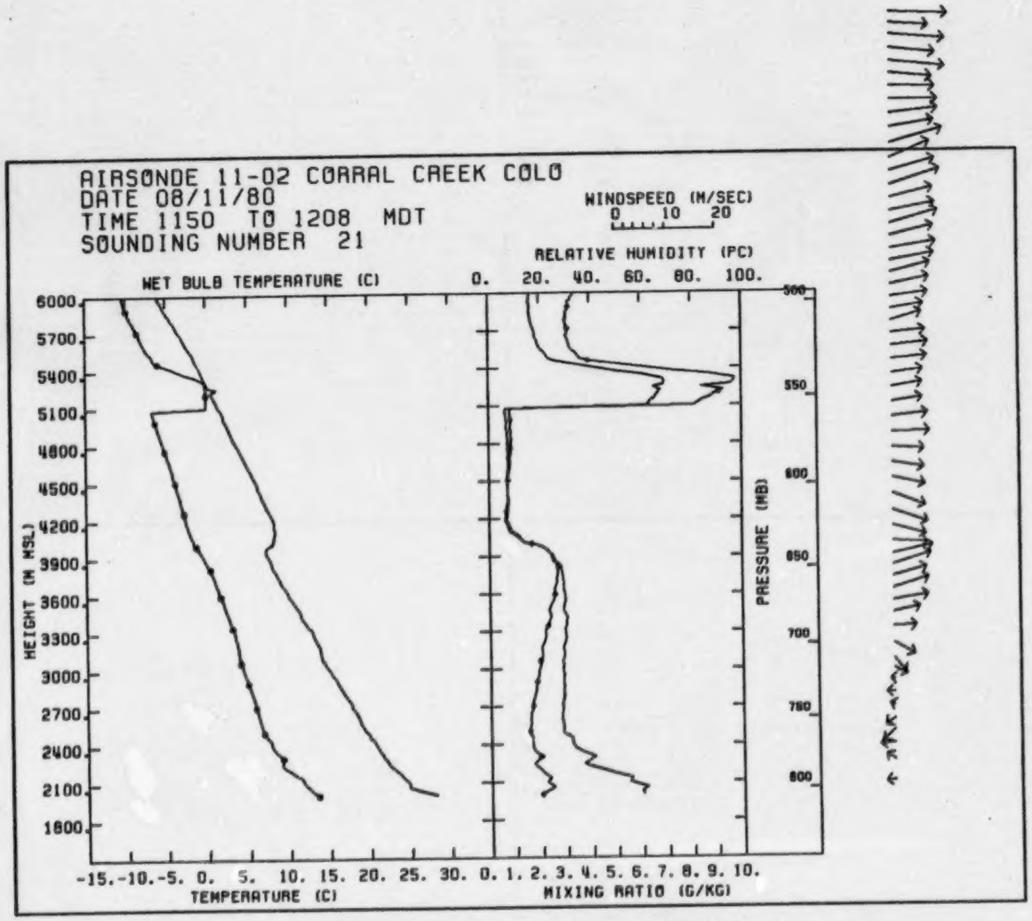

FIGURE 63. Airsonde Sounding #21, 1150 MDT, August 11, 1980.

START LINE
WARNING LINE
ENDING LINE
TYPIST PROOFER CORRECTED BY

START LINE

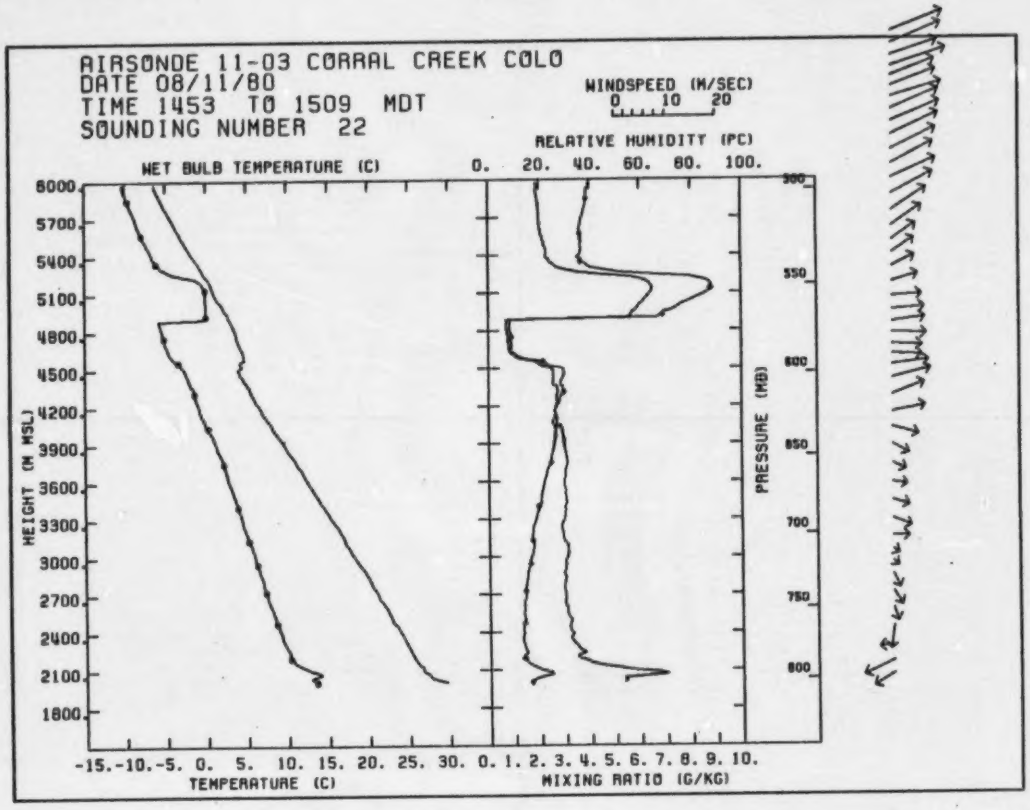

FIGURE 64. Airsonde Sounding #22, 1453 MDT, August 11, 1980.

WARNING LINE
ENDING LINE
TYPIST PROOFER CORRECTED BY

START LINE

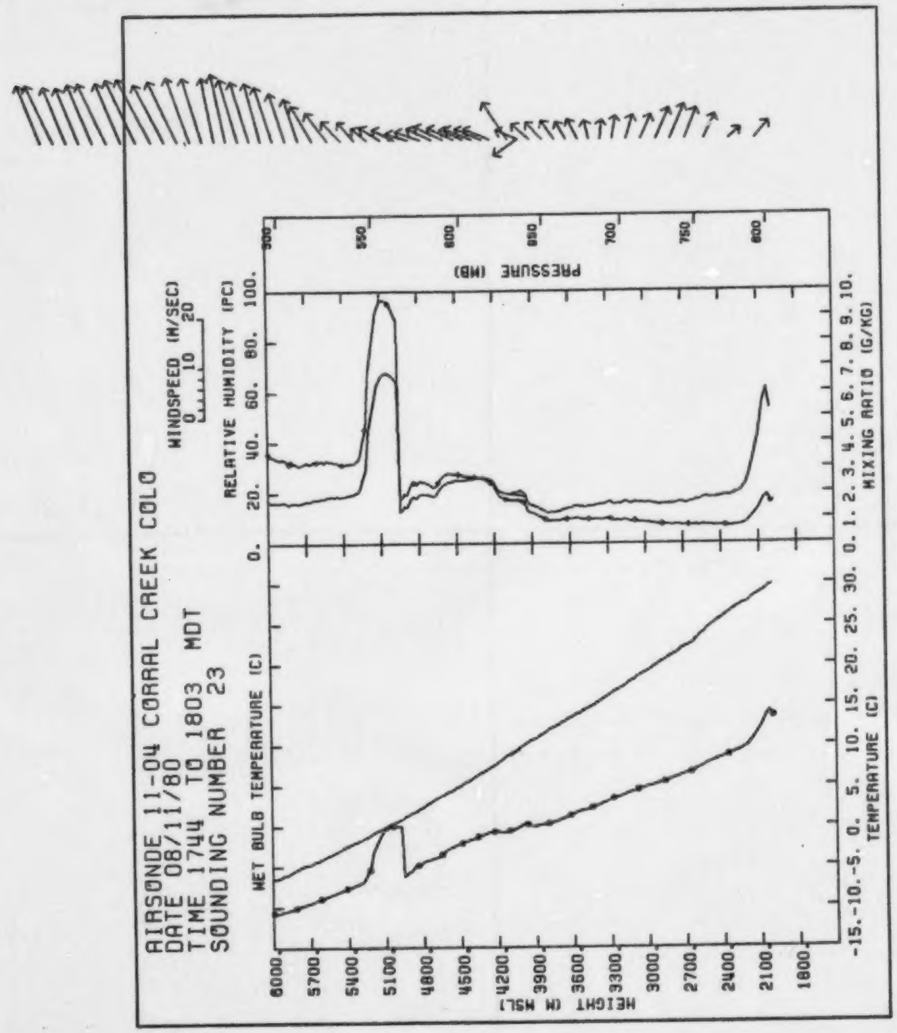

FIGURE 65. Airsonde Sounding #23, 1744 MDT, August 11, 1980.

WARNING LINE

ENDING LINE

TYPIST PROOFER CORRECTED BY

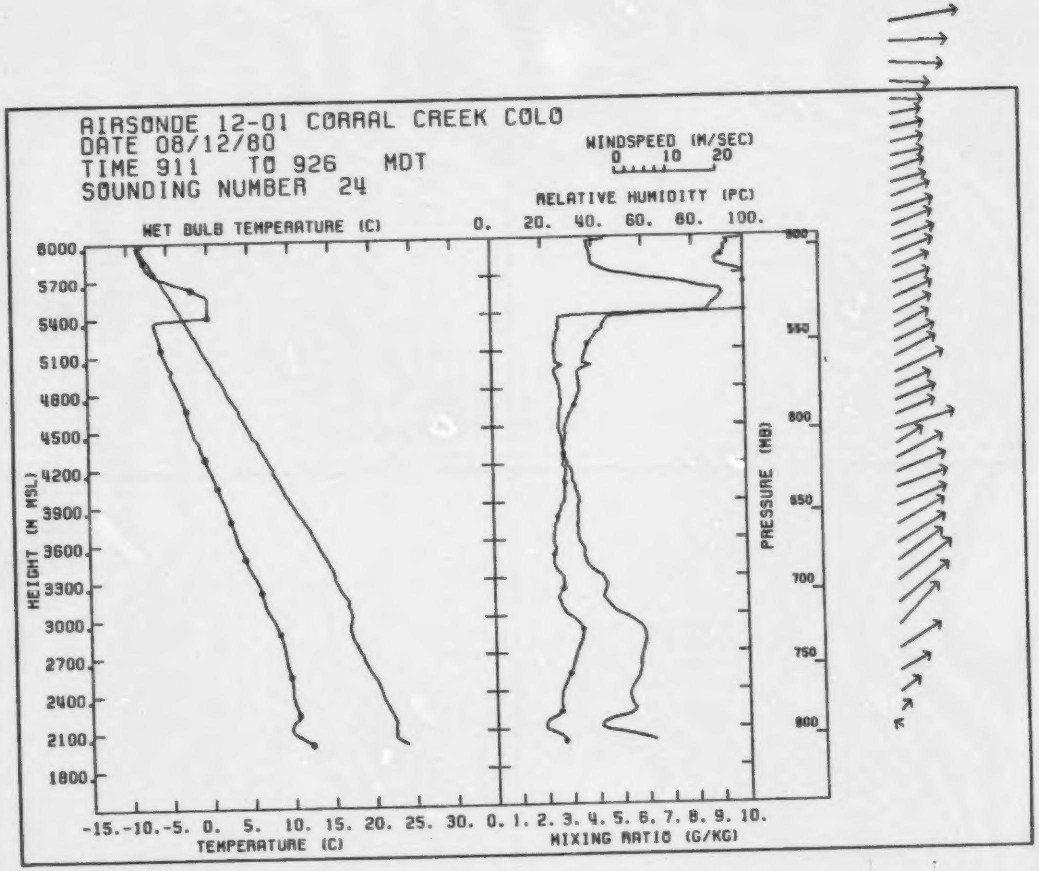

FIGURE 66. Airsonde Sounding #24, 0911 MDT, August 12, 1980.

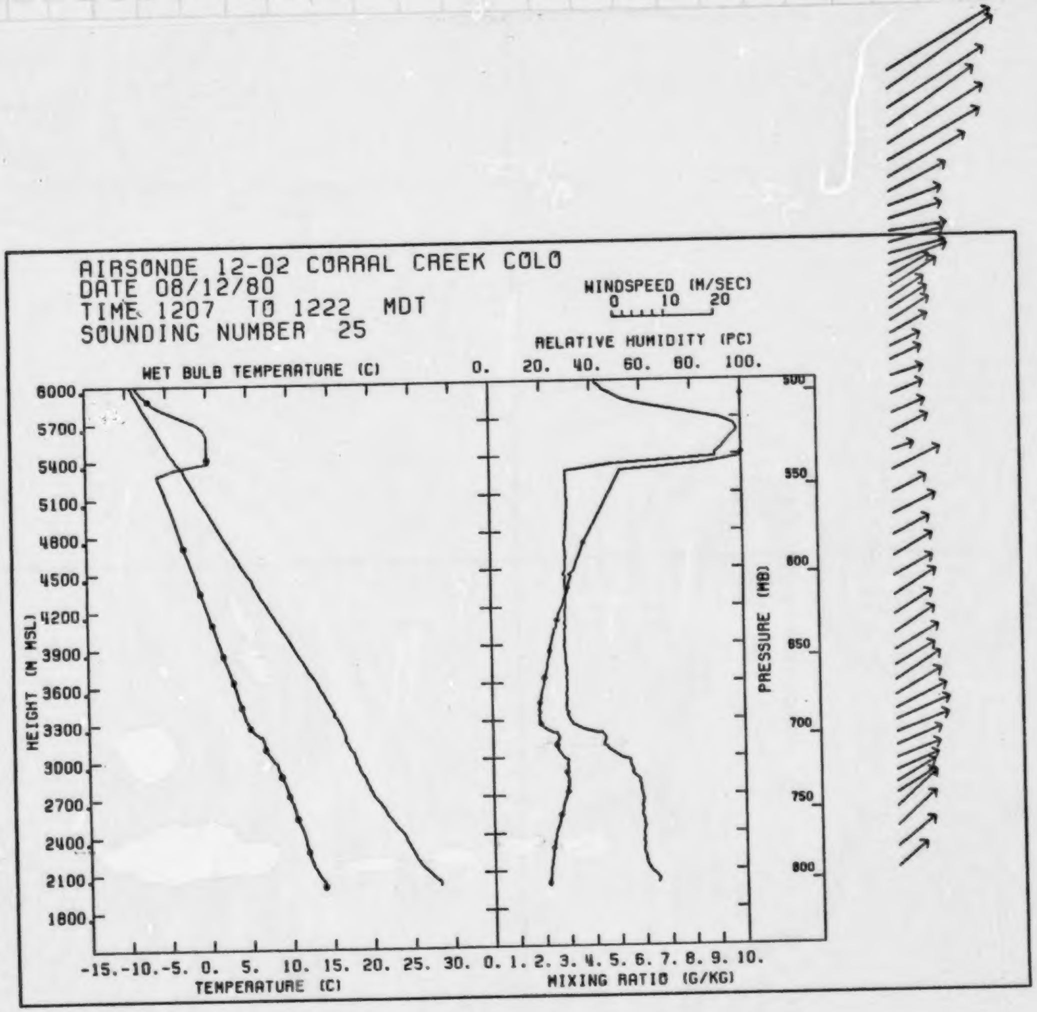

FIGURE 67. Airsonde Sounding #25, 1207 MDT, August 12, 1980.

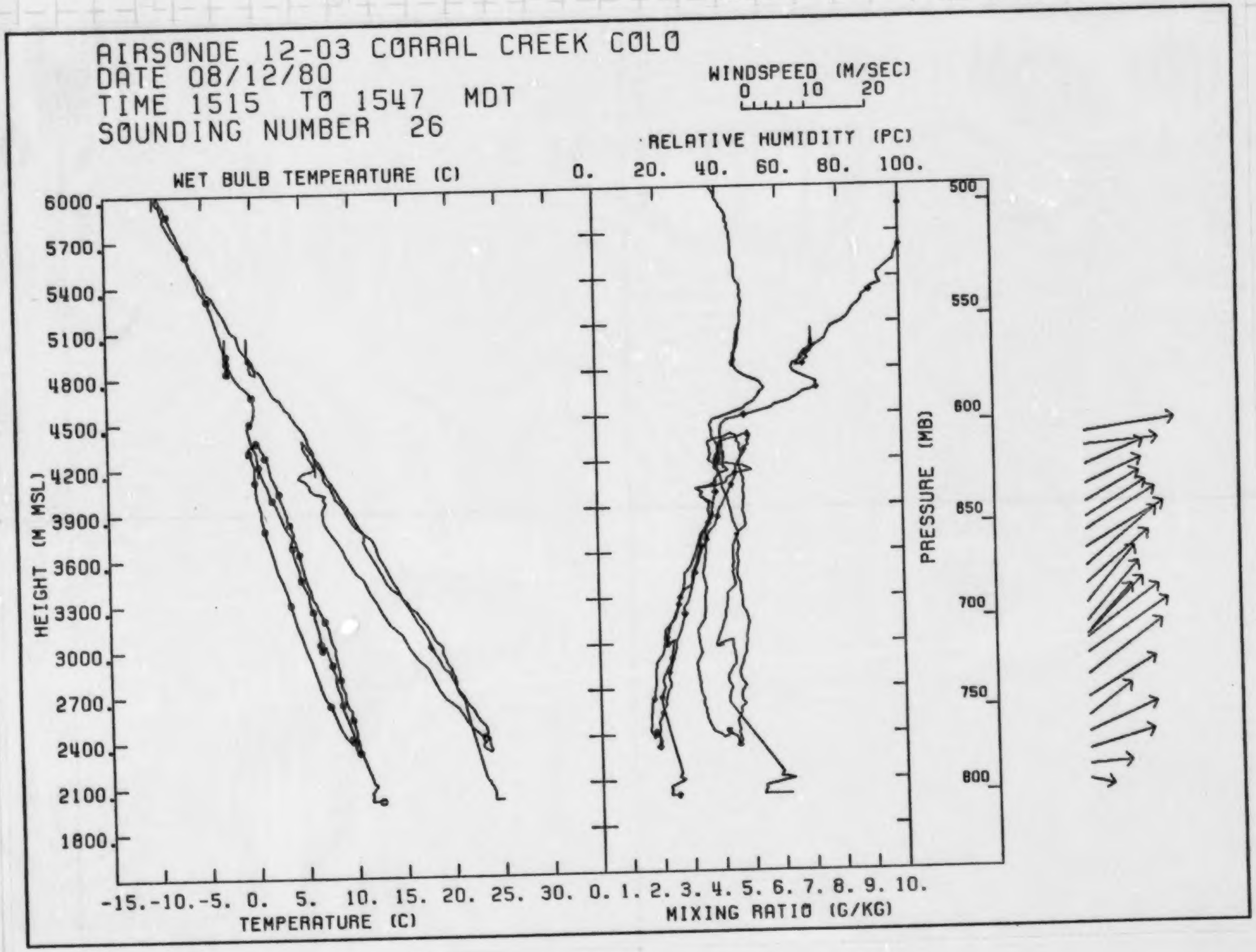

FIGURE 68. Airsonde Sounding #26, 1515 MDT, August 12, 1980.

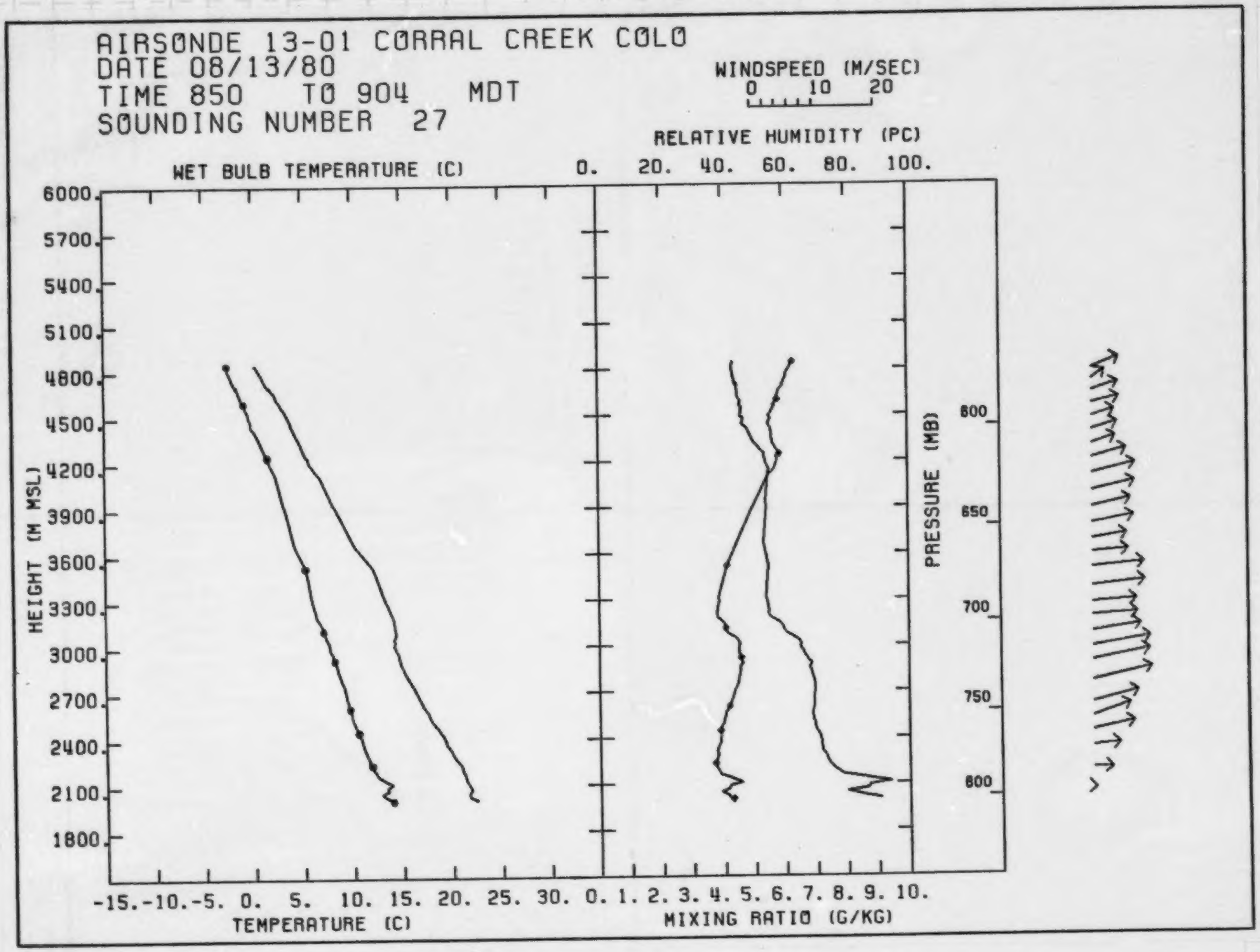

FIGURE 69. Airsonde Sounding #27, 0850 MDT, August 13, 1980.

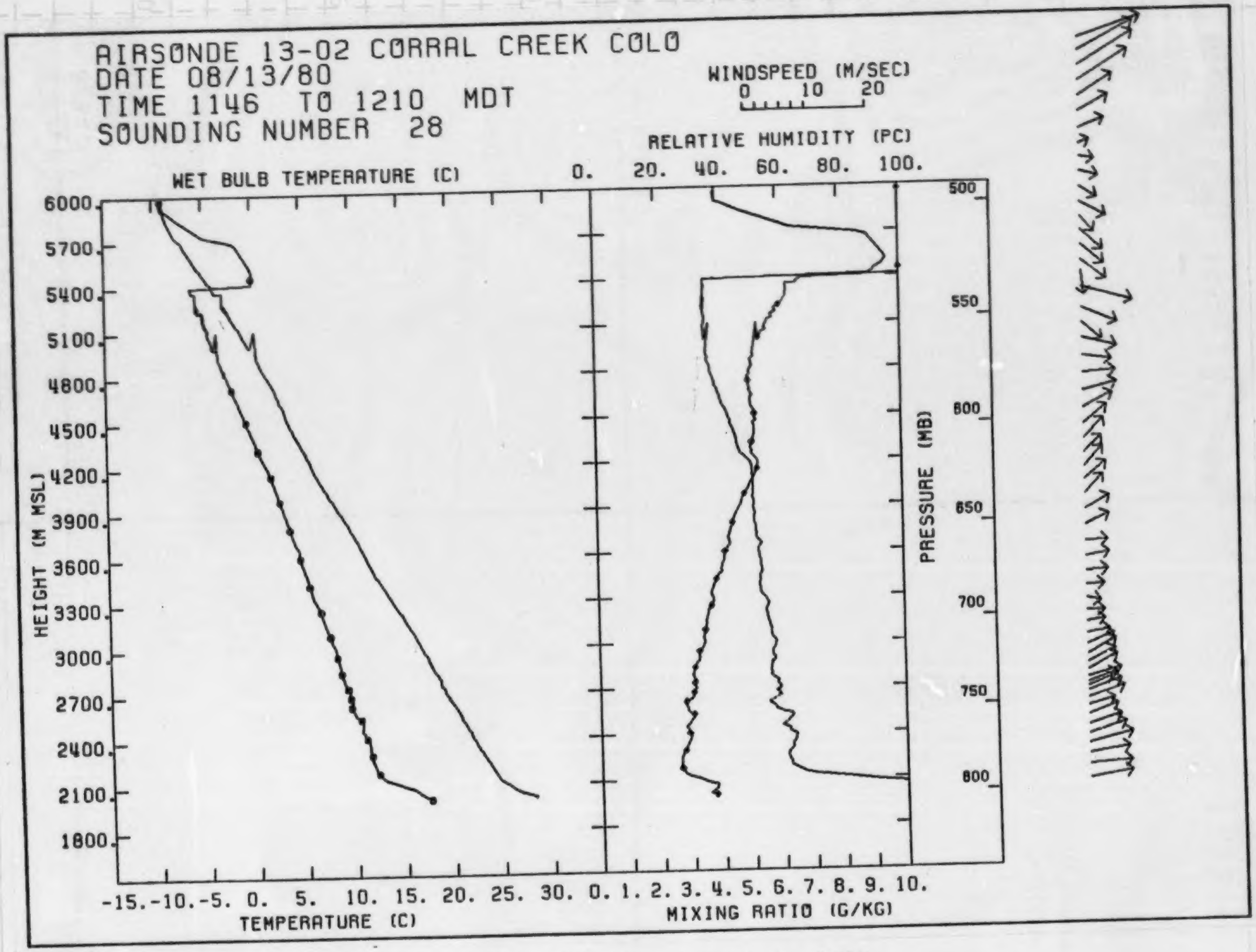

FIGURE 70. Airsonde Sounding #28, 1146 MDT, August 13, 1980.

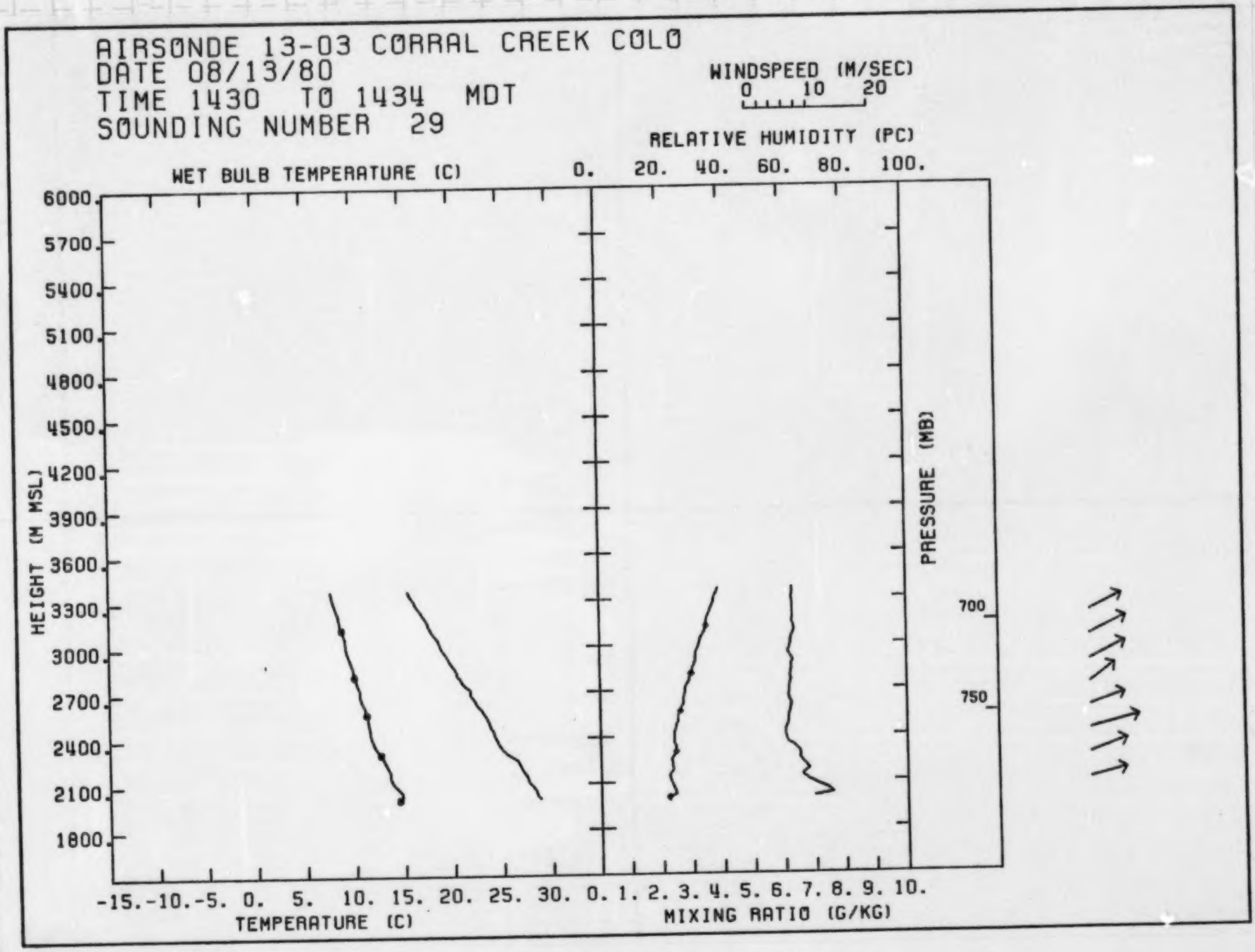

FIGURE 71. Airsonde Sounding #29, 1430 MDT, August 13, 1980.

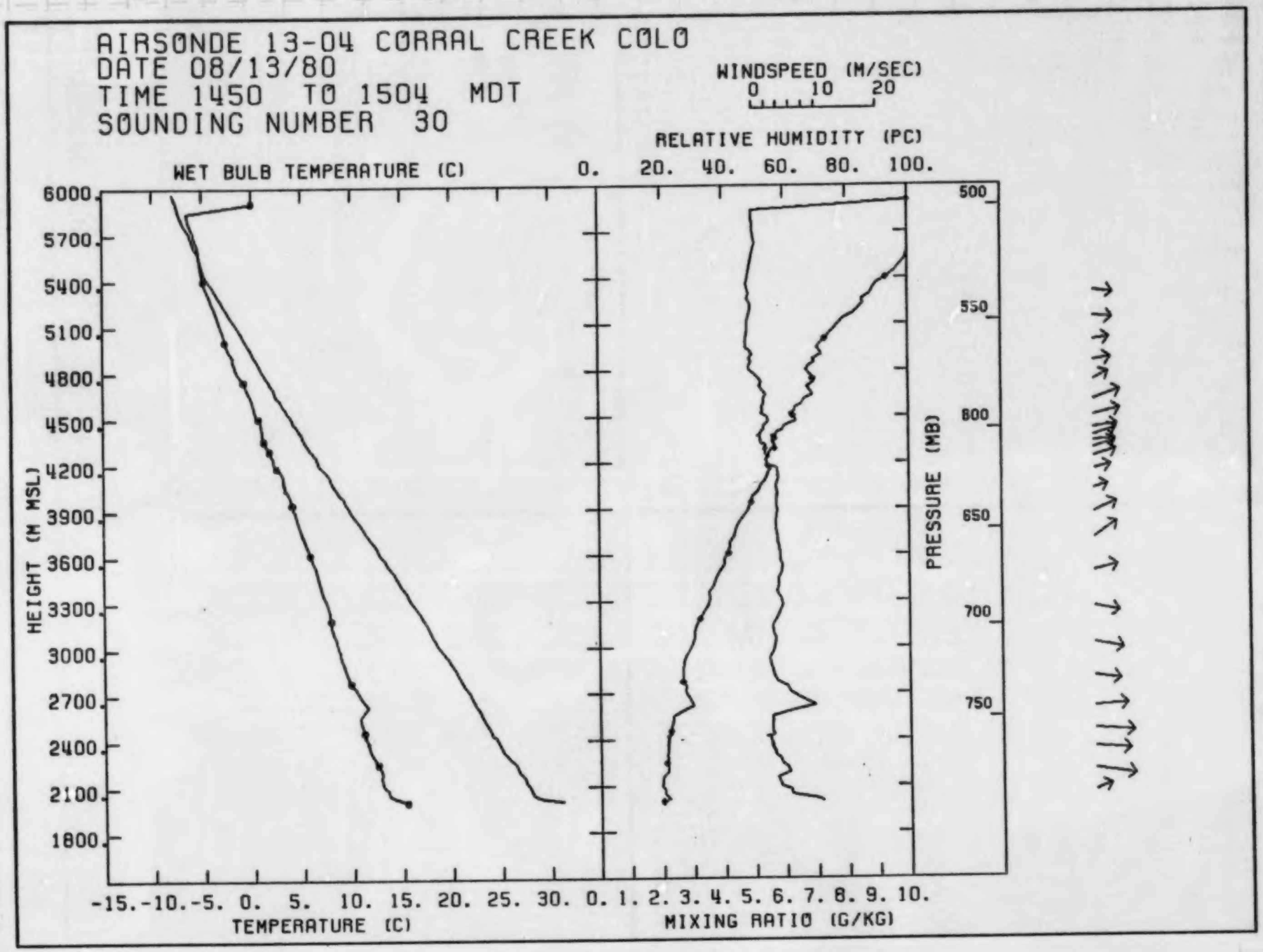

FIGURE 72. Airsonde Sounding #30, 1450 MDT, August 13, 1980.

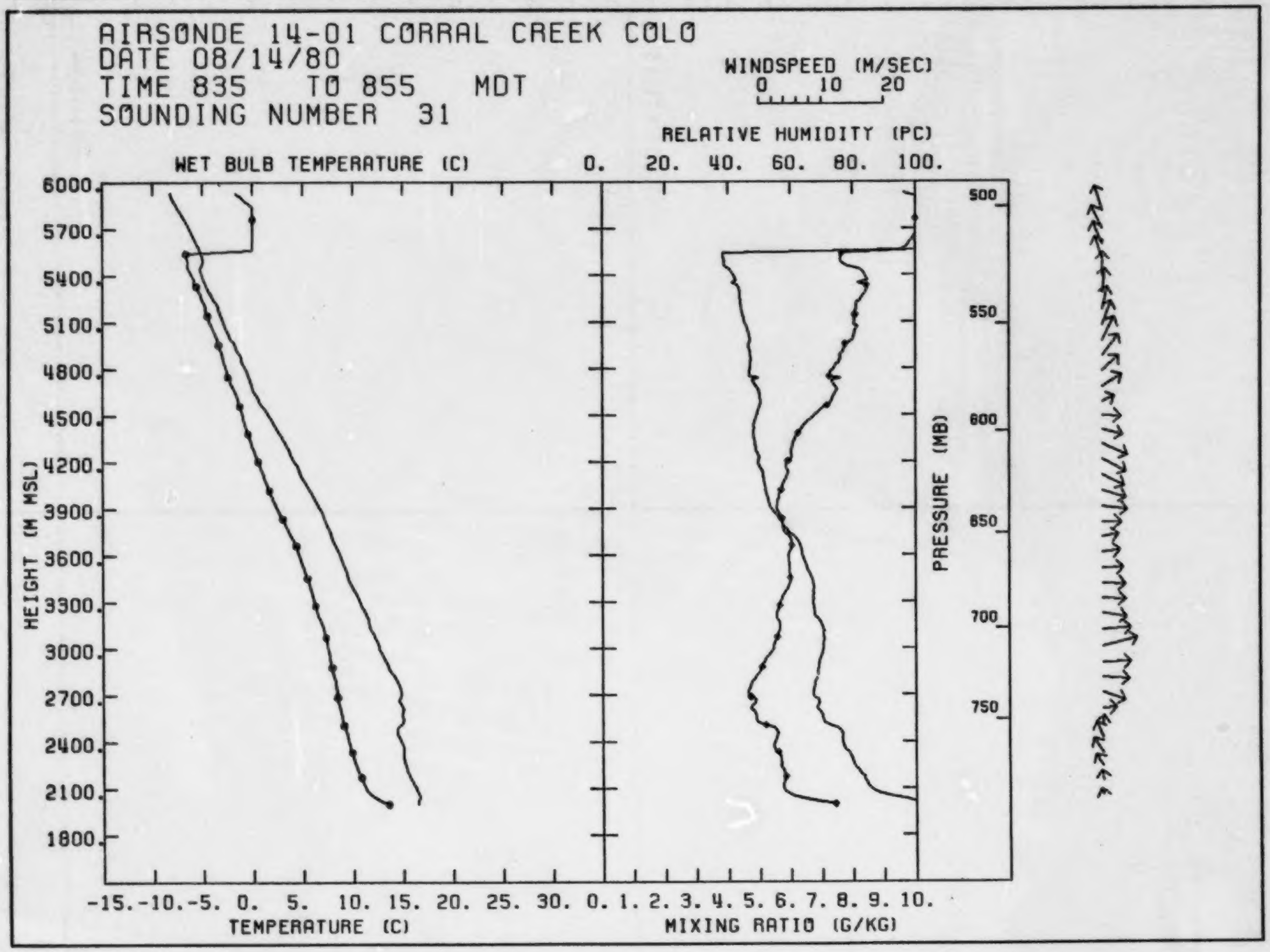

FIGURE 73. Airsonde Sounding #31, 0835 MDT, August 14, 1980.

START LINE
TYPIST PROOFER CORRECTED BY

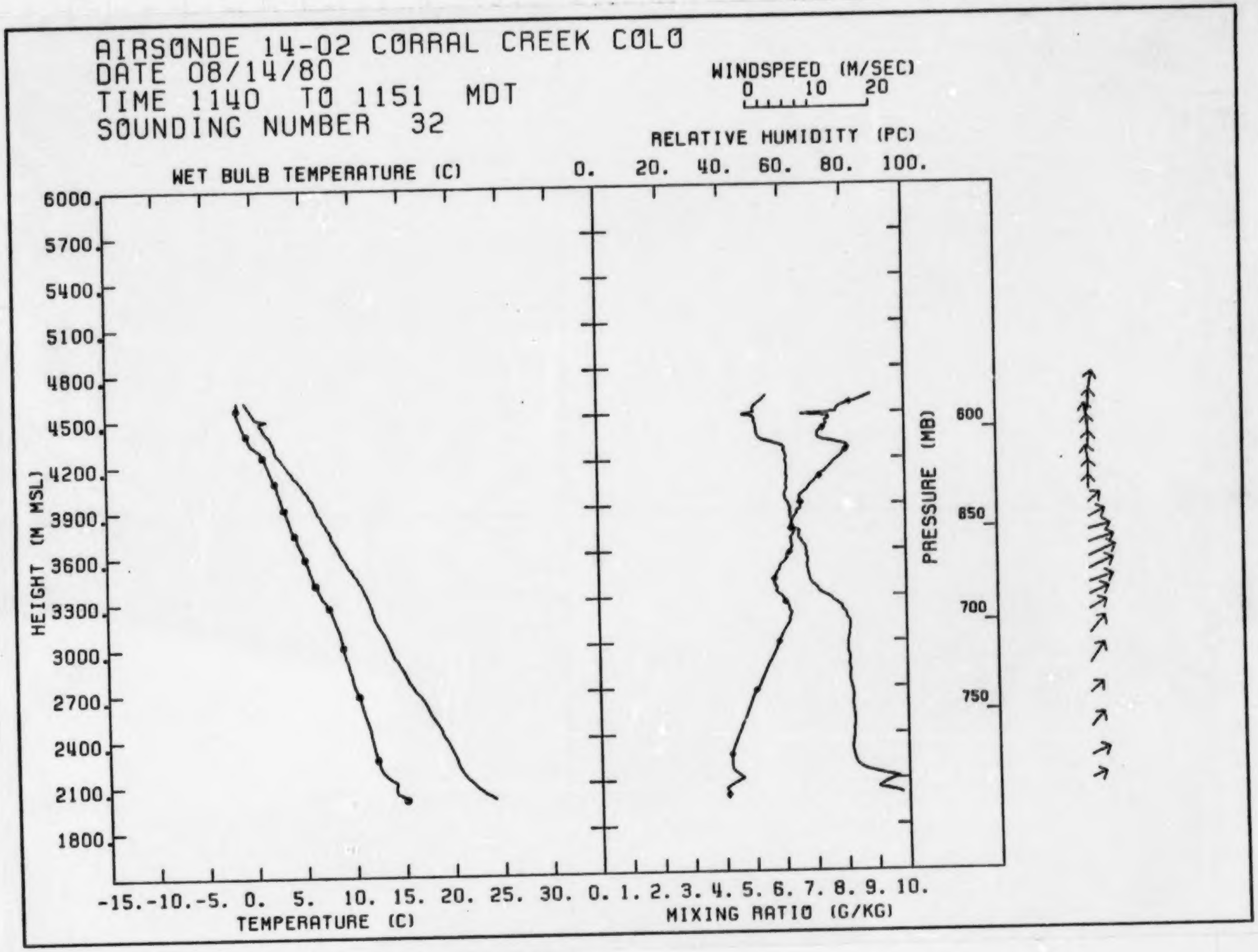

FIGURE 74. Airsonde Sounding #32, 1140 MDT, August 14, 1980.

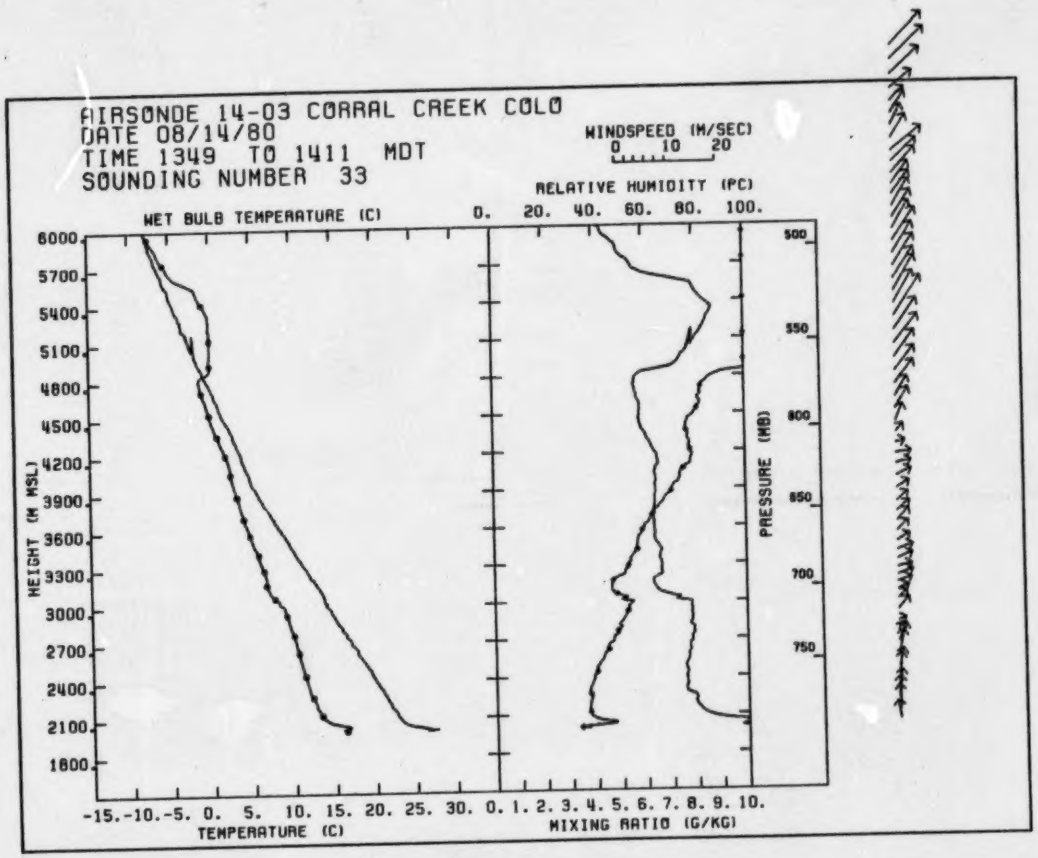

FIGURE 75. Airsonde Sounding #33, 1349 MDT, August 14, 1980.

# APPENDIX B

# COMPOSITE AIRSONDE SOUNDINGS

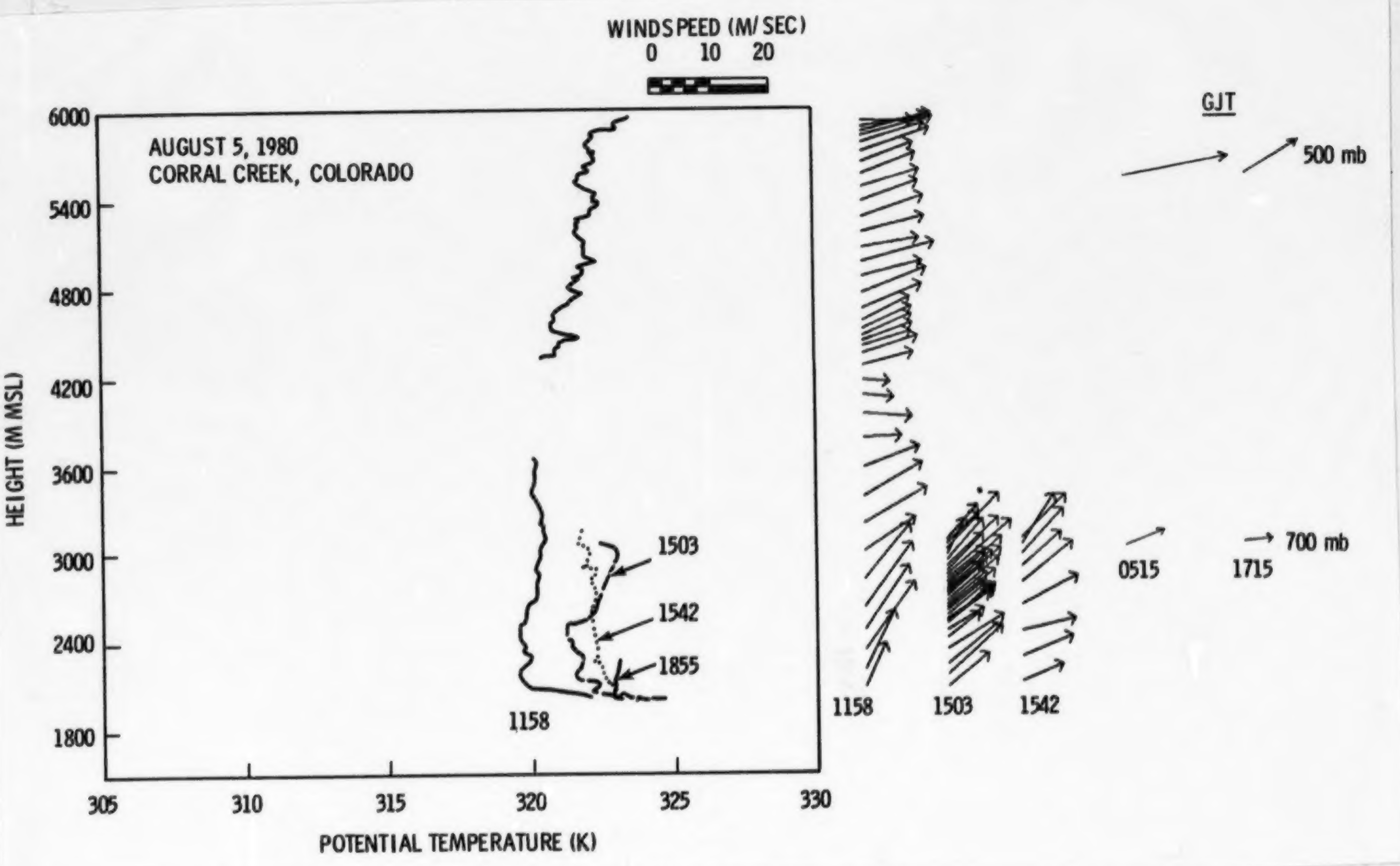

FIGURE 76. Composite Airsonde Profiles, August 5, 1980.

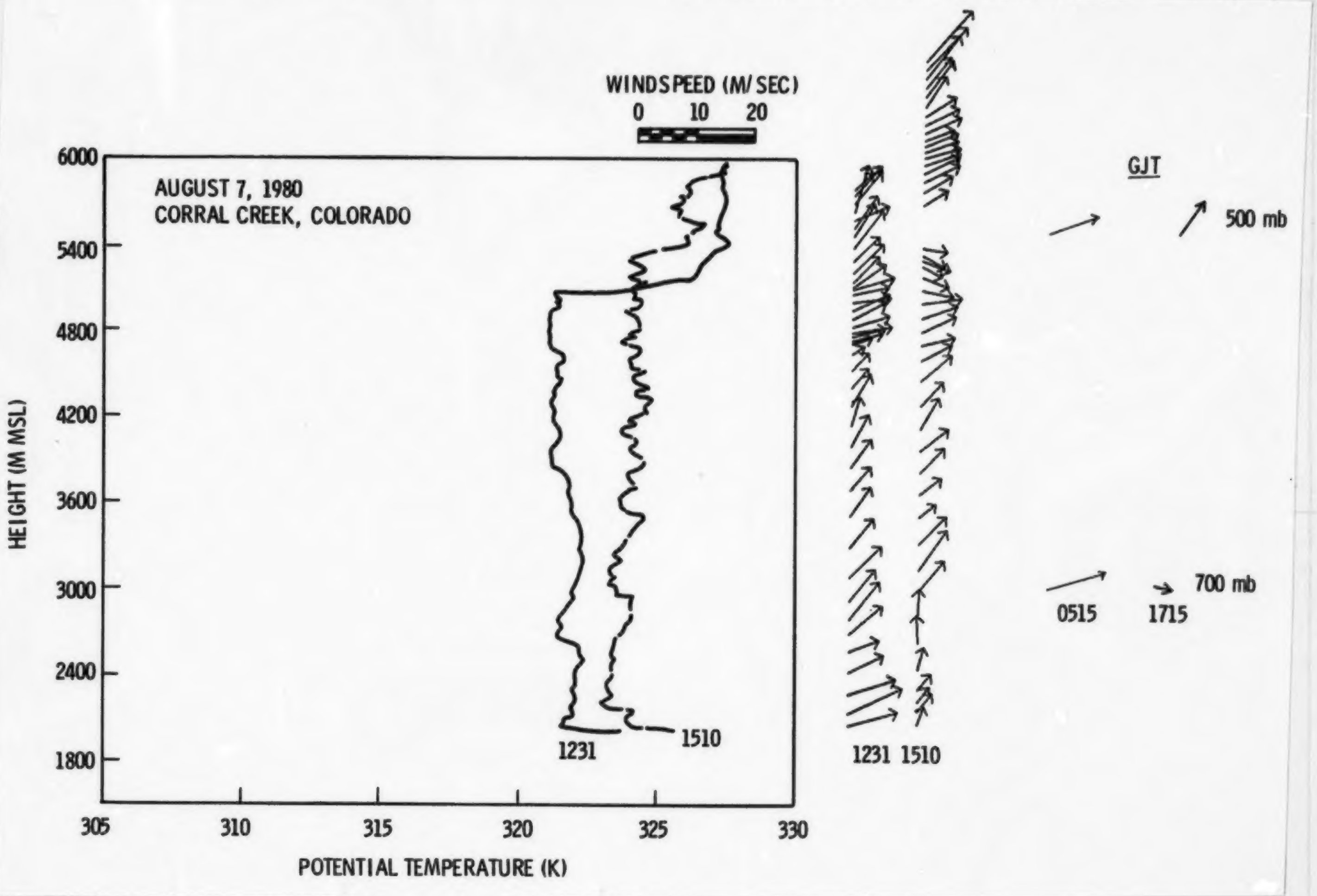

FIGURE 77. Composite Airsonde Profiles, August 7, 1980.

START LINE
PROOFER
CORRECTED BY

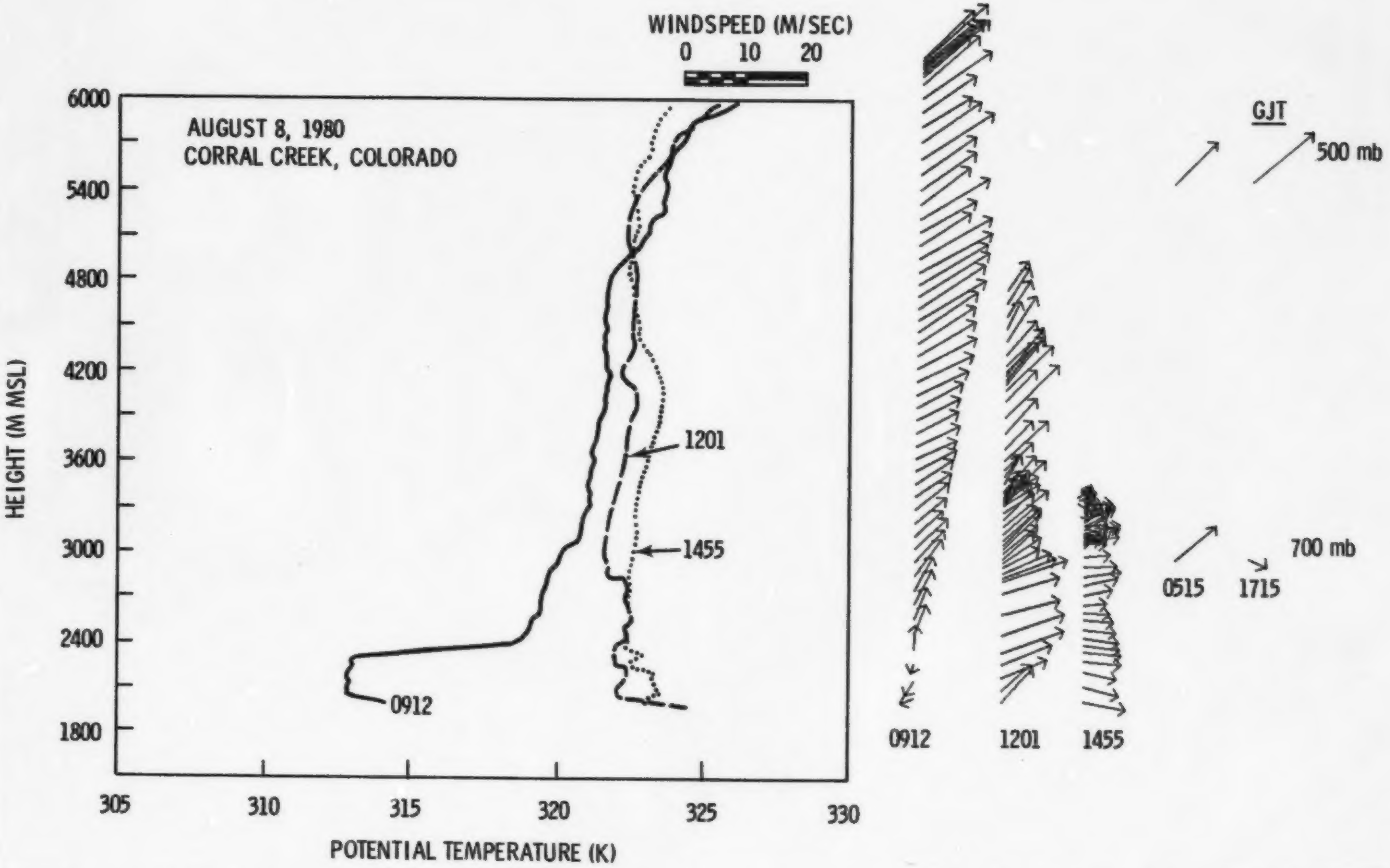

FIGURE 78. Composite Airsonde Profiles, August 8, 1980.

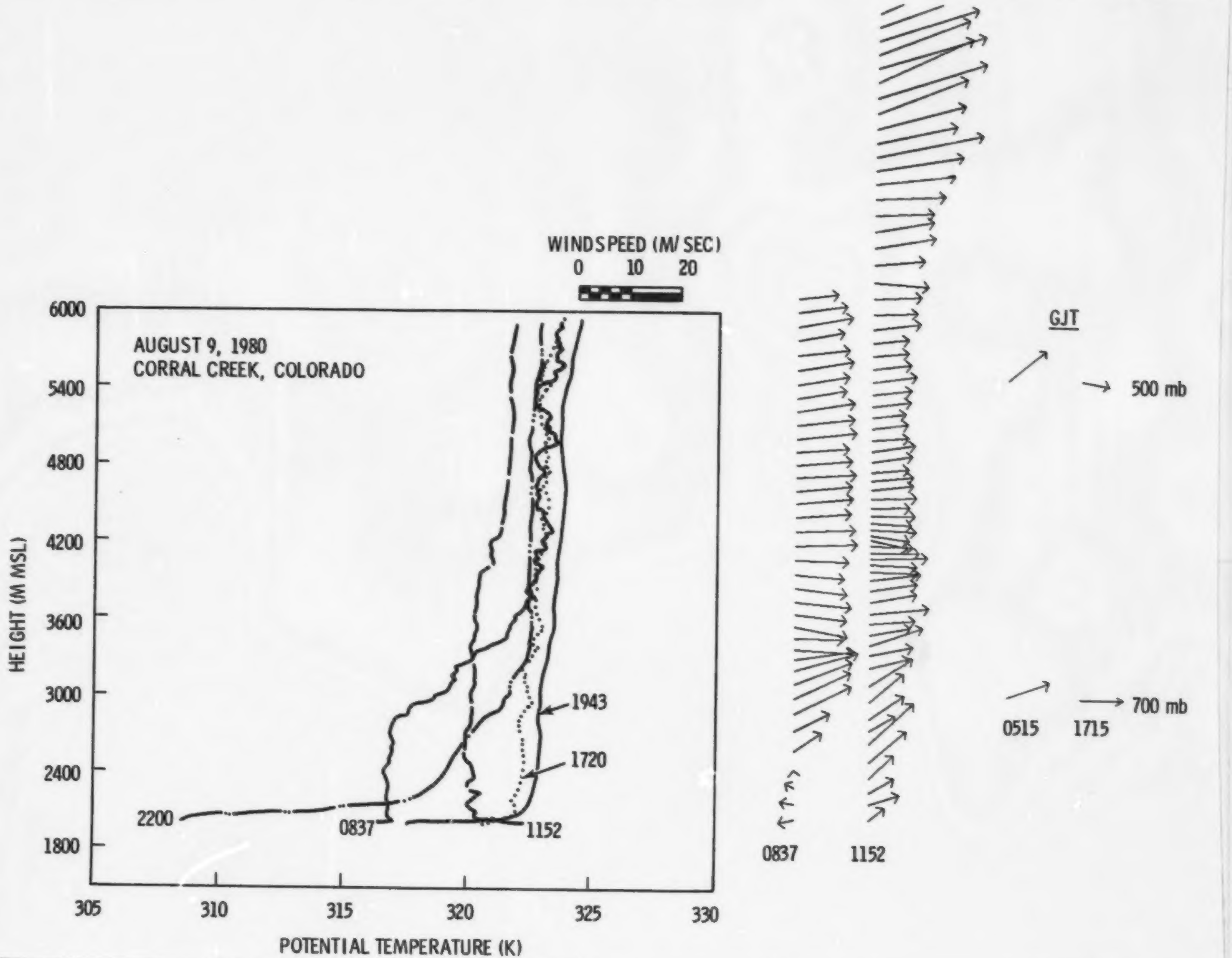

FIGURE 79. Composite Airsonde Profiles, August 9, 1980

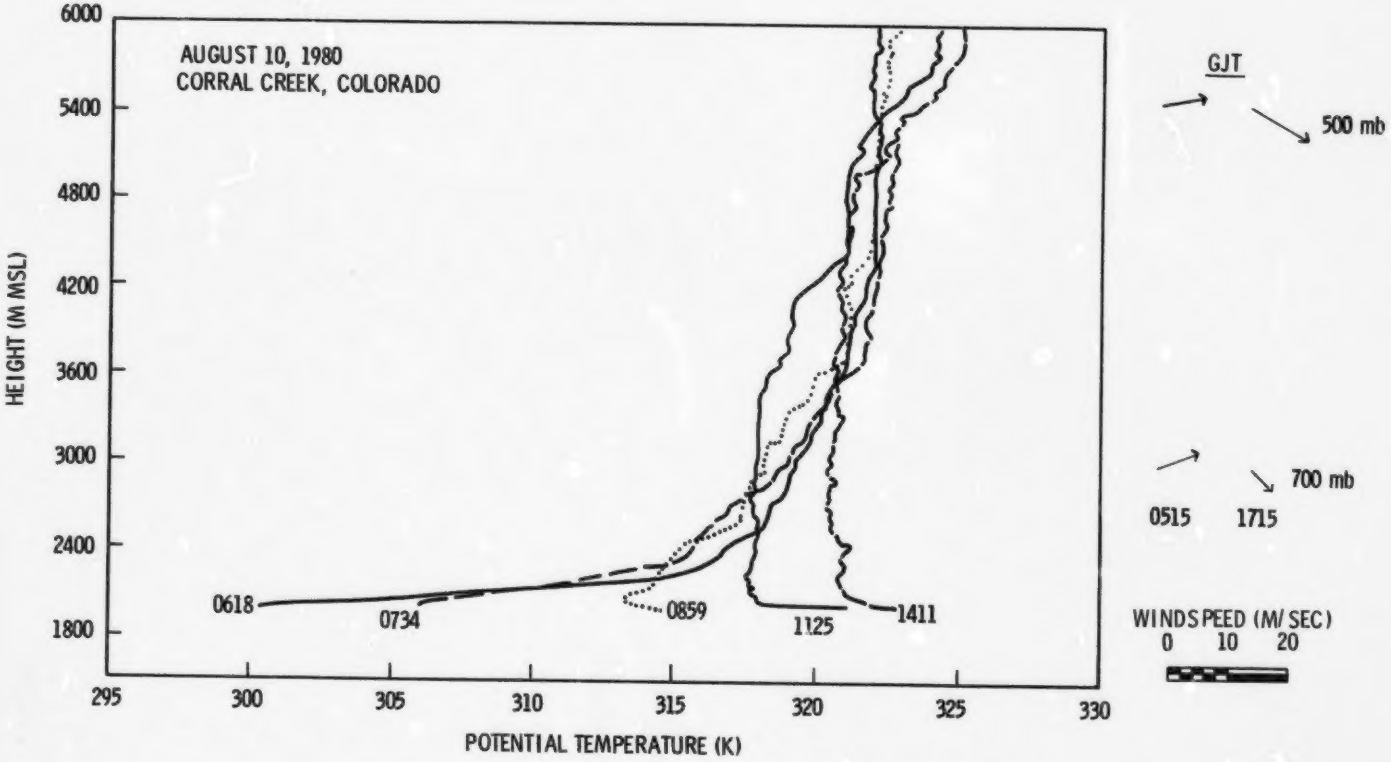

FIGURE 80. Composite Airsonde Profiles, August 10, 1980.

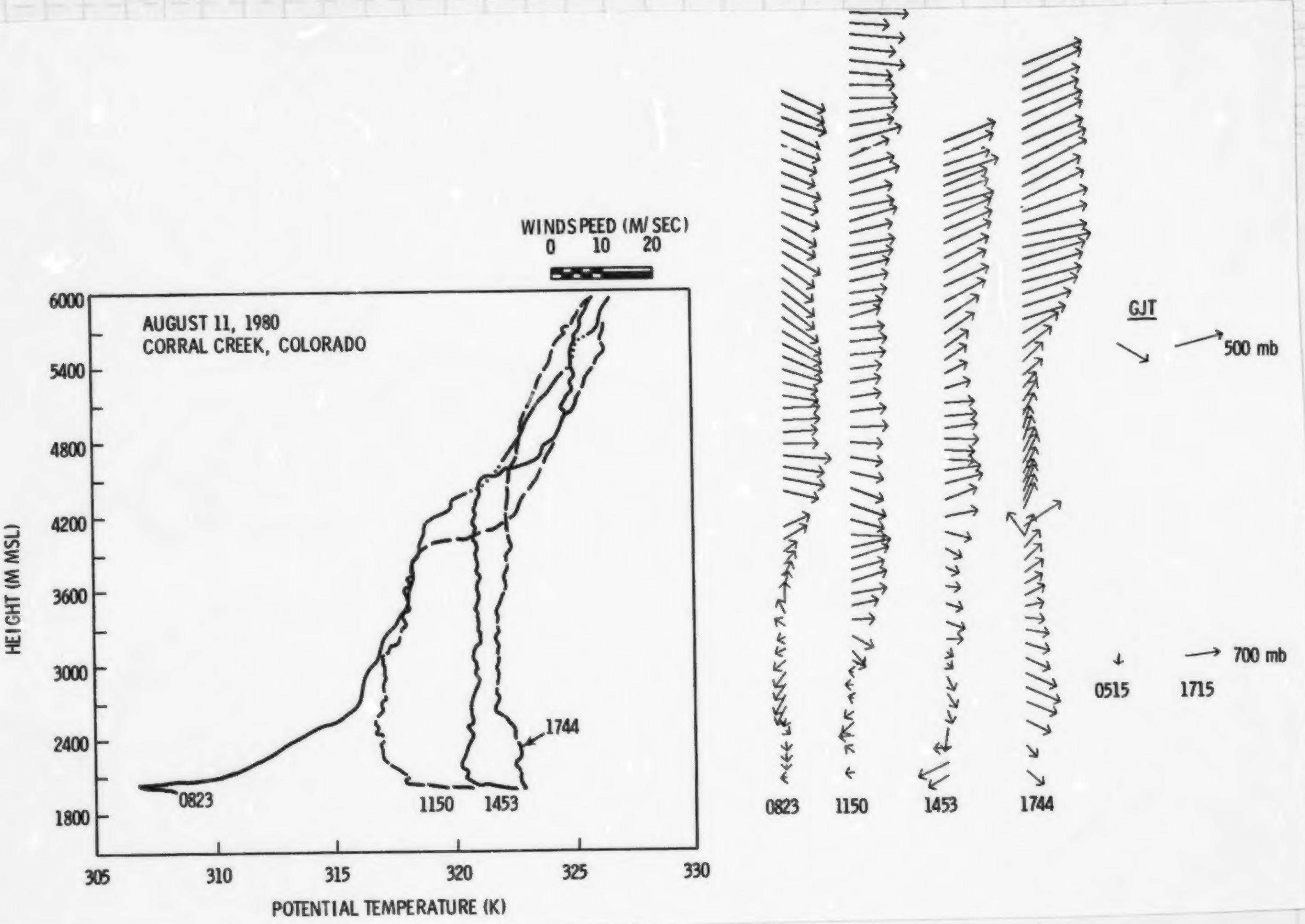

FIGURE 81. Composite Airsonde Profiles, August 11, 1980

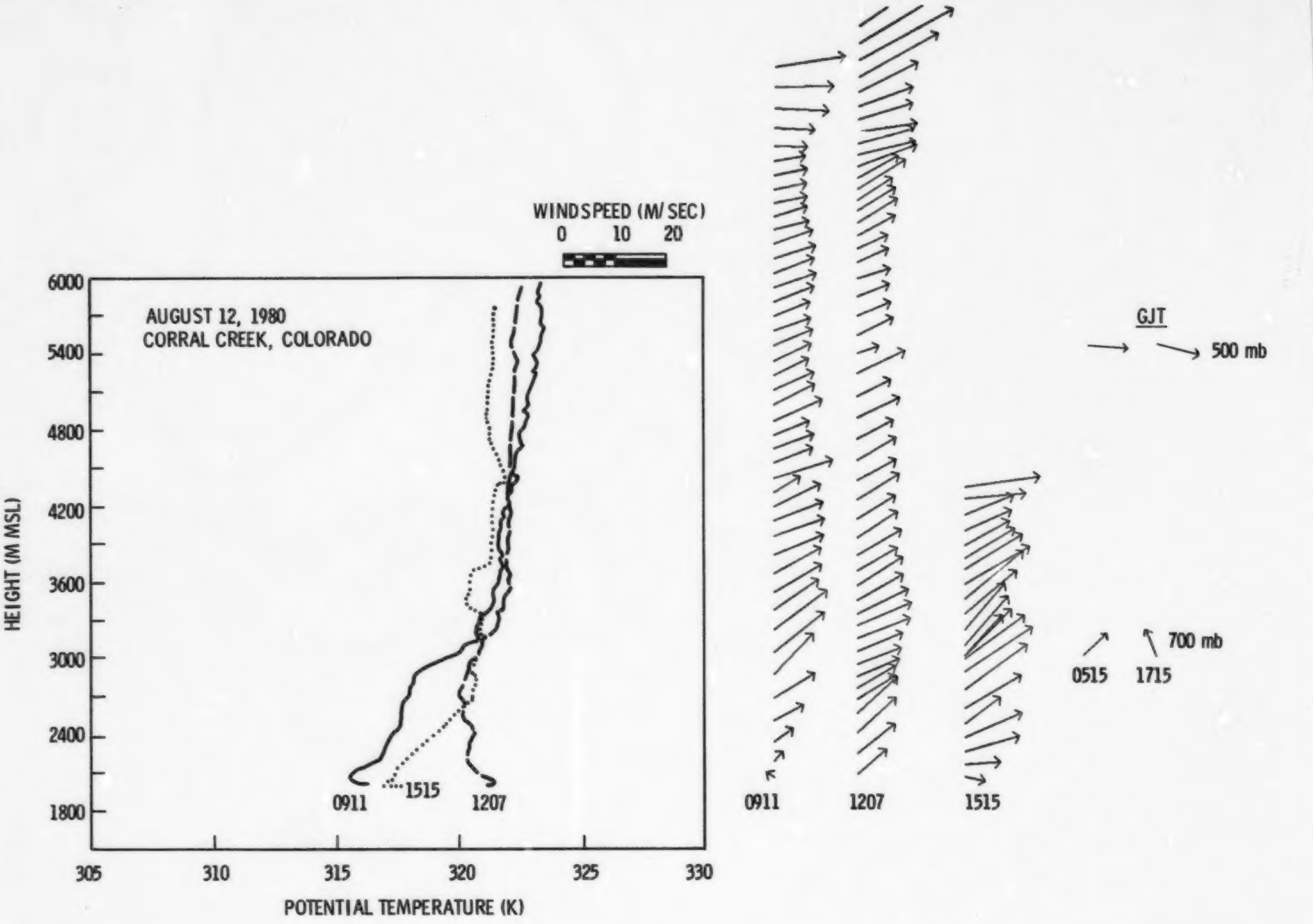

FIGURE 82. Composite Airsonde Profiles, August 12, 1980.

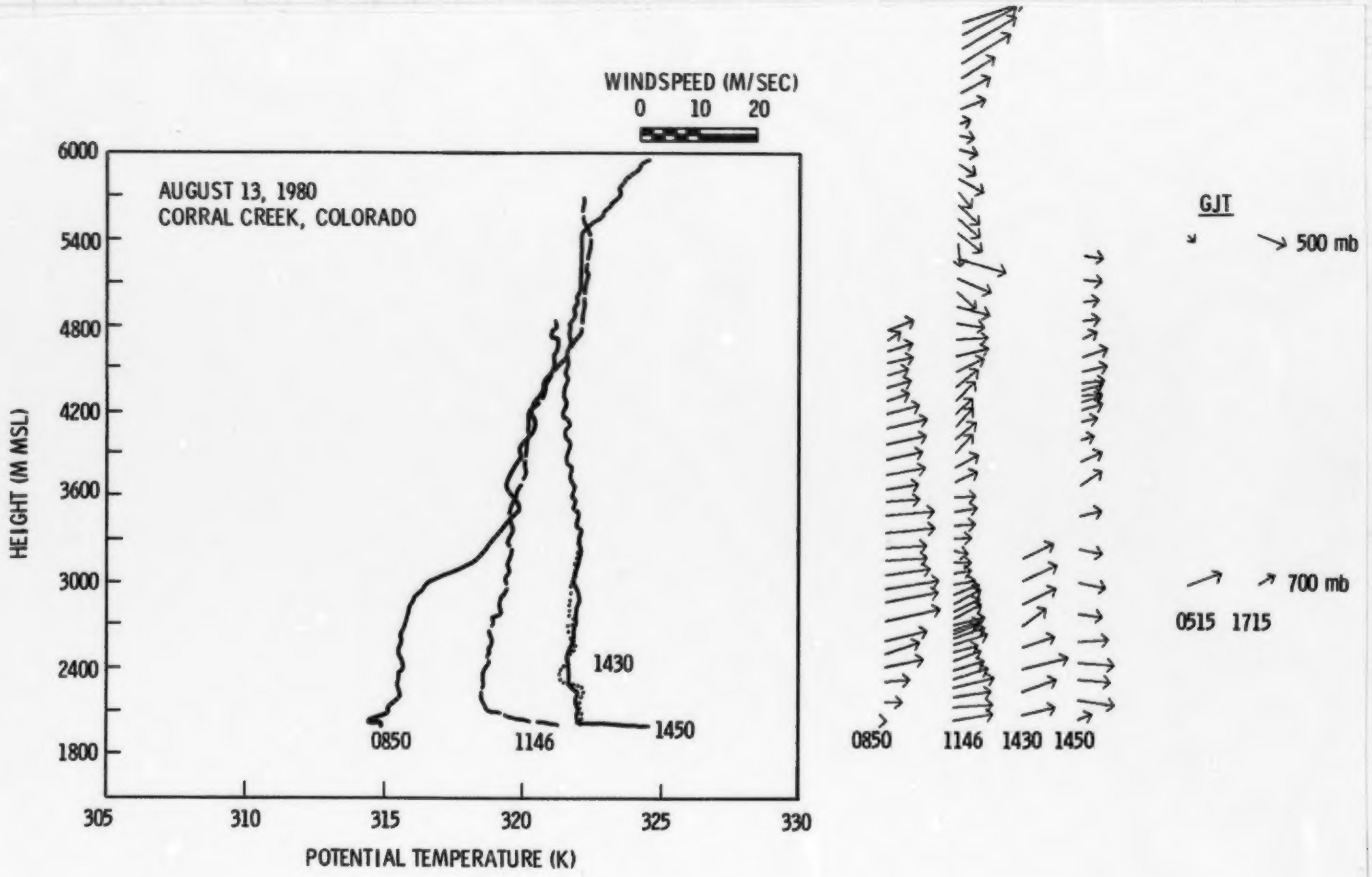

FIGURE 83. Composite Airsonde Profiles, August 13, 1980.

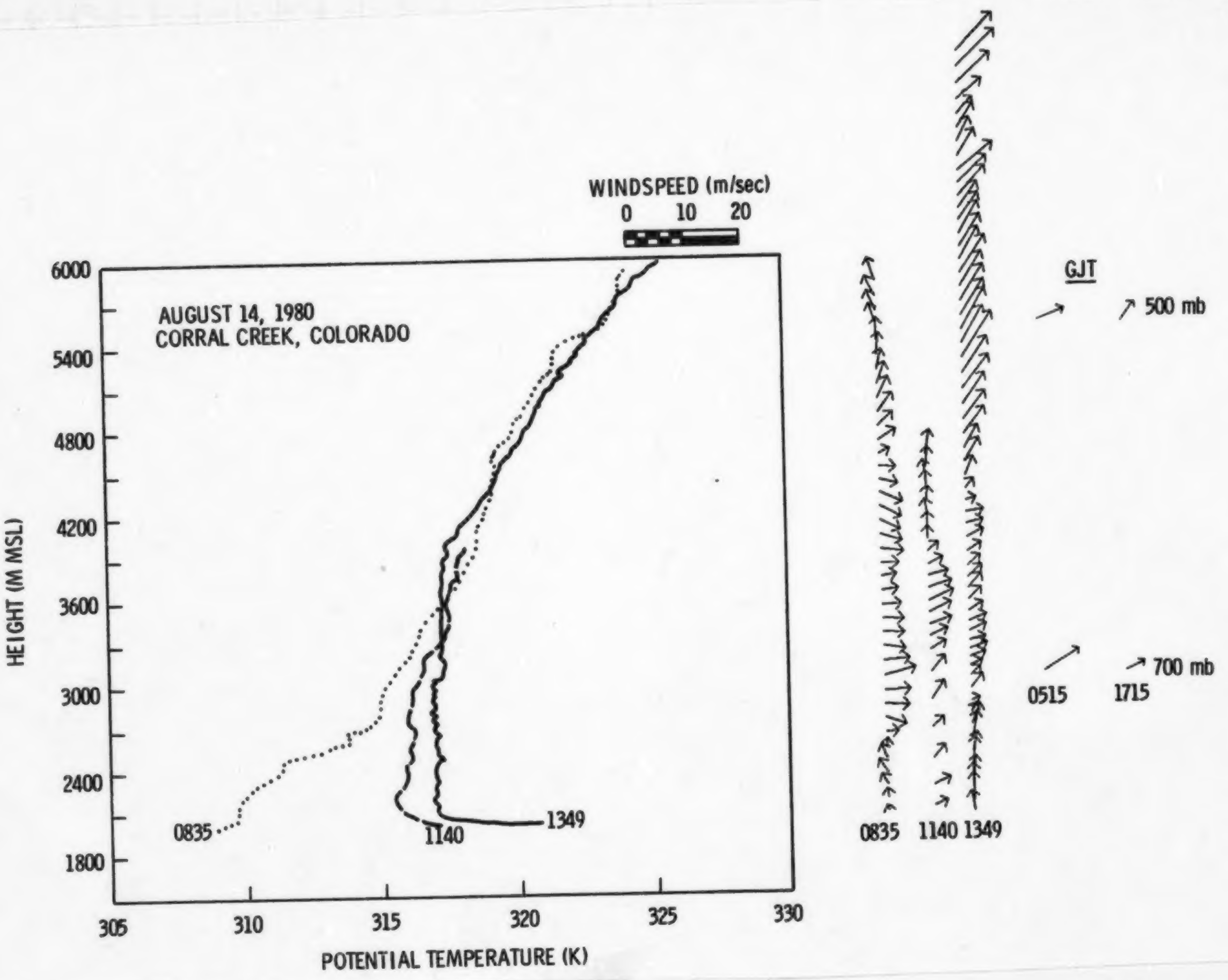

FIGURE 84. Composite Airsonde Profiles, August 14, 1980.

# APPENDIX C

# AIRSONDE SUBPOINT TRAJECTORIES

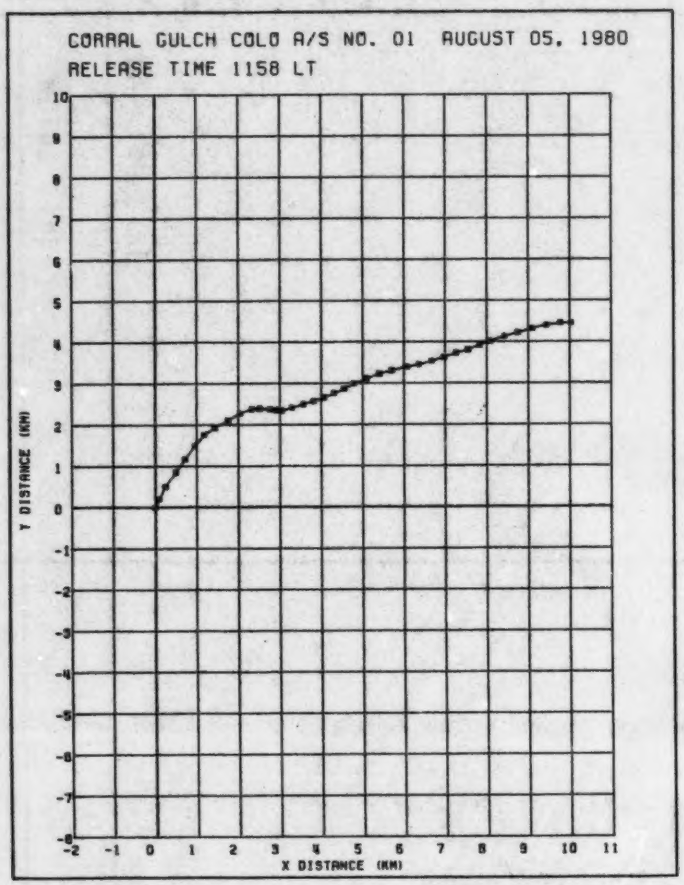

FIGURE 85. Airsonde #1 Subpoint Trajectory, 1158 MDT, August 5, 1980.

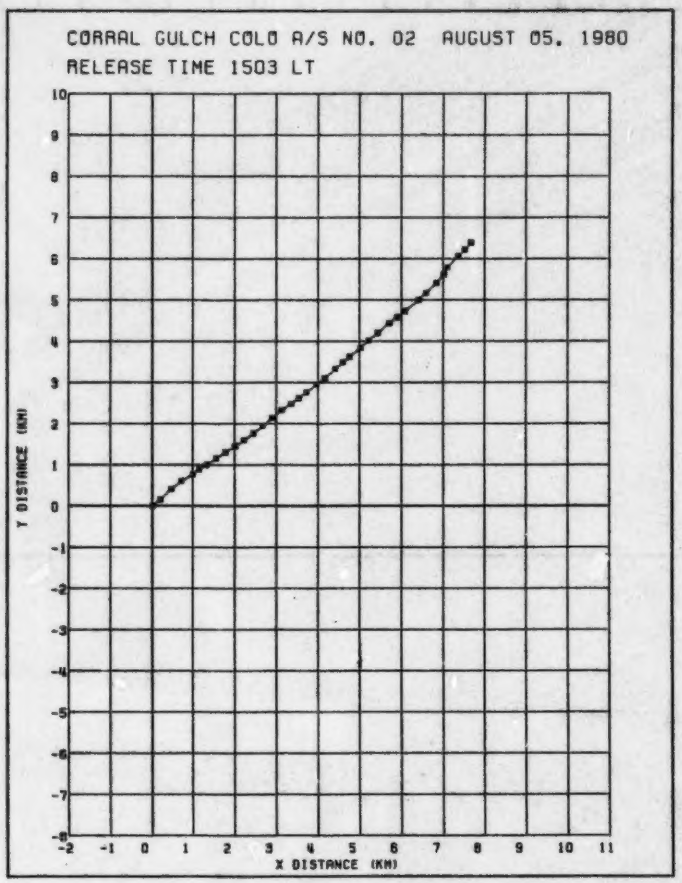

FIGURE 86. Airsonde #2 Subpoint Trajectory, 1503 MDT, August 5, 1980.

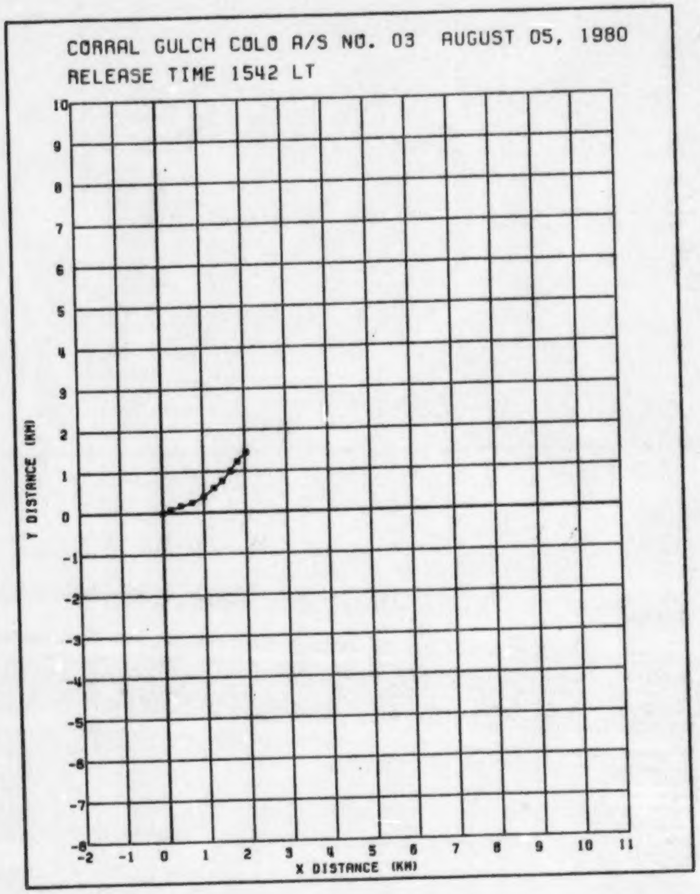

FIGURE 87. Airsonde #3 Subpoint Trajectory, 1542 MDT, August 5, 1980.

Airsonde #4 was not tracked by theodolite. No trajectory data are available.

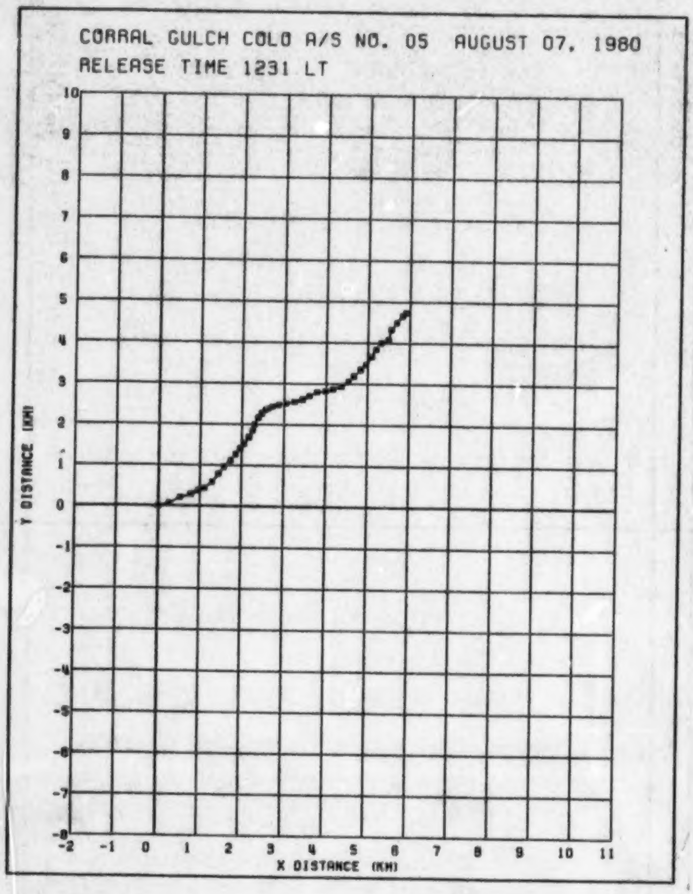

FIGURE 88. Airsonde #5 Subpoint Trajectory, 1231 MDT, August 7, 1980.

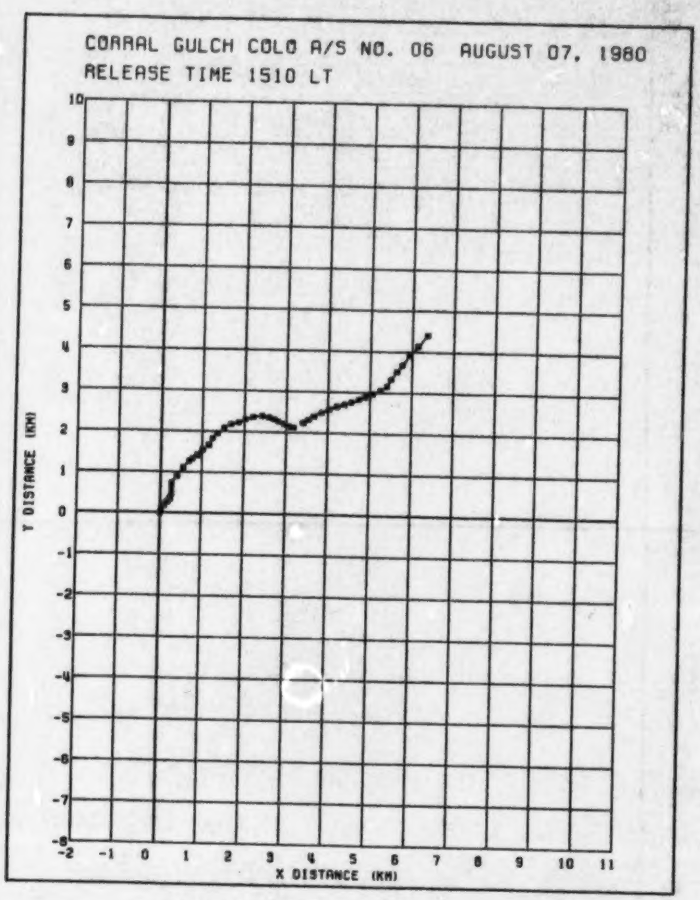

FIGURE 89. Airsonde #6 Subpoint Trajectory, 1510 MDT, August 7, 1980.

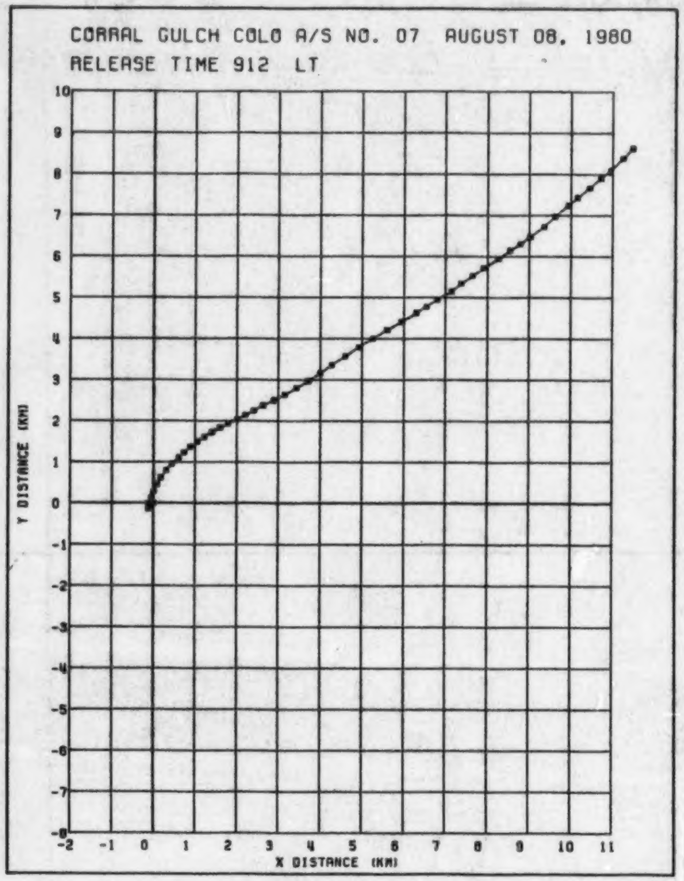

FIGURE 90. Airsonde #7 Subpoint Trajectory, 0912 MDT, August 8, 1980.

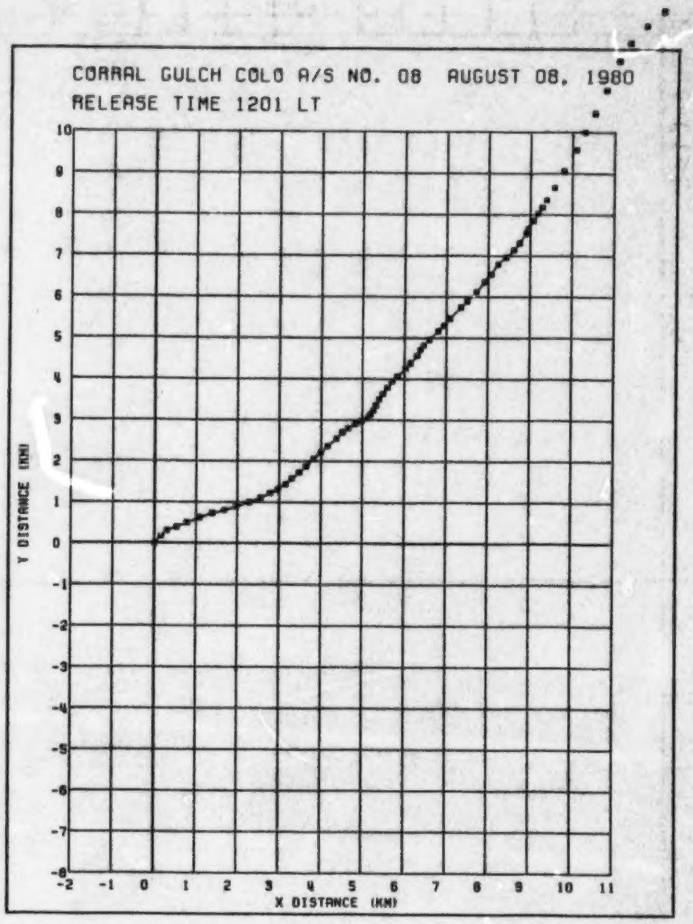

FIGURE 91. Airsonde #8 Subpoint Trajectory, 1201 MDT, August 8, 1980.

IST PROOFER CORRECTED BY

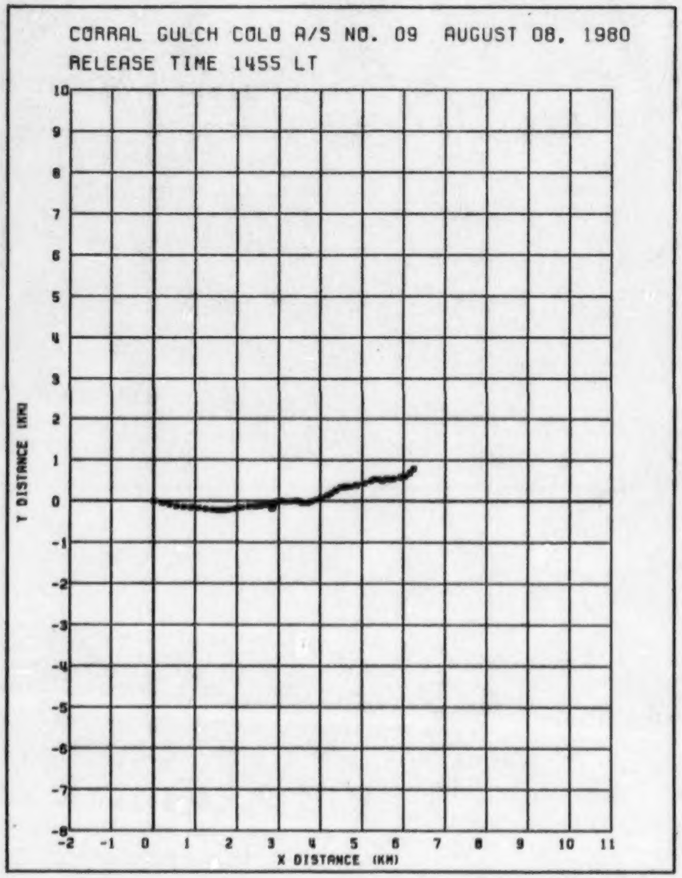

FIGURE 92. Airsonde #9 Subpoint Trajectory, 1455 MDT, August 8, 1980.

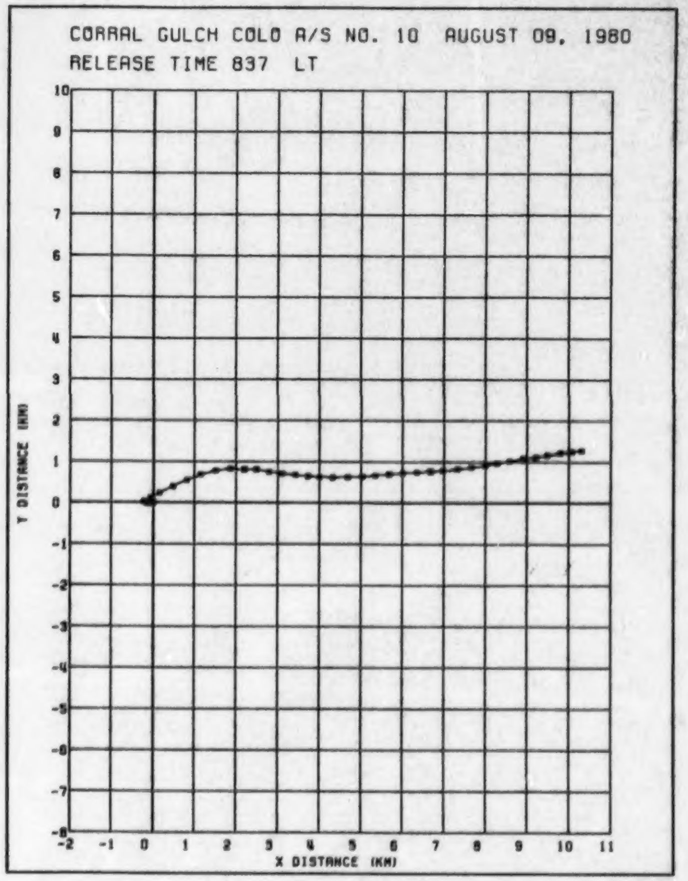

FIGURE 93. Airsonde #10 Subpoint Trajectory, 0837 MDT, August 9, 1980.

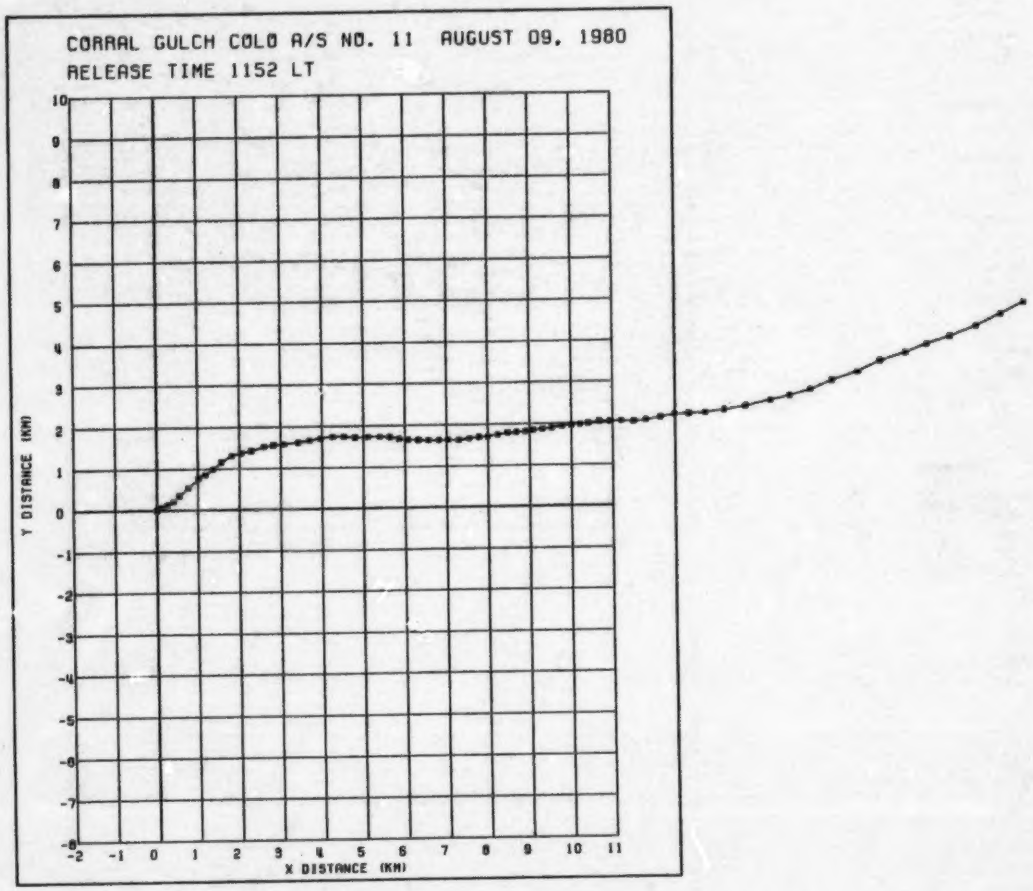

Airsondes #12 - 19 were not tracked by optical theodolite. No trajectory data are available.

FIGURE 94. Airsonde #11 Subpoint Trajectory, 1152 MDT, August 9, 1980.

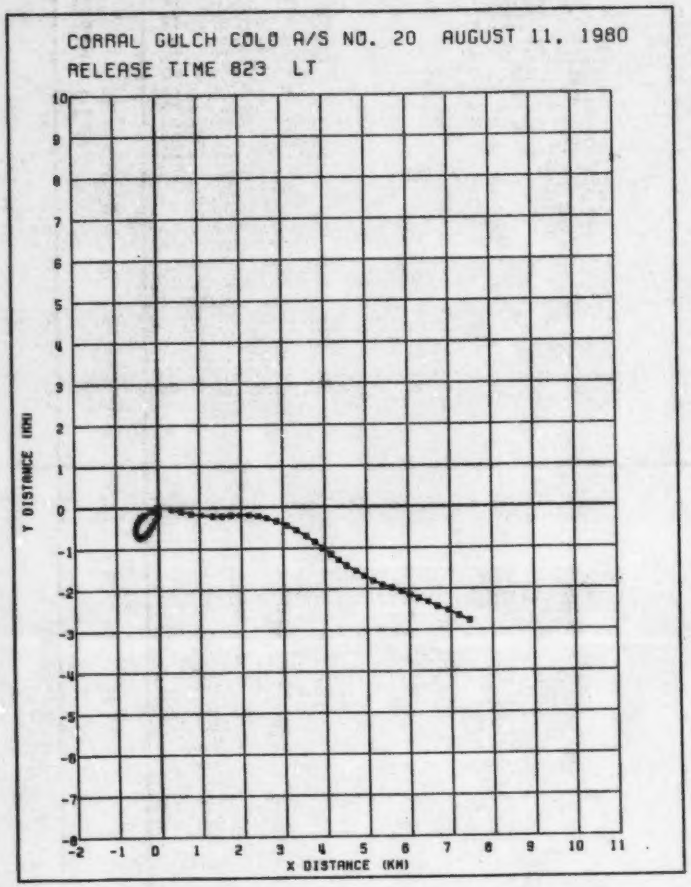

FIGURE 95. Airsonde #20 Subpoint Trajectory, 0823 MDT, August 11, 1980.

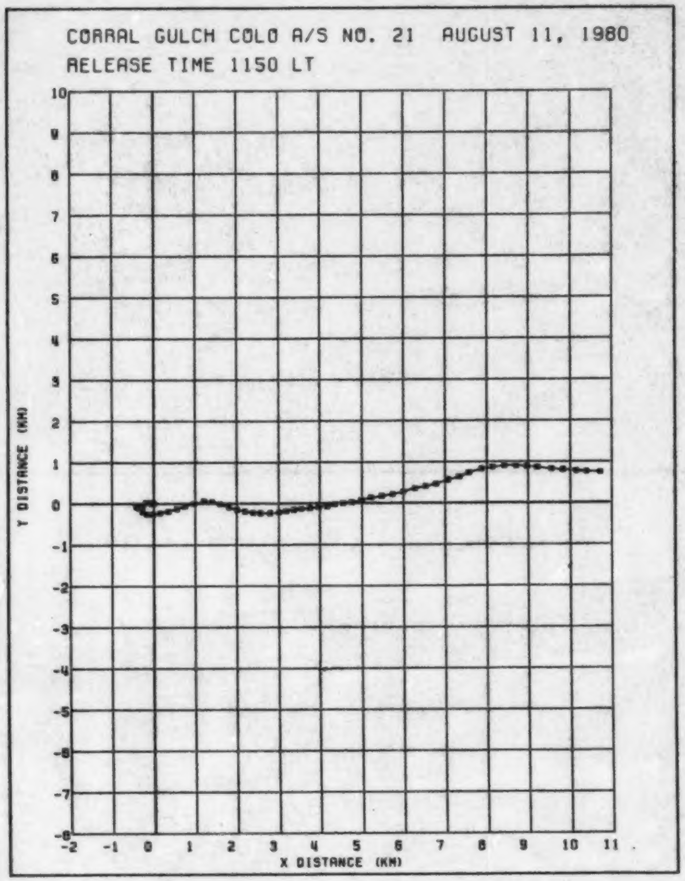

FIGURE 96. Airsonde #21 Subpoint Trajectory, 1150 MDT, August 11, 1980.

START LINE
PROOFER
CORRECTED BY

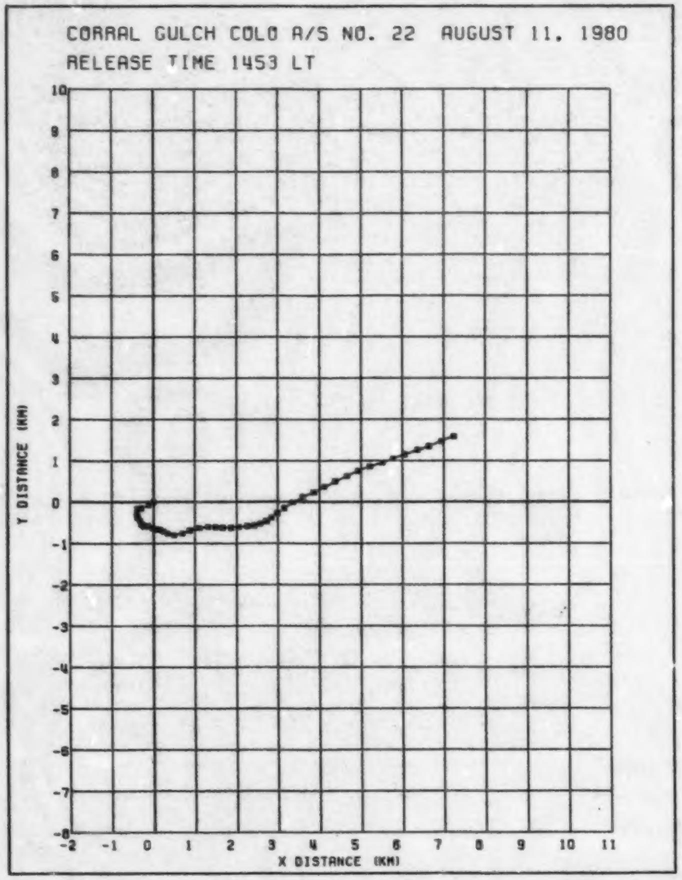

FIGURE 97. Airsonde #22 Subpoint Trajectory, 1453 MDT, August 11, 1980.

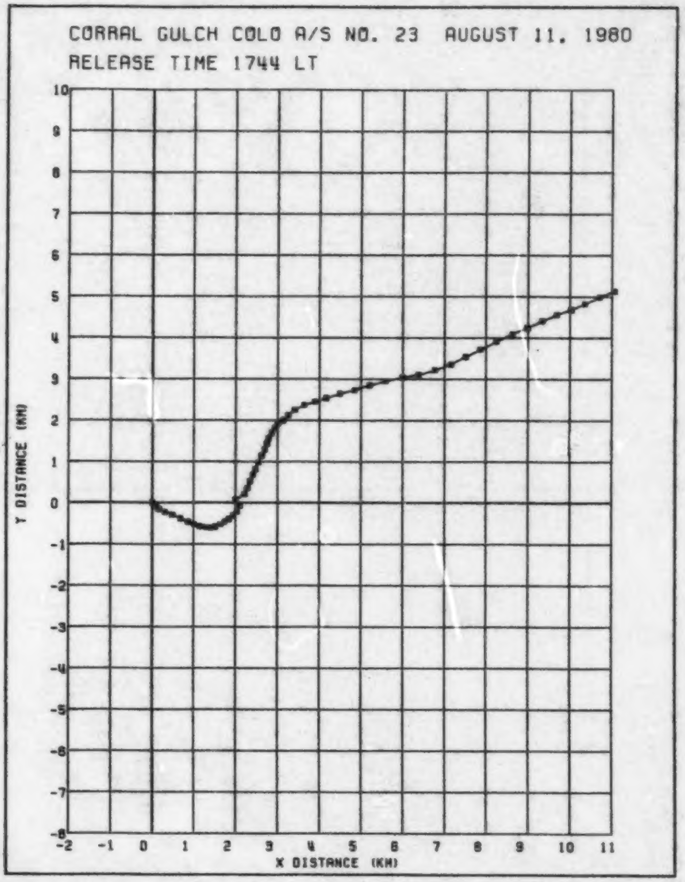

FIGURE 98. Airsonde #23 Subpoint Trajectory, 1744 MDT, August 11, 1980.

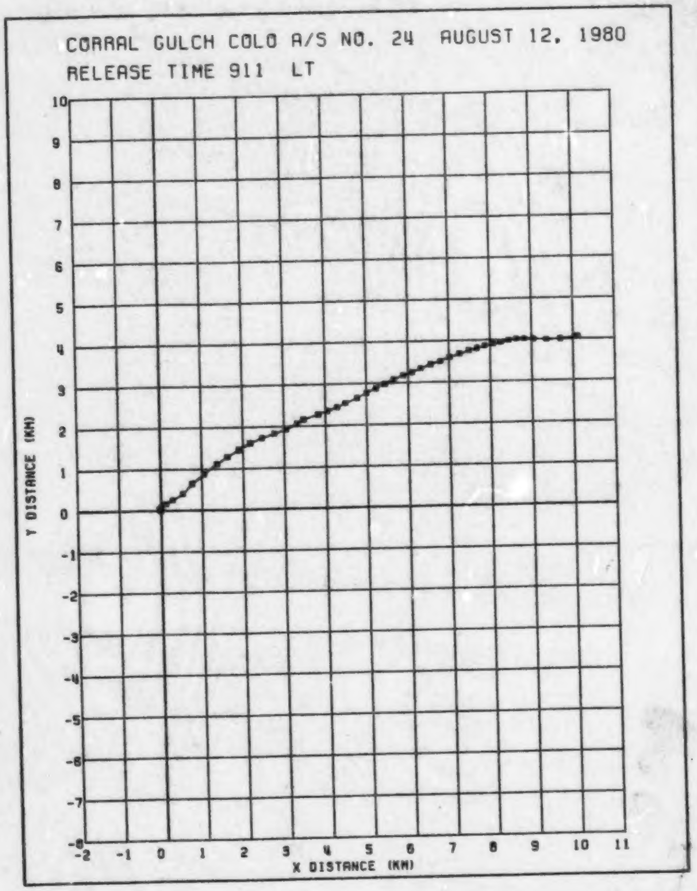

FIGURE 99. Airsonde #24 Subpoint Trajectory, 0911 MDT, August 12, 1980.

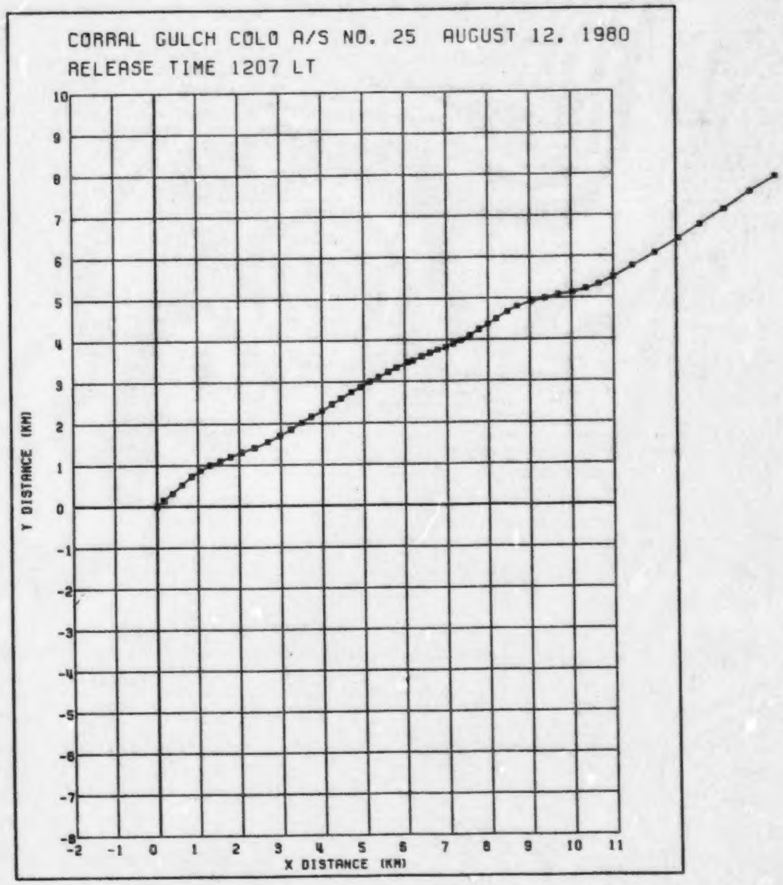

FIGURE 100. Airsonde #25 Subpoint Trajectory, 1207 MDT, August 12, 1980.

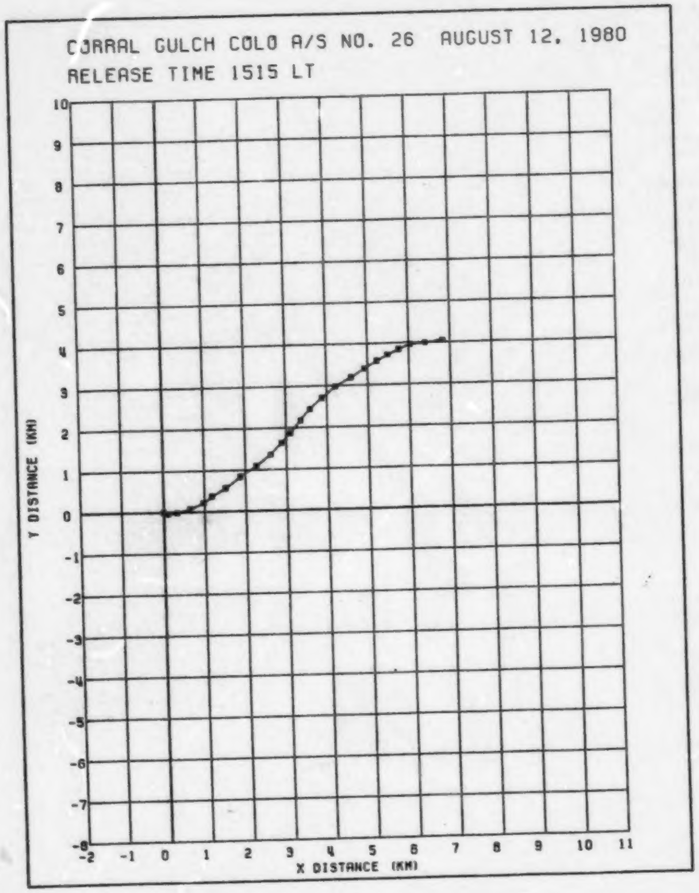

FIGURE 101. Airsonde #26 Subpoint Trajectory, 1515 MDT, August 12, 1980.

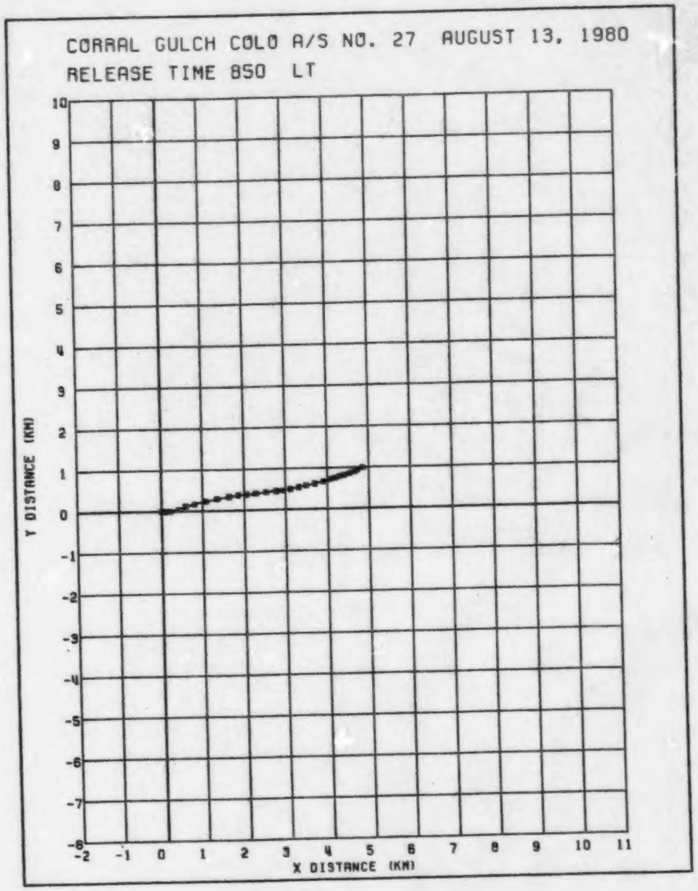

FIGURE 102. Airsonde #27 Subpoint Trajectory, 0850 MDT, August 13, 1980.

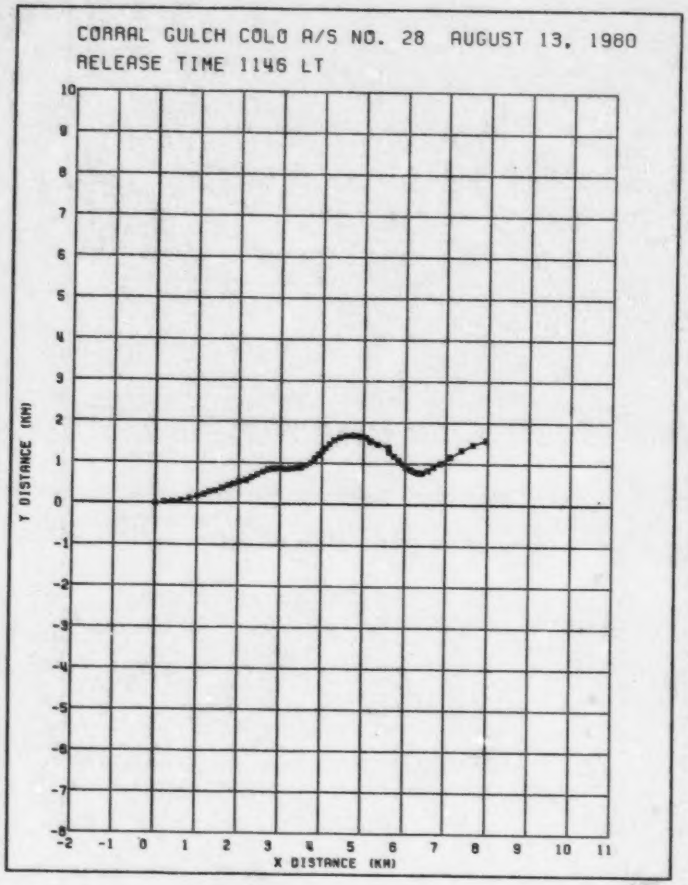

FIGURE 103. Airsonde #28 Subpoint Trajectory, 1146 MDT, August 13, 1980.

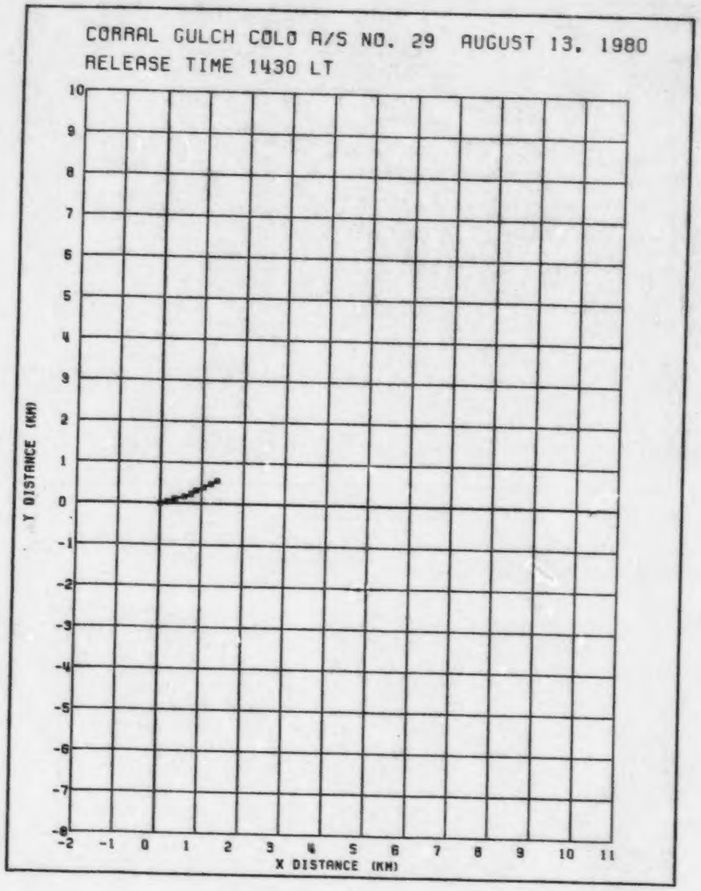

FIGURE 104. Airsonde #29 Subpoint Trajectory, 1430 MDT, August 13, 1980.

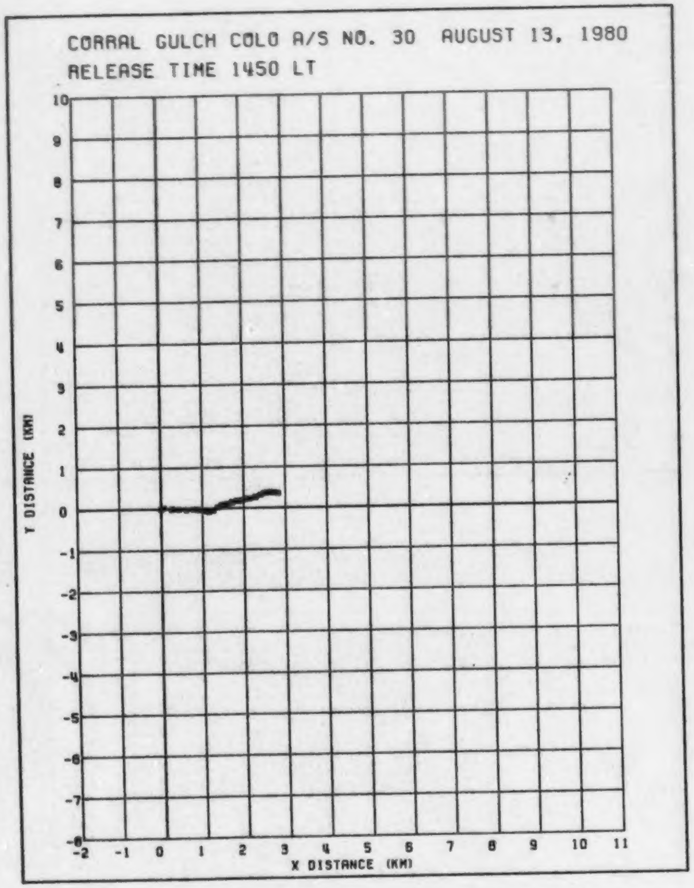

FIGURE 105. Airsonde #30 Subpoint Trajectory, 1450 MDT, August 13, 1980.

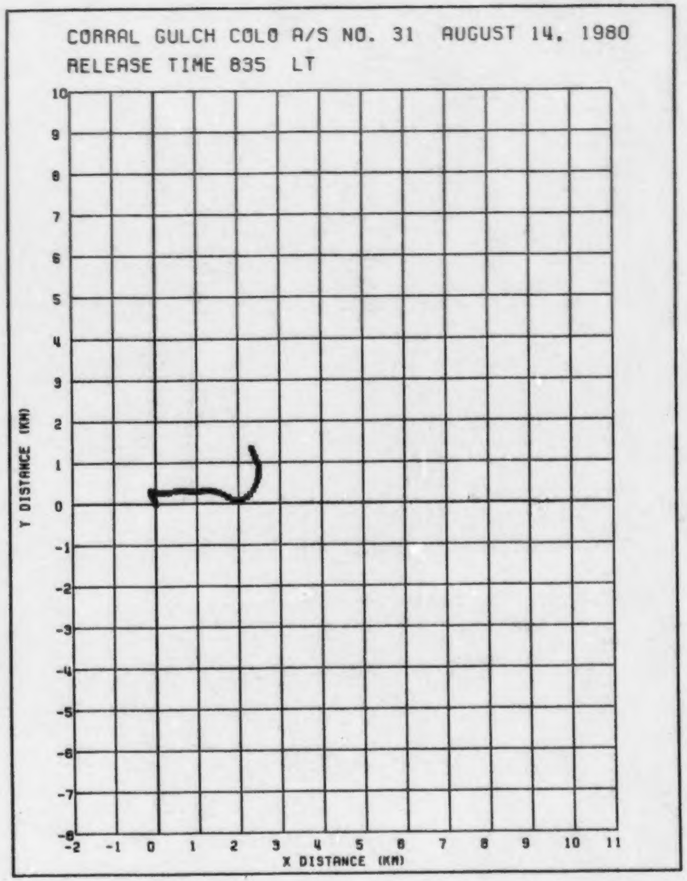

FIGURE 106. Airsonde #31 Subpoint Trajectory, 0835 MDT, August 14, 1980.

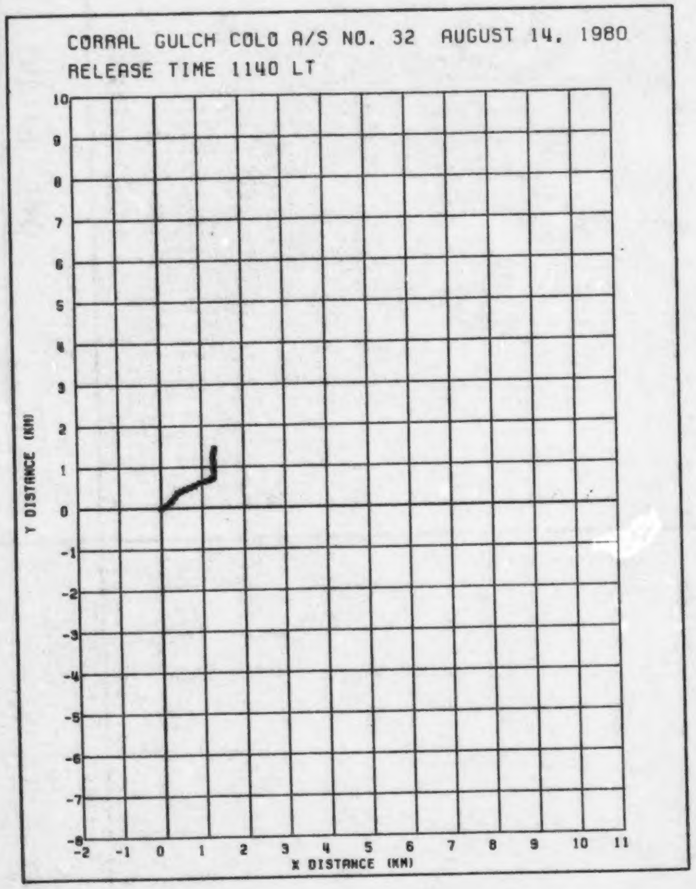

FIGURE 107. Airsonde #32 Subpoint Trajectory, 1140 MDT, August 14, 1980.

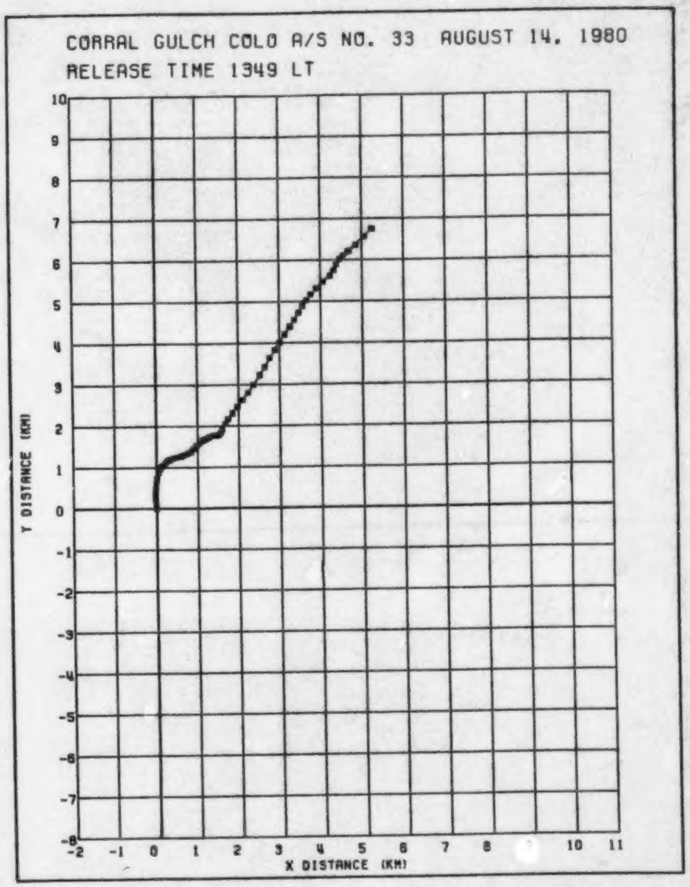

FIGURE 108. Airsonde #33 Subpoint Trajectory, 1349 MDT, August 14, 1980.

# APPENDIX D

# SOLAR AND TERRESTRIAL RADIATION
AND SOIL TEMPERATURE DATA

## TABLE 15. Radiation and Soil Temperature Data, Corral Creek, Colorado, August 8, 1980[1]

| Time MDT | $K\downarrow$ $Wm^{-2}$ | D $Wm^{-2}$ | $K\uparrow$ $Wm^{-2}$ | $Q^*$ $Wm^{-2}$ | $T_2$ °C | $T_5$ °C | $T_{20}$ °C |
|---|---|---|---|---|---|---|---|
| 0 | 9999[2] | 9999 | 9999 | 9999 | 21.0 | 23.2 | 23.9 |
| 30 | 9999 | 9999 | 9999 | 9999 | 20.3 | 22.8 | 23.8 |
| 100 | 9999 | 9999 | 9999 | 9999 | 19.6 | 22.3 | 23.5 |
| 130 | 9999 | 9999 | 9999 | 9999 | 18.8 | 21.7 | 23.4 |
| 200 | 9999 | 9999 | 9999 | 9999 | 18.5 | 21.3 | 23.1 |
| 230 | 9999 | 9999 | 9999 | 9999 | 18.0 | 20.7 | 22.8 |
| 300 | 9999 | 9999 | 9999 | 9999 | 17.8 | 20.5 | 22.7 |
| 330 | 9999 | 9999 | 9999 | 9999 | 17.3 | 20.1 | 22.4 |
| 400 | 9999 | 9999 | 9999 | 9999 | 17.0 | 19.7 | 22.1 |
| 430 | 9999 | 9999 | 9999 | 9999 | 16.3 | 19.4 | 22.1 |
| 500 | 9999 | 9999 | 9999 | 9999 | 16.3 | 19.0 | 21.7 |
| 530 | 9999 | 9999 | 9999 | 9999 | 16.3 | 18.8 | 21.5 |
| 600 | 9999 | 9999 | 9999 | 9999 | 15.6 | 18.5 | 21.4 |
| 630 | 9999 | 9999 | 0 | 9999 | 15.5 | 18.3 | 21.2 |
| 700 | 9999 | 9999 | 18 | 9999 | 14.9 | 18.0 | 21.0 |
| 730 | 9999 | 9999 | 46 | 9999 | 14.9 | 17.8 | 20.8 |
| 800 | 9999 | 9999 | 73 | 9999 | 14.9 | 17.4 | 20.6 |
| 830 | 9999 | 9999 | 91 | 9999 | 15.1 | 17.3 | 20.3 |
| 900 | 9999 | 9999 | 109 | 9999 | 15.6 | 17.3 | 20.2 |
| 930 | 9999 | 9999 | 119 | 9999 | 16.3 | 17.4 | 20.0 |
| 1000 | 9999 | 9999 | 128 | 9999 | 17.8 | 17.5 | 19.9 |
| 1030 | 9999 | 9999 | 147 | 9999 | 20.3 | 18.1 | 19.7 |
| 1100 | 9999 | 9999 | 156 | 9999 | 23.9 | 18.9 | 19.6 |
| 1130 | 9999 | 9999 | 166 | 9999 | 27.0 | 20.3 | 19.6 |
| 1200 | 9999 | 9999 | 184 | 9999 | 29.5 | 21.7 | 19.6 |
| 1230 | 9999 | 9999 | 203 | 9999 | 31.4 | 23.2 | 19.7 |
| 1300 | 1020 | 106 | 203 | 9999 | 33.9 | 24.6 | 19.9 |
| 1330 | 1015 | 112 | 206 | 9999 | 36.3 | 26.1 | 20.3 |
| 1400 | 802 | 182 | 146 | 9999 | 37.3 | 27.6 | 20.6 |
| 1430 | 765 | 263 | 164 | 9999 | 37.5 | 28.7 | 21.2 |
| 1500 | 692 | 237 | 144 | 9999 | 36.5 | 29.4 | 21.6 |
| 1530 | 691 | 243 | 153 | 9999 | 36.5 | 29.5 | 22.1 |
| 1600 | 248 | 205 | 48 | 9999 | 36.9 | 29.8 | 22.4 |
| 1630 | 598 | 204 | 88 | 9999 | 35.9 | 30.0 | 22.8 |
| 1700 | 514 | 184 | 120 | 9999 | 35.3 | 30.0 | 23.2 |
| 1730 | 380 | 165 | 94 | 9999 | 34.3 | 29.8 | 23.5 |
| 1800 | 540 | 156 | 139 | 9999 | 33.3 | 29.6 | 23.9 |
| 1830 | 288 | 90 | 78 | 9999 | 32.5 | 29.3 | 23.9 |
| 1900 | 35 | 35 | 8 | 9999 | 31.0 | 29.0 | 24.2 |
| 1930 | 141 | 44 | 35 | 9999 | 29.6 | 28.4 | 24.3 |
| 2000 | 0 | 0 | 0 | 9999 | 28.7 | 27.9 | 24.4 |
| 2030 | 0 | 0 | 0 | 9999 | 27.1 | 27.2 | 24.4 |
| 2100 | 0 | 0 | 0 | 9999 | 25.7 | 26.5 | 24.4 |
| 2130 | 0 | 0 | 0 | 9999 | 24.3 | 25.7 | 24.4 |
| 2200 | 0 | 0 | 0 | 9999 | 23.5 | 25.0 | 24.3 |
| 2230 | 0 | 0 | 0 | 9999 | 22.7 | 24.4 | 24.2 |
| 2300 | 0 | 0 | 0 | 9999 | 22.1 | 23.9 | 24.1 |
| 2330 | 0 | 0 | 0 | 9999 | 21.4 | 23.4 | 23.9 |

---

1. Radiation data are 5-minute averages about the half-hour indicated.
2. Missing data indicated by 9999.

**TABLE 16.** Radiation and Soil Temperature Data,
Corral Creek, Colorado, August 9, 1980.

| Time MDT | K↓ $Wm^{-2}$ | D $Wm^{-2}$ | K↑ $Wm^{-2}$ | Q* $Wm^{-2}$ | $T_2$ °C | $T_5$ °C | $T_{20}$ °C |
|---|---|---|---|---|---|---|---|
| 0 | 0 | 0 | 0 | -45 | 21.4 | 23.0 | 23.7 |
| 30 | 0 | 0 | 0 | -34 | 21.4 | 22.6 | 23.5 |
| 100 | 0 | 0 | 0 | -45 | 21.3 | 22.4 | 23.2 |
| 130 | 0 | 0 | 0 | -45 | 21.3 | 22.1 | 23.1 |
| 200 | 0 | 0 | 0 | -45 | 20.9 | 22.0 | 22.8 |
| 230 | 0 | 0 | 0 | -57 | 20.6 | 21.9 | 22.8 |
| 300 | 0 | 0 | 0 | -45 | 20.3 | 21.6 | 22.6 |
| 330 | 0 | 0 | 0 | -57 | 19.9 | 21.4 | 22.4 |
| 400 | 0 | 0 | 0 | -54 | 19.2 | 21.0 | 22.4 |
| 430 | 0 | 0 | 0 | -48 | 18.5 | 20.6 | 22.3 |
| 500 | 0 | 0 | 0 | -45 | 17.8 | 20.3 | 22.1 |
| 530 | 0 | 0 | 0 | -57 | 17.0 | 19.9 | 21.9 |
| 600 | 0 | 0 | 0 | -57 | 16.7 | 19.6 | 21.7 |
| 630 | 7 | 7 | 6 | -45 | 16.0 | 19.2 | 21.6 |
| 700 | 72 | 36 | 28 | -57 | 15.6 | 18.8 | 21.4 |
| 730 | 183 | 57 | 55 | 23 | 15.6 | 18.4 | 21.3 |
| 800 | 280 | 61 | 73 | 79 | 15.6 | 18.1 | 21.0 |
| 830 | 366 | 54 | 92 | 102 | 16.3 | 18.1 | 20.8 |
| 900 | 466 | 61 | 110 | 204 | 17.0 | 18.1 | 20.6 |
| 930 | 566 | 79 | 128 | 328 | 18.1 | 18.3 | 20.5 |
| 1000 | 674 | 65 | 143 | 405 | 19.8 | 18.6 | 20.3 |
| 1030 | 753 | 68 | 147 | 452 | 22.4 | 19.2 | 20.3 |
| 1100 | 824 | 72 | 166 | 509 | 25.5 | 20.3 | 20.1 |
| 1130 | 896 | 72 | 172 | 554 | 28.1 | 21.4 | 20.1 |
| 1200 | 939 | 72 | 185 | 588 | 30.3 | 22.8 | 20.2 |
| 1230 | 1118 | 215 | 203 | 649 | 32.5 | 24.3 | 20.3 |
| 1300 | 251 | 222 | 44 | 113 | 35.0 | 26.0 | 20.6 |
| 1330 | 143 | 136 | 27 | 50 | 32.4 | 26.8 | 20.9 |
| 1400 | 108 | 104 | 19 | 34 | 30.2 | 26.8 | 21.3 |
| 1430 | 251 | 215 | 46 | 136 | 27.6 | 26.5 | 21.7 |
| 1500 | 168 | 154 | 29 | 68 | 26.6 | 25.7 | 22.1 |
| 1530 | 179 | 168 | 39 | 90 | 25.8 | 25.2 | 22.3 |
| 1600 | 609 | 161 | 137 | 339 | 26.8 | 24.9 | 22.4 |
| 1630 | 591 | 204 | 128 | 294 | 28.7 | 25.0 | 22.4 |
| 1700 | 287 | 233 | 42 | 102 | 29.5 | 25.5 | 22.4 |
| 1730 | 233 | 204 | 41 | 90 | 28.8 | 25.7 | 22.4 |
| 1800 | 97 | 97 | 15 | -34 | 28.7 | 25.7 | 22.5 |
| 1830 | 412 | 143 | 104 | 192 | 27.9 | 25.7 | 22.7 |
| 1900 | 251 | 79 | 61 | 79 | 27.6 | 25.6 | 22.8 |
| 1930 | 143 | 54 | 35 | -11 | 26.6 | 25.4 | 22.8 |
| 2000 | 36 | 36 | 0 | -57 | 25.4 | 25.1 | 22.8 |
| 2030 | 18 | 18 | 0 | -57 | 23.3 | 24.3 | 23.0 |
| 2100 | 0 | 0 | 0 | -57 | 22.1 | 23.9 | 23.0 |
| 2130 | 0 | 0 | 0 | -57 | 21.0 | 23.2 | 22.9 |
| 2200 | 0 | 0 | 0 | -68 | 20.1 | 22.6 | 22.8 |
| 2230 | 0 | 0 | 0 | -57 | 19.6 | 22.1 | 22.8 |
| 2300 | 0 | 0 | 0 | -57 | 18.6 | 21.3 | 22.4 |
| 2330 | 0 | 0 | 0 | -57 | 18.3 | 21.0 | 22.4 |

## TABLE 17. Radiation and Soil Temperature Data, Corral Creek, Colorado, August 10, 1980.

| Time MDT | K↓ Wm$^{-2}$ | D Wm$^{-2}$ | K↑ Wm$^{-2}$ | Q* Wm$^{-2}$ | $T_2$ °C | $T_5$ °C | $T_{20}$ °C |
|---|---|---|---|---|---|---|---|
| 0 | 0 | 0 | 0 | -57 | 17.8 | 20.3 | 22.3 |
| 30 | 0 | 0 | 0 | -57 | 17.4 | 19.9 | 22.1 |
| 100 | 0 | 0 | 0 | -57 | 17.0 | 19.6 | 21.7 |
| 130 | 0 | 0 | 0 | -57 | 16.3 | 19.2 | 21.7 |
| 200 | 0 | 0 | 0 | -59 | 16.0 | 18.8 | 21.4 |
| 230 | 0 | 0 | 0 | -59 | 15.6 | 18.7 | 21.3 |
| 300 | 0 | 0 | 0 | -59 | 15.2 | 18.3 | 21.1 |
| 330 | 0 | 0 | 0 | -59 | 14.9 | 17.9 | 20.9 |
| 400 | 0 | 0 | 0 | -59 | 14.5 | 17.7 | 20.6 |
| 430 | 0 | 0 | 0 | -59 | 14.1 | 17.4 | 20.6 |
| 500 | 0 | 0 | 0 | -54 | 14.0 | 17.1 | 20.3 |
| 530 | 0 | 0 | 0 | -54 | 13.4 | 16.9 | 20.3 |
| 600 | 0 | 0 | 0 | -59 | 13.3 | 16.6 | 20.0 |
| 630 | 0 | 0 | 0 | -59 | 12.9 | 16.3 | 19.9 |
| 700 | 70 | 17 | 20 | -57 | 12.7 | 16.0 | 19.6 |
| 730 | 152 | 33 | 44 | 11 | 12.7 | 15.8 | 19.5 |
| 800 | 247 | 36 | 66 | 88 | 13.1 | 15.6 | 19.3 |
| 830 | 353 | 49 | 85 | 158 | 13.4 | 15.6 | 19.2 |
| 900 | 460 | 47 | 104 | 226 | 14.1 | 15.6 | 18.8 |
| 930 | 566 | 46 | 113 | 296 | 15.2 | 15.8 | 18.8 |
| 1000 | 661 | 52 | 132 | 373 | 17.0 | 16.1 | 18.6 |
| 1030 | 742 | 58 | 142 | 430 | 20.6 | 17.0 | 18.5 |
| 1100 | 813 | 60 | 155 | 475 | 24.3 | 18.1 | 18.4 |
| 1130 | 883 | 59 | 161 | 520 | 27.2 | 19.6 | 18.4 |
| 1200 | 925 | 61 | 180 | 563 | 30.2 | 21.4 | 18.5 |
| 1230 | 952 | 63 | 183 | 588 | 32.5 | 23.0 | 18.8 |
| 1300 | 987 | 55 | 200 | 611 | 34.7 | 24.6 | 19.1 |
| 1330 | 986 | 54 | 200 | 629 | 36.4 | 26.1 | 19.4 |
| 1400 | 977 | 56 | 201 | 620 | 37.3 | 27.6 | 19.9 |
| 1430 | 958 | 51 | 202 | 599 | 38.3 | 28.7 | 20.3 |
| 1500 | 910 | 50 | 201 | 577 | 39.0 | 29.6 | 20.9 |
| 1530 | 873 | 49 | 186 | 538 | 39.7 | 30.3 | 21.4 |
| 1600 | 800 | 51 | 170 | 475 | 39.4 | 31.0 | 21.9 |
| 1630 | 727 | 50 | 167 | 409 | 38.2 | 31.2 | 22.4 |
| 1700 | 618 | 48 | 150 | 351 | 36.5 | 31.0 | 22.8 |
| 1730 | 527 | 44 | 128 | 271 | 34.9 | 30.6 | 23.2 |
| 1800 | 436 | 42 | 103 | 204 | 33.1 | 30.1 | 23.5 |
| 1830 | 324 | 41 | 84 | 136 | 31.4 | 29.5 | 23.8 |
| 1900 | 215 | 36 | 55 | 57 | 30.0 | 28.7 | 23.9 |
| 1930 | 110 | 31 | 29 | -11 | 28.7 | 28.0 | 24.0 |
| 2000 | 12 | 12 | 0 | -57 | 27.2 | 27.4 | 24.1 |
| 2030 | 0 | 0 | 0 | -57 | 25.3 | 26.5 | 24.1 |
| 2100 | 0 | 0 | 0 | -57 | 23.5 | 25.7 | 24.1 |
| 2130 | 0 | 0 | 0 | -63 | 22.2 | 24.8 | 23.9 |
| 2200 | 0 | 0 | 0 | -68 | 21.3 | 23.9 | 23.9 |
| 2230 | 0 | 0 | 0 | -68 | 20.1 | 23.2 | 23.5 |
| 2300 | 0 | 0 | 0 | -68 | 19.2 | 22.4 | 23.5 |
| 2330 | 0 | 0 | 0 | -68 | 18.5 | 21.7 | 23.2 |

TABLE 18. Radiation and Soil Temperature Data, Corral Creek, Colorado, August 11, 1980.

| Time MDT | K↓ $Wm^{-2}$ | D $Wm^{-2}$ | K↑ $Wm^{-2}$ | Q* $Wm^{-2}$ | $T_2$ °C | $T_5$ °C | $T_{20}$ °C |
|---|---|---|---|---|---|---|---|
| 0 | 0 | 0 | 0 | -68 | 17.8 | 21.2 | 23.0 |
| 30 | 0 | 0 | 0 | -68 | 17.4 | 20.8 | 22.8 |
| 100 | 0 | 0 | 0 | -68 | 16.7 | 20.2 | 22.6 |
| 130 | 0 | 0 | 0 | -68 | 16.1 | 19.7 | 22.3 |
| 200 | 0 | 0 | 0 | -68 | 15.6 | 19.2 | 22.1 |
| 230 | 0 | 0 | 0 | -75 | 14.9 | 18.8 | 21.8 |
| 300 | 0 | 0 | 0 | -75 | 14.5 | 18.3 | 21.5 |
| 330 | 0 | 0 | 0 | -75 | 14.1 | 17.9 | 21.4 |
| 400 | 0 | 0 | 0 | -75 | 13.4 | 17.5 | 21.0 |
| 430 | 0 | 0 | 0 | -79 | 13.2 | 17.1 | 20.8 |
| 500 | 0 | 0 | 0 | -79 | 12.7 | 16.7 | 20.6 |
| 530 | 0 | 0 | 0 | -79 | 12.5 | 16.4 | 20.3 |
| 600 | 0 | 0 | 0 | -79 | 12.0 | 16.1 | 20.1 |
| 630 | 0 | 0 | 0 | -72 | 11.7 | 15.8 | 19.9 |
| 700 | 64 | 32 | 19 | -88 | 11.3 | 15.5 | 19.7 |
| 730 | 146 | 35 | 43 | -11 | 11.2 | 15.3 | 19.5 |
| 800 | 257 | 38 | 69 | 68 | 11.6 | 15.1 | 19.2 |
| 830 | 356 | 41 | 87 | 136 | 12.2 | 15.1 | 19.1 |
| 900 | 467 | 51 | 103 | 204 | 12.7 | 15.0 | 18.8 |
| 930 | 571 | 54 | 119 | 292 | 13.7 | 15.2 | 18.6 |
| 1000 | 669 | 68 | 131 | 357 | 15.8 | 15.4 | 18.4 |
| 1030 | 756 | 54 | 146 | 409 | 19.3 | 16.1 | 18.2 |
| 1100 | 834 | 60 | 154 | 466 | 23.2 | 17.3 | 18.1 |
| 1130 | 898 | 60 | 169 | 516 | 26.7 | 18.8 | 18.1 |
| 1200 | 952 | 66 | 176 | 547 | 29.7 | 20.6 | 18.1 |
| 1230 | 987 | 62 | 182 | 575 | 32.4 | 22.4 | 18.4 |
| 1300 | 1001 | 65 | 187 | 599 | 34.4 | 24.0 | 18.6 |
| 1330 | 1015 | 65 | 191 | 627 | 36.4 | 25.7 | 19.0 |
| 1400 | 1000 | 72 | 189 | 602 | 37.9 | 27.2 | 19.4 |
| 1430 | 974 | 64 | 188 | 572 | 39.0 | 28.4 | 19.9 |
| 1500 | 931 | 67 | 180 | 536 | 40.0 | 29.5 | 20.4 |
| 1530 | 884 | 70 | 177 | 498 | 40.7 | 30.5 | 21.0 |
| 1600 | 819 | 77 | 178 | 450 | 40.7 | 31.2 | 21.5 |
| 1630 | 722 | 87 | 179 | 407 | 39.7 | 31.7 | 22.1 |
| 1700 | 635 | 80 | 172 | 335 | 37.5 | 31.6 | 22.7 |
| 1730 | 538 | 65 | 160 | 274 | 35.2 | 31.2 | 23.2 |
| 1800 | 423 | 61 | 140 | 176 | 33.3 | 30.6 | 23.5 |
| 1830 | 322 | 32 | 113 | 115 | 31.4 | 29.8 | 23.8 |
| 1900 | 232 | 31 | 76 | 48 | 29.8 | 29.0 | 23.9 |
| 1930 | 127 | 23 | 38 | -23 | 28.2 | 28.2 | 24.0 |
| 2000 | 23 | 23 | 1 | -72 | 26.5 | 27.3 | 24.1 |
| 2030 | 5 | 5 | 0 | -77 | 24.5 | 26.5 | 24.1 |
| 2100 | 0 | 0 | 0 | -72 | 22.8 | 25.4 | 24.1 |
| 2130 | 0 | 0 | 0 | -72 | 21.5 | 24.6 | 23.9 |
| 2200 | 0 | 0 | 0 | -68 | 20.4 | 23.5 | 23.7 |
| 2230 | 0 | 0 | 0 | -68 | 19.3 | 22.8 | 23.5 |
| 2300 | 0 | 0 | 0 | -68 | 18.8 | 22.1 | 23.4 |
| 2330 | 0 | 0 | 0 | -68 | 18.1 | 21.4 | 23.2 |

TABLE 19. Radiation and Soil Temperature Data, Corral Creek, Colorado, August 12, 1980.

| Time MDT | K↓ Wm$^{-2}$ | D Wm$^{-2}$ | K↑ Wm$^{-2}$ | Q* Wm$^{-2}$ | $T_2$ °C | $T_5$ °C | $T_{20}$ °C |
|---|---|---|---|---|---|---|---|
| 0 | 0 | 0 | 0 | -68 | 17.7 | 21.0 | 22.8 |
| 30 | 0 | 0 | 0 | -68 | 17.0 | 20.5 | 22.6 |
| 100 | 0 | 0 | 0 | -68 | 16.7 | 19.9 | 22.3 |
| 130 | 0 | 0 | 0 | -57 | 16.0 | 19.5 | 22.1 |
| 200 | 0 | 0 | 0 | -57 | 15.3 | 19.0 | 21.9 |
| 230 | 0 | 0 | 0 | -57 | 14.7 | 18.5 | 21.6 |
| 300 | 0 | 0 | 0 | -57 | 13.9 | 18.1 | 21.4 |
| 330 | 0 | 0 | 0 | -57 | 13.3 | 17.6 | 21.1 |
| 400 | 0 | 0 | 0 | -57 | 12.7 | 17.1 | 20.9 |
| 430 | 0 | 0 | 0 | -57 | 12.9 | 16.7 | 20.6 |
| 500 | 0 | 0 | 0 | -59 | 12.0 | 16.3 | 20.3 |
| 530 | 0 | 0 | 0 | -54 | 11.6 | 16.0 | 20.2 |
| 600 | 0 | 0 | 0 | -57 | 11.2 | 15.6 | 19.9 |
| 630 | 3 | 0 | 1 | -59 | 10.9 | 15.5 | 19.7 |
| 700 | 71 | 35 | 20 | -54 | 10.9 | 15.2 | 19.5 |
| 730 | 160 | 35 | 44 | 23 | 10.9 | 14.9 | 19.2 |
| 800 | 249 | 34 | 66 | 102 | 11.6 | 14.7 | 18.9 |
| 830 | 364 | 48 | 85 | 158 | 12.3 | 14.7 | 18.8 |
| 900 | 464 | 73 | 104 | 224 | 13.4 | 14.9 | 18.5 |
| 930 | 625 | 105 | 131 | 339 | 15.2 | 14.9 | 18.4 |
| 1000 | 717 | 140 | 132 | 464 | 18.1 | 15.6 | 18.1 |
| 1030 | 731 | 93 | 133 | 477 | 22.1 | 16.7 | 18.0 |
| 1100 | 827 | 86 | 148 | 532 | 25.7 | 18.3 | 17.9 |
| 1130 | 892 | 71 | 153 | 566 | 29.1 | 20.1 | 18.1 |
| 1200 | 927 | 117 | 172 | 579 | 31.0 | 21.5 | 18.1 |
| 1230 | 1142 | 264 | 226 | 701 | 33.3 | 23.2 | 18.5 |
| 1300 | 245 | 174 | 50 | 124 | 33.7 | 25.0 | 18.8 |
| 1330 | 998 | 138 | 210 | 645 | 34.5 | 25.7 | 19.2 |
| 1400 | 532 | 352 | 123 | 407 | 36.5 | 26.9 | 19.6 |
| 1430 | 130 | 119 | 41 | 68 | 36.1 | 27.9 | 20.1 |
| 1500 | 212 | 137 | 51 | 113 | 33.3 | 28.3 | 20.6 |
| 1530 | 710 | 298 | 206 | 611 | 31.5 | 27.9 | 21.2 |
| 1600 | 279 | 226 | 60 | 158 | 31.7 | 27.6 | 21.5 |
| 1630 | 207 | 171 | 39 | 113 | 31.0 | 27.3 | 21.8 |
| 1700 | 63 | 63 | 5 | 11 | 30.2 | 27.1 | 22.1 |
| 1730 | 260 | 239 | 59 | 152 | 28.7 | 26.6 | 22.3 |
| 1800 | 124 | 102 | 23 | 57 | 27.9 | 26.4 | 22.4 |
| 1830 | 44 | 44 | 5 | 2 | 27.6 | 25.9 | 22.4 |
| 1900 | 51 | 51 | 9 | 11 | 26.6 | 25.6 | 22.6 |
| 1930 | 98 | 62 | 28 | 23 | 25.7 | 25.1 | 22.6 |
| 2000 | 29 | 29 | 11 | -25 | 25.0 | 24.6 | 22.6 |
| 2030 | 0 | 0 | 0 | -45 | 27.6 | 24.3 | 22.5 |
| 2100 | 0 | 0 | 0 | -34 | 22.8 | 23.7 | 22.6 |
| 2130 | 0 | 0 | 0 | -41 | 21.4 | 23.2 | 22.6 |
| 2200 | 0 | 0 | 0 | -32 | 20.6 | 22.4 | 22.4 |
| 2230 | 0 | 0 | 0 | -34 | 19.9 | 21.9 | 22.4 |
| 2300 | 0 | 0 | 0 | -23 | 19.8 | 21.4 | 22.1 |
| 2330 | 0 | 0 | 0 | -23 | 19.6 | 21.0 | 22.1 |

TABLE 20. Radiation and Soil Temperature Data, Corral Creek, Colorado, August 13, 1980.

| Time MDT | K↓ $Wm^{-2}$ | D $Wm^{-2}$ | K↑ $Wm^{-2}$ | Q* $Wm^{-2}$ | $T_2$ °C | $T_5$ °C | $T_{20}$ °C |
|---|---|---|---|---|---|---|---|
| 0 | 0 | 0 | 0 | -23 | 19.2 | 20.7 | 21.8 |
| 30 | 0 | 0 | 0 | -23 | 18.7 | 20.5 | 21.7 |
| 100 | 0 | 0 | 0 | -38 | 18.1 | 20.2 | 21.5 |
| 130 | 0 | 0 | 0 | -34 | 17.4 | 19.8 | 21.4 |
| 200 | 0 | 0 | 0 | -23 | 17.0 | 19.4 | 21.4 |
| 230 | 0 | 0 | 0 | -25 | 16.3 | 19.0 | 21.0 |
| 300 | 0 | 0 | 0 | -34 | 16.0 | 18.7 | 21.0 |
| 330 | 0 | 0 | 0 | -34 | 15.6 | 18.4 | 20.8 |
| 400 | 0 | 0 | 0 | -34 | 14.9 | 17.9 | 20.6 |
| 430 | 0 | 0 | 0 | -29 | 14.5 | 17.6 | 20.5 |
| 500 | 0 | 0 | 0 | -29 | 14.1 | 17.2 | 20.3 |
| 530 | 0 | 0 | 0 | -34 | 13.8 | 17.0 | 20.0 |
| 600 | 0 | 0 | 0 | -34 | 13.4 | 16.7 | 19.9 |
| 630 | 0 | 0 | 0 | -29 | 13.3 | 16.3 | 19.7 |
| 700 | 54 | 18 | 15 | -34 | 12.8 | 16.1 | 19.6 |
| 730 | 143 | 36 | 42 | 34 | 12.9 | 16.0 | 19.3 |
| 800 | 251 | 54 | 61 | 111 | 13.4 | 15.8 | 19.2 |
| 830 | 287 | 54 | 62 | 136 | 14.1 | 15.8 | 18.9 |
| 900 | 430 | 54 | 99 | 233 | 14.9 | 15.8 | 18.8 |
| 930 | 538 | 72 | 118 | 339 | 16.3 | 16.1 | 18.6 |
| 1000 | 645 | 72 | 137 | 407 | 18.5 | 16.5 | 18.5 |
| 1030 | 143 | 108 | 14 | 57 | 20.2 | 17.4 | 18.4 |
| 1100 | 824 | 97 | 157 | 520 | 20.4 | 18.1 | 18.4 |
| 1130 | 860 | 82 | 158 | 543 | 25.0 | 18.7 | 18.4 |
| 1200 | 932 | 115 | 177 | 599 | 28.7 | 20.3 | 18.4 |
| 1230 | 950 | 90 | 196 | 622 | 31.7 | 21.9 | 18.5 |
| 1300 | 681 | 115 | 145 | 498 | 34.1 | 23.6 | 18.7 |
| 1330 | 645 | 161 | 128 | 362 | 36.1 | 25.4 | 19.0 |
| 1400 | 932 | 197 | 165 | 588 | 37.3 | 26.8 | 19.4 |
| 1430 | 466 | 233 | 104 | 283 | 37.3 | 27.9 | 19.9 |
| 1500 | 233 | 204 | 47 | 124 | 36.5 | 28.7 | 20.4 |
| 1530 | 168 | 143 | 36 | 79 | 34.5 | 29.1 | 21.0 |
| 1600 | 430 | 358 | 91 | 283 | 32.1 | 28.7 | 21.4 |
| 1630 | 627 | 305 | 145 | 407 | 32.9 | 28.1 | 21.7 |
| 1700 | 287 | 233 | 58 | 170 | 32.5 | 28.1 | 22.1 |
| 1730 | 125 | 97 | 15 | 79 | 31.7 | 27.9 | 22.4 |
| 1800 | 54 | 54 | 2 | 0 | 30.2 | 27.7 | 22.4 |
| 1830 | 36 | 36 | 0 | 0 | 28.7 | 27.2 | 22.8 |
| 1900 | 36 | 36 | 0 | 11 | 27.2 | 26.5 | 22.8 |
| 1930 | 29 | 29 | 0 | 0 | 25.7 | 25.9 | 22.8 |
| 2000 | 0 | 0 | 0 | 0 | 24.5 | 25.2 | 23.0 |
| 2030 | 0 | 0 | 0 | 0 | 23.5 | 24.6 | 23.0 |
| 2100 | 0 | 0 | 0 | 0 | 22.8 | 23.9 | 22.8 |
| 2130 | 0 | 0 | 0 | -5 | 21.9 | 23.4 | 22.8 |
| 2200 | 0 | 0 | 0 | 0 | 21.4 | 22.8 | 22.8 |
| 2230 | 0 | 0 | 0 | -7 | 20.6 | 22.4 | 22.6 |
| 2300 | 0 | 0 | 0 | 0 | 19.9 | 22.0 | 22.4 |
| 2330 | 0 | 0 | 0 | 0 | 19.9 | 21.5 | 22.3 |

TABLE 21. Radiation and Soil Temperature Data, Corral Creek, Colorado, August 14, 1980.

| Time MDT | K↓ $Wm^{-2}$ | D $Wm^{-2}$ | K↑ $Wm^{-2}$ | Q* $Wm^{-2}$ | $T_2$ °C | $T_5$ °C | $T_{20}$ °C |
|---|---|---|---|---|---|---|---|
| 0 | 0 | 0 | 0 | -5 | 19.6 | 21.2 | 22.1 |
| 30 | 0 | 0 | 0 | -5 | 19.2 | 20.9 | 22.0 |
| 100 | 0 | 0 | 0 | -5 | 19.1 | 20.6 | 21.7 |
| 130 | 0 | 0 | 0 | -5 | 18.6 | 20.3 | 21.7 |
| 200 | 0 | 0 | 0 | -11 | 18.5 | 20.1 | 21.5 |
| 230 | 0 | 0 | 0 | 0 | 18.3 | 19.9 | 21.4 |
| 300 | 0 | 0 | 0 | -23 | 17.8 | 19.6 | 21.3 |
| 330 | 0 | 0 | 0 | -23 | 17.6 | 19.4 | 21.0 |
| 400 | 0 | 0 | 0 | -11 | 17.0 | 19.2 | 21.0 |
| 430 | 0 | 0 | 0 | -11 | 16.8 | 18.8 | 20.8 |
| 500 | 0 | 0 | 0 | -23 | 16.3 | 18.7 | 20.6 |
| 530 | 0 | 0 | 0 | -34 | 16.0 | 18.4 | 20.5 |
| 600 | 0 | 0 | 0 | -34 | 15.2 | 18.1 | 20.3 |
| 630 | 0 | 0 | 0 | -23 | 14.5 | 17.7 | 20.3 |
| 700 | 54 | 36 | 0 | -23 | 14.1 | 17.3 | 20.1 |
| 730 | 190 | 90 | 55 | 90 | 14.5 | 17.0 | 19.9 |
| 800 | 115 | 90 | 32 | 45 | 15.5 | 16.9 | 19.7 |
| 830 | 90 | 72 | 23 | 11 | 16.1 | 17.0 | 19.6 |
| 900 | 556 | 143 | 129 | 323 | 16.5 | 17.1 | 19.4 |
| 930 | 412 | 90 | 85 | 260 | 17.4 | 17.4 | 19.2 |
| 1000 | 509 | 143 | 129 | 385 | 19.2 | 17.7 | 19.1 |
| 1030 | 340 | 287 | 64 | 215 | 21.4 | 18.3 | 19.1 |
| 1100 | 287 | 240 | 50 | 181 | 22.1 | 19.1 | 19.0 |
| 1130 | 591 | 412 | 94 | 385 | 22.8 | 19.7 | 19.1 |
| 1200 | 573 | 441 | 103 | 385 | 25.0 | 20.3 | 19.1 |
| 1230 | 538 | 376 | 94 | 362 | 26.5 | 21.2 | 19.2 |
| 1300 | 860 | 358 | 173 | 464 | 28.3 | 22.1 | 19.2 |
| 1330 | 484 | 394 | 85 | 328 | 30.2 | 23.2 | 19.4 |
| 1400 | 842 | 394 | 165 | 543 | 31.0 | 24.1 | 19.6 |
| 1430 | 1021 | 197 | 209 | 9999 | 33.3 | 25.0 | 19.9 |

# APPENDIX E

## AIRCRAFT-MEASURED PROFILES OF AIR QUALITY

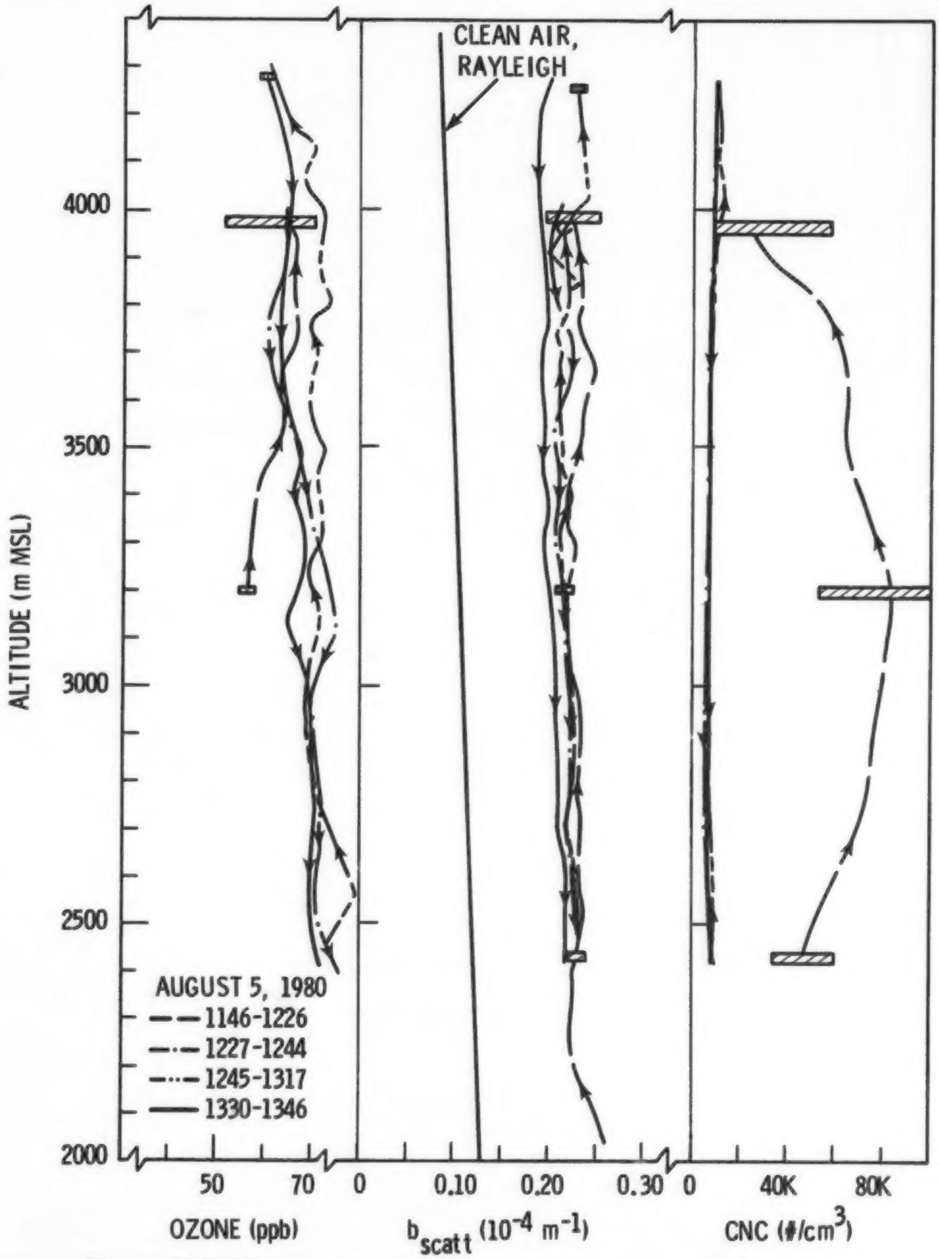

FIGURE 109. Vertical Profiles of Ozone Concentration, Light Scattering Coefficient, and Condensation Nuclei Concentration for Aircraft Flights of August 5, 1980. Rayleigh Scattering Coefficients for Clean Air are Plotted for Reference.

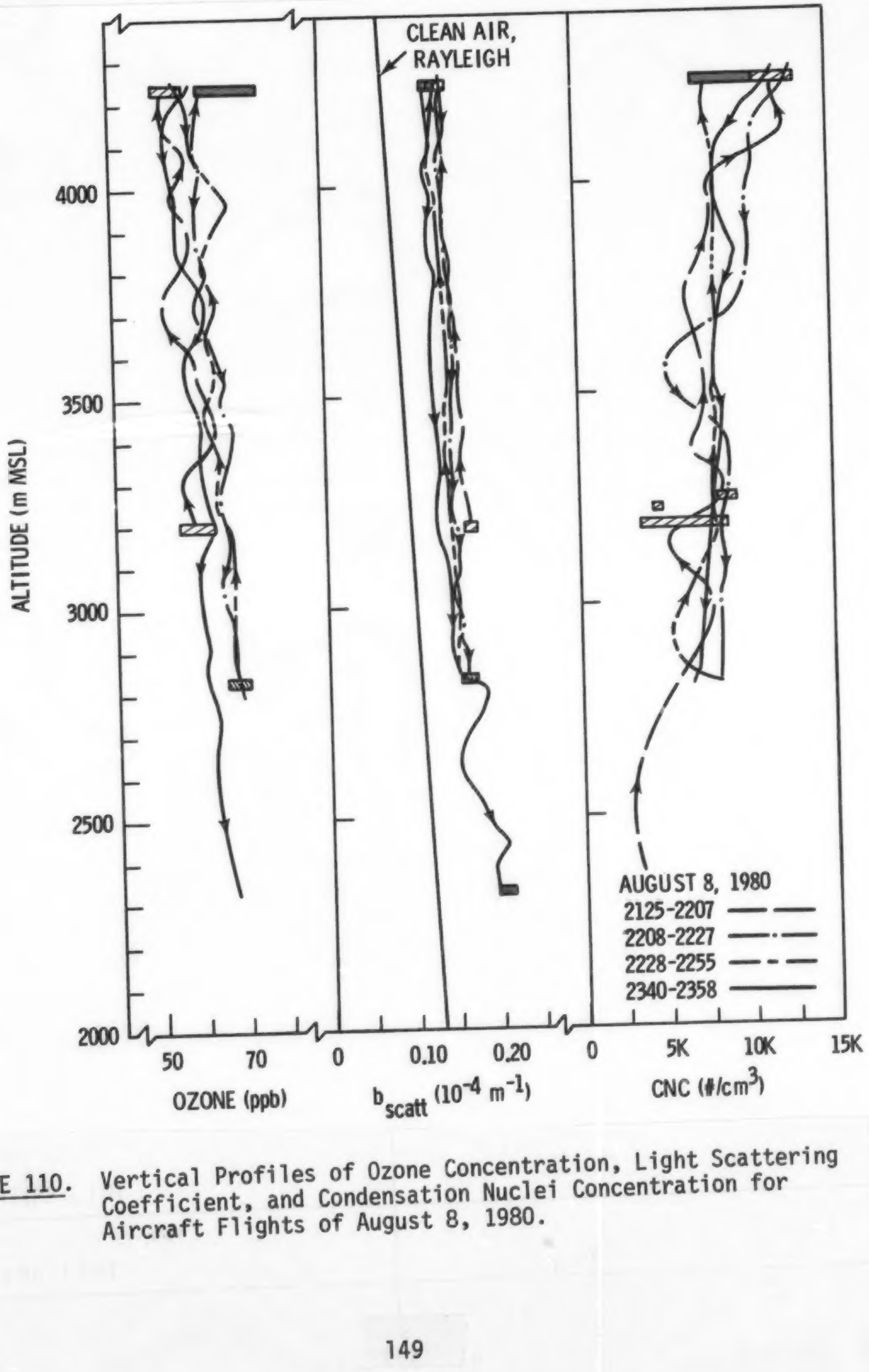

FIGURE 110. Vertical Profiles of Ozone Concentration, Light Scattering Coefficient, and Condensation Nuclei Concentration for Aircraft Flights of August 8, 1980.

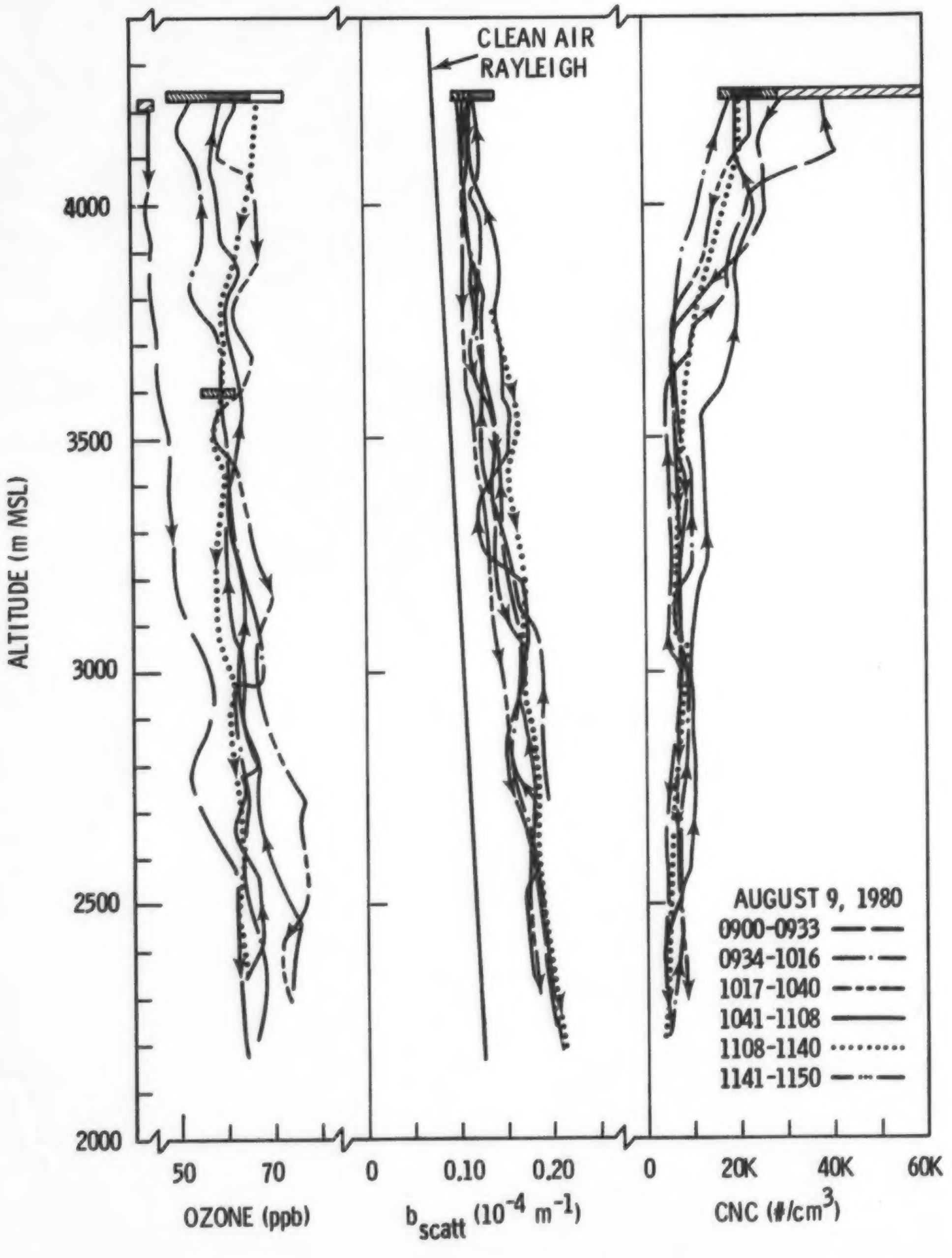

FIGURE 111. Vertical Profiles of Ozone Concentration, Light Scattering Coefficient, and Condensation Nuclei Concentration for Aircraft Flights of August 9, 1980.

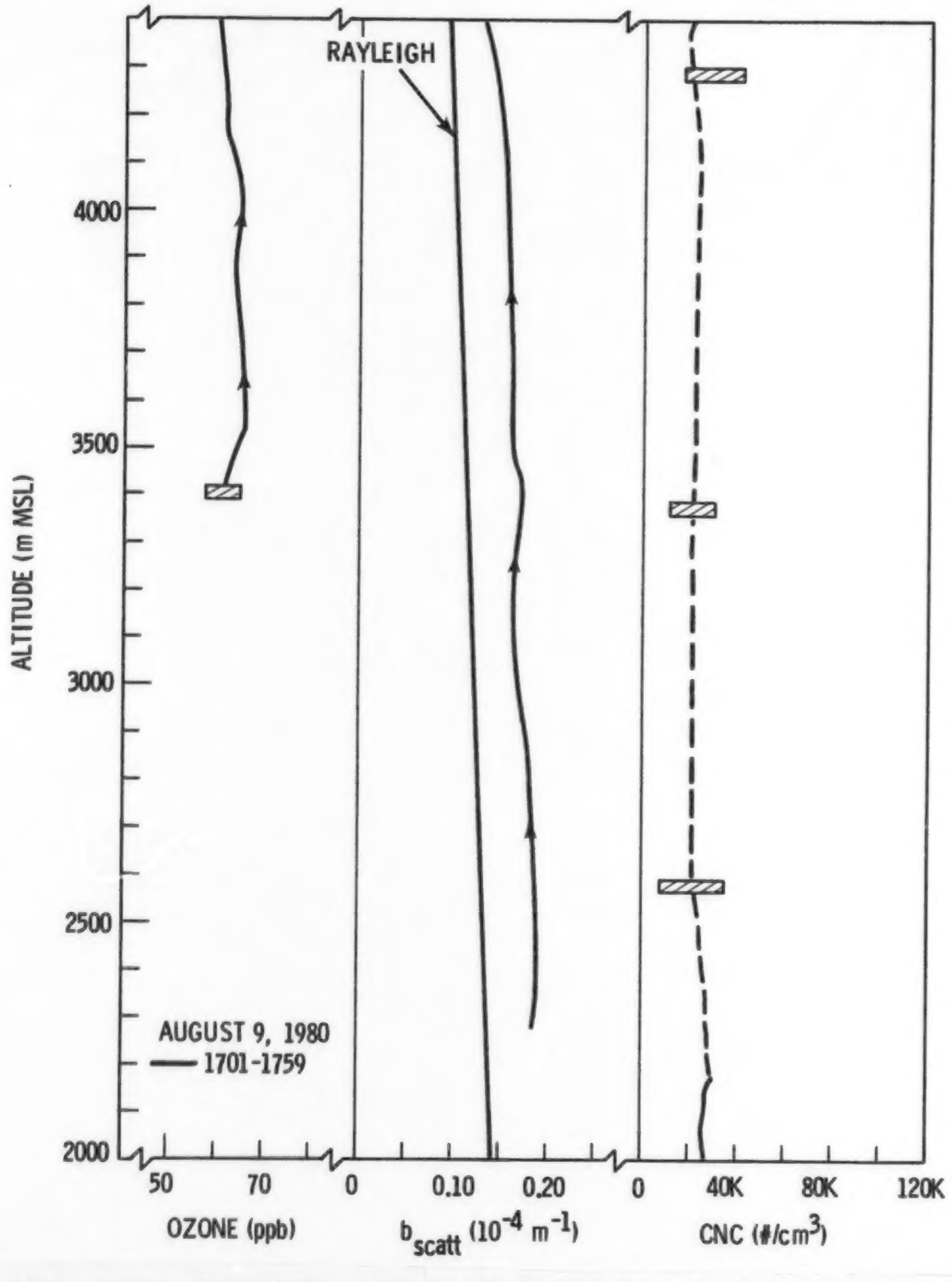

FIGURE 112. Vertical Profiles of Ozone Concentration, Light Scattering Coefficient, and Condensation Nuclei Concentration for Aircraft Flights of August 9, 1980.

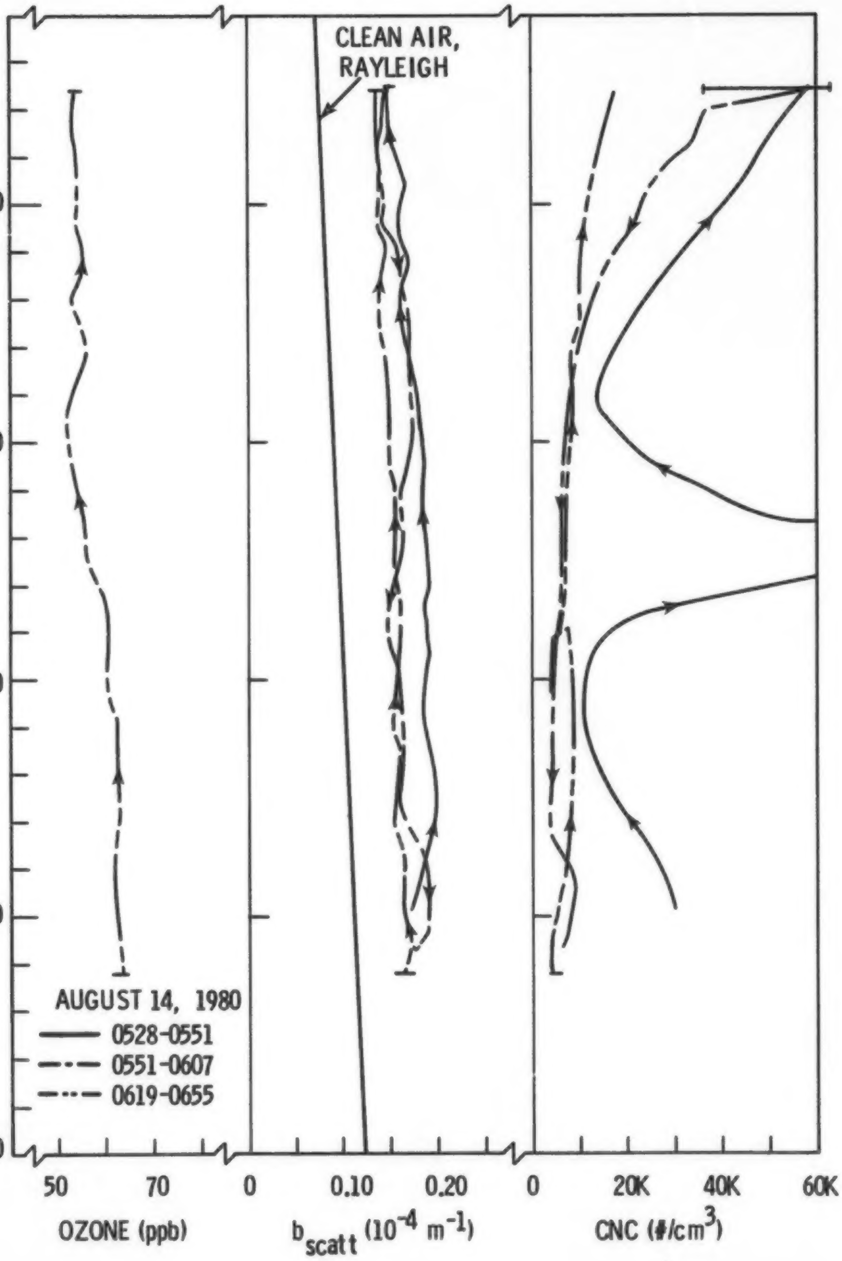

FIGURE 113. Vertical Profiles of Ozone Concentration, Light Scattering Coefficient, and Condensation Nuclei Concentration for Aircraft Flights of August 14, 1980, 0528 - 0655 MDT.

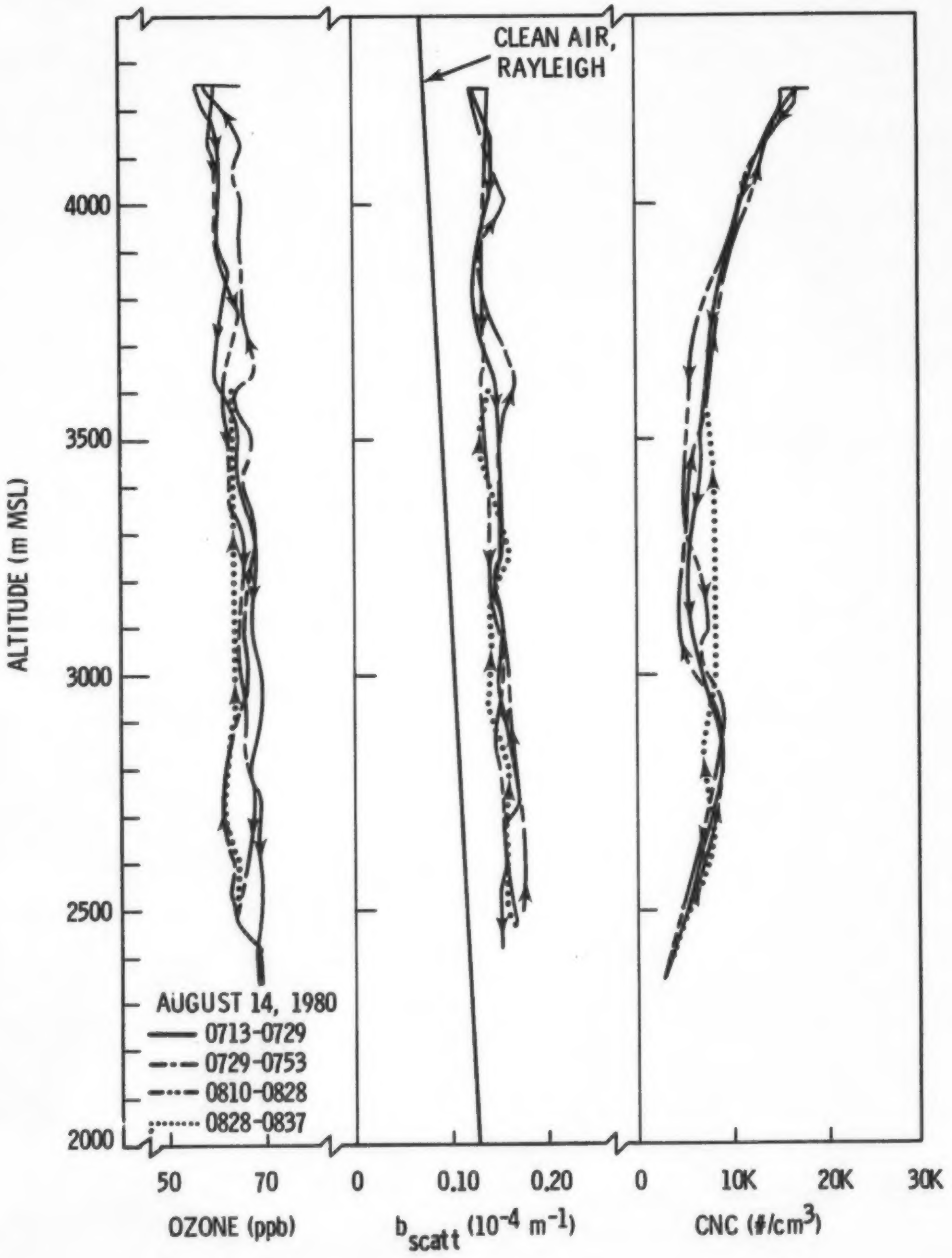

FIGURE 114. Vertical Profiles of Ozone Concentration, Light Scattering Coefficient, and Condensation Nuclei Concentration for Aircraft Flights of August 14, 1980, 0713 - 0837 MDT.